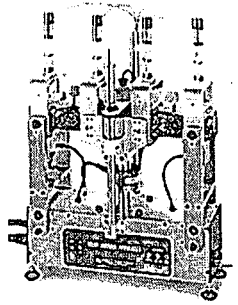


CHARACTERISATION OF FATIGUE PERFORMANCE OF SELECTED COLD BITUMINOUS MIXES



By

TWAGIRA ELIAS MATHANIYA, BSc.(Eng)

A Thesis

Submitted in partial fulfilment of the
Requirements for the degree of
MASTER OF SCIENCE IN CIVIL ENGINEERING, MSc. (Eng)
(PAVEMENT ENGINEERING)

In the
Faculty of Engineering, Department of Civil Engineering
University of Stellenbosch

Promotor

Professor KIM J. JENKINS PhD
SANRAL CHAIR OF PAVEMENT ENGINEERING

STELLENBOSCH, APRIL 2006

DECLARATION BY THE CANDIDATE

I, the undersigned hereby declare that the work presented in this thesis is my own work and has not previously in its entirety or in part been submitted for a degree to any other University.

3rd March 2006.

Date

ABSTRACT

The use of cold mixes (bitumen emulsion and foamed bitumen mixes) in road rehabilitation and construction is gaining favour globally due to its advantage of conservation of environment, resources, and money.

Cold bituminous treated materials exhibit to a certain degree aspects of basic characteristics of granular materials, cement-treated materials and hot mix asphalt depending on the mix proportion of bitumen, mineral aggregates and active filler. Where high binder contents are used to improve strain-at-break (flexibility) and fatigue performance of these mixes, the material approaches loading-frequency and temperature dependency, i.e. visco-elastic behaviour, similar to that of hot mix asphalt. An understanding of the strain-at-break behaviour and fatigue relationship of cold mixes in a pavement layer, therefore, is of considerable importance to ensure correct mix design and analysis of the cold mix layer in a pavement structure.

The main objective of this thesis is to characterize the fatigue performance of selected cold bituminous treated materials, by providing a fundamental understanding of the fatigue properties and its link to strain-at-break properties and visco-elastic behaviour associated with dependency of temperature and rate of loading on the performance of these mixes.

The study investigates the fatigue, strain-at-break, and stiffness modulus (master curve) properties of the different materials types, i.e. virgin crushed limestone, and reclaimed asphalt pavement (RAP) millings blended in two different proportions. Either the limestone or the RAP was selected as the dominant portion, i.e. 75% by mass. These blends were treated with various bitumen contents of either bitumen emulsion or foamed bitumen. The influences and effect of active filler in these mixes were investigated too; 1% cement was added to the 75% limestone blends.

The characterization of these mixes fatigue properties, as well as strain-at-break and flexural stiffness (master curve) properties were developed using a four-point beam testing apparatus. The apparatus is believed to provide an insight on fatigue failure mechanism of specimen by performing flexing tests in the form of an alternating stress or strain of certain amplitude.

It was found in the investigation that the fatigue test under controlled displacement mode of these mixes show that the fatigue life is dependent on the loading rates. On a log-log scale plot, linear fatigue functions are obtained. The foamed bitumen and emulsion mixes without

active filler (cement) show no significant difference in fatigue life at high strain levels. However with the addition of small quantity of cement (1%) a notable shift in the fatigue line for the foam mixes occurs with an increase in fatigue life compared with that of the emulsion mixes. When emulsion or foam is used for the treatment of the mixes with higher percentage of RAP a decrease in fatigue life occurred.

The significant differences occurred in the strain-at-break properties of selected mixes indicate that the test protocol needs further development to provide a reliable link of this parameter to fatigue performance. Further more it cannot define accurately the flexibility behaviour of the cold mixes but provides some indication of flexibility which can be used in the mix design process. The flexural stiffness response of the selected mixes however proves to be both temperature and loading rate dependent.

OPSOMMING

Die gebruik van koue mengsels (bitumen emulsies en geskuimde bitumen mengsels) in padoppervlakrehabilitasie en –konstruksie, wek tans wêreldwyd belangstelling as gevolg van die voordele wat dit inhou in die vorm van finansiële besparings en die behoud van hulpbronne en die omgewing.

Koue bitumineus-behandelde materiale vertoon tot 'n sekere mate die basiese eienskappe van granulêre materiale, sement-behandelde materiale en warmgemengde asfalt afhangende van die verhouding waarin die bitumen, mineraalaggragate en aktiewe vulstof gemeng word. Wanneer 'n hoë inhoud van bindstof gebruik word om die reck-by-breek (buigsaamheid) en die vermoeingseienskappe van hierdie mengsels te verbeter, vertoon die materiale 'n belastingsfrekwensie en temperatuur afhanklikheid (visko-elastiese gedrag), wat benaderd ooreenstem met dié van warmgemengde asfalt. 'n Beter begrip van die reck-by-breek gedrag en die vermoeiings gedrag van koue mengsels in die plaveisel struktuur is dus van groot belang om die korrekte mengselontwerp en analise van die koue mengsels in die plaveiselstruktuur te verseker.

Die hoofdoelwit van hierdie studie is om die vermoeiings gedrag van geselekteerde koue bitumineus-behandelde materiale te karakteriseer deur 'n fundamentele begrip van die vermoeingeienskappe, en die effek van die reck-by-breek eienskappe en die visko-elastiese gedrag op die vertoning van hierdie mengsels te verskaf.

Die studie ondersoek die vermoeiing, reck-by-breek, en styfheidsmodulus (meesterkurwe) eienskappe van die materiaalipes, bestaande nuut-vergruisde kalksteen en herwinde asfalt padoppervlak skerwe wat gemeng is in twee verskillende verhoudings. Kalksteen, óf die padoppervlak skerwe was gebruik in oormaat, d.w.s 75% van die totale massa, waarna verskeie hoeveelhede bitumen in die vorm van óf bitumen emulsie óf geskuimde bitumen daarby gevoeg is. Die invloed en effek van aktiewe vulstof in hierdie mengsels was ook ondersoek. Vir hierdie studies was 1% sement toegevoeg tot die 75% kalksteen mengsels.

Die karakterisering van die vermoeiingseienskappe, asook die reck-by-breek en die buigingstyfheid (meesterkurwe) eienskappe van hierdie mengsels, was ontwikkel deur gebruik te maak van 'n vier-punt balk toetsingsapparaat. Die apparaat verskaf 'n beter begrip van die meganisme van monsters deur 'n buigingstoets in die vorm van 'n alternerende druk of spanning van 'n sekere amplitude uit te voer.

In die ondersoek was daar gevind dat vermoeiings trette van hierdie mengsels in 'n beheerde verplasingsmodus toon dat vermoeiingsleeftyd afhanklik is van die belastingsfrekwensie. Liniêre vermoeiingsfunksies was dus op 'n log-log plot verkry. Die geskuimde bitumen en emulsie mengsels sonder aktiewe vuller (sement) wys geen beduidende verskil in vermoeiingsleeftyd ten opsigte van die

binderstofipe by hoë vlakke van belasting nie. Byvoeging van 'n klein hoeveelheid sement (1%) veroorsaak wel 'n merkbare skuif in die vermoeiingslyn van die skuimmengsels in vergelyking met die emulsiemengsels waarby die vermoeiingsleeftyd verleng word. Wanneer emulsies of skuim bitume gebruik word vir die behandeling van die mengsels met hoër persentasies herwinde asfalt padoppervlak, het 'n verkorting in vermoeiingsleeftyd plaasgevind.

Die verskille in reek-by-breek eienskappe van die geselekteerde mengsels toon dat die toetsprotokol verdere ontwikkeling vereis om 'n betroubare skakel met vermoeiingsgedrag te verskaf. Dit verskaf wel egter 'n oorweging van buigsaamheid in die samestelling van mengsels. Die buigveerkragsmodulus van die geselekteerde mengsels het bewys dat dit temperatuur- en beladingstempo afhanklik is.

ACKNOWLEDGMENT

I, gratefully wish to acknowledge the following persons:

- The Lord God for his grace in giving me strength and endurance enabling me to complete this work.
- Professor Kim Jenkins for sound advice, guidance and interest in my research and also for his selfless time on reviewing and valuable comments in my thesis. Further more for facilitating financial support for the completion of my thesis.
- Lucas-Jan Ebels selfless assistance on setting up test equipment, comments and suggestions with regard to my research. Further more his acceptance to edit and review my thesis.
- Lee-Ann Mullins for assistance on drafting spacemen preparation protocols and testing procedures.
- The laboratory technicians Gavin Williams and Colin Isaacs, and workshop personnel Dion Viljoen and Louis Fredericks for their tireless help on carrying out the spacemen preparations and repairs of the equipment.
- Government of Rwanda for awarding me a scholarship.
- Janine Myburgh and Delysia Baard for kind and patient assistance.
- Dr Carey Malcolm and Oosthuizen of Tygerberg hospital for the successful (L) cataract surgery.
- The family of Jurie and Maggie Goosen, and Strauss Erick for fellowship, support and encouragement.
- My fellow students, Kavii Musango, Pasha Petro, Abela Munyagi, Eben de vos and Dithinde for moral and encouragement on the period of studies.
- My wife Annociata and the children Diana and Derrick for endurance sacrifice and steady love throughout.

LIST OF CONTENTS

1.	INTRODUCTION	1
1.1	BACKGROUND	1
1.2	OBJECTIVE OF THE STUDY	3
1.3	SCOPE OF THE STUDY.....	4
1.4	REFERENCES	4
2.	LITERATURE SURVEY ON MIX DESIGN OF COLD MIXES.....	6
2.1	INTRODUCTION.....	6
2.2	MATERIALS CONSIDERATION.....	7
2.2.1	Aggregates properties	7
2.2.1.1	Grading	7
2.2.1.2	Filler content.....	9
2.2.1.3	Plasticity	10
2.2.2	Bitumen properties	11
2.2.2.1	Foam bitumen.....	11
2.2.2.2	Bitumen Emulsion.....	15
2.2.3	Active filler properties	17
2.2.4	Moisture condition	18
2.2.4.1	Curing conditions	19
2.2.4.2	Temperature condition	21
2.2.5	Engineering properties.....	22
2.2.5.1	Moisture susceptibility.....	22
2.2.5.2	Temperature susceptibility	23
2.2.5.3	Unconfined compressive strength (UCS and ITS)	23
2.2.5.4	Stiffness modulus	24
2.2.5.5	Fatigue resistance	25
2.2.4.6	Resistance to permanent deformation.....	26
2.3	MIX DESIGN CONSIDERATION.....	27
2.3.1	Binder interaction and contents typically used.....	29
2.3.2	Aggregate suitable type and grading.....	30
2.3.3	Moisture consideration.....	32
2.3.3.1	Mixing and Placement.....	33
2.3.3.2	Compaction	34
2.3.3.3	Curing rate.....	35
2.3.3.4	Engineering properties	36

2.4	INFLUENCE OF ACTIVE FILLER ON MIX PROPERTIES AND PERFORMANCE.....	36
2.4.1	Active filler types, used, percentage and its role.....	36
2.4.2	Interaction with bitumen binder, aggregate type and characteristics	36
2.4.3	Moisture condition	37
2.4.4	Engineering properties and mix type classification	39
2.4.5	Performance of mixes and failure, mechanism.....	42
2.5	CONCLUSION.....	44
2.6	REFERENCES	44
3.	LITERATURE SURVEY ON FATIGUE PROPERETIES OF COLD MIXES	49
3.1	INTRODUCTION.....	49
3.2	PRINCIPLES OF FATIGUE TESTING.....	51
3.2.1	Overview of fatigue testing methods	51
3.2.2	Factor affecting fatigue response	55
3.2.2.1	Specimen preparation.....	55
3.2.2.2	Mode of loading	56
3.2.2.3	Mixture variables.....	58
3.2.2.4	Load variables	60
3.2.2.5	Environmental variables.....	62
3.3	FATIGUE CHARACTERIZATION USING DIFFERENT APPROACHES	63
3.3.1	Conventional approach	63
3.3.2	Dissipated energy approach	64
3.3.3	Simplified approach	67
3.4	FATIGUE RELATIONSHIP BETWEEN LAB AND FIELD PERFORMANCE	68
3.4.1	Shift factor.....	68
3.4.2	Transfer function.....	70
3.5	FATIGUE LIFE ANALYSIS.....	71
3.5.1	End of fatigue life.....	71
3.5.2	Damage factor.....	72
3.6	CONCLUSION.....	73
3.7	REFERENCES	75
4.	FATIGUE TESTING METHODOLOGY.....	80
4.1	INTRODUCTION.....	80
4.2	SPECIMEN PREPARATION	81
4.2.1	Materials (blending of mineral aggregates).....	81
4.2.2	Binder content	83
4.2.2.1	Bitumen- emulsion	83

4.2.2.2	Foamed-bitumen.....	83
4.2.3	Active filler.....	85
4.2.4	Moisture content and mixing process.....	86
4.2.5	Compaction.....	87
4.2.5.1	Slab compaction.....	87
4.2.5.2	Compaction and after test moisture content.....	88
4.3.6	Curing.....	89
4.3.7	Cutting of Beams.....	89
4.3.8	Specimen relative density.....	93
4.3.9	Storage of beams.....	93
4.3	IPC 4PB FATIGUE TESTING SYSTEM.....	94
4.3.1	IPC beam fatigue apparatus (BFA).....	94
4.3.2	Loading frame, testing model and pneumatic system.....	95
4.3.3	Microcomputer, control data acquisition system (CDAS) and software.....	97
4.3.4	Principal operation of the fatigue testing system.....	98
4.4	4PB FATIGUE TESTING PROCEDURE.....	100
4.4.1	Flexural stiffness testing of beam specimen.....	100
4.4.2	Testing parameters.....	102
4.4.3	Termination criteria and cycles to failure.....	102
4.5	FLEXURAL STIFFNESS CALCULATIONS.....	103
4.6	CONCLUSION.....	105
4.7	REFERENCES.....	107
5.	CHARACTERIZATION OF FATIGUE PROPERTIES.....	109
5.1	INTRODUCTION.....	109
5.2	FATIGUE TESTING PARAMETER AND RESULTS.....	111
5.3	CHARACTERIZATION OF FATIGUE PROPERTIES OF BITUMEN EMULSION MIXES.....	112
5.4	EFFECTIVE FATIGUE TRANSFER FUNCTION OF BITUMEN EMULSION MIXES....	118
5.5	CHARACTERIZATION OF FATIGUE PROPERTIES OF FOAMED BITUMEN MIXES.....	122
5.6	EFFECTIVE FATIGUE TRENSEFER FUCTION OF FOAMED BITUMEN MIXES.....	127
5.7	COMPARISON OF FATIGUE PERFORMANCE OF EMULSION AND FOAM MIXES..	131
5.8	CONCLUSION.....	139
5.9	REFERENCES.....	141

6.	STRAIN-AT-BREAK PROPERTIES AND TRANSFER FUNCTION.....	144
6.1	INTRODUCTION.....	144
6.1.1	Strain-at-break materials classifications	150
6.2	4PB STRAIN-AT-BREAK TESTING	152
6.2.1	Monotonic beam testing.....	152
6.2.2	Testing parameters and recording of results	153
6.3	STRAIN AT BREAK CALCULATION	154
6.4	STRAIN-AT-BREAK PROPERTIES OF BITUMEN EMULSION MIXES	157
6.5	STRAIN-AT-BREAK PROPERTIES OF FOAMED BITUMEN MIXES.....	159
6.6	COMPARISON ON STRAIN-AT-BREAK PROPERTIES OF EMULSION AND FOAM MIXES	161
6.7	CONCLUSION.....	167
6.8	REFERENCES	169
7.	DEVELOPMENT OF STIFFNESS MASTER CURVES.....	171
7.1	INTRODUCTION.....	171
7.2	TIME-TEMPERATURE SUPERPOSITION PRINCIPLE.....	174
7.2.1	Graphical shifting of experimental results	176
7.2.2	Arrhenius type equation	177
7.2.3	William-Landel-Ferry (WLF) equation.....	178
7.3	CONSTRUCTION OF STIFFNESS MASTER CURVES	178
7.3.1	Determination of the mix stiffness at different temperature and frequencies.....	179
7.3.2	Fitting the experimental results using Arrhenius type equation	180
7.4.	STIFFNESS MASTER CURVE MODELS OF BITUMEN EMULSION MIXES.....	181
7.5	STIFFNESS MASTER CURVE MODELS OF FOAMED BITUMEN MIXES	186
7.6	COMPARISON ON STIFFNESS MASTER CURVES OF EMULSION AND FOAMED MIXES	190
7.4	CONCLUSION.....	194
7.5	REFERENCES	196
8.	CONCLUSIONS AND RECOMMENDATIONS FOR FUTURE WORK	199
8.1	INTRODUCTION.....	199
8.2	SAMPLE PREPARTION AND TESTING PROCEDURE	199
8.3	FATIGUE PROPERTIES.....	201
8.4	STRAIN-AT-BREAK PROPERTIES.....	202
8.5	RECOMMENDATIONS FOR FUTURE WORK.....	203

APPENDICES:

APPENDIX A:	TEST SET-UP FOR THE FOUR POINT BENDING BEAM TESTING .	205
1.	IPC 4PB testing procedure and operating the BFA.....	205
2.	Additional procedure for the strain-at-break test.....	207
APPENDIX B:	VOLUMETRIC PROPERTIES OF EMULSION AND FOAM MIXES	208
1.	Moisture records for emulsion mixes.....	208
2.	Bulk relative density and percentage Mod AASHTO for emulsion mixes.....	209
3.	Moisture records for foam mixes.....	210
4.	Bulk relative density and percentage Mod AASHTO for foam mixes.....	211
APPENDIX C:	GRAPHS OF FATIGUE TEST RESULTS FROM SPREADSHEET DATA FILES CPATURED BY CDAS	213
1.1-1.3	Graphs of fatigue test results for the emulsion mixes.....	213
1.4-1.6	Graphs of fatigue test results for the foam mixes.....	225
APPENDIX D:	DERIVATION OF MATHEMATICAL RELATIONSHIP FOR THE 4PB STRAIN-AT-BREAK RESULTS	238
1.	Calculation of peak deflection on four point bending beam loading.....	238
2.	Calculation of tensile strain for the four point beam loading. (UTM 21 feedback controlled beam fatigue testing calculation)	242
APPENDIX E:	STRAIN-AT-BREAK DATA SPREADSHEET FILES FOR 4PB TEST	244
1.1-1.3	Detail records of deformation controlled test for the emulsion mixes.....	244
1.4-1.6	Detail records of deformation controlled test for the foam mixes.....	247
APPENDIX F:	REPEATABILITY OF FLEXURAL STIFFNESS MASTER CURVES...	251
1.	Superimposition of flexural stiffness master curves of repeat test for the emulsion mixes.....	251
2.	Superimposition of flexural stiffness master curves of repeat test for the foam mixes.....	254

DEFINITION OF TERMS

TERM	DEFINITION
Breaking of bitumen emulsion	The ability of bitumen emulsion as binder to bound aggregates after the evaporation of water content from the mixes though field climate.
Cold mix or cold bituminous mix	A road building materials comprising mineral aggregates that has been treated with bituminous binder and workable at ambient temperature, with the ability to be replaced, leveled and compacted without the addition of heat.
Cycles to failure	The number of loading cycles elapsed when the failure condition has been reached commonly referred to as the fatigue life.
Cradles	The lading frame of the fatigue testing apparatus for flexing beam specimen
Expansion ratio	Ratio of the maximum volume of foamed bitumen produced relative to the original volume of the bitumen, usually measured in vessel of know capacity
Fatigue failure in laboratory	The condition of the specimen when it is deemed to have failed in fatigue when the flexural stiffness has decreased to 50% of its initial value.
Four point loading	Loading applied to beam which is simply supported at two points, such that equal loading is applied at those points which trisect the distance between the support points.
Half-life	The time taken for the foamed bitumen to subside from its maximum volume to half of the maximum volume, recorded in seconds i.e. a measure of foamed bitumen stability.
Haversine sine loading	Cyclical loading such as that the displacement of the beam at its mid length is a range from zero to a maximum in a cyclic manner.
Sine loading	Cyclic loading such that the displacement of the beam at its mid-length is a sine function i.e. minimum to maximum in cyclic manner.

LIST OF SYMBOL AND ABBREVIATIONS

SYMBOL	DESCRIPTION
$\tau_{1/2}$	Half-life of foamed bitumen
4PB	Four point beam that utilizes two simple supports and two line loads equally spaced between the supports. Flexural test are used.
BFA	Beam fatigue apparatus
CDAS	Control and data acquisition system
EBTM's	Emulsion bitumen treated materials
ER _m	Measured expansion ratio recorded at the moment discharge into vessel is complete i.e. at the end of the spray time.
FBTM's	Foamed bitumen treated materials
FI	Foam index
HMA	Hot mix asphalt
HVS	Heavy Vehicle Simulator
IPC	Industrial Processing Control LTD.
LVDT	Linear variable displacement transducer
MDD	Maximum dry density
OFC	Optimum fluid content
OMC	Optimum moisture content
OPC	Ordinarily Portland cement
RAP	Reclaimed or recycled asphalt pavement materials
δ, ω	Peak deflection of centre of beam due to applied load
ϵ	The tensile strain in the extended (stretched) face of the beam at its mid-length which is associated with the peak displacement.

CHAPTER 1

1. INTRODUCTION

1.1 BACKGROUND

Fatigue cracking of bound pavement layers is one of the primary structural distress modes found in flexible pavements. While the fatigue properties of hot-mix asphalt have been extensively studied in the past, the fatigue behaviour of bituminous cold mixes is still relatively unknown (Jenkins, 2000).

Bitumen emulsion and foamed bitumen treated materials exhibit, to a certain degree, aspects of basic characteristics of granular materials, cement treated materials and hot-mix asphalt depending on the mix proportion of aggregate, bitumen and cement. The behaviour of bitumen treated mixes with low bitumen and cement contents, or no cement at all will tend towards the stress dependent behaviour of unbound materials. However, if the amount of bitumen increases (cohesive requirement) the strain-at-break (flexibility) of the mix improves and may even approach the loading rate and temperature dependant behaviour, i.e. visco-elastic behaviour, of HMA (Long et al., 2001). On one hand, if the cement content is increased (strength requirement) while keeping bitumen content low, the behaviour of the bitumen-treated materials mix will approach the stiff, brittle behaviour of cement-treated materials with associated a high resistance to permanent deformation 'rutting' (Theyse, 1993).

Most of the developed models for cold mixes are centred around rutting. However the possibility does exist to improve the modelling of fatigue and flexibility in order to obtain a better understanding of the materials properties and structural behaviour of the cold mixes. There are two primary structural distress modes of pavement layers which require consideration in modelling the materials properties. These are fatigue cracking of the bound layer and excessive deformation (rutting) of both bound and the unbound material layers. An analytical approach to the design of pavements layers requires two aspects of material characteristics; Firstly the analysis of load-deformation or stress-strain characteristics in order to determine strain-at-break (flexibility) properties of the pavement structure. Secondly the analysis of fatigue performance characteristics of the materials that determines the likely mode of pavement failure in fatigue cracking.

Fatigue has been defined as; "the phenomenon of fracture under repeated or fluctuating stress having a maximum value generally less than the tensile strength of the material". Under traffic loading the layers of flexible pavement structures are subjected to flexing and therefore possible fatigue failure in bound materials (Airey, 1995). The criterion for fatigue cracking is generally accepted as the maximum tensile strain on the underside of the bituminous layer

(Pell, 1973). The magnitude of strains is independent of the overall stiffness and the nature of the pavement structure, but analysis confirmed by measurements, has indicated that tensile strains of the order of 40 – 200 microstrain are generally found for a standard wheel load (Cooper, 1992). Under these conditions the possibility of fatigue cracking of the pavement layer exists. Consequently fatigue is one of the criteria to be considered in pavement design for bituminous treated materials.

The researchers has assessed the fatigue properties and strain-at-break properties of cold mixes based on dynamic triaxial fatigue under uniaxial stress conditions either in bending or in direct loading (Pell, 1973) and on four point bending beam tests (Liebenberg, 2003 and IPC, 1998). These tests improve the insight in the failure mechanism of cold mixes by performing flexing test on specimens in the form of an alternating stress or strain of certain amplitude, and determine the number of load applications to crack initiation of specimens, called “failure point or fatigue life”. However due to the cost of equipment and time required for such testing, these tests are still at research level and generally not used as the mix design requirement.

Laboratory four-point beam tests to determine fatigue and strain-at-break properties generally show scattered values. Therefore it is common to test several specimens to increase the level of reliability of the model. Fatigue results at different stress or strain levels are plot versus load cycles to failure on log-log scales to normalize the scatted results.

Traditionally the classification of cold bituminous treated materials adopted in South Africa was based on the CBR and UCS. However since 1990's the ITS (split test) has been used to try to account for flexibility behaviour, but it appears that flexible material properties are not sufficiently captured by ITS tests (Jenkins et al., 2004). The guideline for the design and use of foamed bitumen treated materials TG2 (Asphalt Academy, 2002) classified these mixes according to UCS and ITS values and categorized them as FB1, FB2, FB3, FB4. The bitumen emulsion mixes are categorized as EB1, EB2, EB3, EB4 (Liebenberg, 2003). Although the distinction is made between the FB2/EB2 and FB3/EB3 materials, early indications are that the structural behaviour of these materials are similar. Therefore, the classification of FB2/EB2 does not imply better materials than FB3/EB3 (Verhaeghe and Long, 2004).

Classification of cold mixes based on fatigue and strain-at-break properties is still under investigation. It has however been observed that the strain-at-break test appears to provide a balance in the mix design by introducing a flexibility consideration in addition to the strength requirement. However, the test protocol needs further development or adjustment to provide a reliable link to fatigue performance of cold mixes.

1.2 OBJECTIVE OF THE STUDY

The main objective of this study is to characterize the fatigue performance of selected cold bituminous treated materials by providing a fundamental understanding of the fatigue properties and its link to the strain-at-break properties and visco-elastic behaviour associated with dependency of temperature and rate of loading on the performance of these mixes.

The study investigates the fatigue, strain-at-break, and stiffness modulus (master curve) properties of the materials types, i.e virgin crushed limestone, and reclaimed asphalt pavement (RAP) millings blended in two different proportions (one with 75% limestone and the other with 75% RAP). These blends were treated with either bitumen emulsion or foamed bitumen. A residual bitumen content of 3.6% was used for 75% limestone blends and 2.4% for the 75%RAP blends. The influences and effect of active filler in these mixes were investigated too; 1% cement was added in 75% limestone blends. The same protocol for the specimen preparations and testing procedure of the tests specimen was used for these mixes

The characterization of the fatigue properties of these mixes as well as the strain-at-break and flexural stiffness (master curve) properties was developed using a four-point beam testing apparatus. The apparatus is believed to provide insight into the fatigue failure mechanism of the specimens by performing flexing tests in the form of an alternating stress or strain of certain amplitude. The IPC 4PB apparatus (1998) was employed in this study with the advantage that specimen preparations and testing procedures are similar for investigating fatigue, strain-at-break and stiffness modulus properties.

It is a further objective of this study, through the characterisation of fatigue performance on selected cold bituminous treated materials to obtain an intrinsic comparison of emulsion and foam mixes in three areas, namely;

- Fatigue properties of bitumen emulsion and foamed bitumen mixes in order to quantify the relative fatigue performance of these mixes
- Strain-at-break properties of bitumen emulsion and foamed bitumen in order to understand its link with the fatigue performance and whether it is a normalising parameter of fatigue analysis of these mixes.
- Flexural stiffness modulus properties from developed master curve of bitumen emulsion and foamed bitumen to be used as tool for determining stiffness modulus in the analysis of cold mixes layer in a pavement structure

1.3 SCOPE AND EXTENT OF THE STUDY

The scope and extent of the study can be divided into three main sections. The first section, Chapter 2 and 3, consists of an intensive literature survey into cold mix design considerations and detailed assessment of fatigue characterisation. The second section, Chapter 4, deals with the specimens preparation and testing methodology which includes: laboratory protocols for specimen preparation (i.e. blending of materials, mixing, compaction, curing and cutting of beams, fatigue testing system by IPC (1998)) and fatigue testing procedures used for the IPC 4PB apparatus

The final section, deals with the test results of the selected study materials. This can be further divided into three sections, namely:

- Characterisation of fatigue properties for bitumen emulsion and foamed bitumen mixes
- Characterisation strain-at-break properties of emulsion and foam mixes and,
- Characterization of flexural stiffness master curves properties of emulsion and foam mixes.

The characterisation of fatigue properties of bitumen emulsion and foamed bitumen is dealt with in Chapter 5. The strain-at-break properties of bitumen emulsion and foamed bitumen mixes are dealt with in Chapter 6 and Chapter 7 deals with the flexural stiffness master curves properties of bitumen emulsion and foamed bitumen mixes.

Finally, Chapter 8 provides the conclusion and recommendation of this study.

1.4 REFERENCES

AIREY G.D., 1995. **Fatigue testing of asphalt mixtures using the laboratory third-point loading fatigue testing system**. Masters Dissertation, University of Pretoria, Pretoria, South Africa.

ASPHALT ACADEMY., 2002. **The design and use of foamed bitumen treated materials**. Interim Technical Guideline TG2, Pretoria, South Africa.

IPC (Industrial Process Controls Ltd),1998. **Beam fatigue apparatus**. Reference Manual, Boronia, Australia.

JENKINS K.J, 2000. **Mix design considerations for cold and half-warm bituminous mixes with emphasis on foamed bitumen**. PhD Dissertation, University of Stellenbosch, South Africa.

LIEBENBERG J.J.E., 2003. **A structural design procedure for emulsion treated pavement layers**. Masters Dissertation, University of Pretoria, Pretoria, South Africa.

THEYSE H.L., 1993. **Testing of the fatigue characteristics of bound wearing courses to more accurately predicted pavement behaviour and field performance in design**. Report no. RR 93/565, Dept. of Transport, South Africa Council for Scientific and Industrial Research (CSIR), South Africa.

VERHAEGHE B.M.J.A and LONG F.M, 2004. **Cold in-place recycling with bitumen emulsion and foamed bitumen: South African perspective**. International Seminar on Asphalt Pavement Technology II, Kuala Lumpur, Malaysia.

CHAPTER 2

2. LITERATURE SURVEY ON MIX DESIGN OF COLD MIXES

2.1 INTRODUCTION

For many years lime and cement has been used for the modification and stabilisation of materials for pavement construction. The use of bitumen (cold mixes) in modification and stabilisation of materials in road construction and rehabilitation (recycling) has recently gained popularity due to its advantages of conservation of environment, resources and money. Cold mixes can result in stable pavement at a total expenditure of 40-50% less than the required conventional constructions methods (Annapolis, 1991 and Wirtgen, 2004). However, like conventional hot mix asphalt, cold mixes used for road rehabilitation and construction must be designed properly to ensure reliable performance in terms of shear (cohesion), bearing strength, permanent deformation, fatigue, moisture resistance etc. Furthermore, the mix design should also consider the changes in mixture properties with time and reduction of aged binder consistency (Santucci and Hayashida, 1983).

The lack of standardisation of pavement design procedures in cold mixes and failure of Mobil to exploit their patent in foam bitumen stabilisation contributed to its limited implementation of the technology. Recent research initiatives in upgrading poor quality materials to be used to their full potential in the pavement structure have been focused on two aspects; Mix design process (lab and field) and structural design process. The objective was to provide sound guidelines to the designer with a high level of confidence with respect to understanding the materials properties and structural behaviour in the use of cold mixes. This chapter will be focusing on the literature survey of the mix design aspect. This does not include the structural design aspect.

The effort of preparing cold mix guidelines such as the GEMS Manual (SABITA, 1993) for Granular Emulsion Mixes and the TG2 guideline (Asphalt Academy, 2002) for the design and use of foamed bitumen treated materials in South Africa has improved the use of technology in terms of design and construction as well as reducing the premature failure of cold mix products. However, these manuals did not address all the needs for understanding the material behaviour under laboratory and field conditions. Hence the scope for improving the methodology is apparent.

2.2 MATERIAL CONSIDERATIONS

Material properties of cold mixes are key design parameters that need to be considered with the objective of selecting the mix composition of; mineral aggregates (both RAP and virgin aggregates), bitumen contents, active filler percentages and moisture contents that will achieve the optimum performance of the mix in the laboratory and the field conditions.

2.2.1 Aggregate Properties

A wide range of mineral aggregates ranging from sands, through weathered gravels to better quality crushed stone are suitably treated by bitumen emulsion and foamed bitumen. Aggregate of sound and marginal quality from both virgin and recycled sources have been successfully treated for use in road construction and rehabilitation. However, it is important to establish the boundaries of aggregate acceptability for the different bitumen emulsion types as well as identifying the optimal aggregate composition for foamed bitumen mixes. Emulsion and foamed bitumen can be used with cold and wet aggregate. However, foamed bitumen produces better mixes with half- warm aggregate as shown by Jenkins (2000).

2.2.1.1 Grading

Due to nature of binder dispersion in the mixes the requirements of aggregate grading for bitumen emulsion differs from that for foamed bitumen mixes. From their experiences Mobil Oil established a general grading requirement for foamed bitumen mixes. Figure 2.1 (Akeroyd and Hicks, 1988) defines envelopes for different zones of suitability of aggregates compositions with ideal materials being in grading zone A.

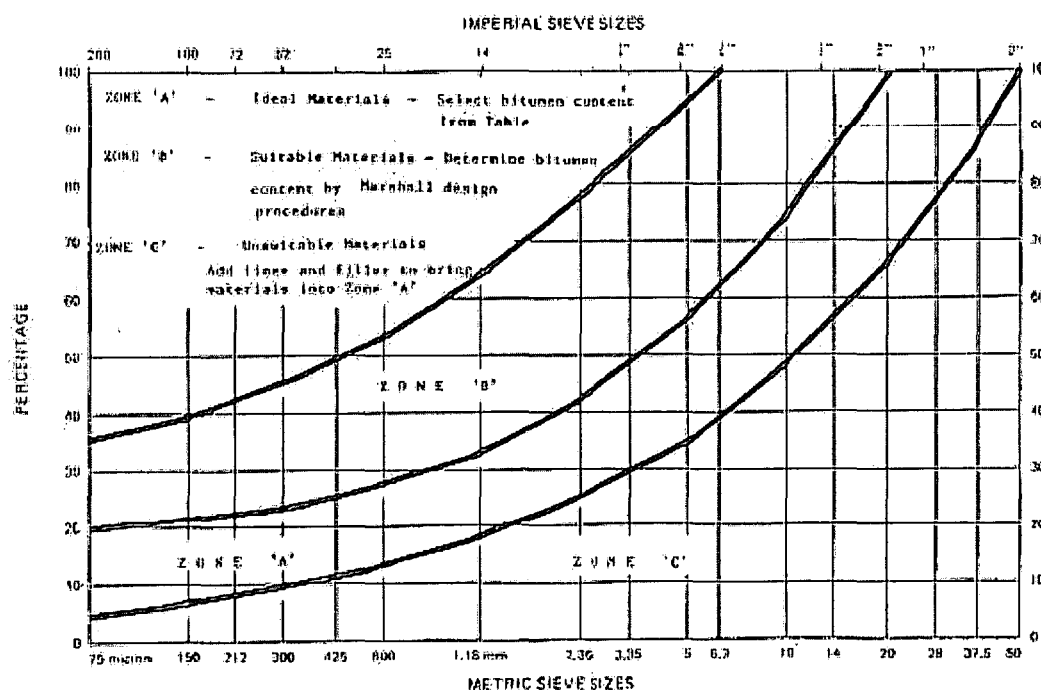


Figure 2.1: Aggregate grading zones for foamed asphalt (Akeroyd & Hicks, 1988)

The envelopes provided in Figure 2.1 are however broad and can be refined by targeting a grading that provides the lowest voids in the mineral aggregate (VMA). Research by Jenkins (2002) has shown that a lower void in the mineral aggregates (VMA) resulted in foamed bitumen mixes with the most desirable mix properties.

Grading has also been utilized as a property to not only classify the suitability of materials, but also to provide an indication of the optimum binder content needed in the cold mixes, see Table 2.1. Bowering and Martin (1976) and later Ruckel et al., (1982) investigated different types of soils and showed that, e.g. crushed stone, rock, gravel sand, silty sand, sandy gravel, slag reclaimed aggregates ore tailing and others are suitable for use in foamed bitumen mixes. Acott (1979) investigated sand, Lee (1981) investigated recycled materials and Dijkink (1992) investigate slag residue and ashes from zinc production etc. No reference has however specified a type of rock that is not suitable for foamed bitumen treatment. This indicates a low dependency of the foaming process on the particle charges of basic or acidic rocks, unlike the bitumen emulsion process, where the rock type has greater influence on the selection and the performance of bitumen emulsion as a binder.

Table 2.1: Ranking of suitability of materials for foamed bitumen treatment (after n Ruckel et al 1982)

Soil type	Suitability for Foamed Mix	Optimum Bitumen Content (% m/m)	Comments
Well graded gravel, little or no fines	Good	2.0 – 2.5	Permeable (improve with crushed fraction)
Well graded gravel + some clayey silt	Good	2.0 – 4.0	Permeable (improve with crushed fraction)
Well graded gravel + sandy silt	Good	2.0 – 4.0	Permeable (improved with crushed fraction)
Poorly graded gravel + sandy clay	Good	2.5 – 3.0	Low permeable (improved with crushed fraction)
Clayey gravel	Poor	4.0 – 6.0	Improve with filler
Well graded sand	Fair	4.0 – 5.0	Need lime
Well graded silty sand	Good	2.5 – 4.0	
Poorly graded silty sand	Poor	3.0 – 4.5	Use lower pen grade bitumen, add filler
Poorly graded sand	Fair	2.5 – 5.0	Need filler
Silty sand	Good	2.5 – 4.5	
Slightly clayey, silty sand	Good	4.0	
Clayey sand	Poor	4.0 – 6.0	Need small % lime
	Good	3.0 – 4.0	After lime modification

Aggregate types that experience moisture susceptible in the form of stripping e.g. 'glassy' granite in hot mixes, can encounter the same problems with foamed bitumen as experienced by Jenkins (2000). This type of aggregate also gives varying results and possible stripping problems with anionic emulsions. The GEMS Manual (SABITA, 1993) shows that non-plastic materials such as granite, quartzite gravels, dolomite/chert gravels, sand stone gravels and crushed stone of various rock, respond well to low emulsion contents. Care should however be taken when selecting the bitumen emulsion type, because aggregate properties have a great influence on the breaking of the emulsions in the mixes. Figure 2.2 (Akzo Nobel, 1997) shows that aggregate with higher silica contents are the most acidic with a strong tendency to adopt a negative surface charged in water (anionic emulsion).

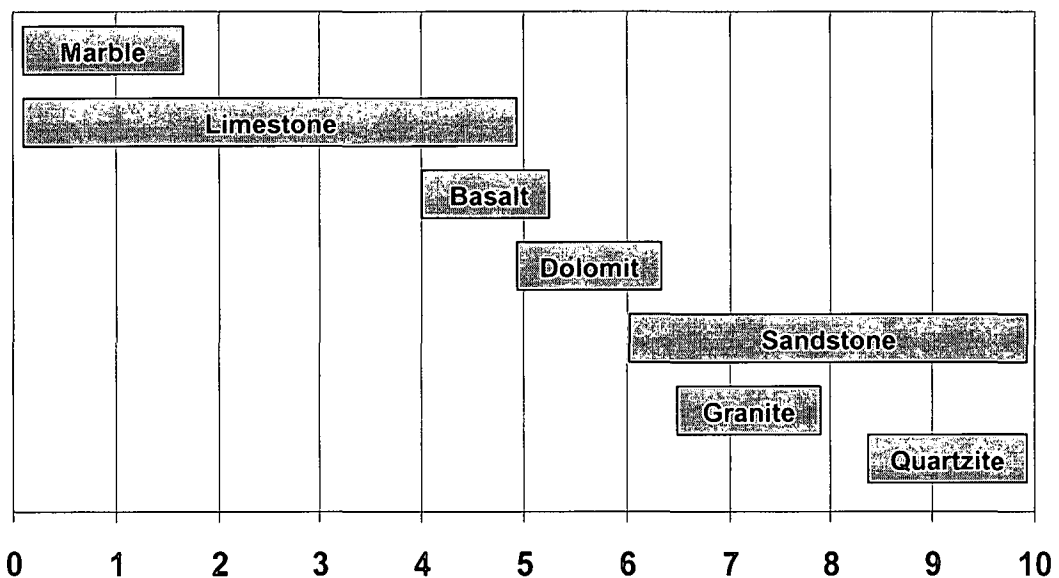


Figure 2.2: Content of Silica (%) on type of aggregates, (Akzo Noble, 1997)

2.2.1.2 Filler Content

The fines content of the aggregates (smaller than 0.075 mm) in the grading is an important consideration in the cold mixes process. TG2 (Asphalt Academy, 2000) shows that the grading for foamed mixes requires a minimum filler content of 5 percentage order to produce good quality mixes, Research of Ruckel et al., (1982) has established a guide for recommended design bitumen content at different aggregate gradings based on the filler content as shown in Table 2.2.

Table 2.2: Guidelines for design bitumen content as a function of filler content targeted for foamed bitumen mix (after Ruckel et al., 1982)

Passing 4.75mm sieve (%)	Passing 0.075mm sieve (%)	Foamed bitumen content (% m/m dry aggregates)
< 50	3.0 – 5.0	3.0
	5.0 – 7.5	3.5
	7.5 – 10.0	4.0
	>10.0	4.5
>50	3.0 – 5.0	3.5
	5.0 – 7.5	4.0
	7.5 – 10.0	4.5
	>10.0	5.0

The ability of foamed bitumen to mix selectively with and coat the fines (creating a mastic or mix of bitumen and filler) results into higher viscosity (than raw bitumen and mixes). The fines act as mortar between the coarse aggregates and hence increase the strength of the mix. The relationship between the fines content and bitumen content is however critical because excess bitumen in the mortar will tend to act as lubricant. This will result in loss of strength and stability. Sakr and Manke (1985) showed that foamed bitumen mixes with higher percentage of fines had higher stability. Bissanda (1987) showed a similar trend for tensile strength. Semmelink (1991) also found that the fines content plays a crucial role in determining the strength stability and workability of foam-stabilize sand.

In a limited study Sakr and Manke (1985) showed that the stability of foamed bitumen mixes is affected to a greater extent by aggregate interlock than by the viscosity of the binder. This behaviour differs from that of hot mix asphalts. Then it implies that foamed bitumen mixes are not as temperature susceptible as HMA. Supporting findings show that the viscosity (grade) of the bitumen used is not very critical for foamed bitumen mixes. However, Wirtgen (2004) commented that hard bitumen (low penetration grade) should not be used in cold mixes due to increased possibility of blockage of the nozzles during spraying. Sakr and Manke (1985) further found that the angularity of fine aggregates is an excellent indication of suitability of foam stabilization and a minimum particle index of 10 was suggested in order to achieve good stabilities.

2.2.1.3 Plasticity

Research has indicated that certain types of soil may require lime or cement treatments and grading adjustments to enable them to perform satisfactorily in cold mixes. Bowering and Martin (1976) confirmed that high plasticity clay gravel responds poorly to the foamed bitumen unless modified prior to the addition of the binder. GEMS Manual (SABITA, 1993), suggests that if the PI of a material exceed 7 percent, the material should be treated with lime or cement

to reduce the PI to less than 7 before addition of emulsion or mixing water. Lee (1981) stated that a limited percentage of plastic fines is acceptable in foam mixes, but that active filler (lime) modification may be advisable and economical if the PI is greater than 8 percent. TG2 (Asphalt Academy, 2002) suggested that natural and weathered gravels be treated with foamed bitumen should have a PI less than 10 percent. Lancaster et al., (1994) suggested that maximum PI limit should be 12 percent before lime modification is necessary.

2.2.2 Bitumen Properties

The high dependency of bitumen properties on time and temperature makes it important to understand the rheological (deformation and flow) characteristics of penetration grade bitumens that are used in the production of foamed bitumen and bitumen emulsion mixes.

Jenkins (2000) indicated that bitumen properties identified to contribute to the foam characteristics include;

- Viscosity versus temperature relationships
- Ratio of Maltene/Asphaltenes
- Composition of the bitumen (Saturates-parafine en naftenes, Aromatics, Resins, and Asphaltenes)

The above properties are determined by both the origin of the bitumen, refining and the manufacturing process. Additives such as silicone oil or anti-foamants used in the refining process are very difficult to monitor or to identify compositionally but result in differences of the foam characteristics.

2.2.2.1 Foam Bitumen

Foamed bitumen, also referred to as expanded bitumen, is a hot bituminous binder that has been temporarily converted from a liquid to a foam state by the addition of small percentage of water (2 percent recommended). The foamed bitumen is characterized in terms of Expansion Ratio (ER) and Half-life ($\tau_{1/2}$). The ER of the foam is defined as the ratio between the maximum volume achieved in the foamed state and the original volume of the binder once the foam has dissipated. The Half life is the time, in seconds, between the moment the foam achieves maximum volume and the time at which it has dissipated to half of the maximum volume. Jenkins (2000) however indicates that Foam Index (FI) provides better characteristics of foamed bitumen than two dependent variable of (ER) and ($\tau_{1/2}$). Figure 2.3 shows foamed bitumen production when small amount of molecuised water, as fine mist (typically 2% by mass) is injected into hot (160°C -180°C) bitumen in an expansion chamber.

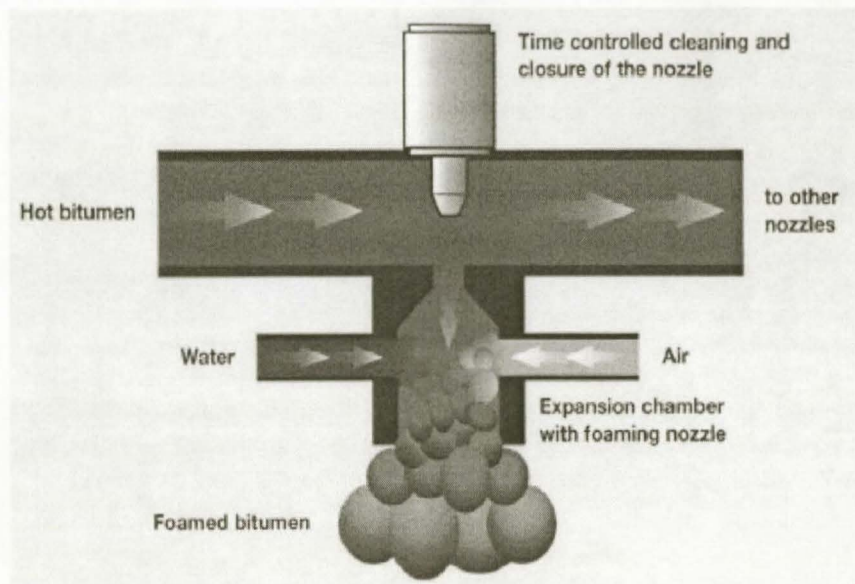


Figure 2.3 Foamed bitumen production, (Wirtgen,2004)

The foaming characteristics of bitumen play an important role during the mixing process of foamed bitumen production. It can be expected that maximized expansion ratios and half life will promote binder dispersion within the mix. Castedo, Franco and Wood (1983) found that any bitumen, irrespective of grading or origin could be foamed with an appropriate combination of nozzle type, water, air and bitumen injection pressure. However experiences from Wirtgen (2004) indicated that the bitumen manufactured from Venezuela has far better foaming properties than many other sources.

Abel (1978) found that bitumen with a lower viscosity foamed more readily and had higher expansion ratios and half life than bitumen with higher viscosities. However, the use of bitumen with high viscosity resulted in superior aggregate coating. Nevertheless, the use of bitumen with high viscosity bitumen is not recommended due to blockage of nozzles during spraying Wirtgen (2004).

Bennen et al., (1983) found that the expansion ratio and half-life of the foam produced from any particular bitumen were affected by the quantity of water used and the temperatures at which the foam was produced. Higher foaming temperature and increased quantities of water both resulted in increased expansion ratios, but resulted in decreased half life. In the laboratory the size of the container was found to affect the foam parameters (Ruckel et al., 1983 and CSIR, 1998). However, critical properties such as container temperature, time of foam discharge, etc. were ignored by the Ruckel et al., Research by Jenkins (2000), found that these factors have significant bearing on the foam properties. However in addition to penetration and viscosity of the bitumen Jenkins (2000), indicates that penetration index (PI) can also influence the foaming characteristics.

In his research Jenkins (2000) also developed the concept of Foam Index (FI) as a measure of both expansion ratio and half life, and recommended that the greater the FI the greater the foaming properties and the better stabilization of the mix. In other words, the more the superior the quality of foam, the more homogenously the bitumen will be dispersed in the mixture. Figure 2.4 shows the concept of FI for characterizing the foamability of bitumen for a given foamant water application rate. He further looked at the effect the temperature of the aggregates and found that as temperature of the aggregates increase foamed bitumen with a lower FI may be used to achieve effective foamed bitumen stabilization.

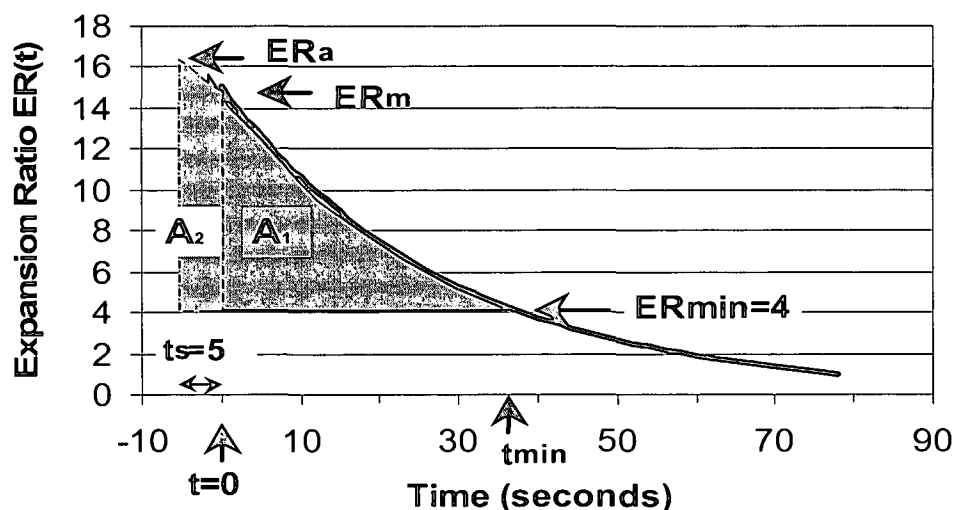


Figure 2.4: The Foam Index (FI) for characterizing the 'foamability' of bitumen for a given water application rate ($FI=A_1 + A_2$), Jenkins (2000).

Ruckel et al., (1983) and Acott and Myburgh (1983) recommend limits of 8:1 to 15:1 for the expansion ratio and at least 20 seconds for the half life for tests in a 1 gallon container. The CSIR (1998) recommends an expansion ratio of at least 10:1 and half life of at least 20 seconds in the same test. TG2 (Asphalt Academy, 2002) characterizes foamed bitumen in terms of foam index (FI) and recommends a minimum FI of 500 and half life of 20 seconds for aggregate temperatures ranging between 10°C to 15°C. Figure 2.5 shows asymptotic curves of Foam Indices (FI) for ranking foamed bitumen suitability in the case of combined (ER) and ($\tau_{1/2}$) characteristics.

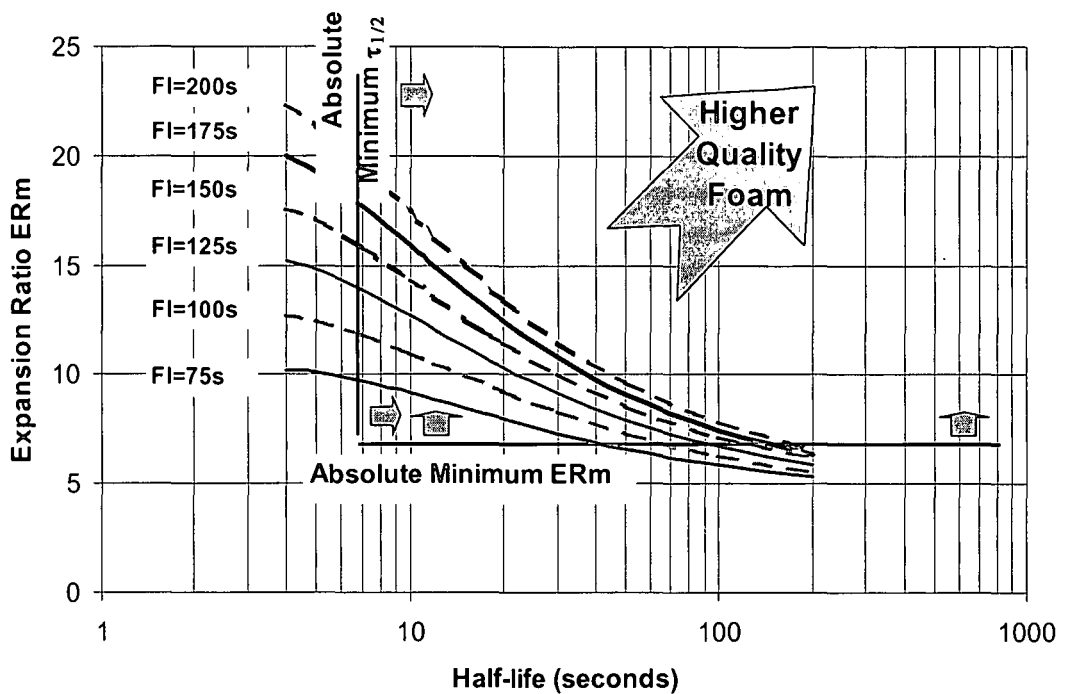


Figure 2.5: Ranking of foamed bitumen suitability on the basis of foaming Characteristics in TG2 (Asphalts Academy, 2002)

Foamed bitumen with at least a moderate classification (FI greater than 125) is recommended to obtain reasonable benefit from the binder used. Table 2.3 provides a ranking of the suitability of foamed bitumen according to the FI and aggregate temperature.

Table 2.3: Classification of the suitability of foamed bitumen mixes in TG2, (Asphalt Academy, 2002)

Foam Index , FI (seconds)	Aggregates at 15°C	Aggregates at 25°C
< 75	Unsuitable	Unsuitable
75 – 100	Very Poor	Poor
100 – 125	Poor	Moderate
125 -175	Moderate	Good
175 – 200	Good	Very Good
> 200	Very Good	Excellent

By using certain surface active additives or “foamants” it is possible to produce highly expanded and stable foamed bitumen with expansion ratio’s greater than 15 and half life exceeding 60 seconds (Maccarrone et al., 1994). Jenkins (2000) indicates that additives can be added not only to the bitumen but also to the foamant water, e.g. 60% Super-Plastazier to reduce the surface tension of water which increases the ER and $\tau_{1/2}$. However, such additions are useful in case the bitumen has been treated with silicon defoamants or anti-foamants, which on the other hand do not produce the desired foaming characteristics. There can be

however significant financial implications by including an additive in foaming process. Bowering and Martin (1976), showed that the cohesion stability and compactive strength of mixes were significantly greater when high expansion (15:1) foamed bitumen was used. Maccarrone et al., (1994) suggested that high expansion foamed bitumen resulted in improved mix properties.

2.2.2.2 Bitumen emulsion

Bitumen emulsion is normally of oil-in-water (O/W) type, although inverted emulsions (water-in-oil (W/O) type based on cutback) can be produced for the specific application see Figure 2.6. Bitumen emulsion is made by the mechanical dispersing of bitumen of a selected penetration grade in the liquid form (at about 60°C -75°C with a viscosity of less than 2 Poise) in water that has been treated with an emulsifying agent. The dispersion of the bitumen is accomplished by shearing the bitumen in an emulsifying mill (of 1000rpm to 6000rpm at 0.25mm to 0.50mm gap clearance) (Shell Bitumen, 1991 and Wirtgen, 2004). Emulsions with 40% - 80% bitumen are brown liquids with consistencies ranging from that of milk to cream. The diameter of the emulsion droplets normally range from 0.001mm to 0.01mm (Wirtgen, 2004) and 0.001mm to 0.05mm (Colas, 2003).

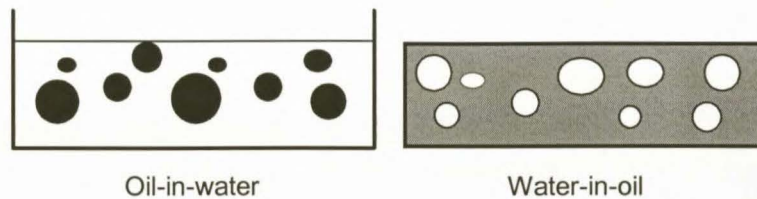


Figure 2.6: Shows two distinct type of emulsions, (Akzo Noble, 1997)

Emulsification is the process by which the two phases (emulsifying agent and water mixture and dispersed bitumen) is intimately mixed under controlled conditions of temperature, dwell time, flows and gap clearance to form bitumen emulsions of the required composition. The emulsifiers used for production of bitumen emulsion are anionic or cationic agents that are absorbed in minute dispersed bitumen droplets and stabilized by means of electric surface charges. These surface charges of the droplets have the same polarity and hence the droplets repel each other and make it difficult for bitumen droplets to coalesce.

Anionic emulsifiers are characterized by the negative surface charges, imparted to the bitumen droplets and cationic emulsifiers are characterized by the positive charges imparted to the bitumen droplets. These are referred to as anionic and cationic bitumen emulsions respectively. Choice of emulsifier is essential in order to get an emulsion with the desired properties. Anionic emulsifiers are sodium or potassium salts of fatty acid that have an alkaline reaction. Cationic emulsifiers are mostly hydrochloride solutions of substituted ammonia compounds or amines with acidic reactions. SABS 309 (1976) and Shell Bitumen (1991),

described that the basic properties of bitumen emulsions are stability (storage and breaking), adhesive (binding) and viscosity (dispersion).

The stability of bitumen emulsions is affected by; inadequacy storage, shearing, boiling or freezing that can result in flocculation and coalescence. Settlement of bitumen droplets occur due to gravitational action on continuous bitumen droplets that have a higher density than water. The velocity of the downwards movement of free bitumen droplets is estimated by Stocke's Law. Shell Bitumen (1991) shows mathematical relationship between the settlement velocity and the gravitational force, droplet radius and viscosity of the bitumen droplets.

$$v = \frac{2/9 \text{ gr}^2 (d_1 - d_2)}{\eta} \quad (2.1)$$

Where,

v	=	settlement velocity
G	=	gravitational force
r	=	particle radius
d_1	=	specific gravity of the bitumen
d_2	=	specific gravity of the aqueous phase
η	=	viscosity of the aqueous phase.

Shell Bitumen (1991) commented that generally, bitumen emulsion droplets are to tightly packed and that Stocke's law might over estimate the particle's velocity. The stability and viscosity of bitumen emulsion can be controlled by proper storage conditions (high temperature), using high penetration grade base bitumen, choice of emulsifier type and percentage, increasing bitumen content and increasing emulsion viscosity. Akzo Nobel (1997) shows that if the viscosity is too low the emulsion will not stay thick (poor adhesion) and if it is too high it will stay in coalesce on the surface.

The breaking behaviour of bitumen emulsions has a great influence on the binding properties of the mix. A good quality emulsion should be stable during storage, transportation and only break during application. Most cationic emulsions show such behaviour because emulsions only and break chemically when brought into contact with most aggregates. In most cases aggregates are negatively charged and therefore the positively charged emulsifier is drawn electrostatically to the aggregates causing the emulsion to break. In addition the emulsifier works as an adhesion agent to the aggregate.

However, the breaking and the quality of the bonds depends on the type of bitumen grade and content, pH of emulsifier solution, particle size distribution of emulsion and aggregates types. Other factors that influence the breaking are temperature and humidity. However an Anionic emulsion does not usually break chemically but the evaporation of water causes the emulsion to break. This is a much slower process that characterizes slow setting emulsions (Colas 2004).

2.2.3 Active filler properties

A considerable amount of research has been done on the influence of active filler on the properties and behaviour of cold mix treated materials. Lime and cement are the commonly used active fillers amongst others in the modification of aggregate properties in order to achieve the required engineering properties.

Cold mixes treated with addition of less than 1.5% (by mass) of cement do not suffer shrinkage cracking. This phenomenon is associated with high percentage of cement treatment. The addition of active filler may allow immediate trafficking due to the initial binding (strength) of the surface particles which prevent raveling under action of traffic. Certain marginal materials treated with bituminous stabilizing agent have poor retained strength properties (i.e. they lose strength when immersed in water). This can be addressed by addition of active filler such as hydrated lime or cement. Colas (2004) shows that small amount of active filler (0.5-1.5% by mass) can significantly increase retained strength without affecting the fatigue properties of the mix. Active filler also acts as a dispersing catalyst with foamed bitumen and promotes breaking when used with bitumen emulsion.

The lime released during the hydration of cement reacts with plastic soil and this result in a fairly rapid reduction in plasticity and increase in strength. Cement is particularly effective in stabilizing medium to low plasticity materials ($PI < 7$). Although it is also possible to treat almost any soil with cement to improve its properties, in practice it is difficult to treat fine, clayey materials with cement owing to high fine (cohesive soil) and become difficult in pulverising the soil for mixing the cement. In such cases lime is preferred as stabilizing agent. However fine single sized windblown or dune soils can be stabilized with cement, although high cement content is usually necessary to obtain the required engineering properties.

Lime is very effective when there is sufficient amount of clay in the soil to react with lime. Therefore, lime is suitable to modify materials with high PI, greater than 7, to reduce the PI and increase the strength. If PI is lower than 7, cement should be used (SABITA, 1993). However this might be a rough guideline as PI is a rough indication of the amount of clay available for reaction with lime. There are materials with PI below 7 that react strongly with lime, e.g. natural gravel, such as certain sandstones, calcretes, decomposed granites, and decomposed dolcrites. The strength of these materials may increase considerable when treated with lime. Materials like calcretes, which containing amorphous silica, react strongly and rapidly with lime and give higher strength than when treated with cement.

Cold mixes have been produced with the application of certain percentage ($< 1.5\%$) of cement or lime in order to improve the engineering properties and applicability of foamed bitumen and bitumen emulsion in the production of quality mixes. The cement applied in bitumen emulsion has four functions viz; it causes the emulsion to break quickly, it increases workability (gel like

behaviour) of the mixes, it absorbs some of the resulting excess free moisture in the soil by hydration and it gives added strength to the processed and compacted mix, when it has hardened. The materials finally produce intermediate properties between soil-cement and true soil-bitumen that possess some rigidity and is also fairly watertight.

2.2.3 Moisture content

The moisture content during mixing and compaction is considered by many researchers to be a very important mix design criterion for cold mixes. Water in bitumen emulsion acts as a densification agent due to evaporation, which sets up a vacuum force, brings individual particles together and densifies the mix (SABITA, 1993). Moisture is required to soften and breakdown agglomerations in the aggregates. This aid is bitumen dispersion during mixing, compaction and promotes shelf life (Csanyi, 1960). Ruckel et al., (1982) recommend that the moisture-density relationship should be considered in the formulation of trial mixes.

Insufficient water reduces the workability of the mix and results in inadequate dispersion of the binder. Too much water lengthens the curing time, reduces the strength and density of the compacted mix and may reduce the coating of the aggregates. Brennel et al., (1983) show that the optimum moisture content (OMC) varies, depending on the mix property that is being optimized (strength, density, water absorption, swelling). However, since moisture is critical for mixing and compaction, these operations should be considered when optimizing the moisture content.

Investigations by Mobil Oil on foamed bitumen mixes suggest that the optimum moisture content for mixing lies at the "fluff point" of the aggregate, i.e. the moisture content at which the aggregates have a maximum loose bulk volume (70 % - 80 % mod AASHTO OMC). However, the fluff point may be too low to ensure adequate mixing (foam dispersion) and compaction, especially for finer materials. Bowering, (1970) observed that where inadequate foam dispersion occurred as a result of insufficient mixing moisture, the compacted densities were low and no benefit was gained from additional moisture after the foamed bitumen treatment. Lee, (1981) found that the optimum mixing moisture content occurs in the range of 65 - 85 percent of the OMC at modified AASHTO compaction for the varying gradations of aggregates, in particular with smaller fractions less than 0.075 mm. This optimum range of moisture content for mixing was confirmed by Bissada (1987) and Jenkins (2000). TG2 (Asphalt Academy, 2002) recommends 70% of the OMC to be used for the foamed bitumen treated materials. Wirtgen (2004) indicated that fluff point can range from 65% to 90% of OMC.

For bitumen emulsion mixes the moisture contents consist of; water in aggregate, water from emulsion and any water added to adjust the workability. Colas (2004) showed that gyratory shear compaction makes it possible for some excess water to drain freely, however too much

water impairs the consistency of the mix by turning in soup (slurry). In addition, it hinders the larger amount of water loss by evaporation; through temperature, relative humidity and force of gravity. Hence it interferes with the mechanical properties of mix through change of the state of the bitumen.

The concept of optimum fluid content (SABITA, 1993) as used in granular emulsion mixes may also be relevant to foamed bitumen mixes (TG2, Asphalt Academy, 2002). This concept considers the lubricating action of the binder in addition to that of the moisture. Thus the actual moisture content of the mix for optimum compaction is reduced in proportion to the amount of binder incorporated. Castedo, Franco and Wood (1982) also agree that the best compactive moisture condition for foam mixes occurs when the total fluid content (%moisture + %bitumen) is approximately equal to the OMC.

Sakr and Manke (1985) developed a relationship (Equation 2.2) to calculate the moisture content for maximum density of foamed bitumen mixes that use sand as aggregate. This relation takes into account the modified AASHTO OMC, percentage of fines (PF) of the aggregate and the bitumen content (BC). As suggested by the equation 2.2, the higher the bitumen content, the lower the compaction moisture content. The compaction maximum moisture content (MMC) equation may not apply to all materials, but the concept is relevant.

$$\text{MMC} = 8,92 + 1,48\text{OMC} + 0,4\text{PF} - 0,39\text{BC} \quad (2.2)$$

The optimum moisture content for mixing is approximately 10 to 20 percent higher than the compaction moisture content, as predicted by Equation 2.2. In order to prevent the time consuming process of drying the mix after mixing (to achieve the MMC), Sakr and Manke (1985) suggested that the MMC should be used for both mixing and compaction. No significant differences in mix properties were observed when this procedure was used.

In recent years the gyratory compaction method has gained popularity for the preparation of samples in the laboratory as it is seen as representing the field compaction. Because the gyratory compaction effort is usually higher than Modified AASHTO effort, the OMC obtained is lower than Modified AASHTO OMC. Hence, when gyratory compaction is used for the preparation of foamed bitumen, the OMC (gyratory) is advocated for mixing and compaction (Maccarrone et al., 1995) (as opposed to the moisture content on the dry side of OMC as used in Mod AASHTO compaction).

2.2.4.1 Curing Conditions

Studies have shown that cold mixes do not develop their full strength after compaction until a large percentage of the mixing moisture is lost. Curing is the process whereby cold mixes

gradually gain strength over time. This is accompanied by a reduction in the moisture content through evaporation, particles charges repulsion or pore pressure induced flow paths.

Ruckel et al., (1982) concluded that the moisture content during the curing period of foamed bitumen mixes has a major effect on the ultimate strength of the mix. However, Lee (1980) provided experimental evidence that suggests that moisture loss is not a prerequisite for strength gain in foamed bitumen mixes. Louw (1996) indicated that the ultimate stability after curing and related properties of bitumen emulsion mixes would take several months, or even up to two years. Whichever the case, a laboratory mix design procedure needs to simulate the field curing process in order to correlate the properties of laboratory- prepared mixes with those of field mixes.

Since the curing of foamed bitumen and bitumen emulsion mixes in the field occurs over several months, it is impractical to reproduce actual field curing conditions in the laboratory. An accelerated laboratory curing procedure is thus required, in which the strength gain characteristics simulates field behaviour, that is the early, intermediate and ultimate strengths attained. This characterization is especially important when structural capacity analysis, based on laboratory-measured strength values, is required. Most of the previous foamed bitumen investigations have adopted the laboratory curing procedure proposed by Bowering (1970), i.e. 3 days oven curing at a temperature of 60° C. This procedure resulted in the moisture content stabilizing at about 0 to 4 percent, which represents the driest state achievable in the field.

The strength characteristics of specimens cured in this manner are representative of the in-service state approximately a year after construction (Maccarrone, 1995). Concerns have been expressed over the binder ageing that may occur at a curing temperature of 60° C. Also, since this temperature is above that of the softening point of common penetration grade bitumen used for road works, changes in bitumen dispersion within the mix are possible during curing. An alternative approach suggested by Lewis (1998) would be to oven dry the foamed bitumen mix to a constant mass, at a lower temperature (40°C). Jenkins (2000) summarized the different curing protocols for foamed bitumen mixes as proposed by different researchers. This is shown in Table 2.3. The targeted equivalent field curing is also shown in this table.

Table 2.3: Different curing protocols proposed for cold mixes, (Jenkins 2000)

Curing method	Equivalent field cure	Reference
3 days @ 60°C + 3 days @ 24°C	Unspecified	Bowering (1970)
3 days @ 60°C	Construction period + early field life	Bowering and Martin (1976)
3 days @ 60°C	Between 23 and 200 days from Vane shear Test	Acott (1980)
1 day in mould	Short term	Ruckel et al (1982)
1 day in mould + 1 day @ 40°C	Between 7 and 14 days (intermediate)	Ruckel et al (1982)
1 day in mould + 1 day @ 40°C	30 days (long term)	Ruckel et al (1982)
1 day @ 38°C	7 days	Asphalt Institute
10 days in air + 50 hours @ 60°C	Unspecified	Van Wijk and Wood (1983)
3 days @ ambient temp. + 4 days vacuum dessicat.	Unspecified	Little et al (1983)
3 days @ 23°C	Unspecified	Robert et al (1984)
3 days @ 60°C	Unspecified	Lancaster et al (1994)
1 day unsealed @ 40°C +2 days sealed @ 40°C	Six months	TG 2 (2002)
3 days @ 60°C	1 year	Maccarrone et al (1994)
1 day in a mould @ambient temp. + 2 days sealed at 40°C	Between 7 and 14 days (intermediate condition)	Malubila, (2005)
2 days sealed @ambient temp. + 2 days @ 40°C	2 years (long term)	Malubila, (2005)

2.2.4.2 Temperature Conditions

The optimum mixing temperature of aggregates for foamed bitumen mixes lies in the range of 13° C to 23° C, depending on the type of aggregate. Temperatures below this range result in poor quality mixes (Bowering and Martin, 1976). This is unlike bitumen emulsion mixes, where mixing and compaction is done at ambient temperature and the temperature of aggregates does not influence the mixture properties. Foamed bitumen mixes may also be prepared with heated aggregates. This will increase the binder dispersion within the mix and aid in the coating of the larger aggregates. This was confirmed by Jenkins (2000) in his research on this property for the half-warm mixes.

Although cold mixes are generally placed and compacted at ambient temperature, research has indicated that possible benefit occurs by heating cold foamed bitumen mixes prior to compaction. Bowering and Martin (1976) heated the surface of the foamed bitumen mixes to 110°C before curing and compaction and compared this with mixes compacted at 23°C. They found that heating the surface resulted in improved densities and significant increase in cohesion value. Robert et al., (1984) achieved substantially higher densities under similar condition with recycled aggregates. TG2 (Asphalt Academy, 2002) recommends heating the aggregates at a range of 10°C to 15°C before mixing. However, Little et al., (1983) reported that a significant decline in the resilient modulus (M_r) has been noted as the temperature of the compacted specimen increases.

2.2.5 Engineering Properties

The results of previous studies all confirm that shear strength parameters and tensile strength properties of cold mixes plays an important role in the long term performance of treated materials. This is due to reduction of moisture susceptibility, increase of fatigue resistance and increase of the cohesion of the untreated aggregate to acceptable levels. In the 1980's, the most common method used in the selection of the design binder content was to optimize the Marshall stability and minimize the loss in stability under soaked moisture conditions. Later the testing procedure shifted away to more fundamental test such as resilient modulus, dynamic creep, tensile strength, flexural bending and strain-at-break and recently introduction of gyratory compactor.

However the limiting values of these tests are uncertain, as the mechanisms of failure are yet not clearly defined, Jenkins (2000). The mixing moisture content and binder content can be optimized using ITS and UCS test results due to its acceptable costs. However, the UCS test is a better option for the moisture content and the combination of UCS and ITS test are used for optimum binder content determination (TG2, Asphalt Academy, 2002).

2.2.5.1 Moisture Susceptibility

The strength characteristics of cold mixes are more moisture-dependent than those of hot mix asphalt. This is because of the relatively low binder contents, moist aggregate at the time of mixing and high air void contents. Lee (1981) found that the immersion Marshall Stability values after 24 hours of soaking at 60°C for most foamed bitumen mixes were low. Little et al., (1983) used vacuum saturation test to determine moisture susceptibility by means of the resilient modulus testing and found that specimens of siliceous gravels and sands foamed stabilized were very moisture susceptible. Van Wijk and Wood (1983) found similar behaviour of RAP and virgin aggregate mixes by means of Marshall Stability testing.

Robert et al., (1984) used a wet curing cycle of 3 days at 24°C and found that a strength decline of 50% compared to that achieved by the dry cured specimen. However Castedo, Franco et al., (1984) found that addition of active filler such as lime or cement reduces the moisture susceptibility of the mixes. Lewis (1998) found that higher bitumen contents also reduce moisture susceptibility because of the higher densities that are achieved. This leads to lower permeability (lower void contents), and increased coating of the moisture-sensitive fines with binder. SABITA (1993) a capillary test indicated that ferricrete materials stabilized with low bitumen emulsion content are more moisture susceptible than those with high bitumen emulsion content. (TG2, Asphalt Academy, 2002) are recommends the following values in Table 2.4 for the retained tensile strength (TSR) for the foamed bitumen mixes.

Table 2.4 Tensile Strength Retained, TSR (%) recommended minimum values for the foamed bitumen mixes based on climatic region using Weinert's N value, in TG2 (Asphalt Academy, 2002)

Terrain Type and Drainage	Dry (N>5)	Moderate (5>N>2)	Wet (N<2)
Rolling- well drained	50	60	70
Flat-poorly drained	60	65	75

Wet ITS tests are based on 24hrs soaking

2.2.5.2 Temperature susceptibility

Foamed bitumen mixes are not as temperature-susceptible as hot-mix asphalt. The mixes tensile strength and stiffness modulus of the former decrease with increasing temperature. Bissada (1987) found that at temperatures above 30° C foamed bitumen mixes after 21 days' curing at ambient temperatures had higher stiffness moduli than equivalent hot-mix asphalt mixes. In foamed bitumen mixes, since the larger aggregates are not coated with binder, the friction between the aggregates is maintained at higher temperatures. However, the stability and viscosity of the bitumen-fines mortar will decrease at high temperatures, which accounts for the loss in strength.

2.2.5.3 Unconfined Compressive Strength (UCS) and Indirect Tensile Strength (ITS)

Ongoing research has indicated that materials stabilized with bitumen emulsion generally have strength and stiffness similar to those of foamed bitumen mixes. Traditional methods such as CBR and UCS borrowed from soil stabilization (Cement) design were used to determine engineering properties of cold mixes. Since the 1990's the ITS (splitting) test has also been used to account for flexibility behaviour of the mixes (Jenkins et al., 2004).

Bowering (1970) established guidelines for foamed bitumen bases underlying thin surfacing layers, including a UCS value of 700kPa for a 3 day cured specimen at 60°C and 500kPa for a specimen treated with a 4 day soak. This was extended by Bowering and Martin (1976) by

stating that the UCS value of foamed mixes at ambient temperature (field condition) lies in the range of 1,8MPa to 5,4MPa and estimated that the tensile strengths of foamed bitumen materials lies in the range of 200kPa to 550kPa, depending on moisture condition. They also found that foamed bitumen treated materials have strength characteristics superior to those of emulsion-treated materials at bitumen contents above 1.5 percent.

Maccarrone (1998) recommended that, for good performance, cured foamed bitumen specimens should have minimum indirect tensile strengths of 100kPa when tested in a soaked state and 200kPa when tested dry.

Liebenberg (2003) stated that little information is available on the limit of ITS values for the bitumen emulsion mixes. Therefore recommended the values suggested by Louw (1997) of 250KPa and 600KPa. And the values for UCS are taken as similar to those of foamed bitumen recommended by TG2 (Asphalt Academy, 2002) of 1000kPa to 2000kPa depending on the classification of the mix.

2.2.5.4 Stiffness Modulus

Cold mix treatment incorporates a binder that is visco-elastic by nature and as such the behaviour of these materials can be expected to be dependent of temperature and loading time (frequency). This is particularly important for the dynamic testing of resilient modulus (M_r) although it also has bearing on tensile and compressive strength, fatigue life etc. The research of Maccarrone et al., (1994) shows that an increase in filler content from 5% to 15% results in an increase in the resilient modulus by 17% for some mixes. In many cases the resilient moduli of foamed bitumen mixes have been shown to be superior to those of equivalent hot-mix asphalt mixes at high temperatures (above 30° C). Foamed bitumen mixes can achieve stiffness moduli comparable to those of cement-treated materials, with the added advantages of flexibility and fatigue resistance (Ramanujan and Fernando, 1997).

Santucci (1997) indicated that the stiffness of bitumen emulsion treated materials depends on the curing period, whereby the ultimate design modulus may be reached after six months to two years depending on the climatic condition. Marais and Tait (1989) suggested that the resilient modulus may be estimated from the indirect tensile strength by Equation 2.3 if the equipment to determine the resilient modulus accurately is not available.

$$M_r = 5.123 \cdot ITS - 75 \quad (2.3)$$

Where: M_r = resilient modulus in (MPa)
 ITS = indirect tensile strength in (kPa at 23°C)

SABITA (1993) proposed the following relationship between stiffness and CBR for estimation purposes where laboratory stiffness data are not available:

$$E = K * CBR \quad (2.4)$$

Where:

E	= stiffness in (MPa)
CBR	= California Bearing Ratio (%) at the required compaction
K	= constant: 5 for G1 and G2 parent materials 6 for G3 and G4 parent materials 7 for G5 parent materials

De Beer and Grobler (1994) reported values for elastic moduli of 800MPa after construction to a value of approx. 3000MPa after 10 months. The highest rate in increase in stiffness was observed between three to four months after construction. ITS values also increased from around 300Kpa to 900KPa. However, reduction of elastic moduli of approx 50% was reported by de Beer and Grobler (1993) after 10000 to 20000 repetitions by the Heavy Vehicle Simulator at various wheel loads. This can be attributed to the development of fatigue cracks within the bitumen emulsion treated layer.

2.2.5.5 Fatigue Resistance

Repeated loading progressively reduces the tensile strength of bituminous treated materials. Fatigue resistance increases as the binder content increases. It is however not as sensitive to the bitumen content as hot-mix asphalt mixes. Small variations will not have a big influence on the fatigue properties. Foamed bitumen with a higher binder content (>3.5%) are considered to behave in a manner that has some similarities to HMA (Jenkins, 2000). For this reason the mixes are expected to have a defined fatigue life, exhibiting cracks as a form of distress. This concept will be explored more in chapter 5 as one of the objectives of this study.

Bissada (1987) considers that the fatigue characteristics of foamed bitumen mixes will thus be inferior to those of hot-mix asphalt materials. Little et al., (1983) provided evidence of this when he showed that certain foamed bitumen mixes exhibit fatigue responses inferior to those of conventional hot-mix asphalt or high quality granular bitumen emulsion mixes. However the binder content was not considered in this study. SABITA (1993) indicated that fatigue characteristics of bitumen emulsion mixes have not being considered for the design purposes but as an indication of the performance. Research by Marais and Otte (1979), showed that on road section S12 (Witbank and Johannesburg) no cracks were visible on the bitumen emulsion treated section after 9 years with load repetition of approx. 3.5 mill E80's.

Tensile strength is considered to be a primary factor influencing the fatigue performance of the material. Maccarrone (1994) recommended that the foamed bitumen mix specimens should have a minimum ITS value of 200kPa (dry) and 100kPa (soaked) after curing for good performance when tested at 25°C and 0.87 mm/sec. The tensile strength is not a deterministic value and varies according to curing condition. More references on the fatigue performance of the bituminous treated materials are presented in Chapter 3 and Chapter 5 of this study.

2.2.5.6 Resistance to permanent deformation

Permanent deformation is result of the accumulation of repeated plastic strain due to traffic loading. It is caused by a combination of consolidation and shear movement. Proper compaction prevents consolidation to a larger extent, while shear deformation could be minimized by proper mix design. Unlike foamed bitumen mixes, bitumen emulsion mixes are sensitive to permanent deformation in its early life. This is mainly because of the fact that the curing process is not completed. Once curing has been more or less completed, permanent deformation is rarely the primary mode for failure (Marais and Otte, 1979 and Wirtgen, 2004).

Measurement of the shear parameters of cold mixes has been used to analyse its engineering properties. Acott and Myburgh (1982) utilized the vane shear test in a CBR mould to evaluate cohesion and triaxial tests on similar specimens. The results showed that cohesion of the mixes increases from 31 kPa to 110 kPa with the addition of 3% foamed bitumen.

Shackel et al., (1974) carried out triaxial tests on foamed bitumen mixes and established that resistance to permanent deformation is function of the binder content and degree of saturation (% void filled with water by volume) of a foamed bitumen mixes treated material. Whereby the ratio of axial strain to the peak axial strain ($\epsilon_{\text{axial}} / \epsilon_{\text{peak axial}}$) decreases with increasing binder content and degree of saturation. The trend shows that the relationship is inverted parabolic with the minimum point as the optimum design binder content and increasing rates of deformation at either side of this minimum point.

Research at Delft University of Technology has shown that when a granular material in a pavement structure comes under load, the ratio of the maximum deviator stresses induced in the granular layer relative to the strength of the material (i.e. the stress ratio) will determine the rate of permanent deformation or rutting. Generally the stress ratio should be limited to 0.4 for granular materials. However Jenkins (2000) researched foamed bitumen mixes and indicated that the limiting stress ratio value of 0.40 to 0.45 are applicable to foamed bitumen treated materials to ensure satisfactory materials performance.

2.3 MIX DESIGN CONSIDERATION

The cold mix design procedure requires the combination of numerous ingredients (materials) to be formulated, combined, and processed in order to provide a composite product with necessary quality and consistency in order to fulfill the intended functions in pavement structure. Cold mix design is not only optimizing the mix composition, but also considering the engineering properties of the mix, durability and long term performance. At the same time economics remain of paramount importance in selecting the appropriate mix design (SABITA, 1993).

The selection of optimum mix design differs from one country to another due to lack of internationally standardized design guidelines for the cold mixes. Therefore, the present methodologies applied are broad in terms of formulation and interpretation. Guidelines such as the GEMS Manual (SABITA, 1993) for granular emulsion mixes (TG2, Asphalt Academy, 2002) for the design and use of foamed bitumen treated materials in South Africa have been developed based on the laboratory tests, empirical formulas and or past experience of identical projects. These are however considered to be good departure point for the cold mix technology.

A typical mix design procedure as adopted in South Africa for cold mixes is shown in Figure 2.7 (Jenkins et al., 1999).

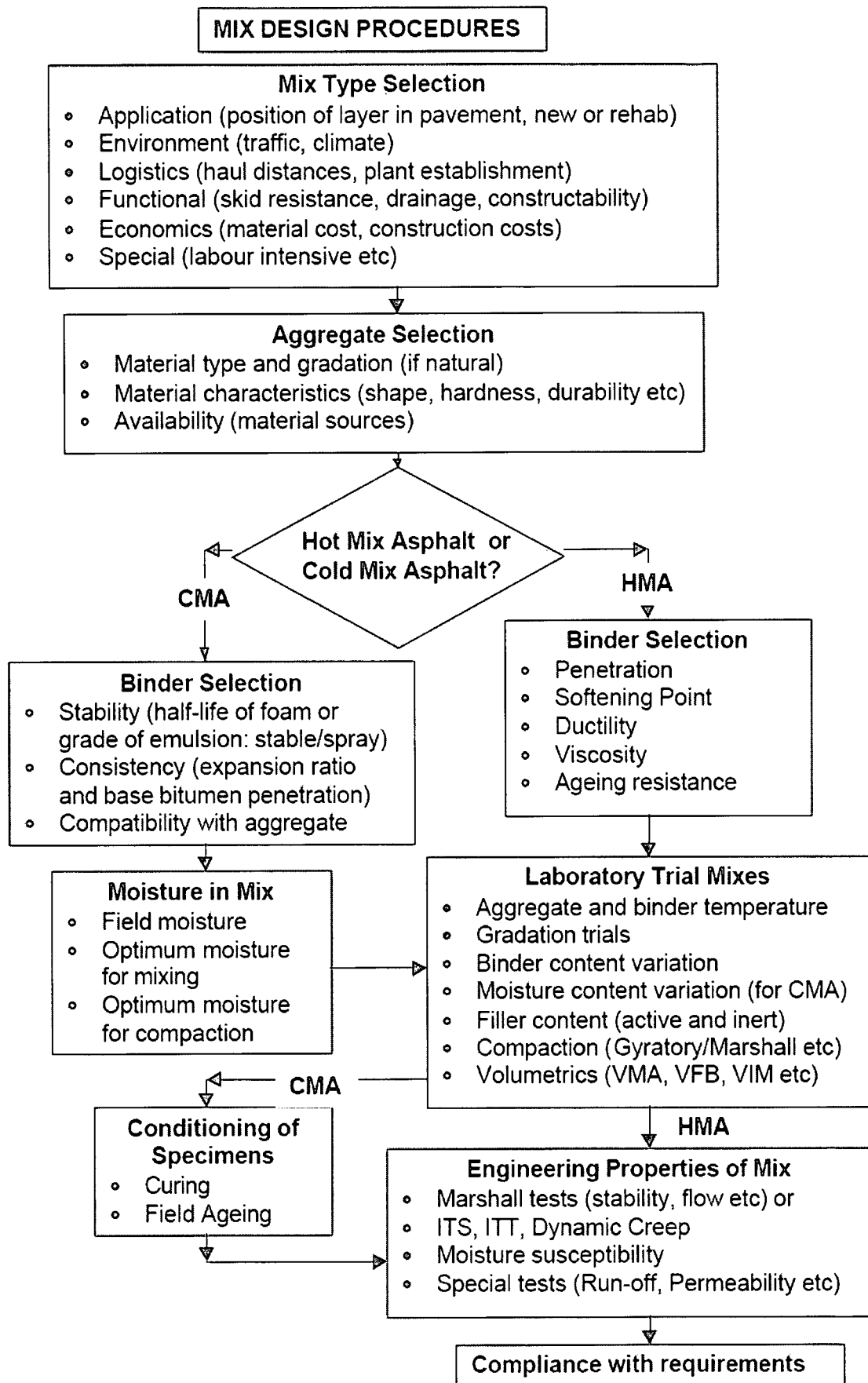


Figure 2.7; Mix Design Procedure for the cold Mixes, Jenkins et al., (1999)

2.3.1 Binder interaction (with filler and water) and content typically used

Bitumen emulsion usually contains 30-40% water. Combinations with varying fines contents may result in uneven curing because the fines retain emulsion water and hence prolongs the curing time of the mix, Myre (1997). Unlike bitumen emulsion research has indicated that a filler component in foamed bitumen mix is extremely important during its metastable life. The interaction of foamed bitumen, filler and water is termed "foamed mastic" (Jenkins, 2000). Ruckel et al., (1993) recommended that the range of filler/binder ratio is 1:1 to 2.5:1 for gravel and 1.2:1 to 2.2:1 for sand. The role of moisture in the filler is an integral part of the stiffening of the foamed mastic. Water provides the lubrication for compaction at ambient temperatures and can be released during consolidation under compaction. Water held within the foamed bitumen mastic assists in explaining the shelf life characteristics of foamed bitumen mixes (Jenkins, 2000).

For the bitumen emulsion mixes, the interaction between aggregates and bitumen is active both physically and chemically as it ionizes the constituents in the aqueous phase, unlike foamed bitumen where the interaction with the aggregates is active only physically (Colas, 2003). Aggregates take up a characteristic surface charge in water that depends on the pH and the nature of the mineral. Acidic aggregates with high silica contents tend to take up negative charged droplets. As the pH raises all aggregates tend to become more negatively charged with presence of calcium salts or other cations in the water tend to make surface less negative (Akzo nobel, 1997).

Jenkins (2000) indicated that the distribution of the foamed bitumen in the mix will depend on a variety of factors including; bitumen content, aggregates temperature and filler characteristics, moisture content of the mix, foam characteristics and mixing technique.

The binder type most frequently used in cold mixes are 70/100, 50/70, but depending on temperature it also varies to 160/200. The residual binder content varies between 2% to 5.5%. Voskuilen et al., (2004) and Didier (2000) shows that pen grade 70/100 is frequently used in Netherlands and France, with the additives of 0.025% to give best properties. 3% of foaming water results in an expansion ratio of 18:1 and half-life time of 18 seconds. Myre (1997) shows that pen grades of 144-210 or 300-430 are preferred in Norway and foaming water is 3% with expansion ratio of 20 seconds. These differences are probably the results of the different climatic condition in the different countries.

Ramanujan (2000) in Australia indicated that class 170 bitumen is preferred for foamed bitumen stabilization and that a foaming agent must be added to the bitumen to counteract the ant-foaming agent (silicon) that is used in the refining process of bitumen. Typically 0.5% foaming additive is required to achieve desirable properties. The foaming water required is 2.5% with 10:1 expansion ratio and 30 seconds half life time. Saleh (2003) indicated that pen

grade 180/200 and 80/100 are commonly used in New Zealand. However, 180/200 pen grade bitumen provides better foaming characteristics than 80/100 with a FI of 224, using foaming water of 2.6% resulting in an expansion ratio of 16.5 and half life time of 13.5 seconds. Overby et al., (2004) indicated that pen grade 80/100 is commonly used in Tanzania; foaming water of 5% used resulting in an expansion ratio of 20 and half –life time of 15 seconds.

The TG2 (Asphalt Academy, 2002) indicates that the pen grade selected for the foamed bitumen is between 80 and 200 with addition of anti stripping agent in wet area of 0.2% to 2% (by mass) of the agent. Foaming water is 2% with the expansion ratio of 10:1, or FI of 500 and half life time of 20 seconds with aggregate temperature of 10°C to 15°C.

In the case of bitumen emulsion mixes, a cationic emulsion of medium setting is commonly used. The residual binder varies from 3%-4.5%. Eckaman (2000) indicated that 65% to 69% bitumen content in emulsion is used in Belgium with the emulsifier content of 0.3%, Didier (2000) shows that 30% to 40% water content in emulsion is use in France with 0.6% emulsifier. Myre (1997) indicated that 30%-40% water content in emulsion is used in Norway but the emulsifier content was not stated.

The TRH 7 manual (SABITA, 1972) shows that a 150/200 pen grade bitumen is used for low traffic roads and 80/100 for high traffic road. GEMS Manual (SABITA, 1993) recommends that the suitable residual binder ranges from 1.5% to 5% for stabilization of materials and 0.6% to 1.5% for the modification of the materials. Emery and O'connell (2004) show that cationic emulsion with a bitumen content of 60% to 70% is commonly used in South Africa (with 65% in the market compared to anionic with 31%). The emulsifier content is 2%. The reason and causes for these differences in the mix design guideline need to be understood in order to optimize the performance of the cold mixes.

2.3.2 Aggregates suitable type and grading

The foamed bitumen process is suitable for treating a wide range of materials, ranging from sands, through weathered gravels to crushed stone and RAP. Materials that are deficient in fines will not mix well with foamed bitumen, unlike bitumen emulsions where materials with less fines produce good quality mixes. Figure 2.8 shows that, the minimum requirement is 5% passing 0.075mm for foamed bitumen and 3% for the bitumen emulsion (Louw, 2003).

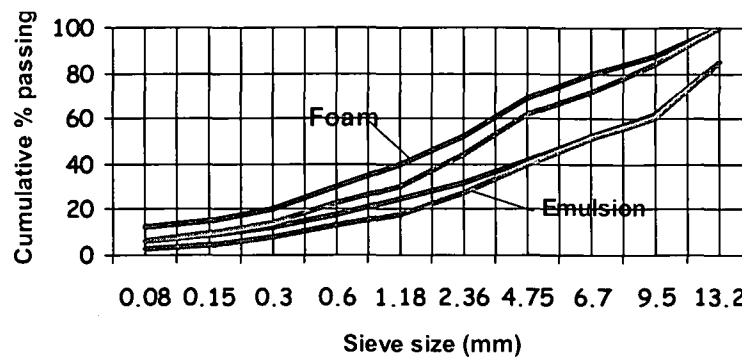


Figure 2.8 Grading suitable for both foamed bitumen and bitumen emulsion

The dispersion of foamed bitumen or the breaking of bitumen emulsion on the mineral aggregate is influenced significantly by the filler fraction and the fine sand fraction. The behavioural tendencies of cold mixes in terms of resilient modulus response to loading at foamed bitumen binder contents lower than 3.5% and bitumen emulsion contents less than 1.5% closely resemble to granular materials behaviour. When binder contents greater than 3.5% for foamed bitumen and 5% for the bitumen emulsion are used in the mixes, the behaviour closely resembles to the visco-elastic behaviour of hot-mix asphalt.

Virgin aggregates such as crushed alluvial, granites and lime stone, dorite and cemented treated ferricrete, sand and RAP, are suitably used aggregates. Myre (1997) indicated that filler contents ($<0.075\mu\text{m}$) suitable for foamed bitumen vary from 2 to 20%. The percentage passing 2mm should not be less than 30%. However, for the bitumen emulsion mixes the filler content ($<0.075\mu\text{m}$) vary from 1 to 7%. Didier (2000) indicates that maximum aggregate size used in cold mix are 0/10, 10/14, 0/19. Gunnar (2000) indicates that up to 15% of 8mm virgin aggregates (sand) can be added to RAP. Saleh (2003) indicates that the maximum aggregate size used in foamed bitumen mixes is 19mm and the filler content is up to 12.5% with additional of fly ash to adjust the fraction of fine fraction.

TG2 (Asphalt Academy, 2002) recommends maximum aggregate sizes of 19mm for foamed bitumen mixes and filler content ($<0.075\mu\text{m}$) varying from 5% to 15%. The addition of virgin aggregates can vary from 15% to 20% of the coarse fractions. The aggregates should be heated to 10°C to 15°C to improve in engineering properties. Bitumen emulsion mixes the GEMS Manual, (1993) recommends a maximum aggregate size of 26.5mm and a filler content varying from 3% to 15%. TRH7 (SABITA,1972) indicates that for wearing coarse the maximum aggregate size is 19mm and the filler content can vary from 0% to 12% depending on the intended use.

Figure 2.9 shows the spatial composition for sand skeleton mixes that produce the densest grading for the foamed bitumen as well as bitumen emulsion (Jenkins, 2000 and Louw, 2003).

However, care should be taken when the gradation is approaches a stone skeleton as these mixes are characterized by balling where bitumen enriched conglomerations cling together. Also, where weak aggregates are used crushing can occur within the layer.

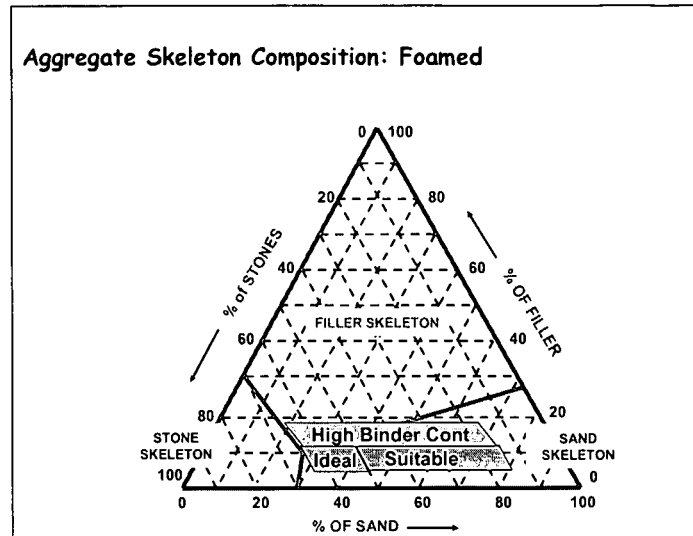


Figure 2.9: Suitability of aggregates grading for foamed bitumen relative to the skeleton structures.

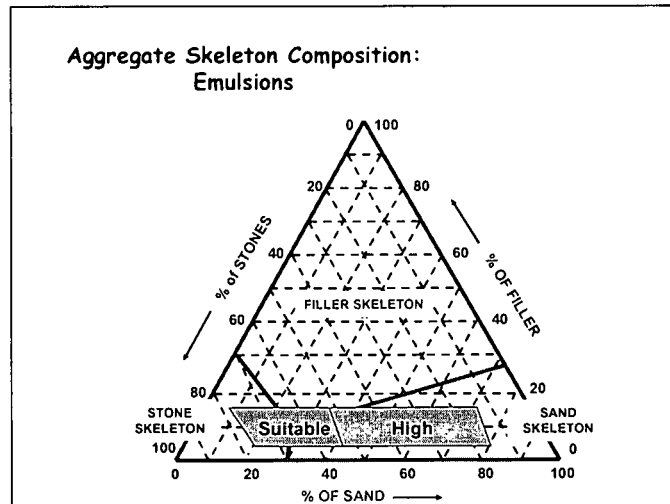


Figure 2.10: Suitability of aggregates grading for bitumen emulsion relative to the skeleton structures

2.3.3 Moisture consideration

The fluid content (FC) of the materials is defined as the moisture content (MC) plus the bitumen content (BC) as shown in equation 2.5. Jenkins (2000) indicated that bitumen has similar lubrication properties to water during the compaction process of the bitumen emulsion mixes. However, this relation was found to be variable for the foamed bitumen mixes.

Compaction of foamed bitumen mixes is achieved by optimizing the fluid content (OFC) which is determined as shown in equation 2.6. The optimum combination of moisture content and foamed bitumen content in the mixes yield the maximum dry density for specific compaction method, TG2 (Asphalt Academy, 2002).

$$FC = MC + BC (\%) \quad (2.5)$$

$$OFC_{\text{compaction}} = OMC + BC (\%) \quad (2.6)$$

From equation 2.6 it can be seen that the higher binder content results (for compaction reasons) in lower moisture content. Due to high compaction energy in the field relative to laboratory compaction it is possible to compact at 1.5% lower fluid contents in the field than the OFC used in the laboratory.

In the bitumen emulsion mixes the total fluid content is used instead of moisture content in identifying the moisture content/density relationships, unlike foamed bitumen, bitumen emulsion contain a high percentage of water ranging from 30% to 40%. The moisture from the aggregates and water added should also be counted. Wirtgen (2004) indicated that compaction above optimum total fluid content (OTFC) results in hydraulic pressure developing under the roller, hence causing materials to heave (zero air voids). Therefore, when the in-situ field moisture content is high, the use of bitumen emulsion can increase the total fluid content beyond the saturation point. Adding cement in these cases is not recommended. Instead the material should be pre-pulverized and allowed to dry sufficiently before stabilization. The recommended optimum OMC is 50% -90% of the binder content.

Bitumen emulsion should not be used in combination with high fines content because bitumen emulsions have high percentage of water. The fines will retain the water resulting into slow curing and low stability of the mix, in particularly soon after laying. Foamed bitumen mixes have much less water in the mix and therefore does not suffer the same problem (Wirtgen, 2004).

2.3.3.1 Mixing and placement

The moisture in bituminous treated materials cannot be analyzed in isolation of the mixing technique. Various mixing technique are utilized in the laboratory and field to distribute binder (bitumen emulsion and foamed bitumen) and moisture over the mineral aggregate during mix production.

Jenkins (2000) indicates that the distribution of binder in the mix, which in part depends on the mixing method, is the key success good to quality mixes. Generally mixing techniques adopted for the cold mixes in laboratory and in the field are; free fall mixer, vertical shaft mixer,

in-place recyclers, pugmills and drum-mixer, and blenders. Limited investigation has been done into the selecting of mixing technique in laboratory that simulates plant mixing. Research conducted in laboratory is primary carried out with mixers that are used in combination with a laboratory foaming plant such as Hobart ® type mixer. However, TG2 (Asphalt Academy, 2002) shows that the mixing time of 30 seconds used in laboratory is longer than the in-situ mixing time due to differences in energy of the laboratory mixer compared to field mixing.

Eggers et al., (1990) state that it is imperative to utilize a laboratory mixer that emulates the mixing that takes place in the field. The rotary mixing motion of the blenders used in the laboratory are neither ideal for restricting particles segregation nor for simulating site manufacture. The methods such as twin-shaft pugmill, drum mixers, free fall mixers and milling-drum mixers all provide sufficient volume in the mixing chamber and energy of agitation to ensure that the mineral aggregates is airborne when it makes contact with the binder (bitumen emulsion and foamed bitumen). Blender type laboratory mixers do not emulate this, which has implications on the mix behaviour.

Colas (2002) indicates that the recommended laboratory mixer for cold mixes is the vertical shaft or twin-shaft pugmill, which influences double coating or sequenced coating of aggregate fractions. However, the laboratory pugmill mixer has the disadvantage of spoiling foam mixes when the paddles get stuck on the larger aggregate particles during production process.

2.3.3.2 Compaction

The mix requirement of compaction strength, durability, and performance depend on the compaction level, which is important in the mix design. Compaction not only improves particle contact and reduce voids contents, but also improves binder adhesion to the stone aggregates (Jenkins, 2000).

The distribution of binder within cold mixes differs from that of HMA and the inclusion of water phase sets these two mixes apart, hence difference in compatibility, (TG2, Asphalt Academy, 2002). Colas (2002) indicate that cold mix compaction has the effect of forcing the elimination of two fluids i.e. air and water from the mixes. The influence of compaction level and technique is significant. Insight into this is required in order to establish a link between the density measured in the laboratory and that which will be obtained on site. Berneel et al., (1998) indicated that gyratory compaction of foamed bitumen mixes doubled the Marshall stability of specimen compacted by 75 blows with the Marshall hummer. Saleh (2003) carried out comparative compaction methods on foamed bitumen mixes using gyratory (80 cycles, at 240kPa with 2° gyratory angle), Marshall (75 blows per face) and vibratory compaction to determine the optimum moisture content of the mix. He found that the gyratory compactor provides the higher density and the lower optimum water content relative to the other methods.

Hodgkinson et al., (2004) shows that the major advantages that the gyratory compactor method offers over standard Marshall compactions are the ability to monitor the volumetric properties with the increase in the number of load repetitions. This provides the ability to "simulate the compaction" that occurs as a result of traffic after the construction is completed. TG2 guideline (Asphalt, Academy 2002) commented that the correlation between the numbers for certain gyrations to traffic levels have not been established yet due to varying properties of cold mixes from granular to visco-elastic. Therefore, by using the gyratory compactor, the number of gyrations should be selected to achieve the level of compaction targeted using drop-hammer technique (Mod AASHTO or Mod Proctor).

Colas (2002) indicated that using the gyratory compactor (0.9MPa, angle 3° and rotation of 6r/min) a minimum volume of voids filled with air is achieved; hence voids will be filled with water which characterizes the beginning of water expulsion from the mix.

It is apparent from the literature that much research has been done on laboratory compaction using Marshall, Mod AASHTO, gyratory compactor, vibrating hammer, slab compaction etc. However, the ideal laboratory compaction technique for the mix design of cold mixes to link between laboratory and field compaction is not yet properly defined (Jenkins, 2000).

2.3.3.3 Curing rates

Curing of foamed bitumen mixes after compaction is important in order to further displacing of water and establish an important moisture regime within the mix. However the hydrophobic nature of bitumen assists in relatively rapid strength gain. The rapid strength gained enables the road to be trafficked immediately without detrimental effects, provided that traffic volumes are not too high (Jenkins, 2000). This is not the same for bitumen emulsion mixes, which takes more time to cure.

Adequate curing for the development of sufficient strength in a foamed bitumen mix is very important since premature failure in the foamed bitumen mix pavements tend to occur in days rather than weeks or months after construction (Jenkins,2000). Curing in bitumen emulsion is important to prevent deformation in the early part of service life of an emulsion treated layer. Small amounts of bitumen emulsion require a shorter period for full curing (Liebenberg, 2003).

Wirtgen (2004) indicates that although some bitumen treated materials may achieve full strength within a shorter time of curing, other materials may take longer than a year. The length of this period is affected by the rate at which aggregates absorb water, moisture content of the mix after compaction, void content in the mix, type and quality of emulsion, mineral composition of aggregates, field climate and addition of active filler if any. However if

the road has to accommodate traffic shortly after treatment, addition of 1% to 2% cement can influence the rate of gain of strength positively.

2.3.6 Engineering properties

Classification of foamed bitumen materials as adopted in South Africa is based on UCS and ITS properties, however on going research has shown focus on investigating the behaviour of the cold mix materials in terms of fatigue life (reduction of the stiffness by loads repetitions to granular materials stiffness), flexibility with strain at break tests and triaxial test for the permanent deformation. Wirtgen (2004) indicated that materials stabilized with bitumen emulsion have strength and stiffness characteristics similar to those stabilized with foamed bitumen. However many researchers have indicated that addition of active filler on the mix improve performance of foamed bitumen mixes. Long and Ventura (2003) showed that UCS and ITS increase with the increase in cement content, however, decrease with increasing binder content. Hodgkinson and Visser (2004) used RAP as test materials and indicated that by addition of 1.5% cement the dry ITS of foamed bitumen mixes increased more than for bitumen emulsion mixes.

2.4 INFLUENCE OF ACTIVE FILLER ON MIX PROPERTIES AND PERFORMANCE.

2.4.1 Active filler type used, percent and its role

A considerable amount of research has been carried out on establishing the influence of active filler on the properties and behaviour of cold mixes. Lime and cement are the commonly used active fillers among others for improvement of the engineering properties of the mix. SABITA manual 21 (1999) recommended 1% of cement to be added to the parent materials in emulsion treated base to assist the breaking process, promote adhesion of emulsion, and increase the early strength when layer is to be opened to traffic soon after the construction.

Saleh (2000) indicated that the use of 2% OPC and lime can reduce moisture sensitivity in the foamed bitumen mixes. Myre, (1997) showed that the OMC is limited to OMC-(0.5-residual binder) of Mod AASHTO. Ramanujam (2000) indicated that 2% hydrated lime is used to act as anti-stripping agent to help dispersion of the foamed bitumen. Colas, (2004), shows that a small amount of active filler 0.5%-1.5% (by mass) applied in cold mixes can significantly increase retained strength without affecting the fatigue properties of the mix. Lancaster et al., (1994) and Wirtgen (2004) state that cementitious additives should be limited to 2% by mass of the dry aggregate to minimize the potential shrinkage cracks and negative effect to fatigue properties of the stabilized cold mix layer.

2.4.2 Interaction with bitumen binder, aggregate type and characteristics

In the interaction of the bituminous binder and cement, the cement acts as an dispersing catalyst in case of foamed bitumen and promotes breaking when used with bitumen emulsion. Giulian (2001) confirmed that bitumen emulsion together with cement does not generate a new binder when observed at molecular level. The rigidity effect is due to two simultaneous mechanisms of the emulsion breaking and the cement hydrating during the watery phase of the bituminous emulsion. He further observed that cement proved to be a regulating element of the emulsion setting, by increasing the viscosity of the bitumen and contributing to the creation of new bonds in the mixture.

Cement actually influences both the physical and chemical properties of an asphalt mixture, even though it is in small dosage. Wirtgen (2004) indicated that care should be taken when adding cement to foamed bitumen mixes because hydration of cement commences as soon as it comes into contact with moisture. Hence it binds the fines and effectively reduces the 0.075mm fractions which are required for effective dispersion of bitumen on particles when foamed bitumen is added. Therefore cement should be added in conjunction with the foamed bitumen.

Brown (2000) indicated that hydration of cement causes a noticeable rise of temperature in the mix. Tests carried out on acidic bitumen emulsions indicated that a small temperature rise from 22°C to 25°C in 30 minutes occurred and change in pH from 3.47 before addition to 12.62 immediately after addition of cement. This indicates that addition of cement can also contribute the early curing strength of the cold bituminous mixes. Hodgkinson and Visser (2004) found that an anionic emulsion does not break as readily as a cationic emulsion, but that cement can be used to enable the layer gaining the early strength.

Mixing performance of foamed bitumen and bitumen emulsion are influenced by plasticity of aggregates, Bowering and Martin (1976), confirmed that the higher plasticity clayey gravels respond poorly to the foamed bitumen treated process unless modified (with lime/cement) before the addition of binder. Lee (1981) suggested that a limited percentage of plastic fines are acceptable, but lime pretreatment may be advisable. Lancaster et al., (1994), suggested that maximum PI limit of 12% before lime modification is necessary. In addition Lancaster (1994) and Wirtgen (2004) state that cementitious additive should be limited to 2% by mass of the dry aggregates.

2.4.3 Moisture condition

Moisture in bitumen emulsion mixes consists of water in emulsion, hygroscopic and added water. When 1% or 2% cement is added to the mixture the cement-water ratio is very high 1:6 or 2:6. Brown (2000) indicated that cement would be unable to set initially until a substantial

amount of water has evaporated. This is a probable cause of steady increase in stiffness of the mixtures that contain cement. In an advanced stage of curing, when the water content is low, cement would have set properly and acts as a competent binder.

Brown (2000) further indicated that the total water loss in the bitumen emulsion mixes is influenced by the percentage of cement used during early curing period (see Figure 2.11). Myre (1997) showed that aggregates in cold mixes are cold and damp during production. therefore the moisture content reduces gradually as mixes cure for up to 1-2 years before materials have developed full strength. However with the addition of cement curing is much quicker.

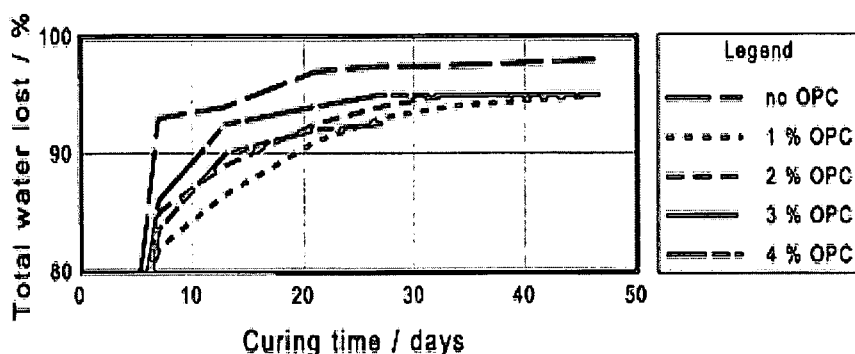


Figure 2.11; Water loss from the mix tested at various cement content (Brown, 2000)

Johansen (1997) indicated that foamed bitumen materials do not give prolonged instability in the curing period. Overby (1996) comment that foamed bitumen gives easier control of the moisture content compared to bitumen emulsion the use of which introduces large amounts of water into the layer hence causing sensitivity during construction.

The curing method for the cold mix is still optimized. TG2 (Asphalt Academy, 2002) recommends curing of foamed bitumen for 24 hours in mould and 72 hours at 40°C (sealed) as equivalent to six months in the field condition. Writgen (2004) suggested 48 hours at 40°C (sealed) + several hours cooling at ambient (unsealed) as equivalent to medium field cure. The University of Stellenbosch (2004) recommended 20 hours at 30°C (unsealed) and 2 x 24 hours at 40°C and change bag (sealed) as equivalent to medium curing. Jenkins (2000) recommended aiming for equilibrium moisture by sealing the specimen at desirable moisture content.

The in-service time related effect of cold mixes is the sign of ageing of binder in the mix that may be due to a high void content as a result of improper compaction. Overby et al., (2004) showed that the softening point and viscosity of the recovered bitumen was increasing with the age against decreasing penetration due to hardening of the binder in the foamed bitumen mixes, Figure 2.12.

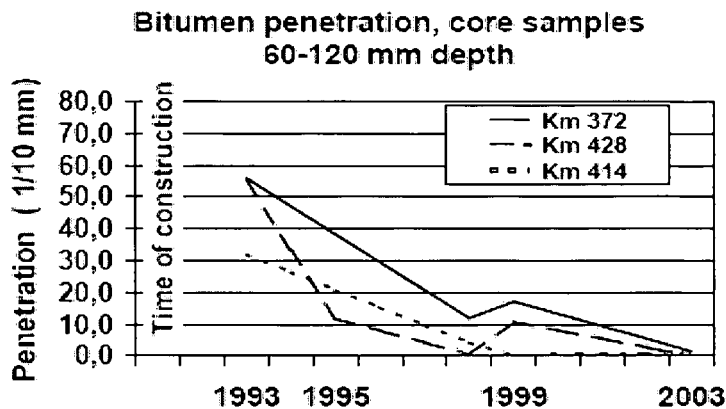


Figure 2.12: Properties of binder recovery from core sample (Overby et al 2004)

2.4.4 Engineering properties and mix type classification

The engineering properties of cold mix materials play an important role in the long-term performance in terms of permanent deformation and flexibility of the mixes. Long and Ventura (2003) show that the test performed on recycled (N7) materials indicate that the UCS, ITS and CBR values increase with the increase in cement contents, whereas an increasing foamed bitumen binder content decreases the strength properties. Table 2.5 shows the engineering properties of foamed bitumen mixes (Long and Ventura 2003).

**Table 2.5; Engineering properties ITS, UCS for the recycled (N7) test results,
Long and Ventura, (2003)**

Mix blend formulation	Cement content (%)	Binder content (%)	ITS average (kpa)	UCS average (kPa)
HSN	0	2.25	27.6	2266
HSN	1	0	293.1	329
HSB	1	1.5	297.5	2330
HSS	1	2.25	320.5	2372
HAS	1	3.0	243.2	1827
HAS	2	2.25	410.8	3116

The results indicate that the UCS increases as the percentage of cement increases. However, at 1% cement there is not much difference in UCS results for the mix of 2.25% or less binder. However, 3% binder cause decreases in the UCS. The ITS results show that a larger amount of binder negatively influences the tensile strength of a mix.

Verhaeghe and Long (2004) suggest that cold mixes exhibit a relative strong cohesion. The ratio of cement to residual binder content can be increased as long as the cohesive bond is retained. The materials will have relative high resilient moduli compared to the resilient

modulus of the untreated materials. The resilient modulus could be 100MPa or higher depending on the amount of residual binder and active filler added to the materials. Jenkins et al., (2004) commented that ITS results on the N7 recycled material mixed with 1 percentage of cement in both foamed bitumen and bitumen emulsion show that the bitumen emulsion mixes were better than foamed bitumen mixes. Bondiotti et al., (2004) also indicated that for decomposed granular materials treated with emulsion and addition of 1% cement the UCS and ITS of the mixture increased with increasing cement, content and reduced with increasing binder content. Figure 2.13 shows that at lower binder contents (0% to 3%) The UCS increases more rapidly (steep slope) by adding 0% to 2% cement and more gradually at more than 2%. However at 4% to 5% binder content the UCS values increase consistently with increasing cement content.

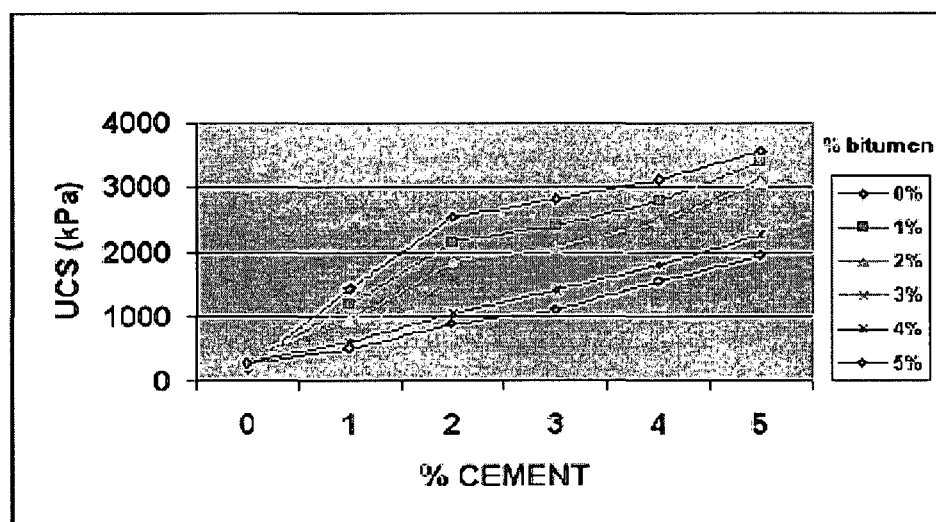


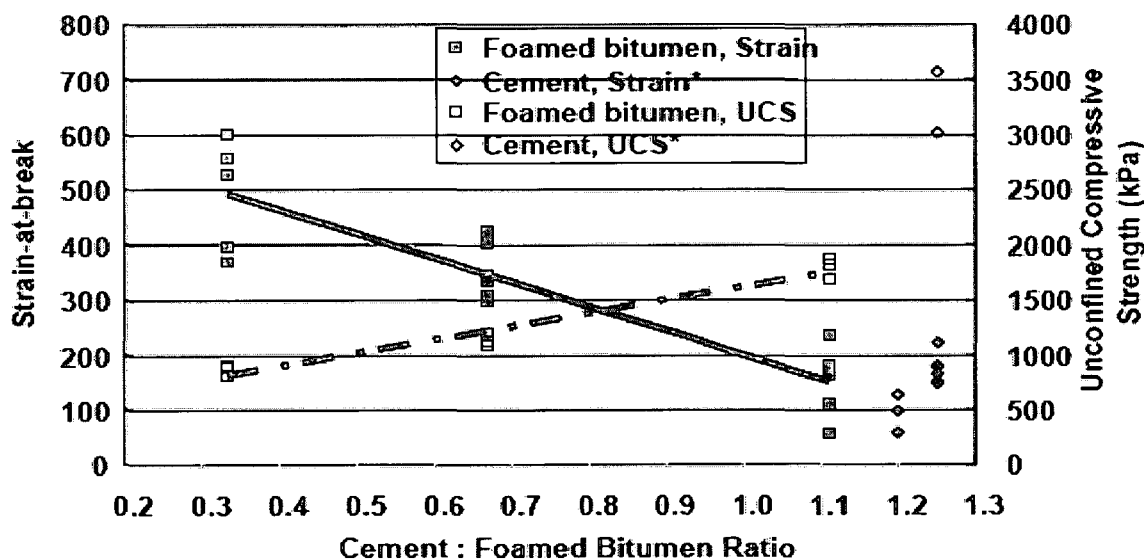
Figure 2.13: UCS of decomposed granite/asphalt mixture at different percentages of bitumen and cement, (Bondiotti et al., 2004)

Classification process of bitumen treated materials as adopted in South Africa is based on the UCS and ITS values. However there is a tendency to include flexibility measure (strain at break test) for cold mixes in an attempt to capture the complex behaviour of these materials that exhibit on interaction between the shear strength (permanent deformation) and flexural characteristics.

It has been observed that the flexibility of the treated materials as determined by the strain-at-break from the flexural beam test can increase by increasing the residual binder content, and consequently by decreasing the ratio of the active filler to bitumen-emulsion content. The effect of cement: bitumen ratio on strain-at-break and UCS was investigated by Verhaeghe and Long (2004) as shown in Table 2.6 and Figure 2.14 below.

Table 2.6; Classification of cold mixes (foamed bitumen and bitumen emulsion)
(Verhaeghe et al., 2004)

Foamed Bitumen Treated Materials			
Material Code		ITS* at 25°C (kPa), or Strain-at-break (microstrain)	
UCS at 25°C (kPa)	700 – 1400	FB4	FB3
	> 1400	FB2	FB1
FB1, FB2, FB3, FB4: Foamed-bitumen materials of classes 1,2,3 & 4			
* unsoaked ITS			
Bitumen Emulsion Treated Materials			
Materials Code		Strain-at-break (microstrain)	
		100 – 300	> 300
UCS at 25°C (kPa)	400 – 1400	EB4	EB3
	> 1200	EB2	EB1
EB1, EB2, EB3, EB4: Emulsion bitumen treated materials of classes 1,2,3 & 4			



* Cement treated with 2 percent cement and no foamed bitumen. Values plotted at an arbitrary ratio of 1.25 for 2 percent cement and 1.2 for 1 percent cement.

Figure 2.14; Engineering properties of foamed bitumen, (Verhaeghe et al., 2004)

The research into the performance properties of the cold mixes has shown that the resistance to permanent deformation increases as cement content increases. Brown (2000) commented that cold mix materials with cement as active filler offered better resistance to permanent deformation than the hot mix asphalt under unconfined test condition. This was because the cement acts as a secondary binder in cold mixes and hydration is necessary to activate the cement. This can only occur in cold mixes where water is available. In absence of water cement acts as inert filler. Verhaeghe and Long (2004) indicated that the cohesive bonds that developed due to hydration of the cement deteriorated by repeated flexing of the materials

under traffic loading to a point where the effective resilient modulus of the layer decreases to a minimum. This reduced effective resilient modulus is comparable to the modulus of untreated materials and is in order of 300-500Mpa.

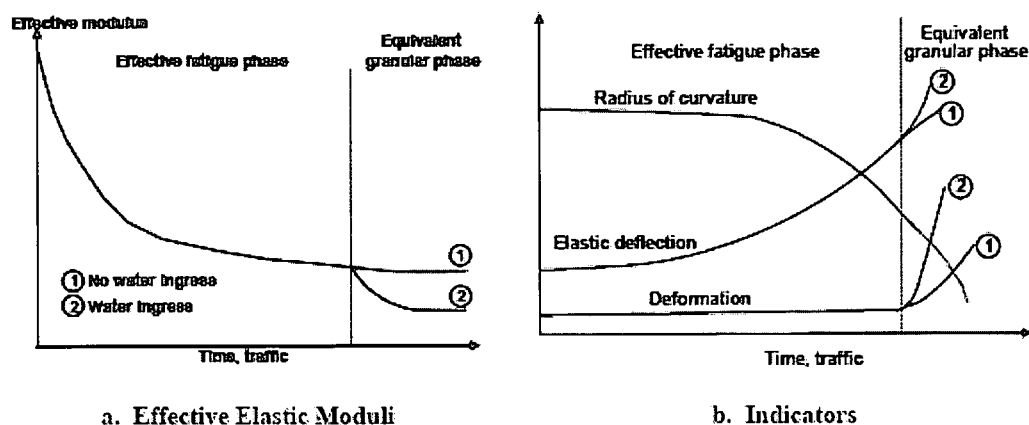


Figure 12.15; Behaviour of pavement with bitumen-emulsion and foamed bitumen treated materials, (Verhaeghe et al., 2004)

Brown (2000) suggested that above 200 microstrain the addition of cement causes a reduction in fatigue life. Below 200microstrain the reverse is true. This depends however on the mixture, subgrade stiffness, load and layer thickness.

Long and Ventura (2003) showed that for tests on G2 recycled material treated with foamed bitumen, the strain-at-break increases (hence the flexibility increases) with increasing binder content. However, tests on mixes without cement and 2.25% binder showed a higher strain-at-break than mixes with 1% or 2% cement content at the same binder content. This demonstrates that addition of higher percentage of cement cause a larger reduction in flexibility of the mix. This is because the cement absorbs the fines in early stage of mixing and affects the dispersion level of the foamed bitumen.

Erosion tests on the same materials indicated that a loss of 17 to 19mm after just 1500 repetition occurred. The same materials treated with 50% less cement reduced the erosion loss to less than 10mm. The permeability test indicated that mixes with 1% or 2% cement have reduced permeability. The shrinkage test however indicated that the mixes without cement show high shrinkage. This may be due to the loss of water in early stage of curing (sealed and unsealed). However addition of cement shows less shrinkage. This might be the result of the presence of cement in the mix that leads to some kind of internal structure, that does not allow much shrinkage once the water evaporates.

2.4.5 Performance of the mixes and failure mechanism

Research into the performance properties of the cold mixes indicated that resistance to permanent deformation increases as cement content increases. Figure 2.16 (Verhaeghe and Long, 2004) illustrates the behavioural characteristics of bitumen-emulsion and foamed bitumen treated materials depending on the proportion of aggregates, bitumen and cement compared to asphalt mixes and unbound materials.

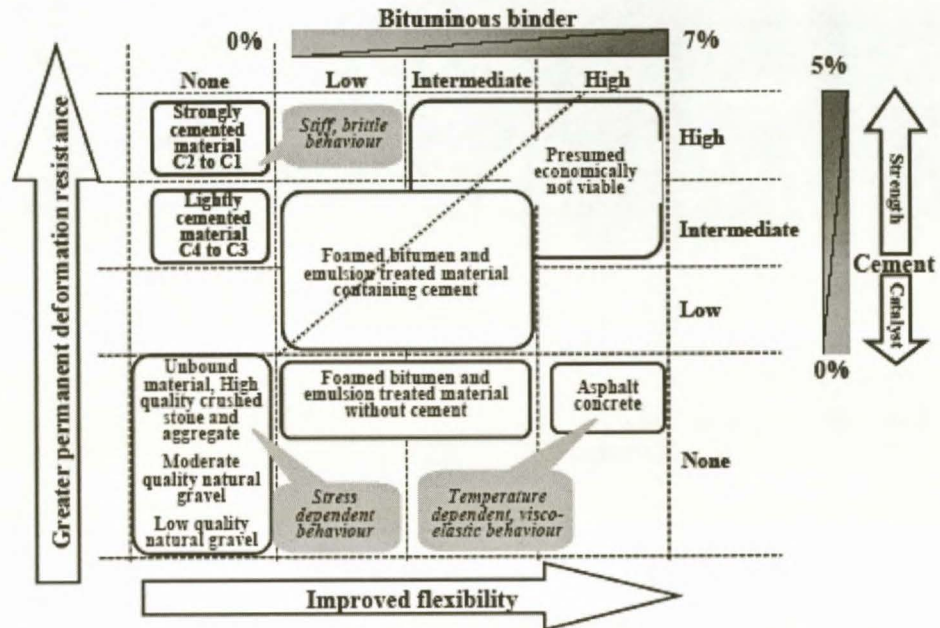


Figure 2.16; Conceptual representations of the behavioral characteristics of pavement materials, (Verhaeghe et al., 2004)

Bitumen-emulsion and foamed-bitumen treated materials exhibit, to a certain degree, aspects of basic characteristics of granular materials, cement-treated materials, and hot-mix asphalt depending on the mix proportion of aggregate, bitumen, and cement. The behaviour of bitumen treated mixes with low bitumen and cement contents or no cement at all will tend towards the stress dependent behaviour of unbound materials. However, if the bitumen content increases, the flexibility of the mix improves and may even approach the temperature dependent, visco-elastic behaviour of HMA. On the other hand if the cement content is increased while keeping the bitumen content low, the behaviour of the bitumen-treated materials mix will approach the stiff, brittle behaviour of cement-treated materials with associated a high resistance to permanent deformation.

2.5 CONCLUSIONS

The mix design of cold mixes requires appropriate selection of numerous ingredients (i.e mineral aggregates (both virgin and RAP), bitumen content, active filler content and moisture content for combination, formulation and processing of the mix to achieve the best properties for the intended use. From the literature survey the following conclusions can be drawn:

- Moisture content during mixing and compaction is considered to be a very important. It acts as a densification agent for emulsion and aids bitumen dispersion for the foam mixes. The optimum moisture content occurs at a range of 65% to 85% of OMC at Mod AASHTO compaction for foamed bitumen mixes, and 50-90% of binder content for the bitumen emulsion mixes.
- The gain in strength of cold mixes is mainly due to loss of moisture (state of curing of moisture). However curing methods for cold mix are still not clear. A large variety of curing methods to simulate the field curing process are currently used in laboratories worldwide,. This advocate for the standardization of curing protocols. However researchers have indicated that for early trafficking of the cold mixes the addition of active filler (1% to 2%) assists in the early strength development of the mixes.
- The interaction of the bitumen with cement has plays a significant role in the long term performance of the cold mixes in terms of increasing flexibility, fatigue life and resistance to permanent deformation. Therefore, there should be a fine balance of these components determined in the mix design process to achieve the targeted engineering properties of the mixes.
- Conventional tests such as CBR and UCS were used in the past for mix design purposes and to determine the engineering properties of the cold mixes. However since 1990's ITS (splitting) tests are also used in an effort to account for flexibility behaviour. It appears however that flexible material property is not sufficient captured by ITS tests. Therefore recent research assesses the flexibility behaviour of cold mixes based on triaxial and four point beam bending tests. These tests improve the insight in the failure mechanism of cold mixes. However these tests are still at research level due to the cost of equipment and time requirement for the testing process.

2.6 REFERENCES

ACOTT S.M. and MYBURGH P.A. 1983. **Design and performance study of sand bases treated with foamed asphalt.** In: **Low-volume roads: 3rd International Conference.** Washington, DC: (Transportation Research Record; 898), pp 290-296.

- ACOTT S.M., 1979. **Sand stabilization using foamed bitumen.** 3rd Conference on Asphalt Pavements for Southern Africa, Durban, pp.155-172.
- AKERROYD F.M.L. and Hicks B.J. 1988. **Foamed Bitumen Road Recycling.** Highways, Volume 56, Number 1933, pp 42, 43, 45.
- AKERROYD F.M.M. 1989. **Advances in foamed bitumen technology.** In: 5th Conference on Asphalt Pavements for Southern Africa; (CAPSA), Swaziland, pp 1-4.
- AKZO NOBEL CHEMICAL, 1997. **Bitumen emulsifier,** Technical paper presented in 24th AEMA meeting, Conzun, Mexico.
- ANNAPOLIS, MD. 1991. **Guidelines for Cold- in Place Recycling,** Asphalt Recycling and Reclamation Association.
- ASPHALT ACADEMY. 2002. **Interim technical guideline: The design and use of foamed bitumen treated materials.** Pretoria: Asphalt Academy. (AsAc Technical Guideline TG2).
- BISSADA A.F. 1987. **Structural response of foamed-asphalt-sand mixtures in hot environments.** Asphalt materials and mixtures. Washington, DC: Transportation Research Board.(Transportation Research Record, 1115), pp 134-149.
- BOWERING R.H. and MARTIN, C.L. 1976. **Foamed bitumen production and application of mixtures evaluation and performance of pavements.** Proceedings of the Association of Asphalt Paving Technologists, Vol. 45, pp. 453-477.
- BOWERING R.H. 1970. **Properties and behaviour of foamed bitumen mixtures for road building.** Proceedings of the 5th Australian Road Research Board Conference, Canberra, Australia, pp. 38-57.
- BOWERING R.H. and MARTIN C.L. 1976. **Performance of newly constructed full depth foamed bitumen pavements.** Proceedings of the 8th Australian Road Research Board Conference, Perth, Australia
- BRENNEN M., TIA M., ALTSCHAEFFL A.G. and WOO L.E. 1983. **Laboratory investigation of the use of foamed asphalt for recycled bituminous pavements. Asphalt materials, mixtures, construction, moisture effects and sulfur.** Washington, DC: Transportation Research Board.(Transportation Research Record; 911), pp 80-87.
- BROWN SF, NEEDHAM D. 2000. **A study of Cement Modified Bitumen Emulsion Mixtures.** Proceedings Association of Asphalt Pavement Technologist, Reno, Nevada Vol. 69, Pp 92-121.

CASTEDO-FRANCO L.H., BEAUDOIN C.C., WOOD E.L. and ALTSCHAEFFL A.G. 1984. **Durability characteristics of foamed asphalt mixtures**. Proceedings of the 29th Annual Canadian Technical Asphalt Association Conference, Montreal, Canada.

CASTEDO-FRANCO L.H. and WOOD E.L. 1983. **Stabilisation with foamed asphalt of aggregates commonly used in low volume roads**. Low-volume roads: 3rd international conference. Washington, DC: Transportation Research Board. (Transportation Research Record; 898), pp 297-302.

CSANYI L.H. 1960. **Bituminous mixes prepared with foamed asphalt**. Ames, IA: Iowa State University, Iowa Engineering Experiment Station. (Bulletin; 189).

Dijkink H, 1992. **Immobilization of slag materials by foamed bitumen**. R&E consult. The Netherlands.

HORAK E., MYBURGH P.A. and ROSE D.A. 1984. **Rehabilitation of a cement treated base pavement**. Proceedings of the 4th Conference on Asphalt Pavements for Southern Africa, Cape Town, South Africa, Volume 1, pp 316-326.

LANCASTER J., MCARTHUR L. and WARWICK R. 1994. **VICROADS experience with foamed bitumen stabilisation**. 17th ARRB Conference, Proceedings in Gold Coast, Queensland, 15-19, Vol. 17, pp193-211.

LEE D.Y. 1981. **Treating marginal aggregates and soil with foamed asphalt**. Proceedings of the Association of Asphalt Paving Technologists, Vol. 50, pp 211-150.

LOUW L, 1997. **ETB mix design: Summary for the best practice**, Contract report CR96/079, Transportek, CSIR, Pretoria, South Africa

MACCARRONE S., HOLLERAN G., LEONARD D.J. and HEY S. 1994. **Pavement Recycling using foamed bitumen**. 17th ARRB Conference, Proceedings in Gold Coast, Queensland, 15-19, Vol. 17, pp 349-365.

MACCARRONE S., HOLLERAN G, and LEONARD D.J. 1993. **Bitumen Stabilisation - A New Approach to Recycling Pavements**. AAPA Members Conference

MYRE J, 2000. **The use of cold bitumen stabilization base course mixes in Norway**. Public road administration NRRL. Oslo.

OVERBY C, JOHANSEN R. and MATAKA M, 2004. **Bitumen foaming; An innovative technique used on a larger scale for pavement rehabilitation in Africa. Case study Same-Himo monitored pilot project.** Proceedings of the 8th Conference on Asphalt pavements for Southern Africa.

RAMANUJAN J.M. and FERNANDO D.P. 1997. **Foam Bitumen Trial at Gladfield-Cunningham Highway.** Proceedings of the Southern Region Symposium, Australia

ROBERTS FL, ENGELBRECHTJC, and KENNEDY TW, 1984. **Evaluation of recycled mixtures using foamed bitumen.** Transportation Research Records 968. Pp 78-85

RUCKEL P.J., ACOTT S.M. and BOWERING R.H. 1982. **Foamed bitumen paving mixtures: preparation of design mixes and treatment of test specimens. asphalt materials, mixtures, construction, moisture effects and sulfur.** Washington, DC: Transportation Research Board.

JENKINS KJ. 2000. **Mix design considerations for cold and half-cold bituminous mixes with emphasis on foamed bitumen.** PhD Thesis, University of Stellenbosch, South Africa.

JENKINS KJ, ROBROCH S, HENDERSON MG, WILKINSON J, MOLENAAR AAA, 2004. **Advanced testing for cold recycling treatment selection on N7 near Cape Town.** 8th conference on asphalt pavements for Southern Africa.

LONG, FM. 2002. **The development of structural design models for foamed bitumen treated pavement layers.** Pretoria: Transportek, CSIR. (Contract Report CR-2001/76).

JENKINS KJ., 1999. **Mix design considerations for foamed bitumen mixtures.** Conference on asphalt pavements for Southern Africa (CAPSA'99)., Swaziland

LONG, FM and Theyse, HL. 2003. **Mechanistic-empirical structural design models for emulsified bitumen treated materials.** Pretoria: Transportek, CSIR. (Contract Report CR-2003/44).

SAKR HA, and MANKE PG, 1985. **Inovations in Oklahoma foamix design procedures.** Transportation Research Records 1034.Pp 26-34.

SALEH MF, 2004. **New Zealand experience with foamed bitumen stabilization.** Annual TRB meeting USA.

SEMMELINK CJ, 1991. **The effect of materials properties on the compactibility of some untreated road building materials.** PhD Dissertation, University of Pretoria. South Africa.

SOUTHERN AFRICAN BITUMEN ASSOCIATION. 1993. **GEMS - The design and use of granular emulsion mixes**. Cape Town: SABITA Manual 14.

SOUTHERN AFRICAN BITUMEN ASSOCIATION. 1999. **ETB – The design and use of emulsion-Treated Bases**. Cape Town: SABITA Manual 21.

SOUTH AFRICAN BUREAU OF STANDARD, 1972. **Standard specification for anionic bitumen road emulsions**. Second revision. SABC 309-1972.

SHELL BITUMEN, 1991. **Shell bitumen handbook**. Shell bitumen South Africa.

THEYSE HL and MUTHEN M. 2000. **Pavement and Analysis Design software (PADS) based on the South African Mechanistic-Empirical Design Method**. Transportation Infrastructure, South African Transport Conference, Pretoria.

VERHAEGHE B.M.J.A and LONG F.M, 2004. **Cold in-place recycling with bitumen emulsion and foamed bitumen: South African perspective**. International Seminar on Asphalt Pavement Technology II, Kuala Lumpur, Malaysia.

CHAPTER 3

3. LITERATURE SURVEY ON FATIGUE PERFORMANCE OF BITUMINOUS MIXES

3.1 INTRODUCTION

Most materials bound by cement and/or bitumen show fatigue resistance properties that will resist the formation of tensile failure areas (cracks) when subjected to tensile stresses or strains. Fatigue by definition has been described as “phenomenon of fracture under repeated or fluctuating stress having a maximum value generally less than the tensile strength of the materials” (Airey, 1995). ASTM (1964) define fatigue as ‘the process of progressive localised permanent structural change occurring in a materials subjected to conditions that produce fluctuating stresses and strains at some point or points and which may culminate in cracks or complete fracture after a sufficient number of fluctuations”.

Fatigue, will therefore start when a material is repeatedly subjected to a load that induces a tensile strain in the materials. Early in their life, as a component in a pavement structure, the in-situ materials act similarly to a loaded beam. Tensile strains develop mainly at the bottom of these layers and will initiate the breaking up of the bonds formed by cement or bitumen. This will lead subsequently to the formation of cracks, which may in some cases be of microscopic size (Liebenberg, 2003).

Fatigue cracking is one of the major load-related distresses experienced in bituminous layers and it occurs when a pavement is subjected to repeated application of the induced traffic. The fatigue resistance of the mixes therefore is the ability of the mixture to resist cracking and fracture under this repeated bending.

The other modes of failure induced by repetitive nature of the loading on bituminous materials are permanent deformation and failure of bound materials through thermal and reflective cracking. Consideration of fatigue behaviour of bituminous materials is therefore important to be addressed in the mix design, analysis and pavement design in order to simulate the repeated stressing of the type encountered in-situ.

Characterisation of fatigue performance of hot asphalt mixtures has been intensively researched in past. Shell (1966), Pell (1965), Pell and Cooper (1975), SHRP (1992) and Delft University of Technology, are among those who researched in this area. Their research however was mainly using the dissipated energy approach, in which the number of cycles to fatigue failure is related to the amount of energy dissipated during repetitive loading using a dynamic bending test (rectangular and trapezoidal specimens) subjected to sinusoidal loading. However, fatigue behaviour of cold treated materials is relatively unknown. Research of cold

mixes has indicated that mixes with a relatively high binder content (foam >3.5% and emulsion > 2%) are considered to behave in a manner similar to HMA with the mixes exhibiting fatigue cracking at the bottom of the layer. However, for the mixtures with low binder content the behaviour of the materials will primarily be similar to that of untreated gravels or aggregates, SABITA (1993) and Marais and Tait (1989). Little et al., (1983) researched foamed bitumen mixes using controlled stress beam tests and found substantially lower fatigue lives for foamed bitumen mixes than for HMA and high quality emulsion. The binder contents were however, not considered in the study. Jenkins (2000) in research on half -warm foamed bitumen mixes found that cold mixes have less sensitivity to increasing strain level (fatigue cracks) compared to HMA, which has a steeper slope of the fatigue line as indicated in Figure 3.1

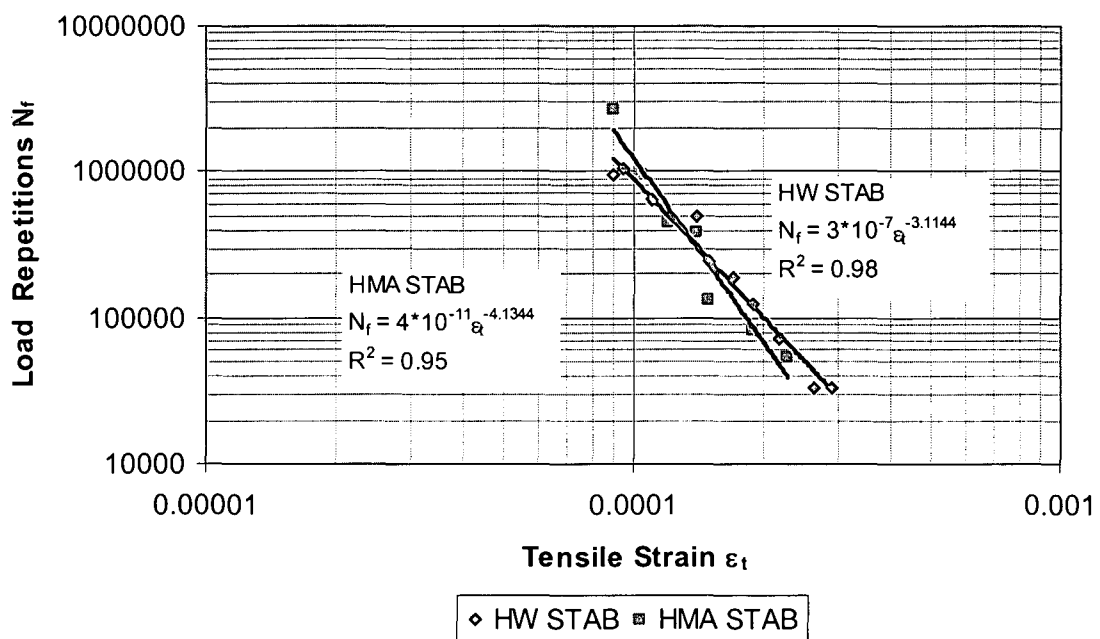


Figure 3.1: Fatigue characteristics of HMA and HW-STAB from 4PB test at 20°C in Displacement Control (10Hz), Jenkins, (2000).

Santucci (1977) and Marais and Tait (1989) used fatigue cracking at the bottom of the layer to characterize failure mechanism of emulsion treated materials. De Beer and Grobler (1994) described that the development of fatigue-like cracking in the layer started mainly at the bottom of the layer and progressing upwards through the weak areas and around the large aggregates. At an advanced stage most of the initial fatigue cracks emerge mainly around the large aggregates. The layer is then transformed into the fracture or advanced granular state. During this process, the elastic moduli of the emulsion treated materials reduce to levels known for unbound gravel materials. Theyse (1998) concluded that the general behaviour of emulsion treated materials is most likely to be equivalent to granular and lightly cemented materials. However, Wirtgen (2004) and Long (2001) argued that the term “equivalent granular state” implies that the effects of stabilisation are lost. This is a misleading concept because the

reduced stiffness levels of the treated materials are always far in excess of the untreated materials.

TG2 (Asphalt Academy, 2002) recommends triaxial and flexural testing to be used to assess the flexibility behaviour of cold mixes. However, these tests are not possible in many cases, because research done by Long and Ventura (2003) indicates that fatigue tests using 4PB on foamed bitumen mixes were not successful. Liebenberg (2003) also indicated that during fatigue testing using 4PB the specimen of emulsion mixes with no cement broke under their own weight when tested and no strain at break value could be obtained. However, the emphasis on specimen preparation was possibly insufficient. Different experiences have been observed by the author. Specimen preparation will be explored more in Chapter 4.

In this chapter, the development and assessment of the fatigue performance of bituminous treated materials will be addressed. This includes: overview of the fatigue testing with regards to different fatigue testing methods and the factors affecting fatigue responses (properties). Fatigue properties characterisation using different approaches is further explained, which includes: conventional, energy dissipated, and simplified methods. These methods are applicable to high binder content cold treated mixes. Fatigue relationship between laboratory testing results and field performance is discussed and finally the effective fatigue live analysis is presented and discussed.

3.2 PRINCIPLES OF FATIGUE TESTING

3.2.1 Overview of fatigue testing methods

There is a wide variety of possible fatigue testing procedures in both laboratory and field testing that could be applied to define the fatigue properties bituminous treated materials. These testing procedures involve a variety of test technique, equipment types, specimen configurations, type and modes of loading, test conditions (e.g. frequency of loading, temperature, etc) and analysis procedure (Tangella, et al., 1990).

The available test methods have been classified into the following categories (Tangella, 1990); Simple flexure, supported flexure, direct axial, diametral, fractural mechanics and Wheel-traffic testing (HVS).

The criteria used to evaluate each method for its potential use as a laboratory standard includes:

- Sensitivity to mixture variables,
- Reasonable ability to simulate field conditions,

- Prediction of fundamental properties that can be used in appropriate design performance models,
- Easy and simplicity of use,
- Time requirement to perform test,
- Ease of implementation and equipment costs, and
- Reliability, accuracy and precision.

Evaluation done by Airey (1995) indicated that based on advantages and disadvantages of the different fatigue testing methods mentioned above, the simple flexural test is the preferred method of defining fatigue parameters. The advantages of this test are; the method is well known, (widely used and readily understood), the results obtained can be used directly in pavement design and the basic technique can also be used for different concepts such as the dissipated energy and fracture mechanics.

Airey (1995) further indicated that, of the different simple flexure test, the third-point loading or four-point loading researched by Tangella (1989), Monismith (1981;1973), Deacons and Monismith (1967) or IPC (1998) respectively, are preferred to cantilever and centre-point load researched by Gerritsen and Jongenell (1988), Van Dijk (1977), Bennot (1972) and Bennaure et al, (1982), Kigham and Kallas (1972) because fatigue failure is initiated in a region of uniform stress. These methods were also confirmed during the SHRP-program.

Tangella (1990) provides a summary of the basic characteristic of the fatigue test methods. From the Table 3.1 it is apparent that repeated load diametral tests are different from other methods. It has a biaxial stress state while flexural, rotating cantilever and axial tests have a uniaxial state of stress. Flexural tests use pulsing load of triangular or square shape, while rotating cantilever has a continuous sinusoidal loading. The axial test uses a sinusoidal or haversine pulse with or without a rest period. Generally, a continuous loading pattern, such as that used in rotating cantilever test, usually yields a smaller fatigue life.

Pronk (1999) commented that due to difference in tests configurations i.e. four point beam (4PB), two point trapezoidal (2PB), semi-circular bending (SCB) and circular bending (NAT) and interpretations of these tests methods, harmonization of the different tests to obtain the same fatigue lives are not possible. However, he suggested that in the evaluation of fatigue lives using dissipated energy approach, it is possible with Weibull volume effect to statistically account for the observed differences.

Table 3.1,a: Summary of fatigue tests characteristics: Tangalle,(1990)

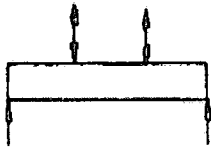
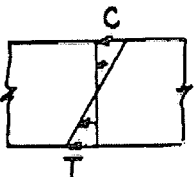
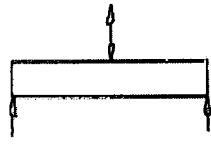

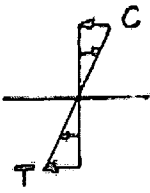

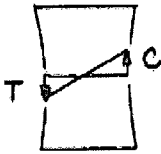
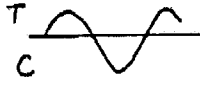
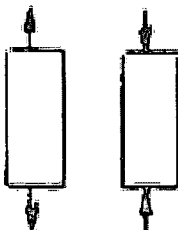
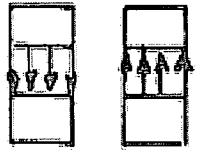
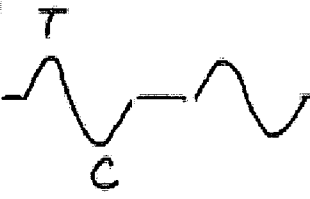
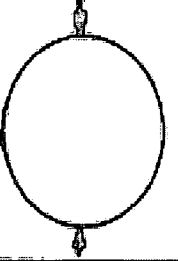

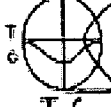


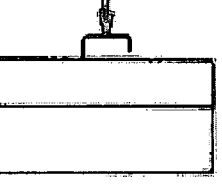
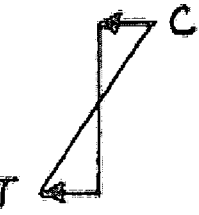
Test	Loading Configuration	Stress Distribution	Loading Waveform	Loading Frequency, cps	Performance Deformation Allowed?	State of Stress	Does failure occur in a Uniform Bending Moment or Tensile Stress Zone?
Third Point Flexure			Halfsine Load Rest - 1.9	1-1.67	No	Uniaxial	Yes
Center Point Flexure		Same as above	Sine, Triangular Rectangular Load Rest - 1:100 max	1:100	No	Uniaxial	No
Cantilever			Sine (Bonnot), Sine, Triangular Load Rest - 1:100 (van Dijk) max	25 (Bonnot) 1:100 (van Dijk)	No	Uniaxial	No
Rotating Cantilever				16.67	No	Uniaxial	Yes

Table 3.1,b: Summary of fatigue tests characteristics, (Tangella,1990)

Test	Loading Configuration	Stress Distribution	Loading Waveform	Loading Frequency, cps	Performance Deformation Allowed?	State of Stress	Does failure occur in a Uniform Bending Moment or Tensile Stress Zone?
Axial				8.33-25.0	No	Uniaxial	Yes
Diametral		<p>Horiz </p> <p>Vert </p>	<p>Horizontal </p> <p>Vertical </p>	1.0	Yes	Biaxial	No
Supported Flexure (Beam)			Haversine	0.75	Yes	Uniaxial	No

Raithby and Sterling (1972) indicate that three continuous loading pulses are applied by a moving wheel over a pavement layer, in lieu of single pulse applied in the laboratory (i.e. compressive stress as wheel approach the layer, then tensile stress as the wheel moves over the point, and finally a compressive stress again as the wheel moves away). Therefore, the magnitude of the initial compressive strain is approximated as one seventh that of the tensile strain pulse at the bottom of the pavement layer. Barksdale (1977) commented that without this small initial compressive stress pulse, the decrease in fatigue life should have been at most in the order of only 10 to 15 percent.

3.2.2 Factors affecting fatigue response

The results from any fatigue tests are dependent on the following factors (Porte, 1975 and Adedimila, 1975):

- Method of specimen preparation (compaction)
- Mode of loading consideration, and
- The influence of the variables which are grouped as follows;
 - Mixture variables
 - Loading variables
 - Environmental variables

3.2.2.1 Specimen preparation

The objective of specimen preparation or compaction is to produce realistic test specimens in the laboratory that, reasonably duplicate the corresponding in-situ paving, in respect to: mix composition, density and engineering properties. Researchers have indicated different methods of compaction utilised to fabricate test specimens such as: static compaction, impact compaction, gyratory compaction, and rolling wheel-compaction.

Von Quintus et al., (1988) indicated that compaction of HMA specimen should be done at selected temperatures such that the asphalt viscosity is maintained by pre-heating the mould, compaction foot, tamping rod etc. However in cold mixes all mixing and compaction is done at ambient temperature, (Jenkins 2000). ARE (1986) commented that laboratory compaction such as static compaction (double plunger) and impact compaction (Marshall, using free fall hammer) have a major disadvantage in that the orientation of aggregate particles is different from that obtained in the field in-situ condition, and, hence does not accurately simulated the field conditions. A further disadvantage is that impact compaction employs a high energy transfer on impact, which may cause rupture of bitumen film and also pack aggregates on top of each other. Therefore it is doubtful that the impact compaction procedure results in specimens that duplicate paving conditions.

However, ARE (1980a) indicated that laboratory kneeding compaction induces deformation and particles orientation which are similar to those which take place in field. Therefore laboratory specimen preparation using kneeding action have both physical and mechanical properties equivalent to those of field cores. This is therefore a suitable method for the preparation of beam specimens for fatigue testing.

Von Quintus et al., (1988) indicated that the gyratory shear compactor is unable to fabricate test specimens other than cylindrical shape. Nevertheless he concluded that, based on comparison of various stiffness and strain parameters measured on cores obtained immediately after construction with same parameters obtained from specimens prepared in the laboratory gyratory compactor, the gyratory shear compactor produces specimens that are representative of asphalt materials compacted in-situ. Visser et al., (2004) indicated that the major advantage of gyratory compactor over standard Marshall compaction is to monitor volumetric properties with increasing number of load repetitions, which enables simulation of the compaction that occurs as a result of traffic after the construction is completed.

Von Quintus et al., (1988), Bonnot (1986) and Van Dijk (1975) showed that rolling-wheel compaction can closely simulate field compaction where aggregates particles are oriented and the density of the mixture closely corresponds to field compaction. This method has been adopted for compacting slab-size specimens (500mm x 150mm x 100mm) using a small-scale compactor (Brown and Cooper, 1984). Tangella (1990) suggested that laboratory compaction using rolling-wheel, kneeding and gyratory methods produces HMA test specimens that are more like the in-situ pavement properties than either static or impact compaction. However, Jenkins (2000) indicated that ideal laboratory compaction technique for cold mixes to provide the link between laboratory and field compaction is not yet defined.

In the literature survey it was indicated that the possible effect of the compaction method on the fatigue response of bituminous materials has not been fully investigated. However fatigue testing programs should be carried out to define the relative effect of compaction techniques on the mix performance. Orientation of the test specimen relative to compaction direction should be such as to ensure that the in-situ situation is correctly modelled (e.g. cutting of a beam from a rolled slab or drilling of a cylindrical core from a rolled slab for direct tension fatigue testing should be in the direction of compaction to maintain orientation and binding of the aggregates in the mix).

3.2.2.2 Mode of Loading

The fatigue life or service life of the test specimen depends on the mode of loading used during the fatigue test. That is the method by which stress and strain are permitted to vary during repetitive loading. Test loading conditions range from the load controlled (controlled-stress) mode where the load or stress amplitude is maintained constant to displacement

controlled mode where the displacement or strain amplitude is maintained constant. Monismith et al., (1977) indicated that mixtures tested in displacement controlled (controlled strain) mode have longer fatigue life than those tested in load controlled tests with all other variables kept constant. The difference between the results of the two modes of testing can be explained in terms of crack propagation through the mixture.

In load controlled test, initiation of crack results in a reduction in the stiffness of the specimen and a subsequent increase in applied energy so that the crack is propagated almost instantaneously. In displacement controlled test considerable time is required to propagate the crack before the specimen is considered to have failed.

Monismith et al., (1977) further indicated that depending on the temperature (and hence mixture stiffness) the results of these tests may be quite different hence leading to varied mixture designs. Monismith and Deacon (1969) proposed qualitative means of differentiating between two modes of loading using a mode factor (MF) and thereby deciding which method of loading is preferable for a particular mixture. The MF is defined as:

$$\text{Mode factor, (MF)} = \frac{|A| - |B|}{|A| + |B|} \quad (3.1)$$

Where, $|A|$ and $|B|$ are the percentage changes in stress and strain respectively, for an arbitrary but fixed percentage reduction in stiffness. The mode factor has a value of -1 for load controlled loading condition and +1 for displacement controlled loading conditions.

Controlled-strain fatigue conditions occur when almost all the applied load is supported by the underlying layers so that the deflections in the bituminous treated materials are substantially independent of the stiffness of the bituminous mixes. Load controlled fatigue conditions occurs when the bituminous layer is relatively thick (> 150mm) and supports a significant portion of the applied load.

Generally, increased mix stiffness results in longer lives at a given stress level in controlled stress testing, and shorter lives in controlled strain testing at a given strain level. The reason is that, in a controlled stress test the formation of crack results in an increase in the actual stress at the tip of the crack due to the stress concentration effect. This leads to a rapid propagation and complete fracture of the specimen and termination of the test. In a controlled strain test, cracking results in a decrease in stress concentration and hence a slow rate (longer time) of crack propagation to failure of specimen.

The stiffness modulus in tension is different to the modulus in compression for test specimens. In tension the entire load is carried by the binder while in compression, the combination of aggregates structure and binder contribute to the formation of stronger structure.

Tangella (1990) indicated that the research on the fatigue life of bituminous mixes beam specimens concluded the following:

- At a given stress levels in load controlled testing, stiffer mixtures have greater fatigue resistance. This indicates that under load controlled testing conditions stiffer asphalt mixtures will have longer fatigue lives than softer asphalt mixtures.
- At a given strain levels in displacement controlled testing stiffer mixtures have less fatigue resistance (negative stiffness power in displacement controlled models regresses on strain). This indicates that under load controlled testing conditions softer, or more flexible asphalt mixes will have longer fatigue lives than stiffer mixes.
- In general, fatigue lives determined under displacement controlled loading are approximately 2.4 times longer than those determined under load controlled loading (for condition at which the test were performed).

Pell (1973) suggested that, based on the mode factors obtained on an experimental pavement the controlled-strain fatigue testing is suitable and applicable for thin asphalt surfacing (< 50mm thick) and controlled-stress tests for thicker, stiffer layers (greater than 150mm thick). However Airey (1995) indicated that although Pell (1973) suggested thicker layer as 150mm, but 100mm is probably more applicable and better for pavement design purposes.

3.2.2.3 Mixture variables

In general, the stiffness of bituminous mixtures is closely related to its fatigue behaviour. The mixtures variables that affect the stiffness also affect the fatigue life. The mixture's variables such as binder content, binder type, aggregates type and grading, and active filler percentages directly influence fatigue performance (Long et al., 2003 and Jenkins, 2000).

The binder content of the mixture directly affects the resistance of the mixture to fatigue cracking. Fatigue resistance increases as binder content increases (Long et al., 2003). Foamed bitumen mixes with higher binder contents (>3.5%) and emulsion (>5%) are considered to behave in a manner similar to HMA. Jenkins (2000) and SABITA, (1993) state that an optimum binder content exists for a maximum fatigue life, but it depends on the type and grading of the aggregates used. TG2 (Asphalt Academy, 2002) recommends that the grading of foamed bitumen mixes have a minimum filler content of 5% to produce good quality mixes.

The GEMs Manual (SABITA, 1993) shows that non-plastic materials respond well to bitumen emulsion. However, aggregate properties have greater influence in breaking results of

emulsion in the mixes. The effects of these variables on fatigue life are summarized in Table 3.2, as reported by researchers in various literature publications.

Table 3.2: Factor affecting stiffness and fatigue behaviour of bituminous mixes, (Tangella et al., 1990)

Factor	Change in factor	Effect of change on factor ^a		
		On Stiffness	On fatigue life controlled-stress	On fatigue life controlled-strain
BINDER				
Viscosity	Increase	Increase	Increase ^c	Decrease
Content	Increase	Increase ^b	Increase ^c	Increase
Temperature	Decrease	Increase	Increase ^c	Decrease
AGGREGATES				
Type	Increase surface texture	Increase	Increase ^c	Increase
Gradation	Open to Dense	Increase ^b	Increase ^c	Increase
Air voids content	Decrease	Increase ^b	Increase ^c	Increase

a- For continuous graded mixture

b- Optimum at level above that reaches affect the mixture performance

c- No significant data

Tensile stresses are needed to propagate cracks in materials, since the bonding of crystalline solid materials is generally much stronger than the bonding of amorphous materials, such as bitumen, and much stronger than the bond which develops between the binder and aggregates. The fracture behaviour of the binder is the primary controlling factor in the crack propagation of bituminous mixture (De Beer and Grobler, 1994).

The stability of cold mixes is ensured by having binder dispersed (foam) with a thin film coating the filler and coarse aggregates (Jenkins, 2000). Breaking of emulsion and binder adhesion on coarse aggregates and evaporation of water through curing will increase the fatigue resistance of the mixture (Wirtgen, 2004; Colas, 2003 and Brown, 2000).

Depending on the filler content, a filler-binder ratio higher or lower than the design ratio may be beneficial or detrimental to the fatigue characteristics of cold mixture. The ability of foamed bitumen to selectively mix with and coat the fines (mix of bitumen and fines) results in higher viscosity than that of the raw bitumen and acts as mortar between the coarse aggregates, increasing the strength of the mix. Sakr and Manke (1985) showed that foamed bitumen mixes

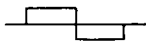
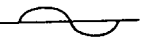
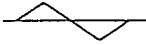
with a higher percentage of fines had higher stability (easy to compact and subsequently lower air voids), while Bisanda (1987) found a similar trend for the tensile strength.

Jenkins (2000) indicated that good mixt design and appropriate compaction techniques will eliminate the high in-situ void content and thereby improving the fatigue resistance of the cold mixes. The fatigue life of bituminous treated materials is direct related to the active filler content as well as to the void content of the mixture. The higher the active filler content, the higher the tensile, compressive and structural strength of the mixture. This results in increasing susceptibility to cracking (Long et al., 2003). Similarly, the greater the air voids content, the lower the tensile, compressive and structural strength of the mixture (Jenkins, 2000). This may result in an increased susceptibility to cracking and hence to reduced fatigue properties of the mixture.

3.2.2.3 Load variables

Loading variables have direct implications for the fatigue life of the mixture; these include the shape and duration of the load pulse, rest period and frequency of loading in the laboratory. Research on HMA performed by Raithby (1972) and Raithby and Sterling (1970) indicated that the type of waveform has a significant influence on the fatigue life of an asphalt mixture. It was found that relative to sinusoidal waveforms, the square waveform produce as shorter fatigue life (relative life of 0.42) and the triangular waveform a longer fatigue life (relative life of 0.45). Table 3.3 summarises the effect of the waveform shape on fatigue life. AUSTROAD (1999) indicates that a haversine waveform is commonly used in USA and sinusoidal waveform is commonly used in Europe.

Table 3.3: Effect of shape of waveform on fatigue life of HMA, (Raithby and Sterling, 1972)

Waveform	Temp, °C	Stress Amp MN/m ²	Initial Strain Amp*	Geometric Mean Fatigue Life, Cycles	Relative Lives
	25	±0.33 (48 psi)	1.7 x 10 ⁻⁴	24,690	0.42
	25		1.2 x 10 ⁻⁴	58,950	1.0
	25		0.67 x 10 ⁻⁴	85,570	1.45

*The values are approximately of 200cycles.

Raithby and Sterling (1970) further commented that if the length of the rest period for a given load duration is increased (low frequency), the fatigue life increases. However there is a limit to which the rest period can be increased to extend the fatigue life. This limit was found to be dependent on the testing temperature. Load duration also has a significant effect on fatigue life. With longer load durations (high frequency for a given rest period) a decrease in the fatigue life of bituminous mixtures is observed.

Work by Raithby and Sterling (1970) and by Van Dijk et al., (1977) showed a considerable beneficial effect of strain recovery if a rest period is present between each load pulse. Therefore laboratory test using continuous loading may well underestimate the fatigue life needed to cause crack initiation in practice. Van Dijk et al., (1977) established empirical relationships for asphalt mixes which estimates the loading time associated with traffic load as follows:

$$\text{Loading time (sec)} = \frac{1}{\text{Traffic speed (Km/h)}} \quad (3.2)$$

Hence, Van Dijk commented that typical loading time representing in the field are as follows:

- Fast moving traffic, 0.01 – 0.1second,
- Breaking and accelerating traffic 0.1 – 1.0 second, and
- Parking vehicles, 1.0 – 10hrs.

However a loading rate of 0.016 second corresponds to a traffic speed of approximate 60km/h which relates the triangular loading frequency of 62.8rad/sec for a sinusoidal loading waveform. An angular loading frequency of 62.8rad/sec is equivalent to a 10Hz sinusoidal waveform. Therefore a loading frequency of 10Hz is generally accepted as a reasonable simulation of randomised traffic for fatigue testing (Airey, 1995).

In most fatigue testing methods creep or permanent deformation is eliminated by the specimen being forced back to its original undeflected position. However Airey (1995) and SHELL (1966) indicates that under field conditions, fracture of materials is the result of progressive internal damage, which can occur as both fatigue and creep fracture. Manson (1968) suggested that at failure the percentage of creep-rapture damage plus the percentage of fatigue damage should be equal to 100%. However, the creep component in fatigue testing is generally limited by testing the bituminous mixture in its elastic stiffness region through the application of high loading frequencies and low testing temperature. The creep component is therefore usually not considered during laboratory testing.

3.2.2.5 Environmental variables

Environmental factors influence the fatigue resistance of a bituminous mixes in two ways, (Jenkins et al., 2004; Brown, 2000 and Long et al., 2003). Firstly, there are the immediate effects produced by moisture and temperature. Secondly, there changes in fatigue characteristics that occur with time, due to changes in the materials properties, i.e. effect of curing, and ageing of the binder.

In a thin layer constructed on a weak foundation, the increased stiffness resulting from hardening of the binder will reduce the fatigue life of the layer. In the case of a relative thick layer constructed on a strong foundation, an increase in the stiffness of the binder will usually result in an increase the fatigue life of the mixture into which is incorporated (Vallerga et al., 1967) and (Van de Ven, 2004).

However the most important environmental factor in laboratory testing is temperature. Fatigue life is found to increase with decreasing temperature in load controlled and displacement controlled tests, due to the materials behaving less visco-elastic to plastically and more elastically.

There is considerable confusion as to which temperature conditions are the most critical for fatigue failure of cold mixes. For HMA, Demons and Metacalf (1964) suggested a temperature of 10°C to 15°C. Brown and Pell (1970) suggested that the average road pavement temperature should be used for the determination of the fatigue performance, further Pell (1965) suggested that fatigue initiate during the hotter part of the year, although the cracking probably only propagate during the cold period.

CSIR (1993) suggested a temperature of 5°C to be used for fatigue testing, however this may overestimate the fatigue life while in the field temperature in South Africa varies from 0°C to 40°C depending on the period of the year. Mullins (2006) found that beam fatigue test at high temperature 10°C and 20°C allow shear cracking to occur at the beam support. However found that 5°C provide a beam failure at the high uniform stress concentration i.e central third section of the test beam specimen. However, an adjustment factor would be therefore necessary to relate laboratory to actual field temperature condition (see section 3.4).

Hawtrey (1964) suggested that crack initiation in HMA under fast moving traffic takes place at low temperatures. There seems to be no definite critical temperature and therefore the resistance of an asphalt mixture probably needs to be determined at high and low temperatures. However Freeme (1971) hypothesised that for pavements with thin surfacings (<50mm thick) the minimum fatigue life is at low temperature conditions. The opposite is true for thick bituminous layer where maximum temperature conditions are most critical with regards to fatigue life.

3.3 FATIGUE PROPERTIES CHARACTERISATION USING DIFFERENT APPROACHES

3.3.1 Conventional approach

Fatigue cracking is considered to be a tensile phenomenon. It is the repetitive application of tensile forces, at levels considerably below that required to induce immediate fracture that is responsible for the initiation and propagation of fatigue cracks. Researchers have found that fatigue life is better correlated with tensile strain than with tensile stress. In the conventional approach (basic failure using Wöhler-type fatigue relationship) the number of load applications to failure, N_f is empirically related to the maximum tensile strain occurring at the bottom of the asphalt layer, ε_t as follows;

$$N_f = a(\varepsilon_t)^n \quad (3.3)$$

Where,

N_f	= number of load applications to failure (fatigue life)
ε_t	= initial strain at the bottom of the bituminous layer (the applied tensile strain)
a, n	= experimental determined materials coefficients

The fatigue parameters a , and n are experimental determined coefficients that vary depending on mixture properties, temperatures and the methods of testing. The relationship is therefore only applicable to the type of bituminous mix tested. Some researchers, Monismith et al., (1985) and Medani and Molenaar (2003) suggested a relationship that is more applicable to asphalt where frequency and temperature varies, and includes the initial mixture stiffness (S_o) with additional parameter (c) in equation 3.3 as follows;

$$N_f = a\left(\frac{1}{\varepsilon_t}\right)^n \left(\frac{1}{S_o}\right)^c \quad (3.4)$$

Where,

N_f	= fatigue life
ε_t	= initial tensile strain
S_o	= initial mixture stiffness
a, n, c	= experimental determined coefficients

Pell and Cooper (1975) indicated that the fatigue life for some materials at different temperatures are presented by the line in Figure 3.2 that is approximately parallel with longer fatigue lives at higher temperature (low stiffness, S_2 under controlled-strain loading condition). A similar effect would be found if tests were carried out at different speeds, with longer lives being found at higher speeds. If the results of the fatigue tests are plotted in terms of strain, ε_t as shown in Figure 3.3, then it will be found that the results from different stiffness coincide, indicating that strain is the criterion of failure.

The effect of temperature and speed of loading are accounted for by their effect on stiffness. This phenomenon is known as the strain criterion in fatigue performance (Cooper, 1992).

Medani and Molenaar (2003) indicated that at low temperature and short loading time the bituminous material are brittle and at higher temperature and high loading time the bituminous materials is flexible. Hence brittle fatigue behaviour shows high n value while flexible behaviour shows low n value.

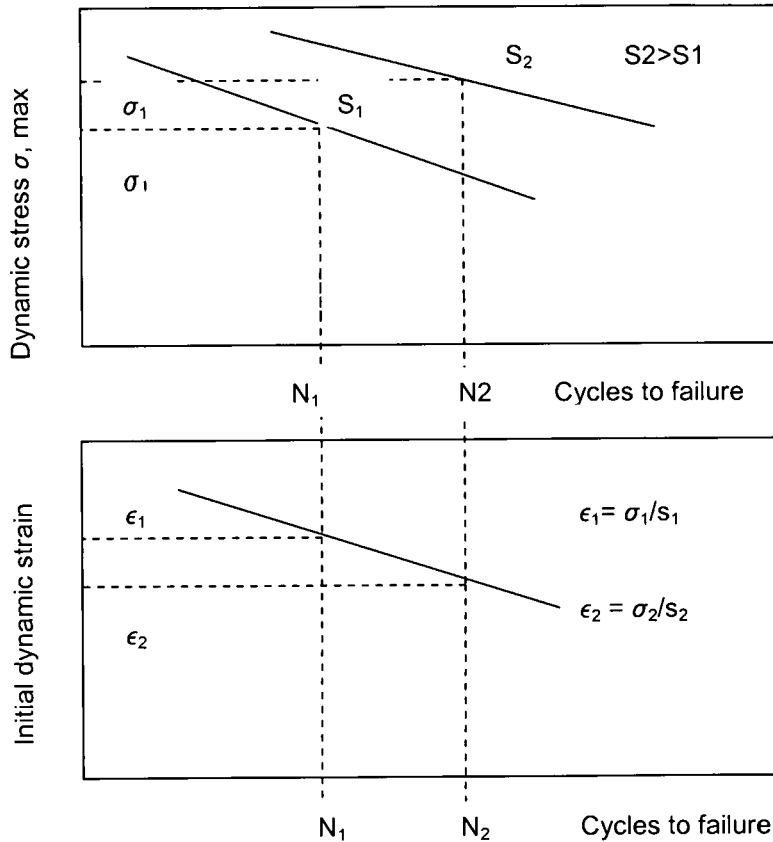


Figure 3.2 and 3.3: The strain criteria, (Pell and Cooper, 1975).

3.3.3 Dissipated energy approach

Literature has advanced the notion that a possibly unique relationship might exist between the number of cycles to failure and the cumulative energy dissipated during repetitive loading (Van Dijk et al., 1977; Tangell, 1990; Tayebali et al., 1992 and Pronk, 1999). They used an energy approach for describing fatigue behaviour and showed that the “total” or “cumulative” dissipated energy to failure is related to fatigue life as follows:

$$N_f = aW_N^{-z} \tag{3.5}$$

- Where:
- N_f = fatigue life
 - W_N = cumulative dissipated energy to failure
 - a, z = experimental determined coefficients

These two different approaches to characterisation of the fatigue behaviour of bituminous mixture, the conventional approach and the energy approach, can be shown to be special

cases of the general fatigue relationship. In the conventional approach, the fatigue life is related to initial test conditions, namely initial strain and initial stiffness. In the dissipated energy approach, the fatigue life is related to a terminal test condition, namely, cumulative dissipated energy to failure. Neither approach directly addresses the problem of how damage to a mixture actually develops as loading accumulates from the beginning to end. Crack initiation and propagation are therefore not analytically assessed.

Van Dijk and Visser (1977) indicated that cumulative dissipated energy to failure, W_N is related to the energy dissipated during the i^{th} cycle w_i , as follows:

$$W_N = \sum w_i \quad (3.6)$$

For sinusoidal loading:

$$w_i = \Pi \epsilon_i^2 S_i \sin \phi_i \quad (3.7)$$

Where:	w_i	= dissipated energy at loading cycle i
	ϵ_i	= strain amplitude at loading cycles i
	S_i	= mixture stiffness at load cycle i
	ϕ_i	= phase shift between stress and strain at load cycle i

For controlled-energy loading, the dissipated energy per cycle remains constant during the test and the cumulative dissipated energy is simply the product of the initial dissipated energy per cycle, w_o , and the number of cycles to failure, N_f :

$$W_N = w_o N_f \quad (3.8)$$

or

$$N_f = \frac{W_N}{\Pi \epsilon_o^2 S_o \sin \phi_o} \quad (3.9)$$

Where:	ϵ_o	= initial strain amplitude
	S_o	= initial mixture stiffness
	ϕ_o	= initial phase shift between stress and strain

Van Dijk (1975) indicated that other than controlled-energy mode of loading, a mode of-loading dependent energy ratio factor may be useful. The energy ratio factor, Ψ is defined as:

$$\Psi = \frac{N_f w_o}{W_N} \quad (3.10)$$

The energy factor, Ψ mainly depends on the test and the mixture stiffness, as shown in Figure 3.4 (Van Dijk, 1975). From the definition of Ψ , it will be clear that for controlled-stress $\Psi \leq 1$ and

for controlled strain test $\Psi \cong$. If the materials are fully elastic ($S_{mix} \approx 26\text{GPa}$) there should no difference between controlled stress and controlled strain tests.

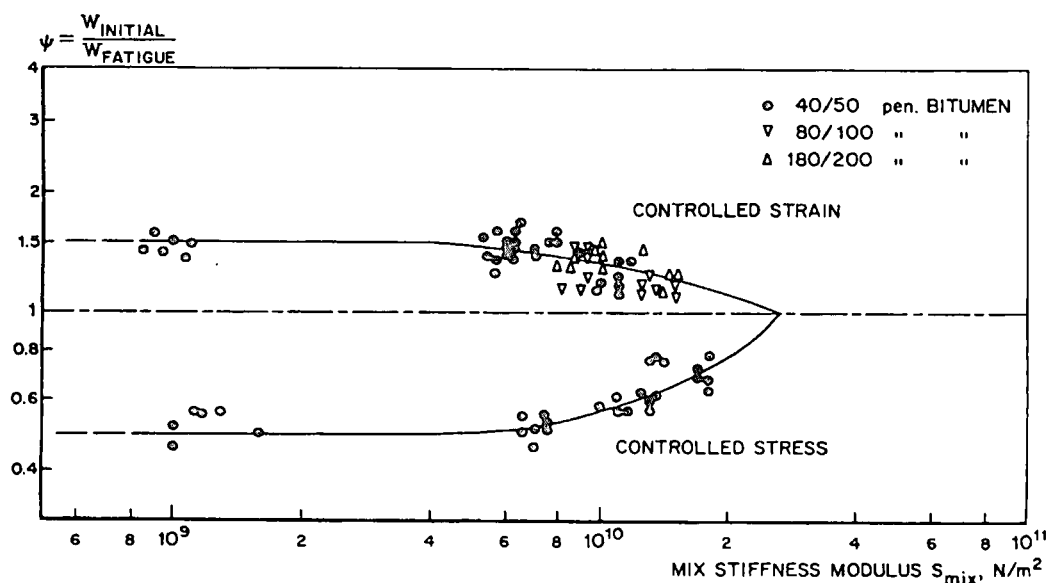


Figure 3.4: Relation between energy factor Ψ , and mixture stiffness, (Van Dijk, 1975)

If Ψ is taken into consideration, the following equation is obtained;

$$N_f = \frac{W_N \Psi}{\Pi \epsilon_o^2 S_o \sin \phi_o} \quad (3.11)$$

and generalising for the purpose of regression analyses:

$$N_f = A (W_N)^a (\Psi)^b (\epsilon_o)^c (S_o)^d (\sin \phi_o)^e \quad (3.12)$$

The general fatigue relationship equation 3.12, indicates that, for any mode of loading (controlled-stress, controlled-strain), fatigue life is a function of both the cumulative dissipated energy, W_N , and the initial energy per cycle, w_o :

$$N_f \propto W_N w_o \quad (3.13)$$

Or
$$N_f \propto W_N \epsilon_o S_o \phi_o \quad (3.14)$$

For all fatigue laboratory tests in which, in addition to stress and strain, the phase angle between the two can be measured. It is possible, with the relation given above to calculate the total dissipated energy during the test up to any number of loading cycles.

The dissipated energy approach lends itself ideally to the characterisation of the fatigue resistance of a particular mixture. Furthermore, this method is based on the physical

phenomenon that explains the fatigue behaviour of visco-elastic materials through the accumulation of the distortion energy resulting from load repetitions. However, for it to be used in mechanistic design, the factor Ψ , Φ and W_N have to be determined.

3.3.3 Simplified approach

In the preceding section the relation between the phase angle and energy ratio factor as a function of the stiffness modulus of the bituminous mixes and the relation between the total dissipated energy per unit volume and the fatigue life were dealt with. In many cases, these data are not available. These relationships however can be simplified if reduced accuracy is acceptable, which in some pavement design studies might be the case:

For those circumstance the following is suggested;

- use the data from other mixtures which resemble the mixture in question, or
- carry out a set of fatigue tests when increase accuracy is required.

To predict fatigue performance for pavement designs purposes, a number of simplified procedures have been adopted (Brown et al., 1982; Shell, 1990; Asphalt Institutes, 1982 and AASHTO, 1977). The Nottingham University developed a general relationship between tensile strain, the number of loadings to failure, binder content (volume basis), and the ring-and ball softening point of bituminous mixes as follows:

$$\log \epsilon_t = \frac{14.39 \log V_B + 24.2 \log T_{RB} - 46.06 - \log N}{5.13 \log V_B + 8.63 \log T_{RB} - 15.8} \quad (3.15)$$

Where:	ϵ_t	= allowable tensile strain
	N	= number of load applications to failure
	V_B	= binder content by volume (%)
	T_{RB}	= initial binder ring and ball softening point ($^{\circ}\text{C}$)

In the Shell approach the fatigue strain is estimated from the following expression:

$$\epsilon_t = (0.856V_B + 1.08) S_{\text{mix}}^{-0.36} N^{-0.2} \quad (3.16)$$

Where:	ϵ_t	= allowable tensile strain
	N	= number of load application to failure
	V_B	= binder content by volume (%)
	S_{mix}	= stiffness of the mixture.

The predicted fatigue strain determined by means of the above model does not differ from the actual one by more than 30 to 40 percent.

In the Asphalt Institute's methodology use is made of the expression:

$$N = 18.4 C \left(4.325 \times 10^{-3} \epsilon_t^{-32.91} S_{\text{mix}}^{-0.854} \right) \quad (3.17)$$

The variable in this expression are the same as those for Equation 3.16, C is a correction factor obtained from,

$$C = 10^M \quad (3.18)$$

Where:

$$M = 4.84 \left(\frac{(V_B)}{(V_A + V_B)} - 0.69 \right) \quad (3.18a)$$

V_v = air void content in the mixture

The phenomenological relationship reported by the Finn et al., (1977) based on laboratory and field data from the AASHTO is defined as follows:

$$\log N_f = 15.947 - 3.219 \log \epsilon_t - 0.854 \log \left(\frac{E^*}{10^3} \right) \quad (3.19)$$

Where:

N _f	= number of 80kN passes which causes 10 percent fatigue cracking in the wheel pass.
ϵ_t	= repeated tensile strain ($\times 10^{-6}$)
E^*	= complex modulus of asphalt (psi) which can be approximated by the resilient modulus (M_R)

In all these relationship, the property of the bituminous mixes is reflected in either the ring-and-ball softening point temperature or the asphalt stiffness. It is emphasised however, that these relationships are merely an approximation and should therefore be considered for pavement design only and not for mixture evaluation.

3.4 FATIGUE RELATIONSHIP BETWEEN LAB AND FIELD PERFORMANCE

A major difficulty with fatigue is developing meaningful relationship between the results of the laboratory tests and field performance. The fatigue life of a pavement determined from laboratory fatigue tests is generally lower than observed in the field (Jenkins, 2000). SHELL (1978) indicates that factors such as crack propagation, traffic wander and even periodic "healing" result in highway pavements being able to sustain from 10 to as much as 100 times the number of load applications as found in the laboratory to their ultimate distress condition.

3.4.1 Shift factor

To account for differences between laboratory and field response, shift factors are necessary to translate laboratory fatigue characteristics to those considered to be representative of in-situ performance. However there is no unique relationship for cold mixes. Shift factors are dependent on the testing methods used to determine fatigue life and on the testing environment. For example diametral fatigue tests underestimate fatigue life considerably by comparison with simple flexure tests. Larger shift factors are required for the former. Also, strain-controlled testing results in fatigue lives in excess of those measured in the stress-controlled mode. The former will thus require lower factors. In the field, compressive (or tensile) residual stress can remain at the bottom of the surface layer after the passage of each load and hence “prestress” the layer so that the tensile stress that occurs when the next heavy load passes cause much less (or much more) fatigue damage, depending on whether the bituminous layer accumulates more (or less) residual stress than the base course layer beneath it. In the field, these residual stresses will remain. In the laboratory, residual stresses also build up in the fatigue samples but these have less opportunity to relax with time, thus contributing to a reduction of fatigue life.

The temperature at which the test is carried out and the rest period also influence the shift factor. It appears that when laboratory fatigue test are conducted at higher temperatures, the shift factor may be lower than when the tests are conducted at lower temperatures. This might be contributed to the healing effect of bituminous materials at high temperature. For tests in which specimens have been flexed at high rates of sinusoidal loading, much greater shift factors have been found than for tests in which rest periods between load applications have been incorporated. In addition the shift factor also depends on the thickness of bituminous-bound layer, increasing as the thickness of the layer increases.

The shift factor for HMA determined by researchers varies from slightly more than one to in excess of four hundred. For cold mixes limited research has done on that factor. Generally, more is known about the laboratory testing than from field observations. Moreover, established correlations between laboratory data and field response are weak. Brown and Pell (1972) suggested that the in-service pavement fatigue life is of order of 20 times the life of test specimen in the laboratory. They also concluded that probably the best that can be achieved with laboratory –derived failure criteria is to obtain an estimate of crack initiation in the in-service pavement.

Kingham and Kalls (1972) investigated the relationship between laboratory fatigue and pavement performance. They found that the results of laboratory, flexural beam, fatigue test over-predicted the actual number of repetitions to failure. The failure of the asphalt field sections was taken as the point where cracks initiated at the bottom of the asphalt layer. Regarding the laboratory fatigue tests, the controlled-stress tests predicted the fatigue life of

the full-depth asphalt pavement better than the controlled –strain tests. This is expected since controlled-stress tests produce fatigue life results for crack initiation, while the controlled-strain tests tends to include an amount of crack propagation in their fatigue life results.

3.4.2 Transfer function

The failure mode for each material type is linked to a critical parameters at a specific position in the pavement structure under loading, Theyse (1998) defines transfer functions for the relationship between the value of the critical parameter and the number of load applications that can be sustained at the value of the critical parameters, before the particular materials type fails in a specific mode of failure. For instance, the failure mode of granular materials is deformation due to densification and a gradual shear under repeated loading (Maree, 1978). Critical parameters are safety factor and major and minor principal stress. For cemented materials the failure mode is effective fatigue and crushing (De Beer, 1998). Critical parameters are maximum tensile strain, ($\mu\epsilon$) at the bottom of the layer during the effective fatigue phase, the stresses in the layer during the equivalent granular phase effective life and vertical compressive stress, σ_v (KPa) on top of the layer in terms of crushing.

For bituminous treated materials, the failure mode is fatigue cracking under repeated loading and critical parameter is maximum tensile strain ($\mu\epsilon$) at the bottom of the layer or the strain ratio. Long and Theyse (2001) developed a transfer function for foam bitumen treated materials (FTBMs) and bitumen emulsion treated materials (ETBMs) by linking the model to the behaviour of cement treated materials. Two phases of materials behaviour were considered, i.e. a stiffness reduction phase and a steady state resilient modulus phase. Permanent deformation occurs predominantly after the constant stiffness phase has been reached, although a small amount may occur during the stiffness reduction phase. However, it is difficult to account for both modes simultaneously.

Long et al., (2002) indicated that depending on the road category the transfer function relates the ratio of the tensile strain at the bottom of the foamed bitumen treated layer to the number of load repetitions to reach the constant stiffness. Equation 3.20 shows a typical transfer function of foamed treated material for maximum tensile strain calculated under and between the tyres.

$$N_{f,FB} = 10^{\left(C - 0.708 \left(\frac{\epsilon_t}{\epsilon_b} \right) \right)} \quad (3.20)$$

Using HVS testing (Liebenberg, 2003) indicated that based on De Beer's (1989) transfer function for cement materials. A typical transfer function for emulsion bitumen treated materials (depending on road categories) can be presented in equation 3.21 as follows:

$$N_{f,EB} = 10^{\left(C - 1.2775 \left(\frac{\epsilon_t}{\epsilon_b} \right) \right)} \quad (3.21)$$

Where:	N_f	= number of load repetition to crack initiation of bitumen emulsion layer
	C	= variable depending of road categories.
	ϵ_t	= maximum tensile strain at the bottom of the layer
	ϵ_b	= strain at break from laboratory testing.

However, with the trend of decreasing cement contents in emulsion mixes, the form of this equation is questionable. This model of cold mix behaviour is somewhat controversial and is still under review by researchers. More discussion on the transfer function of cold mix is explored in Chapter 5 and 6 of this study.

3.5 FATIGUE LIFE ANALYSIS

3.5.1 End of fatigue life

The fatigue life of a treated pavement material is normally characterised by high modulus of elasticity, low elastic deflections and virtually no permanent deformation. The end of fatigue life results in a non-linear behaviour because of the non-homogeneity from the presence of cracks, a reduced modulus of elasticity, increased elastic deflection and decrease in the resistance to permanent deformation. The initiation of cracks in the layer will lead to a reduction in the effective stiffness that will lead to further reduction as the cracks propagate through the layer.

Typical for the behaviour of cold mixes (FBTMs and EBTMs) observed during APT testing is that the resilient modulus (stiffness) of the treated base layer starts at a relatively high value and then decreases under the action of HVS loading to a constant resilient modulus (Long and Theyse, 2001). This occurs relatively early in the life of the pavement under HVS loading. Figure 3.5 illustrates the behaviour of stiffness reduction to end of fatigue life from fatigue beam testing. Liebenberg (2003) indicated that emulsion treated layers start to behave similar to granular materials at the end of the fatigue life (terminal stiffness life) when a stiffness of 500MPa is reached after a large number of 40KN (HVS) load repetitions. When the load increased to 80KN, stiffness reduction toward 500MPa was reached with less number of load repetitions using HVS testing.

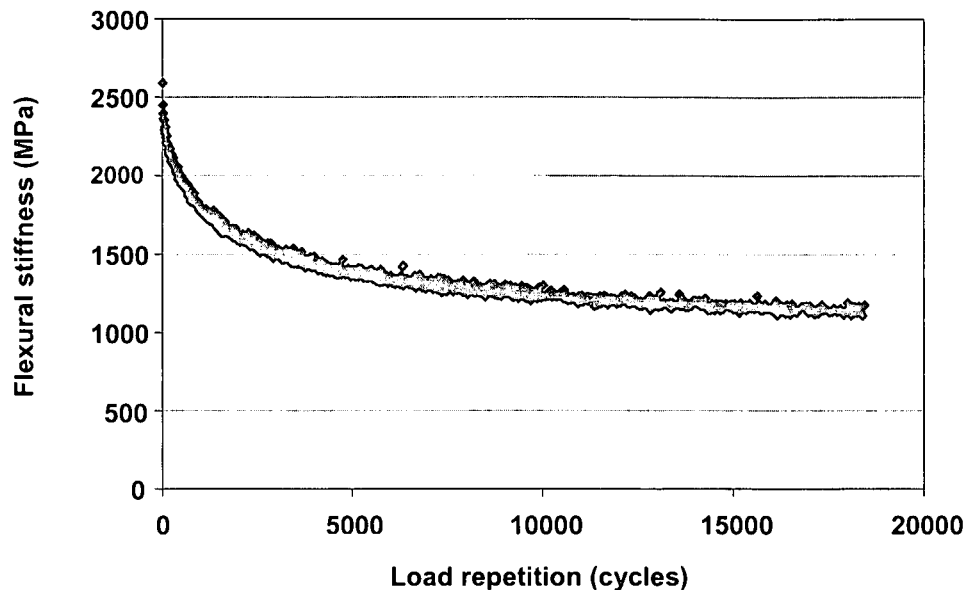


Figure 3.5: Flexural stiffness reduction curve from four-point beam testing, 10Hz at 5°C

The constant stiffness reached is typically representative of the modulus of the untreated parent materials and has been referred to as the “equivalent granular state” for cemented materials (De Beer, 1990). Long and Theyse (2003) indicated that the term “equivalent granular state” is somewhat misleading because the materials are equivalent in resilient modulus only and not in the condition of the material, i.e. the treated material is not in loose particulate state. Hence they recommended that this state to be named “constant stiffness state”.

The number of load repetitions from the initial state to the constant stiffness state has been referred to as the “effective fatigue life” (De Beer, 1990). Long and Theyse (2003) indicated that this term “effective fatigue life is also misleading because the layer is not at the terminal state at the end of effective fatigue life. It is thought that at this phase the micro-bonds between materials particles formed by the bituminous binder or filler break down, thereby reducing the resilient modulus. Therefore, they recommended that the phase be named “stiffness reduction phase” instead of effective fatigue and effective fatigue life as “Phase 1 life”. At the end of phase 1 the pavement is not in a terminal condition. The reduced stiffness increases the tensile strain at the bottom of the asphalt layer, and therefore reduces the life of the surfacing. The shorter this phase, the quicker the surfacing will crack and water will be able to penetrate to the base layer.

3.5.3 Damage factor

For pavements, in- service strains induced in the structure vary widely as result of variation in the type of axles, their loaded weights, tyre pressure, wander, etc. Therefore, some means for accumulating the damaging effects of mixed loading is required. The most common mean is

the Miner's law, which describes the relationship of linear summation of cycle's ratios, to failure shown as follows (Tangella, 1990):

$$\frac{n_1}{N_{1f}} + \frac{n_2}{N_{2f}} + \dots + \frac{n_i}{N_{if}} + \frac{n_m}{N_{mf}} \quad (3.22)$$

Where:

- i = the i^{th} level of applied strain at critical point within the pavement structure
- n_i = the actual number of applications of strain i that is anticipated.
- N_{if} = the number of application of strain i expected to cause fatigue failure if applied in a non-mixed loading environment.

Failure in the pavement under mixed loading is expected when the linear summation of cycle ratios reaches one (1).

In similar way Santucci (1977) indicated that a damage factor is used to compare the predicted and allowable number of load applications. If the cumulative damage factor exceeds 1, the pavement will reach its terminal condition before the required design traffic load and the pavement can be regarded as inadequate. If the cumulative damage factor is less than 1, the pavement will be able to carry the required load before the terminal condition is reached. He therefore defined the Cumulative Damage Factor (CDF) for the i^{th} loading as the number of load repetitions (n_i) of a given response parameters divided by the "allowable" repetitions (N_i) of the response parameters that would cause failure. Summation of the ratio gives the overall damage of the loading in the traffic spectrum, which is calculated as follows:

$$CDF = \sum_{i=1}^n \frac{n_i}{N_i} \quad (3.23)$$

Where:

- CDF = cumulative damage factor
- n_i = damage of the i^{th} load repetition
- N_i = total number of allowable load repetition

This is an iterative process until the required layer thickness is determined.

3.6 CONCLUSIONS

Fatigue cracking is one of the major load-related distresses experienced in a bituminous layer. It occurs when a pavement is subjected to repeated loading applied by the traffic. The fatigue resistance of the mixes therefore, is the ability of the mixture to resist cracking and fracture under this repeated loading. There are many factors that require consideration in the fatigue performance of the bituminous treated materials. This literature survey explored some of these factors and the following conclusion can be drawn:

3.6.1 Factors affecting fatigue response

- It is considered important to examine the influence of compaction on the response characteristics of laboratory prepared specimens. Kneading, gyratory and rolling wheel compaction has shown to be the most promising compaction techniques that simulate in-situ behaviour. However, more research is required for cold mixes to ensure that in-situ situation is correctly modelled.
- Mixture variables, such as binder content, binder type, aggregates type and gradation and active filler percentage have a great influence in the maximum fatigue life. It is essential, therefore for strength and fatigue performance that these parameters to be balanced and optimized in the mix design through laboratory testing in order to achieve the maximum load spread and fatigue resistance.
- Load variables, such as a frequency of load application and environmental variables, such as temperature at which fatigue test are performed will have a strong bearing on the fatigue performance of a particular mixture. 5°C found to be critical for the laboratory test beam specimen of cold mix. However to account for the difference a shift factor is necessary to translate laboratory fatigue characteristics to those considered to be representative of the in-situ response.
- The survey shows that a continuous sine-wave (no rest period between load cycles) is the most practical type of loading application as it reduces the time required for a specimen to fail. However, with this particular wave-shape the resulting fatigue life considerably underestimates the in-situ fatigue performance of a particular material. Thus a relatively large shift factor is required.
- The survey further found that a load frequency of 10Hz is representative of mixed traffic conditions and different pavement thickness, and does not generate excessive heat in the specimen. It is therefore, suggested that the loading frequency in all fatigue testing conducted in the laboratory be standardized at 10Hz.

3.6.2 Evaluation of fatigue life.

- Fatigue cracking is considered to be a tensile phenomenon and the fatigue life is therefore correlated with tensile strain. The conventional approach, using Wöhler-type fatigue relationship is more applicable, where the number of load application to failure, (N_f) is empirically related to the maximum tensile strain occurring at the bottom of the specimen.

- Different methods of determining the fatigue performance of bituminous treated mixtures are applicable. However the simple flexural four point beam bending test was identified as being one suited for the evaluation of the resistance of bituminous bound mixtures to fatigue.
- Most fatigue equations incorporate initial mixture stiffness as variable. However, there is still ambiguity as to how the different definitions of stiffness interrelate. The flexural stiffness of mixtures behaved differently (variability) in four-point beam testing at the same input parameters.
- Generally fatigue failure of the test beam specimen is defined as the reduction of the stiffness to 50 percent of its initial flexural stiffness. Using the conventional method ($N_f = a\epsilon^{-b}$) fatigue relationship can be estimated. The alternative evaluation method is using dissipated energy approach using $N_f \propto W_{N,\epsilon_0,S_0,\phi_0}$ relationship.

3.7 REFERENCES

ADEDIMILA A.S and KENNEDY T.W., 1975. **Fatigue and resilient characteristics of asphalt mixture by repeated –load indirect tensile strength**. Research Report 183-5, Centre for Highway Research, the University of Texas at Austin.

AIREY G.D., 1995. **Fatigue testing of asphalt mixtures using the laboratory third-point loading fatigue testing system**. Masters Dissertation, University of Pretoria, Pretoria, South Africa.

ARE, Inc., Engineering Consultants. 1986. **Development of asphalt aggregate mixture analysis system**. Prepared for NCHRP.

ASPHALT ACADEMY., 2002. **The design and use of foamed bitumen treated materials**. Interim Technical Guideline TG2, Pretoria, South Africa.

ASTM., 1964. **STP 91A: Tentative guide for fatigue testing and the structural analysis of fatigue data**. American Standard Test Methods, 2nd Edition, West Conshohocken, PA, United States.

AUSTROADS., 2001. **Fatigue life of compacted bituminous mixes subject to repeated flexural bending**. AST03, Sydney, Australia.

BARKSDALE R.D and MILLER J.H., 1997. **Development of equipment and techniques for evaluating fatigue and rutting characteristics of asphalt concrete mixes**, Report SCEGIT-77-147. School of Civil Engineering, Georgia Institute of Technology, Atlanta.

BISSADA A.F., 1987. **Structural response of foamed-asphalt-sand mixtures in hot environments.** Transportation Research Record 1115, pp 134-149.

BONNAURE F., HUIBBERS A.H.J.J. and BOODERS A., 1982. **A laboratory investigation of the influence of rest periods on fatigue characteristics of bituminous mixes.** Proceedings, the Association of Asphalt Paving Technologists, Vol. 51, pp 104.

BONNOT J., 1986. **Asphalt aggregate mixtures.** Transportation Research Record 1096, Transportation Research Board, Washington DC, pp 42-50.

BONNOT J., 1972. **Assessing the properties of materials for the structural design of pavements.** Proceedings, Third International Conference on the Structural Design of Asphalt Pavements, London, pp 200-213.

BROWN S. and NEEDHAM A. 2000. **A study of cement modified bitumen emulsion mixtures.** Proceeding of the Association of Asphalt paving Technologists. AAPT, vol. 69, Reno USA.

BROWN S.F., COOPER K.E., GIBB J.M., READ J.M. and SCHOLTZ T.V., 1994. **Practical tests for mechanical properties of hot mix asphalt.** Proceedings, 6th Conference on Asphalt Pavements for Southern Africa, Vol 2, Cape Town, South Africa, pp. 29-45.

COLAS, 2002. **Emulsion cold mixes specific features and new design methods.** Johannesburg, South Africa.

DE BEER M., 1989. **Aspects of the design and behaviour of road structures incorporating lightly cemented layers.** PhD thesis, University of Pretoria, Pretoria, South Africa.

DE BEER M and GROBLER J.E., 1994. **Towards improved structural design criteria for granular emulsion mixes.** Proceedings of the 6th Conference on Asphalt Pavements in Southern Africa, Cape Town, South Africa.

DORMON G.M. and METCALF C.T., 1964. **Design curves for flexible pavements based on layered system theory.** Highway Research Record, no. 71, pp. 69-84.

FREEME C.R., 1971. **The behaviour of bituminous surfacing in asphalt pavements.** PhD Thesis, University of Natal, Durban, South Africa.

HAWTREY L.E., 1964. **Studies on the flexible behaviour of bituminous mixtures**. PhD Thesis, University of Cape Town, South Africa.

IPC (Industrial Process Controls Ltd.), 1998. **Beam fatigue apparatus**. Reference Manual, Boronia, Australia.

JENKINS J.K., 2000. **Mix design considerations for cold and half –warm bituminous mixes with emphasis on foamed bitumen**. PhD Dissertation, University of Stellenbosch, South Africa.

KINGHAM R.I and KALLAS B.F., 1972. **Laboratory fatigue and it relationship to pavement performance**. Third International Conference on the Structural Design of Asphalt Pavements, Vol 1, London, pp 849-865.

LIEBENBERG J.J.E., 2003. **A structural design procedure for emulsion treated pavement layers**. Masters Dissertation, University of Pretoria, Pretoria, South Africa.

LITTLE D.N., BUTTON J.W., and EPPS J.A., 1983. **Structural properties of laboratory mixtures containing foamed asphalt and marginal aggregates**. Transportation Research Record 911, pp 19-24.

LONG F.M and THEYSE H.L., 2001. **Laboratory testing for the HVS sections on Road P243-1**. Contract Report CR-2001/32, Transportek, CSIR, Pretoria, South Africa.

LONG F.M and VENTURA D.F.C., 2003. **Laboratory testing for the HVS test sections on the N7 (TR11/1)**. Contract Report CR-2003/56, Transportek, CSIR, Pretoria, South Africa.

MARAIS C.P. and TAIT M.I., 1989. **Pavements with bitumen emulsion treated bases: Proposed material specification, mix design criteria and structural design procedures for South African conditions**. Proceedings of the 5th Conference on Asphalt Pavements in Southern Africa, Swaziland.

MEDANI T.O. and MOLENAAR A.A.A., 2003. **Estimation of fatigue characteristics of asphalt mixes using simple tests**. Wegbouwkundige werksdagen, The Netherlands.

MONISMITH C.L., 1981. **Fatigue characteristics of asphalt paving mixtures and their use in pavement design**. Proceedings, 18th paving conference, University of New Mexico, Albuquerque.

MONISMITH C.L., HICKS R.G., and FINN F.N., 1985. **Improved asphalt mix design**. Proceedings, Association of Asphalt Paving Technologist, University of California, Berkeley, United States.

PELL P.S., 1965. **Fatigue of bituminous materials in flexible pavements**. Proceedings of the Institute of Civil Engineers, Vol 31.

PELL P.S and COOPER K.E., 1975. **The effect of testing and mix variables on the fatigue performance of bituminous materials**. Proceedings, Association of Asphalt Paving Technologists, Vol 44, pp 1-37.

PORTER B.P and KENNEDY T.W., 1975. **Comparison of fatigue test methods for asphalt materials**. Research Report 183-4, Centre for Highway Research, the University of Texas at Austin.

RAITHBY K.D and STERLING A.B., 1972. **Some Effects of Loading History on the Fatigue Performance of Rolled Asphalt**. Great Britain Transport and Road Research Laboratory Report LR 496, Crowthome, Berkshire.

SABITA., 1993. **GEMS- The design and use of granular emulsion mixes**. Manual 14, Cape Town, South Africa.

SAKR H.A AND MANKE P.G., 1985. **Innovations in Oklahoma foamix design procedures**. Transportation Research Record 1034, pp 26-34.

SANTUCCI L.E., 1977. **Thickness design procedure for asphalt and emulsified asphalt mixes**. Proceedings of the 4th International Conference on the Structural Design of Asphalt Pavements, Ann Arbor, Michigan, United States, pp 424-456.

SHELL., 1966. **The testing of bituminous materials**. Koninklijki / shell-laboratorium, Amsterdam.

STRATEGIC HIGHWAY RESEARCH PROGRAM., 1962. **Fatigue response of asphalt-aggregate mixes**. Executive summary, Washington.

TANGELLA RAO S.C.S., 1989. **Development of an Asphalt-Aggregate Mixture Analysis System (AAMAS)**. Doctor of Engineering Dissertation, Department of Civil Engineering, University of California, Berkeley.

TANGELLA RAO S.C.S., CRAUS J., DEACON J.A and MONISMITH C.L., 1990. **Summary report on fatigue response of asphalt mixtures: Prepared for Strategic Highway Research Project A-003-A**. Report TM-UCB-A-003A-89-3, University of California, Berkeley.

THEYSE H.L., 1998. **Towards guidelines on the structural design of pavements with emulsion treated layers.** Contract Report, CR-97/045, Transportek, CSIR, Pretoria, South Africa.

VALLEGRA B.A., FINN F.N. and HICKS R.G., 1964. **Effect of asphalt ageing on the fatigue of asphalt concrete.** Proceedings of the Second International Conference on the Structural Design of Asphalt Pavements Research Record, no. 71, pp. 69-84.

VAN DE VEN M.F.C., and JENKINS K.J., 1999. **Mix design considerations for foamed bitumen mixtures.** Proceedings, 7th Conference on Asphalt Pavements for Southern Africa, Livingstone, Zimbabwe.

VAN DIJK W. and VISSER W., 1977. **The energy approach to fatigue for pavement design.** Proceedings, Association of Asphalt Paving Technologists, Vol. 46, pp 1-40.

VISSER A.T. and HODGKINSON A., 2004. **The role of fillers and cementitious binders when recycling with foamed bitumen or bitumen emulsion.** Proceedings, 8th Conference on Asphalt Pavements for Southern Africa, Sun City, South Africa.

VON QUINTUS H.L., SCHEROCCMAN T.A, HUGHES C.S. and KENNEDY T.W., 1988. **Development of asphalt-aggregate mixture analysis system: AAMAS.** Brent Rauhut Engineering, Inc., Austin.

WIRTGEN, 2004. **Cold Recycling Manual**, 2nd Edition, Windhagen, Germany.

CHAPTER 4

4. FATIGUE TESTING METHODOLOGY

4.1 INTRODUCTION

The fatigue, strain-at-break and stiffness properties of cold mixes are influenced by the interaction of binder, mineral aggregates and the use of active filler, as well as sample preparation including mixing, compaction, curing, and cutting of the beams and testing procedures.

There are wide varieties of possible testing methods which can be applied to determine the fatigue resistance of bituminous mixes in the laboratory. These methods among others, include simple flexural tests, (third-point or four-point), diametral, indirect tensile test and laboratory or field wheel traffic test (HVS). These methods have been discussed in Chapter 3.

Of the various testing methods, the simple flexural test (third-point or four-point loading) was identified by researchers as the one best suited to evaluate the fatigue resistance of bituminous mixture (Tangella et al., 1990; Raithby and Sterling, 1972; Barksdale, 1977; IPC, 1998; Medani et al., 2000 and Fritz et al., 1999).

The simple flexural tests, be it centre point, third -point , four-point or cantilever loading, provide a direct relationship between fatigue life and stress/strain developed by subjecting beams to pulsing, sinusoidal or haversine loads. The technique thus enables determination of a fundamental property, which can be used in both mixture evaluation and design. A shift factor is nevertheless required in order to relate the laboratory results to field performance (Pell and Cooper, 1995, Theyse, 1998; Long et al., 2001 and Liebenberg, 2003).

In third-point or four-point loading, failure of the specimen is initiated in the region of relative uniform stress. This feature helps to reduce the coefficient of variation of the test results, thus reducing the number of test required for a given confidence level.

The simple flexural test has however, have some limitations, amongst which are (Airey, 1995):

- Validation of laboratory results by comparison with in-situ pavement performance is difficult because of the need for a shift factor.
- The methodology is costly, time consuming and requires specialised equipment.
- Elastic theory is usually assumed to compute the tensile stress or strain. This is not true because the mixes behave visco-elastic under different loading conditions.

IPC, (1998) developed a Beam Fatigue Apparatus®, (BFA) which is a simple flexural four point beam loading (4PB) test, used for determination of fatigue life of bituminous mixture among other tests. This apparatus was adopted in the test methodology for fatigue, strain-at-break and frequency sweep tests

This chapter describes protocols for beam fatigue testing methodology, in which specimen preparation methods (foam and emulsion mixes); including blending of materials, mixing, compaction, curing and beam cutting are presented and discussed. The fatigue testing system used is the IPC 4PB fatigue apparatus and the different components and their functions are dealt with. The operating process of the feedback servo-pneumatic system is explained. The fatigue testing procedures are then described, which includes an explanation of the test set-up and input parameters. Fatigue end point criteria are explained and the equations used to determine the flexural stiffness of the tested beam specimen are presented and discussed. Finally conclusions are drawn with regard to, specimen preparation, BFA fatigue testing system and their effect on fatigue life. Fatigue testing procedures and determinations of initial stiffness and cycles to failure from test data are also discussed.

4.2 SPECIMEN PREPARATION

4.2.1 Materials (blending of mineral aggregates)

Two selected materials type, i.e. virgin limestone and reclaimed asphalt pavement (RAP) with maximum aggregate sizes of 19mm were prepared, i.e. air-dried before sieving, wet-sieving to account for fine fractions and dried-off, then blended at two different proportions; One with 75% limestone Table 4.1 and one with 75% RAP Table 4.2. These blends were stabilised with either bitumen emulsion or foamed bitumen. The 75% limestone blends were tested with both additions of One percent cement (surebuild type) and without cement. The typical combinations are shown in Table 4.3.

Table 4.1: Mixing blend "C" (%passing aggregates and required mass) of two parent materials

Total blend size		28.0 (Kg)			
%crushed rock (lime)		75%			
%milling (RAP)		25%			
Crushed rock – Limestone			Asphalt millings – RAP		
	total mass:	21(kg)		total mass:	7(Kg)
stockpile	ratio in blend	mass in blend (kg)	stockpile	ratio in blend	mass in blend (kg)
19.0 - 12.5	12.32%	2.587	19.0 - 12.5	9.69%	0.678
4.75 - 12.5	37.02%	7.774	4.75 - 12.5	38.03%	2.662
2.2 - 4.75	13.77%	2.892	2.36	23.99%	1.679
1.18	7.36%	1.546	1.18	9.25%	0.648
0.60	7.98%	1.676	0.60	11.22%	0.785
0.30	9.53%	2.001	0.30	5.49%	0.384
0.15	7.17%	1.506	0.15	1.59%	0.111
0.075	3.90%	0.819	0.075	0.61%	0.043
<0.075	0.95%	0.200	<0.075	0.13%	0.009
Total	100.0%	21.00	Total	100.0%	7.00

Table 4.2: Mixing blend "M" (%passing aggregates and required mass) of two parent materials

Total blend size		28.0Kg			
%crushed rock (lime)		25%			
%milling (RAP)		75%			
Crushed rock - Limestone			Asphalt millings - RAP		
	total mass:	7(Kg)		total mass:	21(Kg)
stockpile	ratio in blend	mass in blend (kg)	stockpile	ratio in blend	mass in blend (kg)
19.0 - 12.5	12.32%	0.862	19.0 - 12.5	9.69%	2.035
4.75 - 12.5	37.02%	2.591	4.75 - 12.5	38.03%	7.986
2.2 – 4.75	13.77%	0.964	2.36	23.99%	5.038
1.18	7.36%	0.515	1.18	9.25%	1.943
0.60	7.98%	0.559	0.60	11.22%	2.356
0.30	9.53%	0.667	0.30	5.49%	1.153
0.15	7.17%	0.502	0.15	1.59%	0.334
0.075	3.90%	0.273	0.075	0.61%	0.128
<0.075	0.95%	0.067	<0.075	0.13%	0.027
Total	100.0%	7.000	Total	100.0%	21.000

Table 4.3 Mix name and composition.

Mix No.	Name*	Binder	Aggregates blend	Binder content	Cement content
4	B-75C-0%	Bitumen emulsion	75%limestone -25%RAP	3.6%	0%
5	B-75C-1%		75%limestone- 25%RAP		1%
6	B-75M-0%		25%limestone-75%RAP	2.4%	0%
7	C-75C-0%	Foamed bitumen	75%limestone -25%RAP	3.6%	0%
8	C-75C-1%		75%limestone- 25%RAP		1%
9	C-75M-0%		25%limestone-75%RAP	2.4%	0%

* B = Emulsion mixes, C = Foam mixes

4.2.2 Binder

4.2.2.1 Bitumen Emulsion

The bitumen emulsion type B used in this study is a stable grade cationic emulsion (65% residual binder and 35% emulsion water). The bitumen emulsion content of 5.5% (i.e. 3.6% residual binder) and 3.7% (i.e. 2.4% residual binder) was used for treatment of the 75% virgin limestone and 75% asphalt milling (RAP) blends respectively. The bitumen emulsion were stored in sample containers and heated in the oven at 60°C for three hours, stirred and left to cool before mixing with the aggregates.

4.2.2.2 Foamed-Bitumen

The bitumen used for foaming process was a PG58-28 pen grade. The residual binder content of 3.6% and 2.4% of foam bitumen was used for treatment of 75% virgin limestone and 75% milling asphalt (RAP) blends respectively. Before production of foam bitumen, the foaming properties of bitumen viscosity (expansion ratio) and stability (half life time) were determined at different levels of foamant water as mass percentage of the bitumen.

The expansion ratio and half-life time of the foamed bitumen are shown in Figure 4.1. The half-life time of the foamed bitumen at a foamant water level 1% was in excess of 3 minutes and is not shown on the graph.

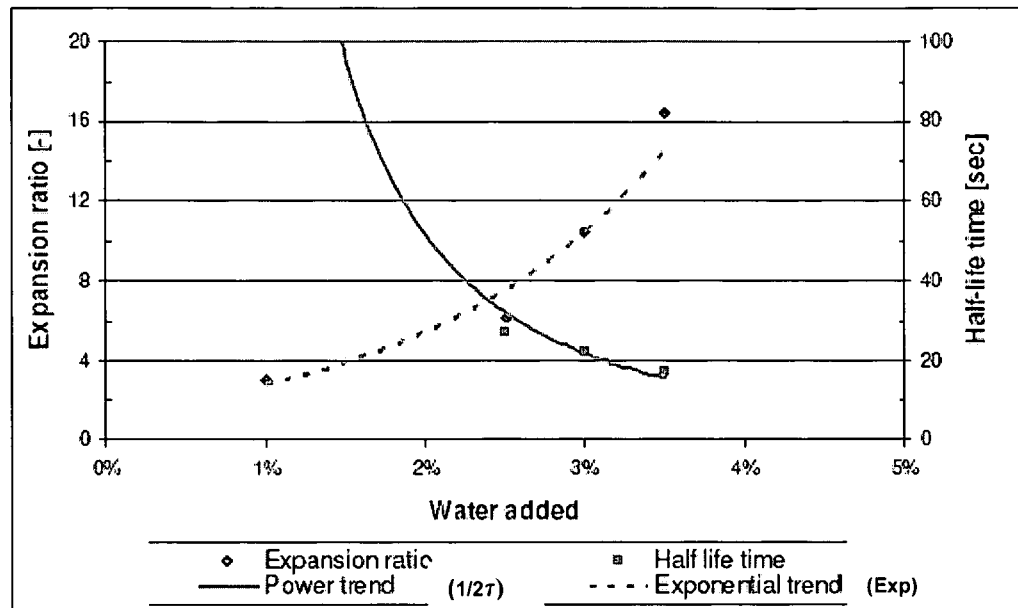


Figure 4.1: Foaming characteristics of (PG58-22) penetration grade bitumen.

A Wirtgen WLB-10 laboratory plant (Figure 4.2) was used for the foamed bitumen production. The temperature of the bitumen was kept constant at 170°C during all foamed bitumen testing and mix production. For every new set-up of the foaming process the half-life time and expansion ratio were checked. The foaming properties of the bitumen usually fluctuated during each new set-up, e.g. half-life time fluctuated between 20 and 29 seconds and expansion ratio fluctuated between 10 and 14. The percentage water in the bitumen for the foaming process was 3% of the mass of the bitumen.

It is assumed that the fluctuation has no large influence on the quality of the mixes, as the half-life time was always higher than 20 seconds, and expansion ratio in excess of 10. In foam index (FI) valuation this is approximate = 130 which lies in the range of FI between 125 and 175 for good foamed bitumen mixes at 25°C aggregates temperature recommended by TG2 (Asphalt Academy, 2002)

Therefore the minimum recommended value was achieved. However, the testing was done during the winter period and it was necessary to heat the aggregates in the oven to 25°C to achieve a aggregate mixing temperature.

Jenkins (2000) indicated that the temperature of the aggregates before mixing has a significant influence on the equilibrium binder-mix temperature. The transfer of heat from the foam at just over 100°C to the aggregates at less than 30°C will influence the rate of collapse of the foam i.e. the rate of viscosity of binder increase during mixing.

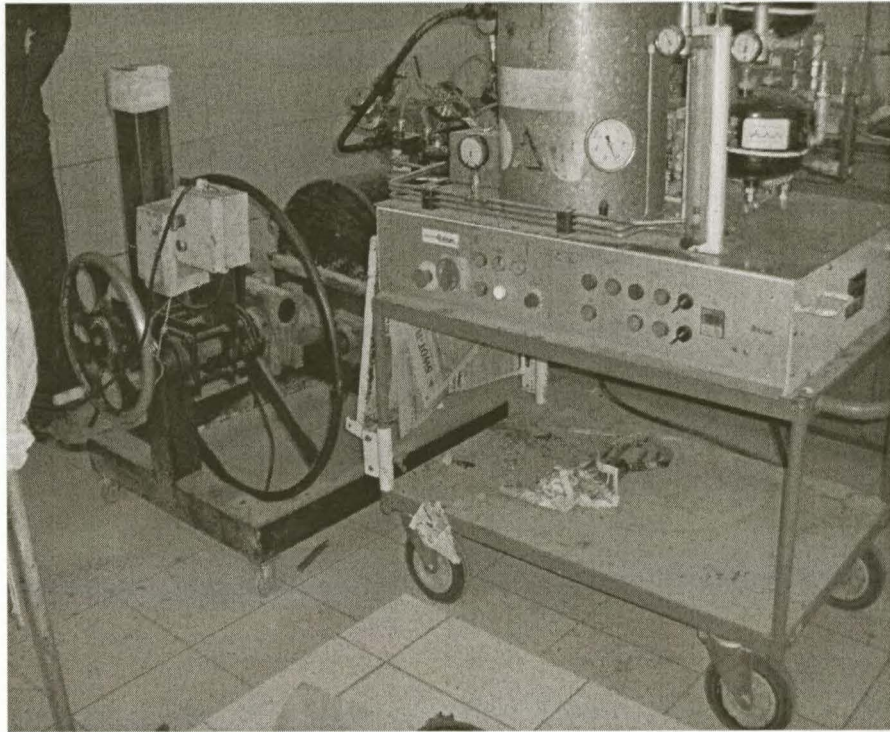


Figure 4.2: Wirtegen, WLB- 10 used as laboratory foam plant

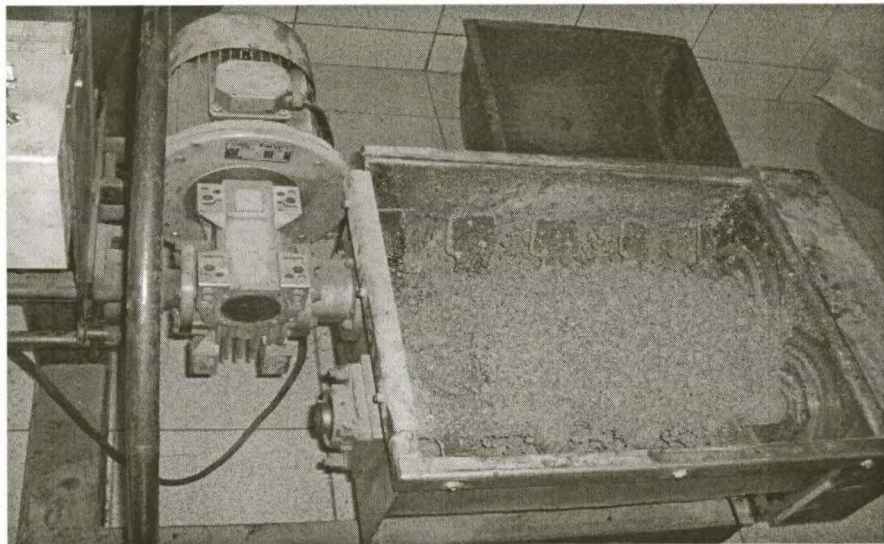


Figure 4.3: Twin-shaft pugmill used as foamed bitumen mixer

4.2.3 Active filler

Ordinary Portland cement (OPC) named Surebuild 42.5 (CEM II-B/M (L/S) according to South African specification) was added to some of 75% limestone mixes as active filler.

4.2.4 Moisture content and mixing process

The optimum moisture content (OMC) and maximum dry density of the materials, were determined by Modified AASHTO compaction and standard Proctor compaction as summarised in Table 4.4 for the two selected blends. The hygroscopic moisture in the mineral aggregates was 0.75% for 75% limestone and 0.5% for the 75% RAP.

Table 4.4: Summary of optimum moisture contents and maximum dry densities of blends

Blend	Compaction	OMC (%)	MDD (Kg/m ³)
75% limestone – 25% RAP	Mod AASHTO	7.5	2106
	Standard Proctor	8.0	2000
25%limestone – 75% RAP	Mod AASHTO	5.2	1930
	Standard Proctor	7.0	1800

The mixing process for the bitumen emulsion and the foamed bitumen mixes was different. The emulsion mixes were mixed in a standard laboratory vertical shaft mixer (see Figure 4.4) and the foamed bitumen mixes were mixed in the twin-shaft pugmill placed in front of the WLB-10 foam plant (see Figure 4.3)

The content of the aggregate during mixing with the bitumen emulsion was 70% of OMC. However, when this percentage produced a fairly wet mix, it was reduced to 65% of OMC. The mixing moisture to 65% of OMC was initially added and mixed for one minute. Then the aggregate was sealed in a bag and left for three hours to allow absorption of the moisture. Prior to the addition of bitumen emulsion, the remaining compaction water was added and mixed for a minute. Any addition of cement (active filler) took place at this stage before adding emulsion and mixed for one minute, followed by addition of emulsion and again mixed for another minute. Prior to compaction, the mixture was placed in a oven at 40°C for 30 minutes to simulate field compaction moisture, i.e. drying/ working with grader.

For the foamed bitumen mixes 70% of OMC as mixing moisture was found rather low to achieve workability and good compaction of the mixes. The mixing moisture for the foamed bitumen was then increased to 80% of OMC. Initially 50% of the mixing moisture was added to the aggregates and left to be absorbed by aggregates for three hours. During this time the aggregate was sealed in a bag and put into the oven heated at 25°C in order to achieve the recommended aggregates temperature prior to addition of foamed bitumen.

Prior to the addition of foamed bitumen, the remaining compaction water was added and mixed for 30 seconds. Any cement (active filler) was added at this stage before the foaming and mixed for

30 seconds. This was followed by the addition of the foamed bitumen, which was and mixed in at 40 r/min of the pugmill for 30 seconds. To maintain mixture temperature the materials were removed from the foam plant and placed directly in the slab mould, and immediately compacted. The moisture contents during mixing, compaction and after testing are summarized and presented in Appendix B.

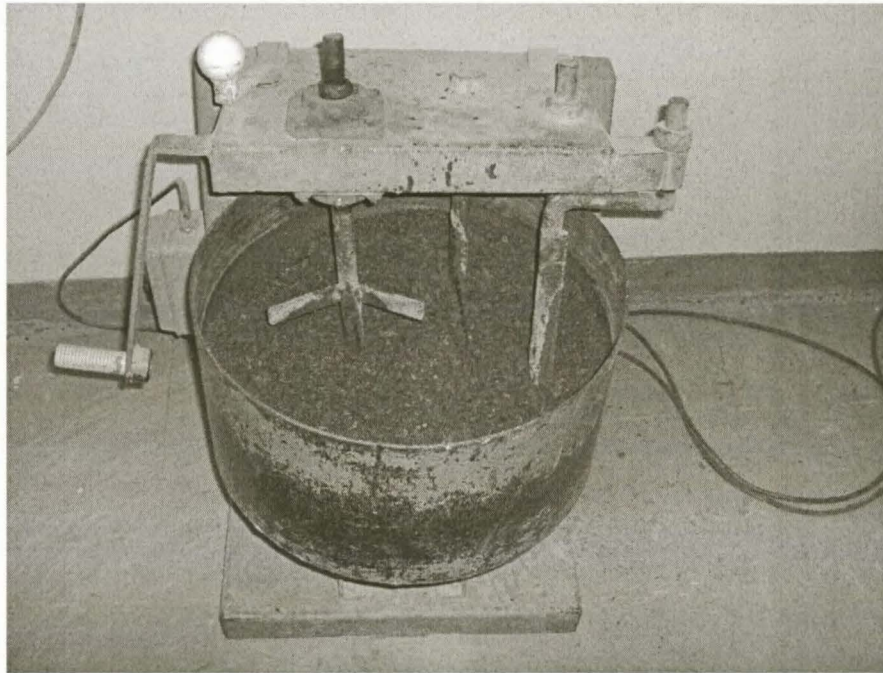


Figure 4.4: Standard laboratory vertical shaft mixer used for emulsion mixes

4.2.5 Compaction

4.2.5.1 Slab compaction

A steel wheel roller of laboratory size (880mm wide by 450mm diameter) with compaction mass of 250Kg was used to compact slabs with both static and vibration action in order to simulate the field compaction. 50 to 60 passes for bitumen emulsion and 60 to 70 for passes foam bitumen were applied to compact the materials in the mould of size 450mm x 450mm x 62mm. The required amount of materials for making the slab was calculated based on the target dry density (98% of Mod AASHTO) and the volume of the mould. These materials were placed in the mould into two layers prior to compaction. The first was lightly tamped (see Figure 4.5) to prevent spillage, followed by the second layer until all the material was placed in the mould. Then compaction by wheel roller commenced. Figure 4.6 shows the laboratory compaction set-up.

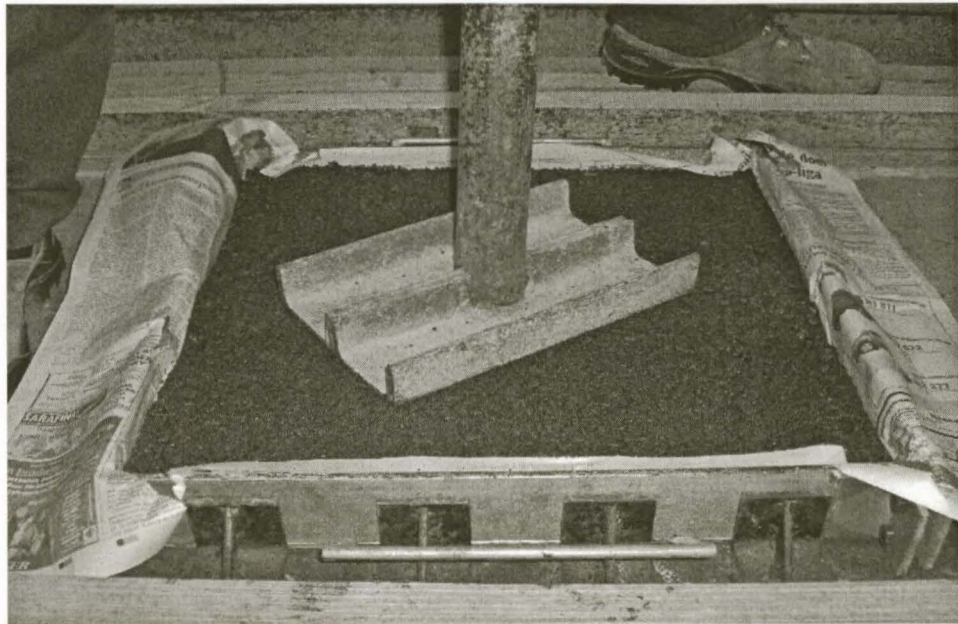


Figure 4.5: Moulding of materials into layers prior to compaction

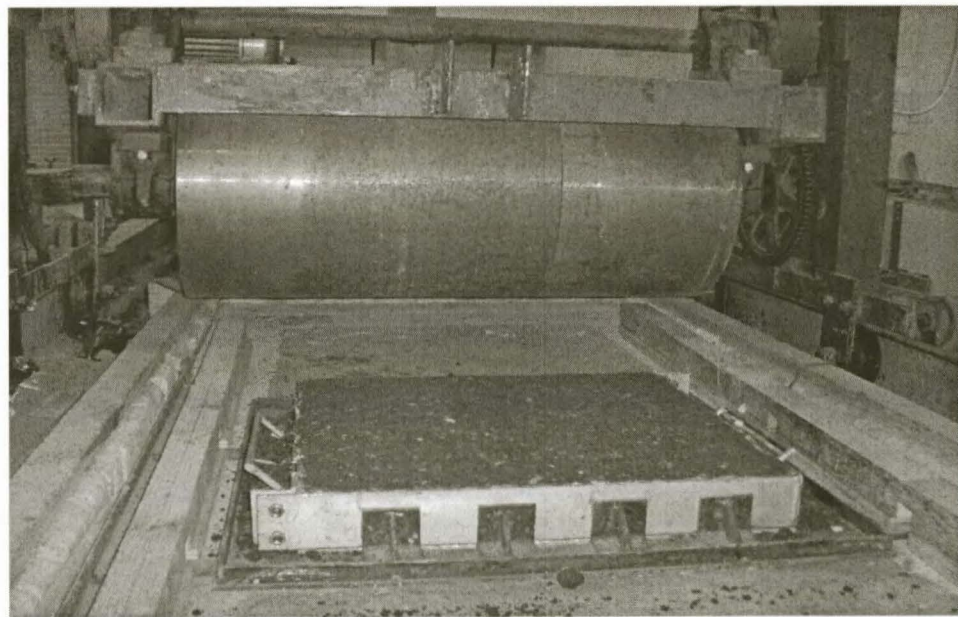


Figure 4.6: Laboratory compaction, Steel wheel roller and Slab mould set-up.

4.2.5.2 Compaction and after test moisture content.

Visual observation of the mixes during the mixing and compaction process showed that the bitumen emulsion mixes appeared 'wetter' than the foamed bitumen with equal mixing moisture content. This indicates that apart from high moisture content, the bitumen in the emulsion acts more like a fluid than of the foamed bitumen mixes. Due to high percentage of moisture in the

emulsion mix the compaction energy of 50-60 passes applied to fit the materials in the mould appeared to over compact the materials and produce densities higher than the target density of 98% Mod AASHTO. However the number of passes 60-70 applied to the foam mixes produced fairly good densities. However, theoretical determination of specimen density might underestimate the actual density of the mix due to variability of the measured beam dimensions.

After the test the beam specimens' moisture content was measured to check the level of moisture lost which gives an indication of full breaking of emulsion or curing of the foamed bitumen mixture.

4.2.6 Curing

The slabs were cured at 40°C for 72 hours as suggested by Jenkins (2000). He further indicated that this curing procedure was aimed at approximating 6 months of curing in the field. The first 24 hrs the specimen was cured within the side frames to ensure sufficient lateral support of the slab (see Figure 4.7). Thereafter the sides were removed and curing continued for 48 hours in the oven (see Figure 4.8). The same curing protocol was followed for both bitumen emulsion and foamed bitumen mixes. After curing the slab was sealed and left to cool at ambient temperature prior to the beam cutting process.



Figure 4.7: 24Hrs of curing with side wall Figure 4.8: 48Hrs of curing without side wall

4.2.7 Cutting of the Beams.

The laboratory saw-cutter (fixed blade and sliding table) was used to cut beams out of the compacted slab. Dry cutting was necessary due to the damage caused by water absorbed by the specimen during wet cutting. However excessive dust as a result of the dry cutting was seen as a major problem which needs further attention. The sliding table was modified to fit the size of the

slab (450mm x 450mm) as well as fitting the base supporting the specimen at bottom in the region of the blade. Lack of such support had been identified to spill edge materials during cutting and trimming. Further improvements to the cutting of the beams were made by using a continuous diamond blade in lieu of diamond slotted blade for trimming the beams, which resulted in better defined faces and the edges. The effect of this is significant due to the fact that stress/strain parameters of the mixture depends on the dimensions of the beam test specimen. This means that irregular surfaces have an adverse impact on the of beam testing for fatigue, flexibility and flexural stiffness as reported elsewhere in this study. The experience reported by other researchers indicated that specimen preparation required considerable attention to ensure acquisition of sound testing results. Figure 4.9 illustrates the cutting process and Figure 4.10 the trimming process. Apart from the modification mentioned chipping of aggregates was still experienced and resulting in inaccuracy of the beam dimensions. This necessitates investigation into the better laboratory saw cutting machine for the cold mixes.

The beam specimen dimensions of 63.5 ± 5 mm in width, 50 ± 5 mm in depth and 380 ± 5 mm in length were cut from slab dimensions of 450mm width by 450mm length by 62mm depth compacted, cured and cooled to ambient temperature. Cutting was carried out in the direction of compaction to maintain the aggregate orientation and bonding strength between particles and to simulate field compaction. A maximum of six beams were obtained from a slab as shown in Figure 4.11.

Due to weak bounding of materials, 62mm slab depth was found to cause chipping of aggregates at the faces in the process of trimming surfaces irregularities. This was found to be more serious on foam mixes at 70% OMC and without cement, which implies that mixture variables such as gradation, binder content (bitumen, active filler), moisture content and compaction are sensitive to the mixture and are likely to introduce variability of the beam test results. Section 4.4 discusses the adversely effect on the surface imperfection of the beam test specimen.

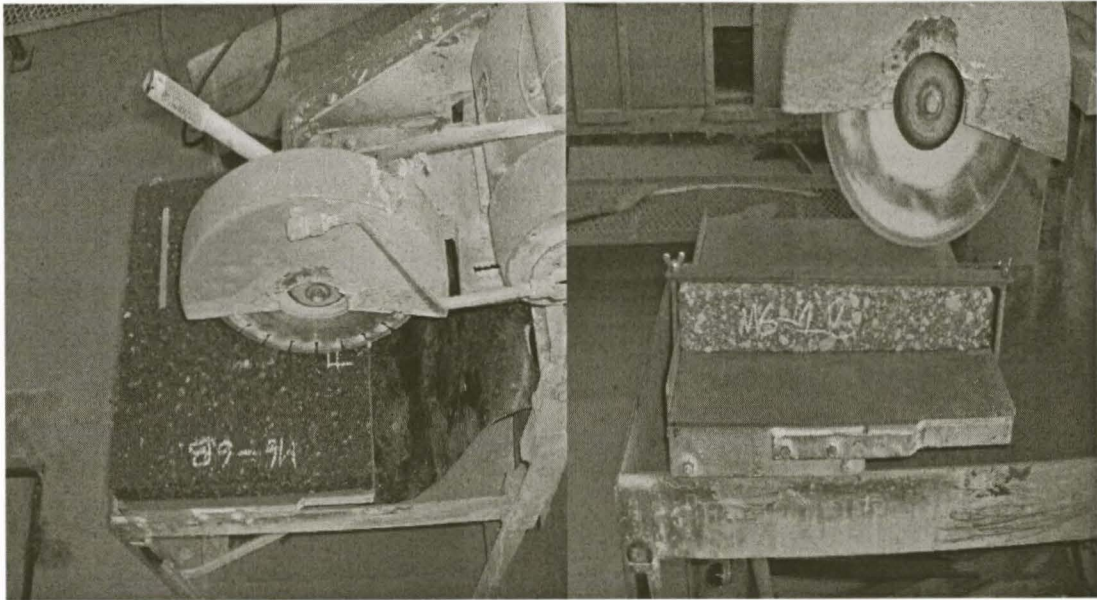


Figure 4.9: Laboratory, cutting of slab set-up using 3 mm slotted blade **Figure 4.10: Trimming of beam faces set-up using 1.5 mm continuous blade**

Labelling of the beams, cutting the beams and then placing into BFA frame were done consistently according to compaction orientation in order to simulate the field loading conditions. For comparison and quality control of the tested beams labels were used as an input file name into the testing software. Figure 4.11 indicates beam labelling style e.g. M(8)-(A)(2), which describes: mix(type)-(Slab no)(Beam no.)

The trimming of the top and bottom beam faces was carried out on approximately 6 mm excess (see Figure 4.12 and 4.13). Due to small trimming thickness (insufficient materials) out of 1.5 mm blade, it was seen to have effect on aggregates oriented to be flushed against the surface which resulted in chipping-off of the aggregates at the edges and the faces of the beam. Therefore sufficient excess material was required in order to be able to produce beams with better defined edges and faces. Therefore, it is recommended that in future the slab thickness be increased to 70 mm.

Further, variability of beams dimensions occurred as a result of trimming set-up. Inappropriate clamping, missing of longitudinal guide and improperly guiding wheels caused inaccuracy of beams dimensions. Therefore the variability of beam dimensions which was in the range of ± 3 mm instead of ± 0.5 mm standard tolerance. This influenced the variability of the test results. Therefore further investigation in modification or better equipment is needed in future research in order to minimise beams dimensions' variability.

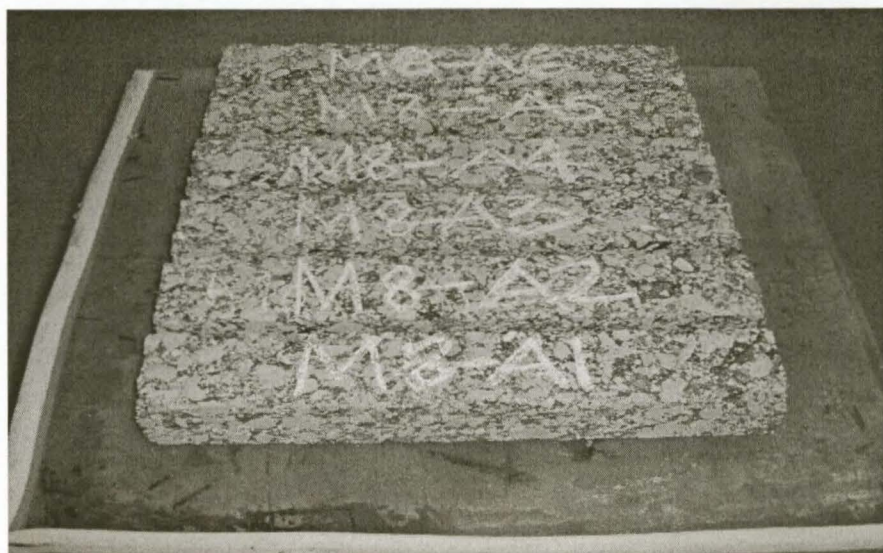


Figure 4.11: Beam labelling style (also used for file name)

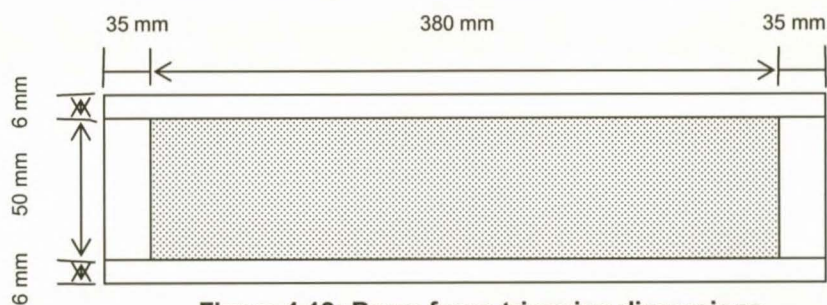


Figure 4.12: Beam faces trimming dimensions

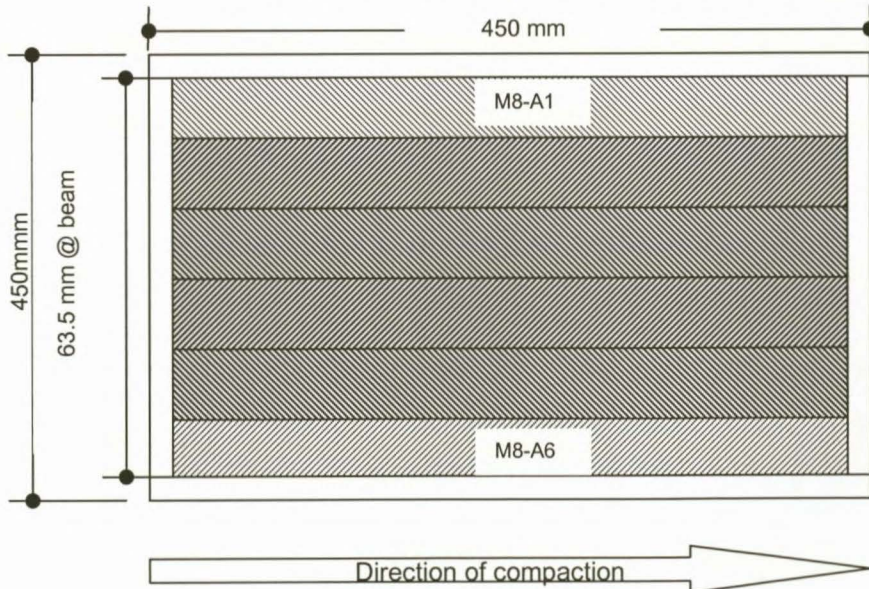


Figure 4.13: layout of cutting beams from compacted slab

4.2.8 Specimens relative density

The fatigue and flexural properties of the bituminous mixes are sensitive dependent on its actual level of compaction (percentage of air void content in the mix) (ARE, 1986). It is for this reason that relative density tests were carried out on each specimen.

The bulk relative density (BRD) can be determined before or after the test, but because of the possible severe damage to the beam during testing, BRD test were carried out before beams were tested. After the BRD tests, the beams were dried at ambient temperature before testing. However this process was not possible for the foam mixes and some emulsion mixes because the beams appeared weak and broke when submerged into water. Hence the BRD's of these beams were preferably calculated from theoretical volume (average volume).

The BRD's and compaction levels of each beam test specimens in all three mixes, of bitumen emulsion and foamed bitumen were summarised and presented in Appendix B1 and B2 respectively.

4.2.9 Storage of the beams

Prior to testing, the beam specimens were placed on the shelves in the climate chamber of the testing apparatus and conditioned for the test temperature of 5°C. However, any excess beam specimens were kept at room temperature between 20°C to 25°C whilst placed on a flat stiff surface. These beams are stored upside down such that the face to be loaded is fully supported until such time they are placed in the in the climate chamber (see Figure 4.19).

The duration for complete testing of 6 prepared beams was for all practical purposes 27 days from the date of compaction of the slab. This was due to the time taken by the tests at low strain levels. However storage at ambient temperature should not exceed 14 days before testing from the date of compaction of slab, so as to avoid long term curing influences. Storage at lower temperature allows longer storage periods without ageing of the beams.

4.3 IPC 4PB FATIGUE TESTING SYSTEM

The IPC fatigue testing system operates as with a pneumatic power closed-loop feedback servo system, which comprises three major components (see Figure 4.14). These include:

- Interface software
- Control and Data Acquisition system, CDAS and
- Testing Apparatus

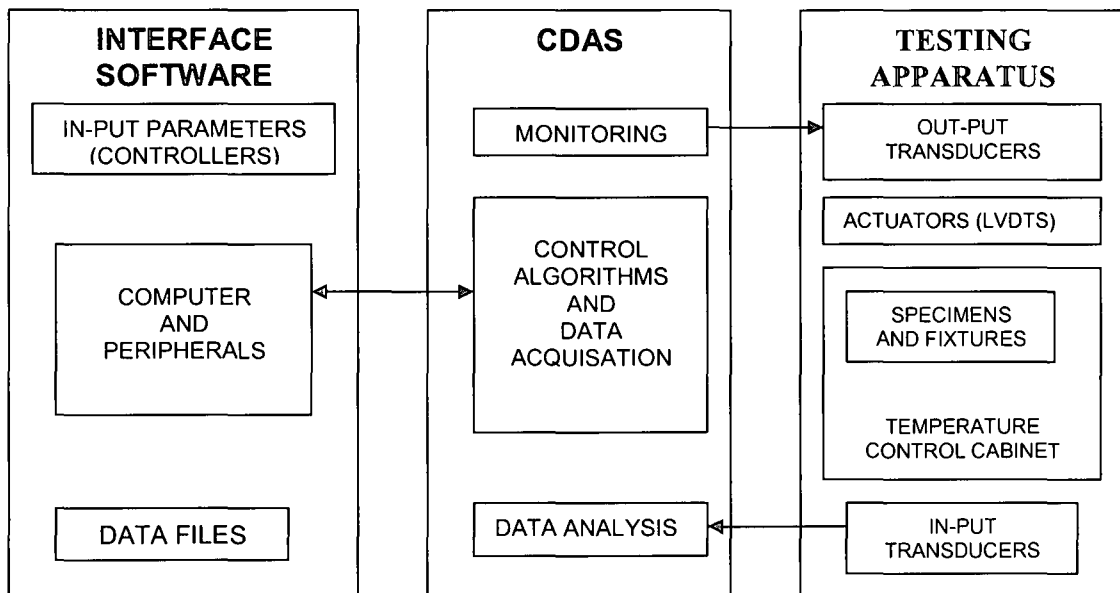


Figure 4.14: Fatigue testing system major components, (IPC, 1998)

4.3.1 IPC Beam Fatigue Apparatus (BFA)

The IPC beam fatigue apparatus is pneumatic type. In this investigation, the pneumatic powered feedback closed loop servo-system was used. The BFA is a stand-alone system for four-point fatigue life testing. The beam specimens are subjected to repeat flexural bending until failure. The cradle mechanism allows for free translation and rotation of the clamps and provides loading at the third points. The pneumatic clamps at either ends of the cradles, centre the beam laterally and clamp it. Servo-motor driven vertical clamps secure the beam at four-points with a predetermined self-adjusted clamp force, which remains constant throughout the test.

The servo-motors are operated continuously during the test to take up the slack resulting from permanent deformation (creeping) of the surface at clamping surfaces. Figure 4.15 shows the IPC, (1998) BFA configuration.

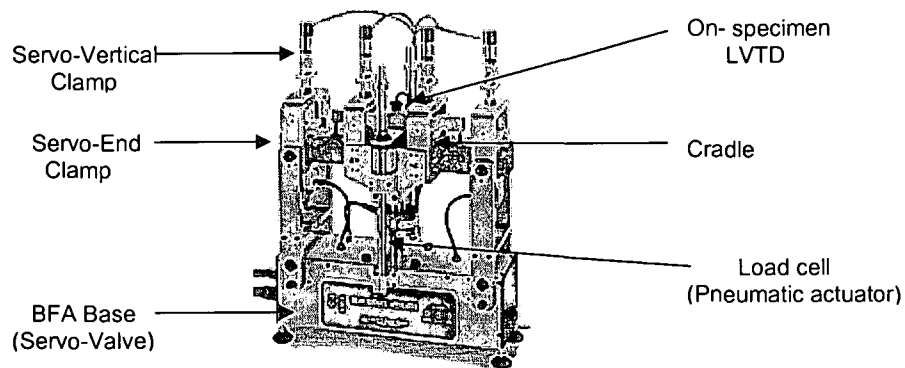


Figure 4.15: Four point loading fatigue apparatus® IPC, (1998)

The environmental temperature control chamber (climate chamber) is part of the testing apparatus. However, it is not part of the closed loop feedback control system. Therefore the specimen testing temperature is adjusted manually. The BFA (Figure 4.15) and test specimen are placed in the environmental chamber (thermostat refrigerator control). A dummy HMA specimen is used to measure the specimen core and skin temperature and to monitor the temperature during testing. However, this dummy is just provides an indication. Due to its sensitivity it is usually an incorrect prediction of the actual core temperature of the test specimen.

The climate chamber has sufficient space to accommodate the loading frame (BFA) and at least six test specimens and permits adjustment of the loading frame during loading of the specimen.

4.3.2 Loading frame, testing model and pneumatic system

The loading frame (cradles) has a servo-controlled pneumatic actuator built into the base of BFA. The actuator span is 9kN (± 4.5 kN), which applied from beneath the test specimen. This is opposite to the loading mechanism found in the field where traffic loads are applied from the top of the pavement layer. However, the failure mechanism in both cases is identical, where cracks develop from the bottom of the layer/specimen.

The loading mechanism (model) of the four point bending fatigue test is illustrated graphically in Figure 4.16. Fatigue testing consists of forcing the two central supports of the central third section of the beam, to deflect and return to its original position (haversine) or deflects in both directions (sinesoidal) by means of CDAS which generate cyclic loading function by operating the servo controlled pneumatic actuator coupled mechanically to the specimen through the loading frame. The loading frame has four points, the outer two reactions (supports) are separated at a distance typically of 355.5 mm and the loading reactions at the third points (supports) at distance of 118.5mm. Although the test specimen is clamped in the cradle it is able to experience free

movements (rotation) and horizontal translation of all load and reaction points. During the running of the test the outer two supports fixed, in the vertical direction, while the central section of testing frame and therefore two central supports are able to move vertically up-and-down. The clamping mechanism at all four locations are servo-electronically controlled.

The fact that the beam is stressed at its central two supports means that the fatigue failure is initiated in a region of uniform stress.

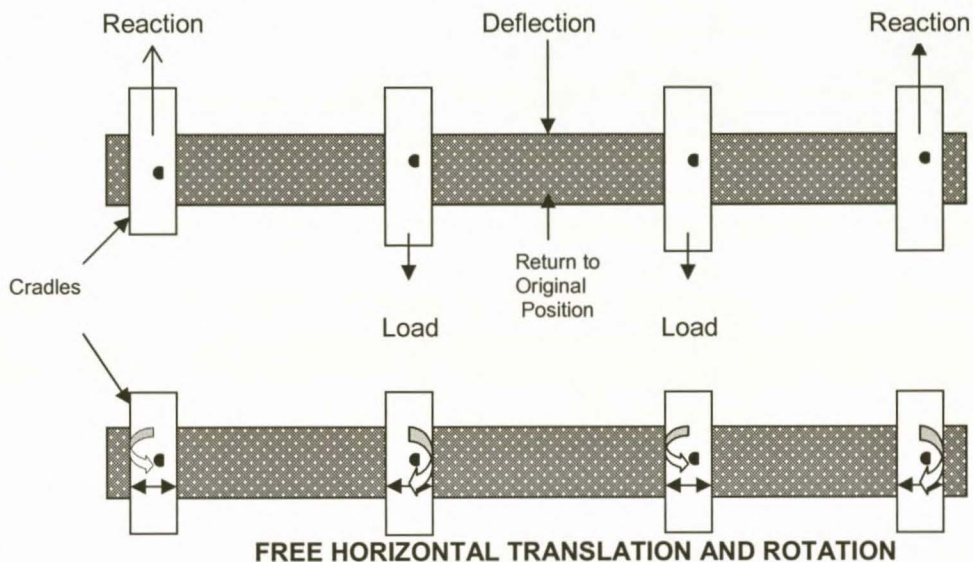


Figure 4.16: Loading characteristics of four-point loading fatigue test, (IPC, 1998).

The performance of the pneumatic servo actuator and transducers depends on servo valve and the pressure of air flow from the pressure supply. The pneumatic system requires a clean, dry air supply at minimum pressure of 600kPa. Low pressure will prevent the system from achieving maximum force.

The presence of water in the air supply may result in severe damage to the servo-valve and/or block the air supply due to icing up of the condensation water in the cooling system at low testing temperatures (say 5°C). It is for this reasons that various filters with drain valves are required to ensure smooth operation of the pneumatic system. The air supply is regulated to 600kPa before passing through the 5micron filter built onto the regulator. A 5 litre accumulator is used to buffer the air supply before further filtering by 0.5 micron filter and micro-mist separator. The number of filters supplied as standard with system was seen to be insufficient to eliminate the large amount of water in the air supply when testing at low temperatures and using untreated compressed air.

Therefore several modifications were made to eliminate water in the supplied air to ensure smooth operation of the BFA in this research. The effective reduction of moist air in the pneumatic system was achieved by fitting after cooler (radiator) to the outlet of the air supply (compressor) with more

filters and drains see Figure 4.17. Furthermore, a heating element was fitted at the base of servo-valve to heat-up the servo slightly in order to prevent moist air condensation inside the servo-valve.

Regular checking and draining of the filters was necessary especially at the water filter and mist separator bowls which are next to servo-valve. A way of preventing condensation water to ice up was to allow a little leak air at the drain valves of the water filter and breather to increase the air circulations speed allowing less time for condensations and accumulation. This resulted in fewer intervals of draining, especially in long testing of low strain level. Figure 4.17 illustrates the pneumatic air supply system to BFA.

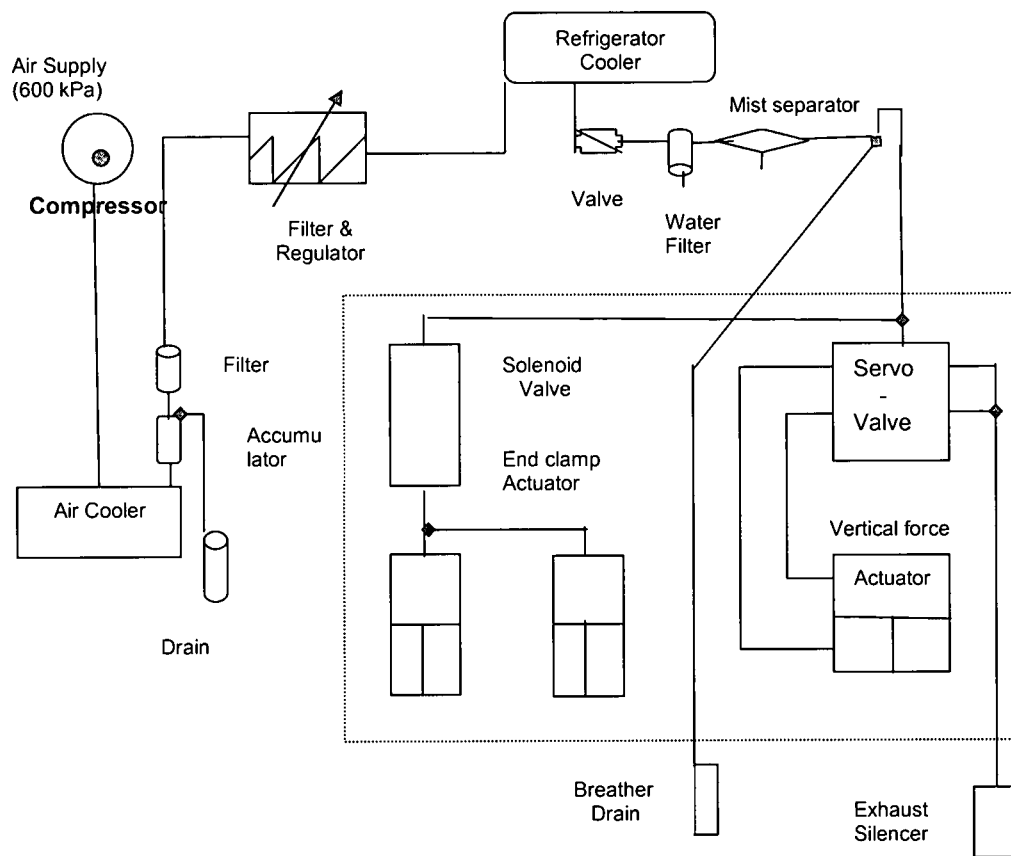


Figure 4.17: Modified beam fatigue pneumatic air flow system.

4.3.3 Microcomputer, control data acquisition system (CDAS) and software

The control and monitoring of the fatigue testing system is achieved through a personal computer, CDAS and fatigue testing software program, (Teyabali et al., 1992, IPC, 1998). The computer instructs the CDAS to control both the specimen loading function and data acquisition from the transducers attached to the specimen tested. The displacement or deflection of the central section

of the beam is measured by linear variable displacement transducer (LVDT) positioned above the specimen during testing, with the deflections being measured on the specimen's top surface. The CDAS provide all critical control, timing and data acquisition functions for the loading frame and transducers by means of the closed-loop feedback system. The test data are gathered from CDAS and displayed in real time on the PC screen.

For correct operation, the CDAS is equipped with various input channels. Among others four input channels are most relevant for fatigue testing, these include:

- Load input from the load cell,
- The ram or actuator displacement measured by internal displacement transducer, LVDT
- The on-specimen displacement is measured by an external linear variable differential transducer, LVDT
- An input from the temperature control unit indicating specimen (core and skin) temperature.

The software package provides the option of setting the test parameters that the CDAS uses to run the test. The software captures every 10th cycle and measures beam deflection and applied load at early stages of the test (up to 10000 cycles). Every cycle transferred to the PC will be stored and plotted, and then it is updated periodically on a logarithmic basis. Various parameters are calculated from the acquired data as the test proceeds and records the following: number of load cycles, the applied load (maximum and minimum) and beam deflection (maximum and minimum) as well as calculating maximum tensile stress, maximum tensile strain, phase angle, flexural stiffness, modulus of elasticity, dissipated energy and cumulative dissipated energy at load cycles interval.

The software creates a data file to archive/store the test results. This data file allows test results to be reviewed, printed, or imported into spreadsheet program for further analysis.

4.3.4 Principle of operation of the fatigue testing system.

The operation procedure of the IPC fatigue testing system is graphically shown in Figure 4.18 and pictorial components are shown in Figure 4.19. A load is applied to the test specimen by a servo-controlled pneumatic actuator mounted in the base and coupled mechanically to the system through the reaction-loading frame. The two input transducers mounted in the system, the load cell and the external LVDT, convert mechanical movement into standard electronic signal and, via the control and data acquisition system (CDAS) provide output display of flexural test information on the personal computer user interface screen.

The CDAS then monitors the test parameters from the feedback of the input transducer and adjusts these parameters in accordance to the requirements of the flexural test instructed by computer. For example, CDAS could adjust the applied load such that the specimen experiences a constant level of strain on each cycle. These adjustments are then conveyed to the pneumatic actuator via an error amplifier, servo driver and servo valve to regulate the air pressure and loading force to eliminate the error. This concept can be expressed as:

$$\text{Drive Error} = \text{Input DEMAND} - \text{Position FEEDBACK}$$

The control loop is therefore closed electronically and the operation continues for each load cycle until failure of specimen. Section 4.4 discusses the failure of beam test specimen or termination conditions.

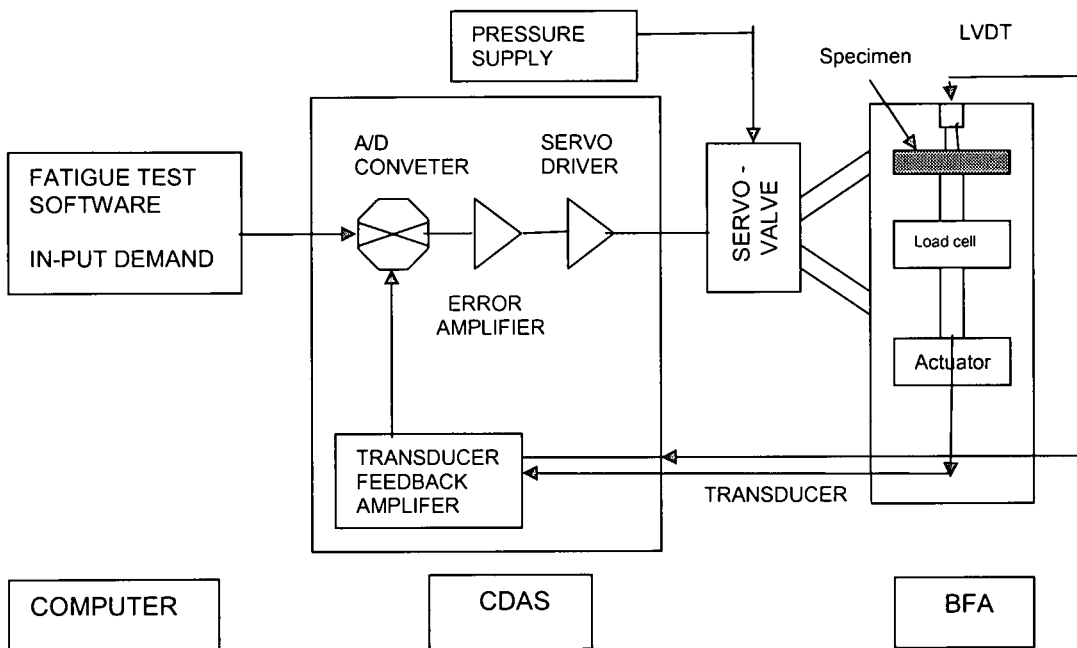


Figure 4.18: Schematic operation of fatigue testing system (Closed loop feedback Servo-control), (IPC, 1998)

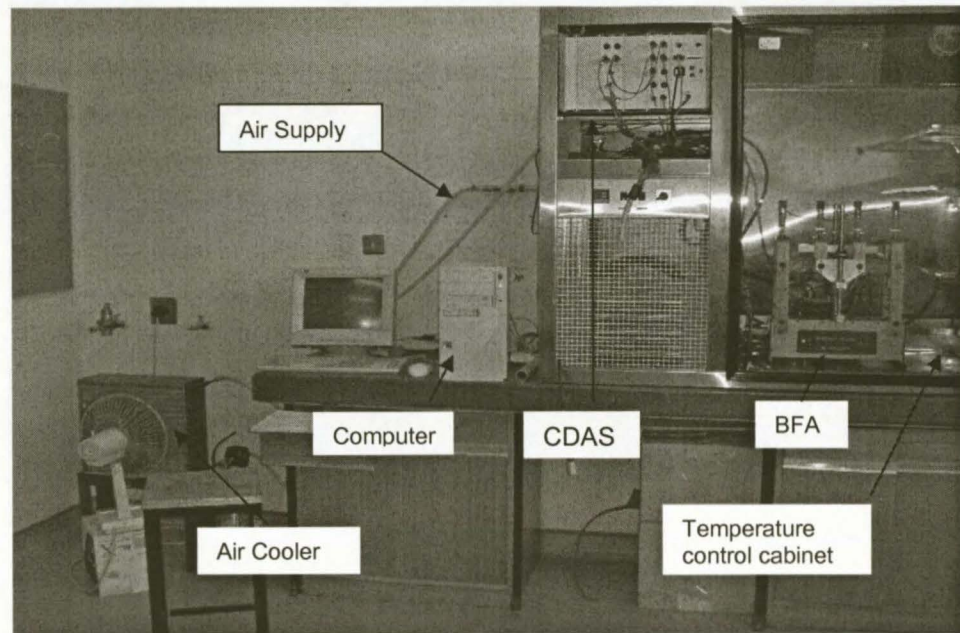


Figure 4.19: Pictorial components of fatigue beam testing system.

4.4 4PB FATIGUE TESTING PROCEDURE

4.4.1 Flexural stiffness testing of beam specimen

The 4PB flexural stiffness set-up of a beam specimen is shown in Figure 4.20. The testing procedure for the characterisation of the fatigue properties of cold bituminous mixes has been based on the "The Standard Method of Testing for determining the Fatigue Life" Designation M-009, SHARP, (1996). This test method was modified by AUSTRROADS, (1998) to suit the IPC 4PB-testing equipment (BFA) and data acquisition system (CDAS).

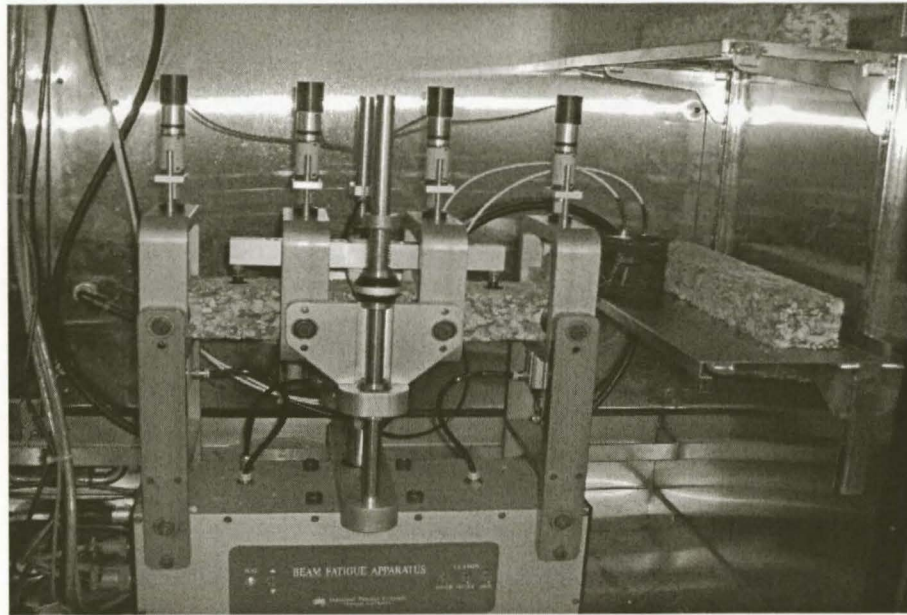


Figure 4.20: Beam set-up and conditioning in the temperature control cabinet at 5°C.

The specimens are conditioned at 5°C in the controlled temperature cabinet see Figure 4.20. This temperature was found to provide beam failure at middle of the with high uniform stress conditions. A constant maximum bending moment occurs at the central third section of the test beam specimen. Higher test temperatures were found to result in shear cracking occurring at the beam supports (Mullins 2006).

The duration for conditioning of beam specimens in the cabinet is at least four hours prior to testing to allow the specimen to stabilise at the testing temperature. The beam temperature is considered stabilised when the core and skin temperature of the dummy specimen in the cabinet differ by not more than 0.5°C at testing temperature. The dummy specimen was seen to be very sensitive to temperature change on the cabinet (opening and closing of the cabinet door). This does not represent the actual fluctuation of the specimen temperature especially at the core. However, in the severe climate the fluctuation has significant impact. Therefore modification by sealing the door front is necessary to reduce the effect of the air exchange when the cabinet door is opened. Provision of the suspended thick sliced plastic curtain might serve the purpose.

The specimen is then set-up in the BFA and subjected into four-point loading, see specimen's - testing procedures illustrated in the Appendix A.

The testing of specimen was carried out in the displacement-controlled mode, with a haversine loading wave (i.e. one direction loading where specimen returns to its pre-test position at the end of each loading cycle) at the load frequency of 10Hz. No rest period was included in the loading wave signal.

4.4.2 Testing parameters

Using computer software (IPC, UTM21), several input test parameters were entered to instruct the CDAS to control and monitor the specimen loading function and data acquisition from testing. The most relevant parameters are:

- Specimen identifications and dimensions (measured precisely using Vernier calliper)
- Peak tensile strain (various levels, between $100\mu\epsilon$ and $480\mu\epsilon$)
- Loading wave (haversine) and loading frequency (10Hz) and
- And termination condition, a maximum allowable number of cycles to failure and/or termination stiffness (50% of initial flexural stiffness), whichever is reached first during testing.

4.4.3 Termination criteria and cycles to failure.

The test is terminated on the first occasion that either of the following criteria is satisfied:

- The flexural stiffness falls below the operator -specified value of termination stiffness, or
- The number of loading cycles applied reaches the operator-specified maximum allowable number.

During the course of the test, the initial flexural stiffness is displayed and the operator is able to change the value of terminal flexural stiffness. To ensure the accurate assessment of the termination conditions, for “cycles to failure” and “flexural stiffness” of the test specimen at the same time to avoiding premature termination of the test, it is necessary to set the terminal stiffness at artificially low values and the allowable number of cycles to failure at artificially high values at the beginning of the test. Subsequently the values can be changed during the course of the test. Care should be taken on every test set-up to re-check the input values and files name to ensure that it corresponds to the intended test.

After the completion of the test the software creates a data file to archive/store the test results. This data file allows test result to be reviewed, printed, or imported into spreadsheet program for further analysis.

4.5 FLEXURAL STIFFNESS CALCULATIONS

The initial flexural stiffness is the flexural stiffness of the beam specimen calculated by the CDAS at the 50th load cycles. After the completion of the first 50 loading cycles, the IPC (UTM 21) software using the input parameters determines, peak force and peak displacement and calculates the following test parameters among others: The derivations of these mathematical relationship are presented in Appendix D.

$$\sigma_t = \frac{GoP \times 10^6}{wh^2} \quad (4.1)$$

Where: σ_t = maximum tensile stress (KPa)
 Go = Outer gauge length (typically 355.5mm)
 P = peak force (kN)
 w = average beam width (mm)
 h = average beam height (mm)

$$\varepsilon_t = \frac{12\delta h \times 10^6}{(3Go^2 - 4Gi^2)} \quad (4.2)$$

Where: ε_t = maximum tensile microstrain, (mm/mm)
 δ = peak deflection at the centre of beam (mm)
 Gi = Inner gauge length (typically 118.5mm),
 = other parameters as mentioned in Equation (4.1)

$$S = \frac{10^3 \times \sigma_t}{\varepsilon_t} \quad (4.3)$$

Where: S = flexural stiffness, (MPa)
 Other variables as explained above

The vertical force (load application) required to provide the desired specimen displacement is measured during pulsing. However, the variation in the initial readings during testing is substantial depending on the stiffness/sensitivity of the mix. This variation reduces considerably within the first 50 pulses. For this reason, the determination of initial flexural beam stiffness (S_i) was determined by plotting stiffness (s) against load cycles (n) of the first initial 500 pulses, and solve the regression relationship of the best-fitting by power/exponential function as shown in Figure 4.21. Where the regression relationship did not show the desired fit, the BFA initial stiffness was adopted.

For the determination of fatigue life (cycles to failure) the best-fit with power/exponential function on cycles after 500 to cycles where initial flexural stiffness value reduced by 50 percent was used to solve the regression relationship as follows;

$$S = Ax^n \quad (4.4)$$

Or

$$N_{f,50} = \frac{\log\left(\frac{S_{f,50}}{A}\right)}{n} \quad (4.5)$$

Where:

- $N_{f,50}$ = load cycles to failure
- $S_{f,50}$ = Stiffness, 50 percent of initial stiffness (MPa)
- A = regression constant
- n = regression constant

Where the regression relationship did not show the best fit the extrapolation of the BFA plot was adapted to predicted fatigue life.

The beam stiffness is related to beam geometry and dimensions. Therefore defected beam specimen (chipped off or inaccurate cut) may results in significant different fatigue results. This is due to the fact that the calculation of beam deflection depends on the beam height in power three factor as shown in the following relationship:

$$d = \frac{23 PL^3}{648 EI} \quad (4.6)$$

$$I = \frac{bh^3}{12}$$

Where:

- δ = displacement at the centre of the beam (mm)
- P = applied load (KN)
- E = modulus of elasticity (MPa)
- I = moment of inertia (m^4)

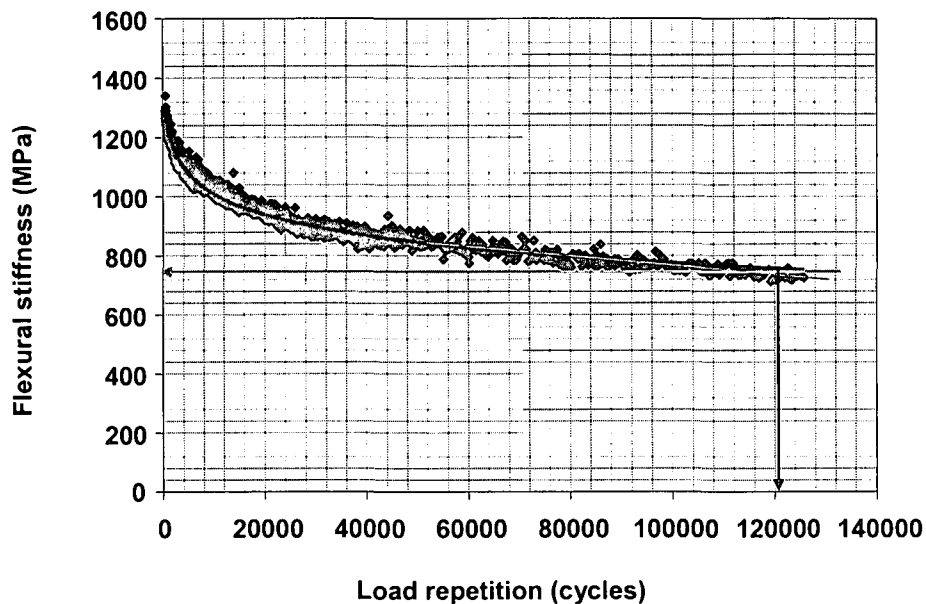


Figure 4.21: Flexural stiffness as a function of load repetition in displacement controlled test.

4.6 CONCLUSIONS

There are many factors that require considerations in the specimen preparation of a selected mix in order to be able to achieve a good quality test specimen. The interaction of binder, cement, mineral aggregates and moisture content has variable characteristics during mixing, compaction, curing and cutting of beams. The optimization of these parameters ensures sufficient level of reliability of the produced test specimen. However the prepared beam specimen in conjunction with the test equipment and testing procedure provide test results that enable proper characterization of the mix properties. The methods used in this study for the specimen preparation and testing procedures provide the following conclusion to be drawn.

4.6.1 Mixing and compaction

- The moisture content and filler percentage during mixing and compaction plays a vital role in the behaviour of the bitumen emulsion and foamed bitumen mixes. The moisture acts as densification agent of individual particles in the mix and aid in bitumen dispersion of foamed bitumen over the filler during mixing. The addition of 70% OMC during mixing was producing fairly dry mixes in

case of the foamed bitumen, which resulted in less workability for proper compaction. This had to be increased to 80% of OMC. For the emulsion mix 70% OMC was seen to produce fairly wet mixes during compaction and was hence reduced to 65% OMC. This is due to fact that bitumen in emulsion acts more like a fluid during compaction than the foamed bitumen.

- The addition of active filler (cement) improves the dispersion of foamed bitumen and breaking of bitumen emulsion. This has an advantage of increasing cohesive strength of the mixes. However the addition of active filler should be done in conjunction with emulsion or foam to ensure the achievement of its role in the mixes.
- The influence of compaction level and technique is significant on the mix behaviour. The use of a laboratory steel-wheel roller with both static and vibration action in the compaction of bitumen emulsion or foamed bitumen mixes provided sufficient compaction effort to compress the required materials in a slab mould (frames). The compaction level applied for emulsion mixes was 50-60 passes and 60-70 passes for foam mixes. For each 10 passes were vibratory. These passes were able to achieve compaction level more than the target of 98% MDD for emulsion mix and fairly low for the foam mix. This might be due to inaccuracy of the theoretical method of determination of the specimens' densities.

4.6.2 Cutting of the test beams

- The cutting technique adopted to produce and shape beams faces plays a significant role in the condition and quality of beams. The materials treated with emulsion or foam are too weak for wet cutting. Therefore dry cutting is preferred. However, this method produces excessive dust, which is hazardous to health and needs extra precautions. The normal laboratory saw cutter (fixed motor and sliding table) seems to produce inferior quality beam. This necessitates a modification to improve the set-up of the specimen and to minimize variability. The details of the modifications are explained in Section 4.2.7.
- The beam conditions and dimensions play a vital role in the quality and variability of the test results. The weakness of the bound bitumen emulsion or foamed bitumen mixes causes the chipping off of aggregates at the edge and faces of beam specimen during the trimming process. Inadequate set-up of the saw cutting machine resulted in some beam depths of $\pm 3\text{mm}$ in lieu of tolerance of $\pm 0.5\text{mm}$. This has a significant impact on the calculation of stiffness values. Therefore, to minimize chipping off aggregates the effective slab thickness should be increased to 70mm instead of 60mm. Alternative solution could be to frozen the slab at i.e. 0°C and cut while brittle, but the prones and cones needs to be investigated.

4.6.3 Testing procedures

- The quality of the acquired data during testing relies on the smooth operation of the servo-pneumatic controlled system. Low testing temperatures might cause condensation of supplied air in the system resulting in non-continuity of air flow due to ice blockage. This impacts on the motion of the loading actuator (jumping motion or weak stroke) hence damaging the test beam specimen and consequently the captured data. The process of filtering the air to avoid excessive water in the system is therefore required. The modifications and additions of filters and heating element to the testing equipment are explained in section 4.32.
- The control and monitoring of the testing system is achieved through a personal computer, CDAS and the software for input parameters. The input parameters determined the type of the test. These parameters therefore need to be correctly verified before running to avoid premature failure of the test beam specimen. Similarly, the beam numbering should be consistent all along from casting of slab until testing for appropriate analysis and to avoid mixing-up specimens.
- The increase or decrease in test temperature affects the performance of the mixes. The test temperature of 5°C is prone to quick raise by opening the door of the climate chamber, especially in summer period. This requires some improvement of the chamber by providing a suspended split curtain at the door which will allow working with BFA while preventing high exchange of air in and out of the climate chamber.

4.7 REFERENCES

AIREY G.D., 1995. **Fatigue testing of asphalt mixtures using the laboratory third-point loading fatigue testing system**. Masters Dissertation, University of Pretoria, Pretoria, South Africa.

ASPHALT ACADEMY., 2002. **The design and use of foamed bitumen treated materials**. Interim Technical Guideline TG2, Pretoria, South Africa.

AUSTROADS., 2001. **Fatigue life of compacted bituminous mixes subject to repeated flexural bending**. AST03, Sydney, Australia

BARKSDALE R.D. and MILLER J.H., 1977. **Development of equipment and techniques for evaluating fatigue and rutting characteristics of asphalt concrete mixes**. Report SCEGIT-77-147. School of Civil Engineering, Georgia Institute of Technology, Atlanta.

IPC (Industrial Process Controls Ltd), 1998. **Beam fatigue apparatus**. Reference Manual, Boronia, Australia.

JENKINS J.K., 2000. **Mix design considerations for cold and half –warm bituminous mixes with emphasis on foamed bitumen**. PhD Dissertation, University of Stellenbosch, South Africa.

LIEBENBERG J.J.E., 2003. **A structural design procedure for emulsion treated pavement layers**. Masters Dissertation, University of Pretoria, Pretoria, South Africa.

LONG F.M and THEYSE H.L., 2001. **Laboratory testing for the HVS sections on Road P243-1**. Contract Report CR-2001/32, Transportek, CSIR, Pretoria, South Africa.

MEDANI T.O., HUURMAN M., HOUBEN L.J.M and MOLENAAR A.A.A., 2000. **A proposed fatigue based design methodology for asphalt mixes applied on orthotropic steel bridges**. Delft University of Technology, the Netherlands.

Mullins L..S, 2006. **Fatigue properties of emulsion treated materials**, Master Thesis, to be submitted to Stellenbosch University, South Africa.

PELL P.S and COOPER K.E., 1975. **The effect of testing and mix variables on the fatigue performance of bituminous materials**. Proceedings, Association of Asphalt Paving Technologists, Vol 44, pp 1-37.

RAITHBY K.D and STERLING A.B., 1972. **Some effects of loading history on the fatigue performance of rolled asphalt**. Great Britain Transport and Road Research Laboratory Report LR 496, Crowthome, Berkshire.

ARE, Inc., Engineering Consultants. 1986. **Development of asphalt aggregate mixture analysis system**. Prepared for NCHRP.

TANGELLA RAO S.C.S., CRAUS J., DEACON J.A and MONISMITH C.L., 1990. **Summary report on fatigue response of asphalt mixtures: Prepared for Strategic Highway Research Project A-003-A**. Report TM-UCB-A-003A-89-3, University of California, Berkeley.

TEYABALI A., ROWE G. and SOUSA J., 1992. **Fatigue response of asphalt-aggregate mixtures**. Paper presented at the annual meeting of the Association of Asphalt Paving Technologists, Charleston, South Carolina.

THEYSE H.L., 2000. **The stiffness, strength and performance of unbound aggregate**. Contract Report CR-2000/35, Transportek, CSIR, Pretoria, South Africa.

CHAPTER 5

5. CHARACTERIZATION OF FATIGUE PROPERTIES

5.1 INTRODUCTION

The characteristic of fatigue properties or fatigue performance is usually expressed as a relationship between the maximum stress or strain and the number of load repetition to failure. Among other methods, used to characterize the fatigue performance of the mixes (see Chapter 3) the conventional method (Wöhler model) was applied to develop fatigue relationships for cold bituminous mixes in this study. In this relationship, the number of fatigue load repetitions to failure (N_f) is related to the maximum tensile strain occurring at the bottom of the asphalt layer (ϵ) or beam specimen as given in Equation 5. 1.

$$N_f = a\epsilon_t^n \quad (5.1)$$

$$\text{Or} \quad \text{Log}(N_f) = A - n \text{Log}(\epsilon_t) \quad A = \text{Log } a \quad (5.1a)$$

Where:

- N_f = number of load repetition to failure (Fatigue life)
- ϵ_t = maximum tensile strain
- a, n = experimental determined coefficients

The fatigue parameters a and n are experimentally determined coefficients that vary with mixture properties, temperature and the method of testing. In four point beam fatigue testing in the displacement control mode, failure of the beam (N_f) is defined as the number of load repetitions to reduce the flexural stiffness to half of its original value (S_i). Rowe et al. (2000) indicated that stopping a test at 50 percent reduction in initial stiffness underestimates the performance of the mix as this point is often reached before crack initiation occurs. The original (initial) stiffness (S_i) of the mix is determined using procedure illustrated in Section 4.5, Chapter 4.

The fatigue characterization guideline for HMA adopted in South Africa is defined by CSIR, (2000). Because the guideline is not strictly applicable for HMA it was used to characterize the fatigue performance of cold mixes for comparison purposes. The guideline indicates that there are unavoidable variations in support conditions, traffic axle configurations and wander, traffic speeds, type pressure and axle loads that can lead to a significant variation in actual tensile strains for a uniform section of road. Hence, the HMA Guideline advises that it is not appropriate to represent the strain condition in a road by a single strain value and suggests that it is more appropriate to

calculate a range of expected strains using a probabilistic response model, and then characterizing the working strain range of pavement as low, medium or high.

The guideline therefore provides the interpretation of four point bending beam fatigue results as presented in Table 5.1. The limits shown in Table 5.1 pertain to controlled displacement tests performed at 5°C and at 10Hz loading rate.

Table 5.1: Guideline for interpretation of fatigue test data at constant strain, (CSIR, 2000)

Relative Fatigue performance	Number of Load repetition to failure for strain regime at 5°C and 10Hz		
	Low Strain 180 - 230 $\mu\epsilon$	Medium Strain 320 - 370 $\mu\epsilon$	High Strain 380-430 $\mu\epsilon$
Good	> 2 400 000	>130 000	> 60 000
Medium	1 000 000 - 2 400 000	30 000 – 130 000	20 000 – 6 000
Poor	< 1 000 000	<30 000	<20 000

The guideline further recommends that beams should be tested at the strain level that falls within the appropriate strain regime and a minimum of 3 beams should be tested at the strain regime. The graphical presentation of the strain regimes are presented in Figure 5.1.

In Figure 5.1 it can be seen that the strain regimes' demarcations are broad thus providing a wide range of poor to good performance relative to the materials fatigue life, e.g. a fatigue life of one million repetitions is poor performance at 180 $\mu\epsilon$ and good performance at 270 $\mu\epsilon$. The 270 $\mu\epsilon$ is usually considered medium to high strain in the pavement layer. It was expected that low strain should range from 180 -200 $\mu\epsilon$, medium from 320-350 $\mu\epsilon$ and high strain should range from 380-400 $\mu\epsilon$ for a better estimated of the fatigue performance. Figure 5.1 illustrates the strain regimes with fatigue performance, where above the upper limit line indicates good fatigue performance of the mixture, in between it is either good-medium or medium-poor and below lower limit line indicates poor performance of the mixture.

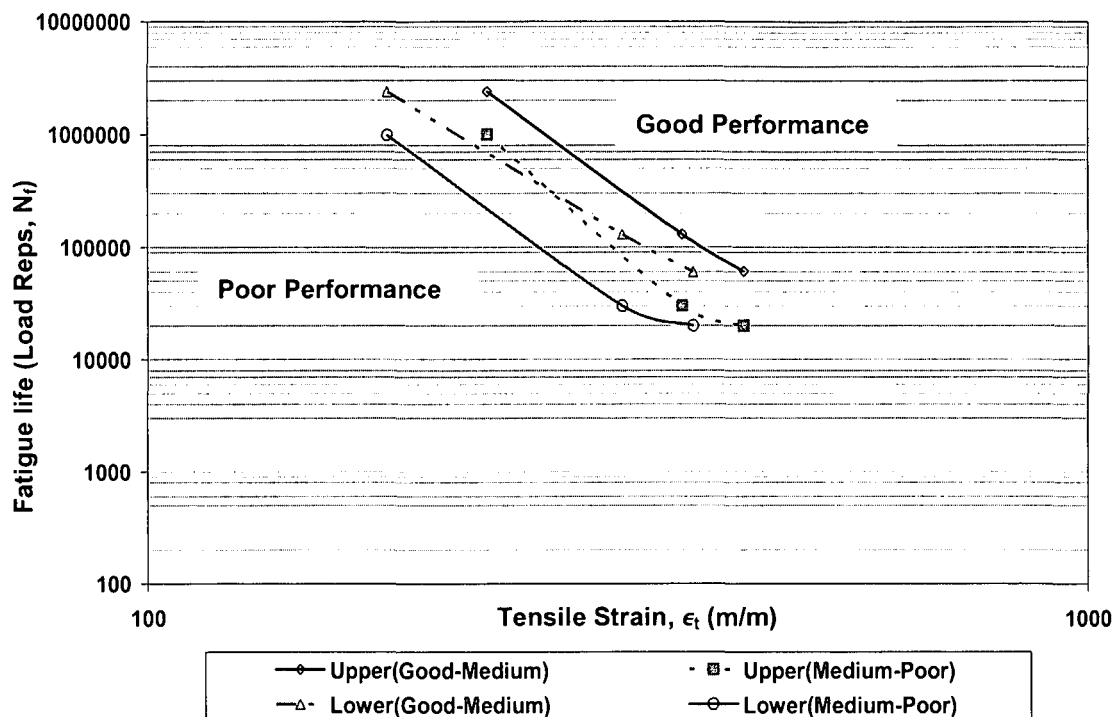


Figure 5.1: Strain regimes for the four point beam fatigue performance of HMA(CSIR, 2000)

The characterization of fatigue properties in this study was established by carrying out a number of fatigue tests at various ranges of strain levels and their respective number of load repetition to failure (fatigue life). The numbers of load repetitions to failure are the numbers of repetition to the point of crack initiation in the pavement layer, or beam specimen. The Wöhler parameters were determined from a regression analysis plotted on log-log scale using strain levels and loads repetitions to failure. The fatigue relationship associated with the cold mixed being tested and parameters of this study are discussed in subsequent sections. The other aspect of the investigation was to establish whether the fatigue relations for these cold mixes were indeed linear on log-log plot.

5.2 FATIGUE TESTING PARAMETERS AND RESULTS.

The fatigue testing methodology is in detail explained in Chapter 4. The testing parameters used to determine the fatigue life were:

- Mode of loading : Controlled displacement mode
- Loading wave form : Haversine
- Loading frequency : 10Hz
- Testing Temperature : 5°C

The fatigue testing were conducted using IPC Four Point Bending Apparatus at strain levels ranging between 100-480microstrain. Due to fairly high amount of variability on the test twelve beams specimens of each mix were tested to increase the statistical reliability of the modeling.

During fatigue testing as the displacement controlled fatigue test progresses, the deflection remains constant, while the load remains at steady state up to the point of initial crack failure and then decreases until complete failure.

However, controlled displacement tests at low strain levels usually indicate a substantial difference between the number of repetitions to initial failure point and the ultimate failure of the specimen, which makes the determination of the exact number of repetitions to initial crack stage sometimes difficult. This has been evident as many tests needed to be stopped due to many days of testing without coming close to reaching the 50 percent reduction in initial stiffness. Consequently, the numbers of load repetitions to failure were merely estimated by extrapolation of the failure trend line captured by the software (BFA).

The acquired test data during flexural beam testing were stored in a computer file. Then these files were imported into spreadsheet and analyzed for fatigue life.

In this chapter, the analysis of fatigue results for characterization of the fatigue properties of the bitumen emulsion and foamed bitumen mixes will be addressed. The normalization of effective fatigue life using strain ratio will be presented and discussed and finally comparisons on fatigue properties of bitumen emulsion and foamed bitumen mixes to quantify their relative fatigue performance will be discussed, then conclusion being drawn on the fatigue characterization of these mixes.

5.3 CHARACTERIZATION OF FATIGUE PROPERTIES OF BITUMEN EMULSION MIXES

This section discusses the fatigue property results from four point flexural beam tests on three different selected bitumen emulsion treated mixes. The variability of the measured fatigue life from 4PB fatigue test generally depends on the mixture properties, geometry of the beam specimen and interpretations of results. The modeling of emulsion mixes in fatigue properties is dealing with the results of twelve beam specimens to characterize the mixes fatigue performance.

The summary of the measured fatigue life of bitumen emulsion mixes; Mix 4 (B-75C-0%), blend of 75%limestone and 25% milling asphalts (RAP) with no cement, is presented in Table 5.2. Mix 5 (B-75C-1%), blend of 75%limestone and 25% asphalts milling (RAP) with 1% cement, is

presented in Table 5.3 and Mix 6 (B-75M-0%), blend of 25%limestone and 75% asphalt millings (RAP) with no cement, is presented in Table 5.4. The summaries include the test maximum tensile strain, the determined initial flexural stiffness, phase angle and the fatigue life (load repetition to failure). Detailed graphs of the mixes fatigue properties are presented in Appendix C.

Table 5.2: Fatigue properties of bitumen emulsion Mix 4(B-75C-0%) at 5°C and 10Hz

Beam Specimen	Strain level ($\mu\epsilon$)	Initial flexural stiffness (MPa)	Phase angle ($^{\circ}\text{C}$)	Fatigue life Load Reps to failure
A2	470	1 672	28	7 674
A5	450	1 572	33	7 059
A1	430	2 059	28	11 114
A3	400	1 521	22	9 323
A4	380	1 753	31	10 215
A6	350	2 349	39	15 050
B1	330	3 621	27	23 020
B6	300	3 563	28	95 250
B2	250	2 799	29	316 220
B3	230	2 626	27	132 350
B5	200	3 544	25	1 177 900
B4	180	3 177	27	416 860

Table 5.3: Fatigue properties of bitumen emulsion Mix 5 (B-75C-1%) at 5°C and 10Hz

Beam	Strain level ($\mu\epsilon$)	Initial flexural stiffness (MPa)	Phase angle ($^{\circ}\text{C}$)	Fatigue life Load reps to failure
C1	420	1 270	21	5 713
C6	380	2 524	12	16 986
B1	350	1 674	11	23 612
B2	300	1 616	10	88 200
B3	280	2 101	15	2 1 300
B6	250	1 617	18	560 000
B5	200	1 832	24	172 000
D4	190	2 850	15	94 000
B4	180	2 370	17	800 000
C3	140	2 785	17	2 400 000
C5	120	3 093	14	1 700 000

Table 5.4: Fatigue properties of bitumen emulsion Mix 6 (B-75M-0%) at 5°C and 10Hz

Beam Specimen (no.)	Strain level ($\mu\epsilon$)	Initial flexural stiffness (MPa)	Phase angle ($^{\circ}$ C)	Fatigue life Load reps to failure
B5	470	3658	20	1 748
A3	450	2 893	23	4 573
A4	400	3 346	25	7 706
B2	380	4173	17	8 000
B6	370	4 061	18	7 120
B4	350	3910	20	15 440
A1	300	4 035	23	27 130
A2	250	4 045	16	132 000
A6	230	3 850	23	168 520
B1	200	4 391	17	1 345 510
A5	180	3 593	20	1 260 000
B3	150	3750	15	2 630 000

The fatigue properties of the emulsion mixes Mix 4, 5 and 6 presented in Tables 5.2, 5.3 and 5.4 show that under controlled displacement mode at selected loading time (frequency) and temperature the fatigue life increases as the maximum tensile strain decreases as in the case with many HMA. However, as strain decreases the stiffness of the Mix 4 and 5 significantly increases unlike Mix 6 see Figure 5.2. This is unexpected in fatigue tests for visco-elastic materials. The reason for this behaviour is not clear, but it might be due to sensitivity of equipment, mixture variable and tests conditions, which need further investigation.

However the lower phase angle of these mixes an average of 10° to 39° show that the mixes are more elastic in visco-elastic behaviour compared to hot mix asphalt. The visco-elastic behaviour of bituminous treated materials assumes homogeneity with respect to stiffness modulus in the whole specimen during fatigue test. However, the beam fatigue test is designed, through its geometry, to initiate cracking at its centre where horizontal stresses are highest. The binder dispersion in the cold mixes is not as uniform as that of HMA; therefore, with a cold mix beam, the decrease in materials stiffness during fatigue testing depends on the location of weakness in the specimen where micro-cracks initiate or where cracking (formation of defects and dislocations) occurs.

The variability in the location of the failure points (weakness) that result from spilling of the beam edges and faces during sawing and no-uniform binder dispersion, leads to higher variability in the

estimation of fatigue life than for HMA. However, the use twelve beam test results will account for the variability in developing a fatigue function (model) for statistical significance.

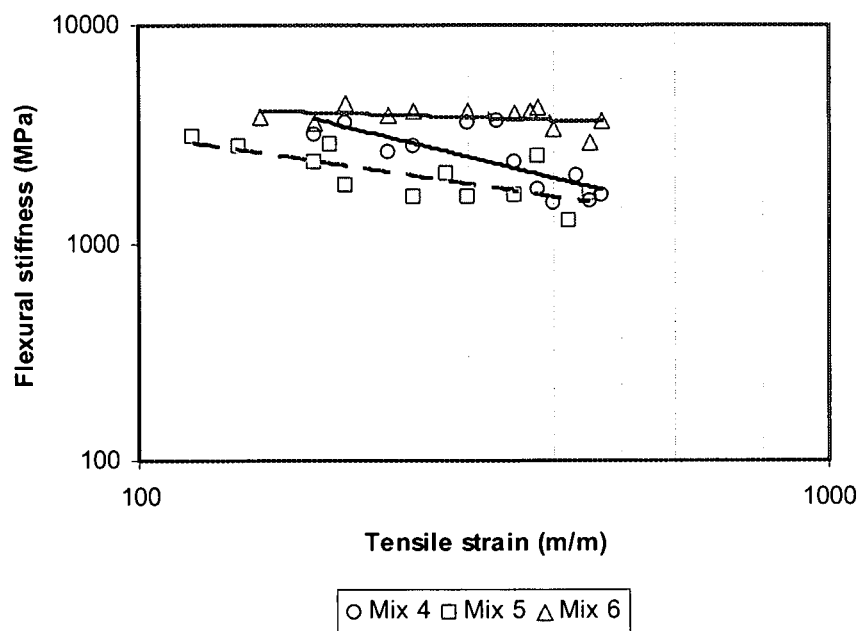


Figure 5.2: Initial flexural stiffness versus strain levels for emulsion Mix 4(B-75C-0%), Mix 5(B-75C-1%) and Mix 6(B-75M-0%) at 5°C and 10Hz

The characterization of fatigue properties (models) of these selected emulsion mixes gives an insight in the comparison of the fatigue behavior in regard to mix characteristic with and without cement and variation of asphalt millings (RAP) in the mix.

The models of emulsion mixes Mix 4(B-75C-0%), Mix 5(B-75C-1%) and Mix 6(B-75M-0%) plotted on log-log scale as load repetitions against tensile strain show linear fatigue lines. The fatigue lines for Mix 4 and 5 of 75% limestone blend with and without cement appears to be parallel Figure 5.3. However, the mix with addition of cement show decrease in fatigue performance compared to the mix without cement. This was unexpected. It might be due to untimely addition of the cement during mixing in conjunction with the addition of bitumen emulsion.

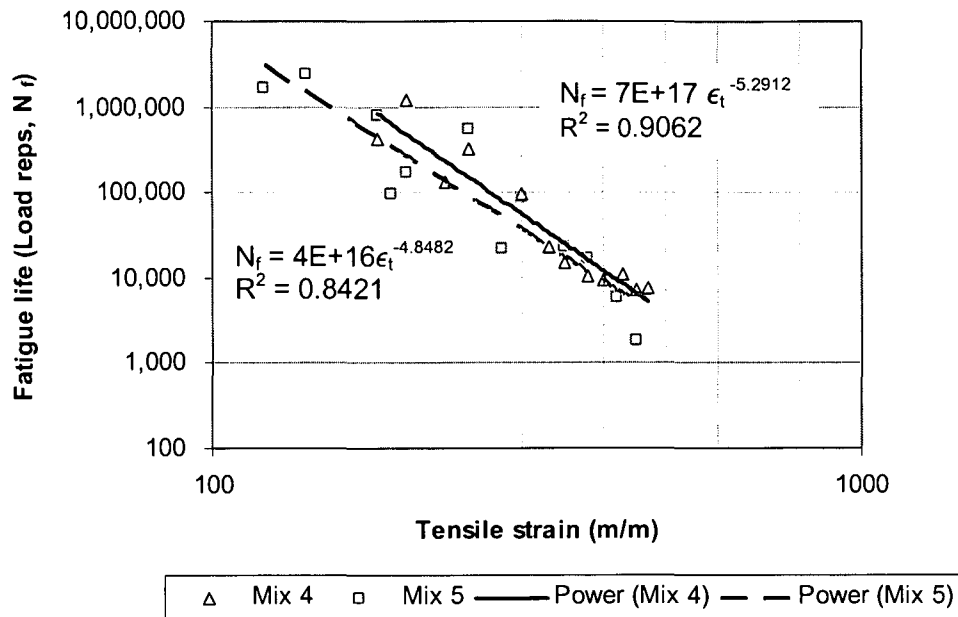


Figure 5.3: Fatigue models of emulsion Mix 4(B-75C-0%) and Mix 5(B-75C-1%) at 5°C and 10Hz

In Figure 5.3, it can also be seen that fatigue properties at low strain regime are more scattered especially in the mix with addition of cement compared to higher strains. This was due to premature failure of the test beam specimens that failed to reach 50% of its initial stiffness after many load repetitions in several days. Hence, premature stoppage was necessary. It was considered impractical to test the specimen for such long. The resulted fatigue data were, therefore extrapolated to obtain expected fatigue life.

The superimposition of emulsion Mix 4 (B-75C-0%), Mix 5 (B-75C-1%), and Mix 6 (B-75M-0%) Figure 5.4 shows that fatigue line for Mix 6 with 75% RAP is not parallel to Mix 4 and 5. This might be due to high stiffness of the mixture. The steeper slope of fatigue line at lower strain regime indicated that it has significant fatigue performance compared to Mix 4 and 5. However, at high strain regime this mix shows a decrease in fatigue performance. The cause of increase or decrease in fatigue performance of this mix is not clear however. It might be due to interactions of bitumen emulsion (added) and old binder in the RAP that needs further investigation.

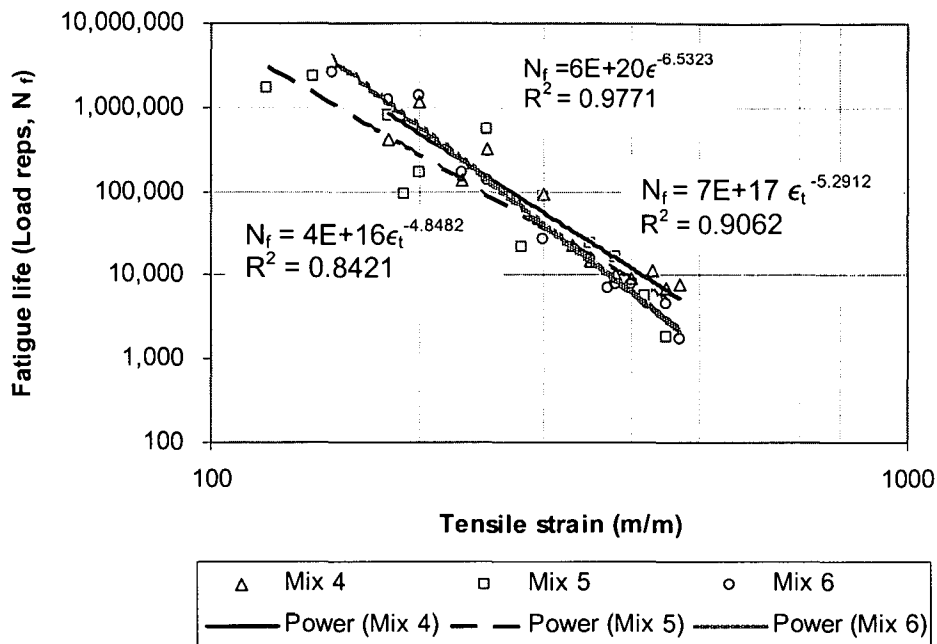


Figure 5.4: Fatigue models of emulsion Mix 4(B-75C-0%), Mix 5 (B-75C-1%) and Mix 6(B-75M-0%) at 5°C and 10Hz

The emulsion mixes fatigue models parameters determined from linear regression of Wöhler equation are presented as shown in Table 5.5.

Table 5.5: Fatigue characteristics of the emulsion mixes for Wöhler Equation

Mix Type	Log (A) (m/m)	N	R ²	ε _b
4: B-75C-0%	17.845	5.291	0.906	1845
5: B-75C-1%	16.603	4.848	0.837	994
6: B-75M-0%	20.778	6.533	0.977	921

For the Wöhler equation, as the slope of the fatigue line increase (high value of n), it implies that the mixture is increasing in resistance to fatigue. While as the slope of the fatigue line decreases (low value of n) it implies that the mixture is decreasing in fatigue resistance. As for the behaviour of these mixtures in pavement layer, the one with high value of n will show high sensitivity to overloading and with low value of n less sensitivity to overloading.

The expected increase in fatigue resistance and sensitivity to overloading with increasing in cement content in not evident as the mixture parameters (n-value) for the Mix 5(B-75C-1) seems to be decreasing compared to mix with no cement and high percentage of RAP. This is

unexpected as the mix with cement would have shown a significant increase in n-values, if the influence of the cement had played its role in improving the mixture properties.

The use of strain-at-break values (investigated in Chapter 6) as shown in Table 5.5 introduce a flexibility consideration as opposed to just strength of the mixture. Mix 4(B-75C-0%) has $\epsilon_b = 1845\mu\text{m/m}$, Mix 5 (B-75C-1%) has $\epsilon_b = 994\mu\text{m/m}$ and Mix 6(B-75M-0%) has $\epsilon_b = 921\mu\text{m/m}$. This shows that Mix 4 is stronger (flexible) compared to Mix 5 and Mix 6, However this does not fully concur with the investigation on the fatigue performances on these mixes. Nevertheless the correlation between fatigue life and strain-at-break properties of the emulsion mixes indicates that there is a link between these parameters that might enable the best analysis on the performance of the mixes in pavement layer.

5.4 EFFECTIVE FATIGUE TRANSFER FUNCTION OF BITUMEN EMULSION MIXES

A major difficulty with fatigue failure is developing a meaningful relationship between the results of the laboratory tests and the field performance. The fatigue life of a pavement incorporating cold mixes as determined from laboratory flexural beam tests is generally lower than observed in the field (Jenkins, 2000). To account for the difference between laboratory and field response, a transfer function is necessary to translate laboratory fatigue characteristics to those considered representative of in-situ performance.

In the mechanistic pavement design method applied in South Africa, the transfer function for effective fatigue life of cemented layer relates the ratio of the tensile strain at the bottom of the base layer and the strain-at-break (maximum tensile strain that the mix can sustain before crack initiation), called "Strain Ratio" to the number of load repetitions to reach the equivalent granular state. This behaviour has been considered applicable for cold bituminous treated materials (Long, 2002). The tensile strain at the bottom of the layer is related to maximum controlled strain, ϵ applied to the flexural beam specimen under laboratory fatigue tests. Strain-at-break, ϵ_b is determined from a monotonic flexural test on a beam specimen, where the applied load and vertical displacement are measured during the test.

The strain-at-break has been investigated as a possible normalizing parameter for the fatigue analysis of the cold mixes. If it can accurately reflect the laboratory fatigue properties of cold mixes, it can be linked to the mix type for the analysis of the layer effective fatigue life in pavement structure, in a similar fashion as for cemented materials (Theyse, 2000).

However many researchers are still questioning the applicability of the strain-at-break properties as a normalizing parameter for the fatigue analysis of the cold mixes. The selected materials treated with bitumen emulsion have shown the strain-at-break values as presented in Table 5.5 above. Using these values and the tensile strain, (ϵ) from the fatigue properties Table 5.2, 5.3 and 5.4 the strain ratio (ϵ / ϵ_b) of these mixes were calculated and these are presented in Table 5.6, 5.7. and 5.8 respectively.

Table 5.6: Strain ratio and effective fatigue life of Mix 4(B-75C-0%) at 5°C and 10Hz

Beam Specimen (no.)	Tensile Strain ($\mu\epsilon$)	Strain Ratio (ϵ/ϵ_b) at $\epsilon_b = 1827\mu\text{m/m}$	Effective fatigue life
A2	470	0.26	7 674
A5	450	0.25	7 059
A1	430	0.24	11 114
A3	400	0.22	9 323
A4	380	0.21	10 215
A6	350	0.19	15 050
B1	330	0.18	23 020
B6	300	0.16	95 250
B2	250	0.14	316 220
B3	230	0.13	132 350
B5	200	0.11	1 177 900
B4	180	0.10	416 860

Table 5.7: Strain ratio and effective fatigue life of Mix 5 (B-75C-1%) at 5°C and 10Hz

Beam Specimen (no.)	Strain level ($\mu\epsilon$)	Strain Ratio (ϵ/ϵ_b) at $\epsilon_b = 994\mu\text{m/m}$	Effective fatigue life
C4	450	0.46	1 819
C1	420	0.43	5 713
C6	380	0.39	16 986
B1	350	0.36	23 612
B2	300	0.31	88 200
B3	280	0.29	2 1 300
B6	250	0.26	560 000
B5	200	0.20	172 000
D4	190	0.19	94 000
B4	180	0.18	800 000
C3	140	0.14	2 400 000
C5	120	0.12	1 700 000

Table 5.8: Strain ratio and effective fatigue life of Mix 6 (B-75M-0%) at 5°C and 10Hz

Beam Specimen (no.)	Strain level ($\mu\epsilon$)	Strain Ratio (ϵ/ϵ_b), at $\epsilon_b = 921\mu\text{m/m}$	Effective fatigue life
B5	470	0.51	1 748
A3	450	0.49	4 573
A4	400	0.43	7 706
B2	380	0.41	8 000
B6	370	0.40	7 120
B4	350	0.38	15 440
A1	300	0.33	27 130
A2	250	0.27	132 000
A6	230	0.25	168 520
B1	200	0.22	1 345 510
A5	180	0.20	1 260 000
B3	150	0.16	2 630 000

The analysis of the pavement layer for the effective fatigue life of these mixes Table 5.6, 5.8, and 5.9 shows that as strain-at-break value increases the strain ratio decreases. For low strain loading, which could occur in very thick layers, the strain ratio becomes small approaching zero. At that stage a longer effective fatigue life is expected. The increasing in strain-at-break of Mix 4 (high strain-at-break value) gives small strain ratio. Depending on the tensile strain, loading this mix will have longer effective fatigue life compared to Mix 5 and 6.

The superimposition of the number of load repetition that can be sustained at that value of the critical parameter before the mix type fail and critical parameter (strain ratio) Figure 5.5 for Mix 4, 5 and 6 provide an intrinsic comparison of the laboratory fatigue performance related to field response of these mixes.

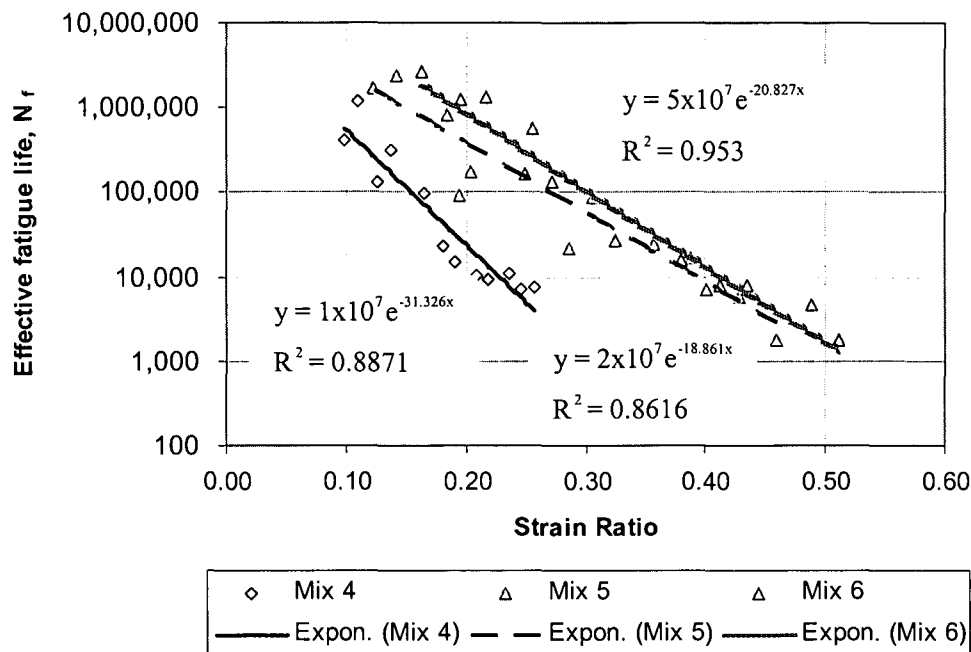


Figure 5.5: Effective fatigue life transfer function for Mix 4(B-75C-0%), Mix 5 (B-75C-1%) and Mix 6(B-75M-0%) at 5°C

The effective fatigue life models for the selected emulsion mixes using strain ratio shows significant differences. In Figure 5.5 it can be seen that Mix 4 having lower strain ratio is due to a high strain-at-break value has lower effective fatigue life for the same strain ratio compared to Mix 5 and 6 with lower strain-at-break values. This behaviour does not concur with the laboratory characterization of fatigue properties of these mixes. This indicates that the strain-at-break property is not a normalizing parameter for the fatigue life analysis of the emulsion mixes. The regression models of these mixes however show a notable decrease in R-square values of data points compared to laboratory fatigue relationship. This might have been caused by the rounding-off of the calculated strain ratios values.

The slope of the fatigue lines of normalized fatigue properties of Mix 4 is steeper compared to Mix 5 and 6. This shows that strain ratios from strain at break test do not correctly translate laboratory fatigue properties to those considered representative of the in-situ performance.

The summary of the effective fatigue life transfer function in Figure 5.4 of the selected emulsion mixes is presented in Table 5.9. The values of the regression coefficients for the transfer function a , and n are significantly different. This indicates that binder content, materials type, and the use of active filler and testing method have a significant effect on the effective fatigue life behaviour of the emulsion mixes.

Table 5.9: Effective fatigue life transfer function for selected bitumen emulsion mixes

Mix Type	Linear Regression (Exponential)	R2	Transfer Function*
B-75C-0%	$y = 1 \times 10^7 e^{-31.326x}$	0.89	$N_f = 10^{\left(7.000 - 13.605 \frac{\epsilon}{\epsilon_b}\right)}$
B-75C-1%	$y = 2 \times 10^7 e^{-18.861x}$	0.86	$N_f = 10^{\left(7.301 - 8.191 \frac{\epsilon}{\epsilon_b}\right)}$
B-75M-0%	$y = 5 \times 10^7 e^{-20.827x}$	0.95	$N_f = 10^{\left(7.698 - 9.045 \frac{\epsilon}{\epsilon_b}\right)}$

* y is substituted by N_f , and x by ϵ / ϵ_b in exponential regression equation after solving the logarithmic relationship.

5.5 CHARACTERIZATION OF FATIGUE PROPERTIES OF FOAMED BITUMEN MIXES

This section discusses the fatigue property results from 4PB tests on three different selected foamed bitumen treated mixes. The modeling of results deals with the results of twelve beam specimens due to variability of flexural beam test results.

The summary of the measure fatigue life of foamed bitumen mixes; Mix 7(B-75C-0%), blend of 75%limestone and 25% milling asphalts (RAP) with no cement, is presented in Table 5.10. Mix 8(B-75C-1%), blend of 75%limestone and 25% asphalts milling (RAP) with 1% cement, is presented in Table 5.11 and Mix 9(B-75M-0%), blend of 25%limestone and 75% asphalt millings (RAP) with no cement, is presented in Table 5.12. The summaries include the test maximum tensile strain, the determined initial flexural stiffness, phase angle and the fatigue life (load repetition to failure). Details of the mix fatigue properties are presented in Appendix C.

Table 5.10: Fatigue properties of foamed bitumen Mix 7(C-75C-0%) at 5°C and 10Hz

Beam specimen	Strain level ($\mu\epsilon$)	Initial flexural stiffness (MPa)	Phase angle (deg)	Fatigue life Load reps to failure
D5	470	2040	23	3 942
C1	450	1763	13	7 680
D3	430	1695	17	2 390
D4	400	2451	17	22 550
D6	380	2276	16	34 400
B4	350	614	24	42 000
D1	330	1836	23	66 000
B3	300	817	25	29 000
B5	250	725	24	3 420 000
D2	230	2858	18	732 820
A6	200	986	18	1 620 000
A5	180	1022	14	3 600 000

Table 5.11: Fatigue properties of foamed bitumen Mix 8 (C-75C-1%) at 5°C and 10Hz

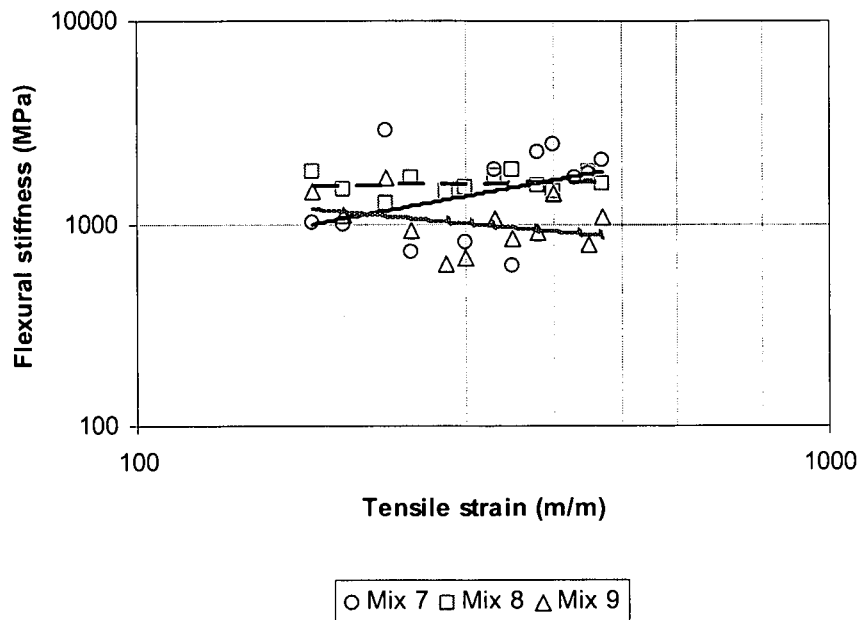
Beam specimen	Strain level ($\mu\epsilon$)	Initial flexural stiffness (MPa)	Phase angle (deg)	Fatigue life Load reps to failure
A4	470	1583	15	19 150
B5	450	1789	13	16 460
A2	400	1449	15	115 000
B3	380	1546	13	58 200
A3	350	1826	17	122 000
B2	330	1720	12	91 000
A1	300	1518	20	840 000
B4	280	1447	11	550 000
A5	250	1673	17	3 310 000
B1	230	1271	14	822 000
A6	200	1480	14	1 236 000
B6	180	1800	11	5 680 000

Table 5.12: Fatigue properties of foamed bitumen Mix 9(C-75M- 0%) at 5°C and 10Hz

Beam specimen	Strain level ($\mu\epsilon$)	Initial flexural stiffness (MPa)	Phase angle (deg)	Fatigue life Load reps to failure
C5	470	1072	22	19 300
C4	450	789	24	14 790
B4	400	1410	21	26 000
A3	380	896	31	39 600
A1	350	842	22	205 000
C2	330	1052	29	310 762
A2	300	682	33	212 588
C3	280	634	24	194 177
A6	250	924	22	830 000
B5	230	1693	16	410 000
A5	200	1096	21	1 980 000
B6	180	1444	18	3 520 000

The fatigue properties of foam mixes; Mix 7(C-75C-0%), Mix 8(C-75C-1%) and Mix 9(C-75M-0%) Table 5.10, 5.11, and 5.12 shows similar behaviour as recorded for the emulsion mixes under controlled displacement mode. The variability in initial flexural stiffness of Mix 7 and 9 as strain level decreases, see Figure 5.6, might have been caused by the weakness in the beam specimen. The fact that mixing moisture was increased from 70%OMC to 80%OMC for Mix 7 indicates that the low moisture content used in making slabs A's and B's resulted in non-uniform binder dispersion in the mixes, hence producing weak beams. It has been mentioned for the emulsion mixes that stiffness during fatigue test depends on the location of the weakness in the specimen where micro-cracking will occur. The spalling of beam edges and faces during sawing is due to weakness of the mix, that leads to higher variability of the stiffness reduction of the mixes.

For Mix 9 (C-75M-0%), the cause of the weakness of the mixtures is not clear, whether it is due to high percentage of RAP or the interaction of the new binder with the old asphalt in the RAP. The work of Voskuilen (2004) on half-warm foamed bitumen mixes shows that it is unlikely that the interaction of the new foamed bitumen and the RAP results in rejuvenation of the old binder. So the significant influence of the binder type and percentage of RAP in the mixture behaviour requires further investigation.



**Figure 5.6: Initial flexural stiffness versus strain levels for foamed bitumen
Mix 7 (C-75C-0%), Mix 8 (C-75C-1%), and Mix 9 (C-75M-0%) at 5°C and 10Hz**

Mix 8 (C-75C-1%) with addition of one percent cement, its stiffness behaviour does not appear to be a function of strain levels. The fact that this mix exhibits consistently uniform stiffness in all strain loading, shows that addition of small quantity of active filler (1% cement) improves the dispersion characteristics of foamed bitumen that results in better interaction of binder, mineral aggregates and moisture in the mixes.

The characterization of fatigue properties (models) of these selected foam mixes gives an insight in the comparison of the fatigue behaviour in regard to mix characteristics with and without cement and variation of asphalt millings (RAP) in the mix.

The superimposition of fatigue models of foam Mix 7(C-75C-0%) and Mix 8(C-75C-1%) in Figure 5.7 shows linear fatigue line in log-log plot. The slope of the fatigue lines shows that there is no significant difference in fatigue life of these mixes at low strain loading. However, significant shift is noted for the mix with additional of active filler (Mix 8) at higher strain loading with increase in fatigue life.

The fatigue model of Mix 9 with high percentage of asphalt millings (RAP) superimposed on Mix 7 and 8 (Figure 5.8) shows a parallel fatigue line with Mix 8 however with a decrease in fatigue life. But when compared with Mix 7 it shows that Mix 9 has higher fatigue life at high strain loading and

low at lower strain loading. This indicates that the mix with 75% RAP blend in the pavement layer might perform better than 75%limestone blend with no cement.

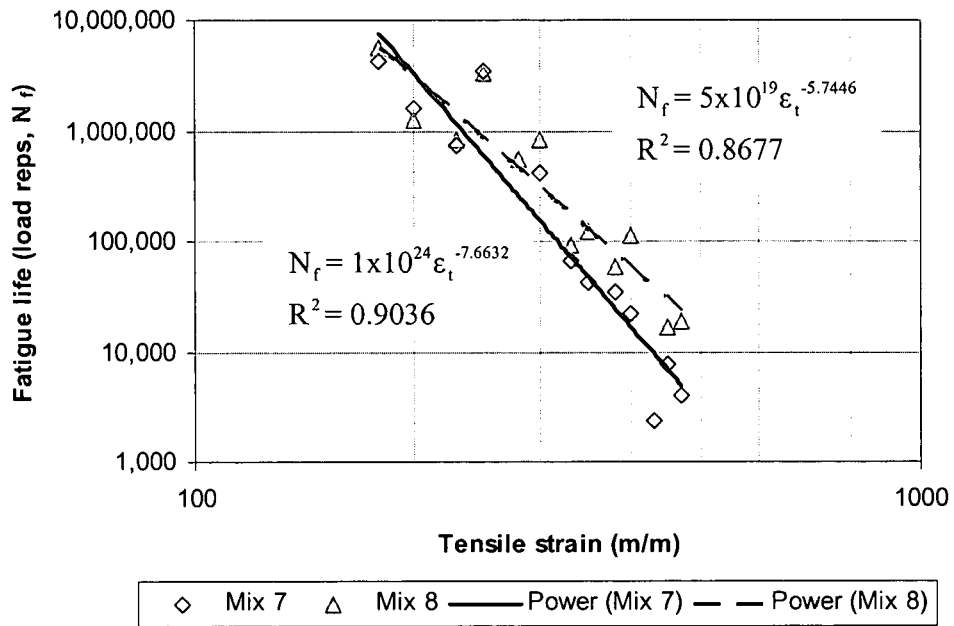


Figure 5.7: Characterization of fatigue properties, Mix 7 (C-75C-0%) and Mix 8(C-75C-1%) at 5°C and 10Hz

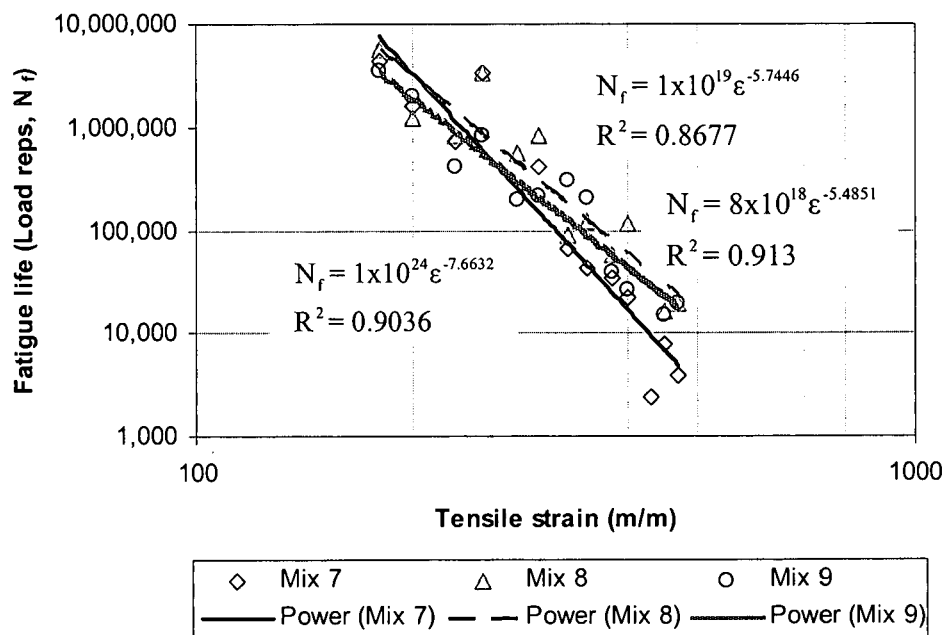


Figure 5.8 Characterization of fatigue properties, Mix 7(C-75C-0%), Mix 8(C-75C-1%) and Mix 9(C-75M-0%) at 5°C and 10Hz

The models of the fatigue properties for Mix 7, Mix 8 and Mix 9 indicated in Figure 5.7 and Figure 5.8 presents the Wöhler parameters determined from linear regression as shown in Table 5.13.

Table 5.13: Fatigue Characteristics of the foamed bitumen mixes for Wöhler Equation

Mix Type	Log (A) (m/m)	n	R ²	ε _b (με)
7: C-75C-0%	24.000	7.637	0.904	1790
8: C-75C-1%	19.699	5.745	0.868	2495
9: C-75M-0%	18.903	5.485	0.913	1271

Following the discussion in the emulsion mixes. The Wöhler parameters for the foam mixes (Table 5.13) do not define the fatigue life consistently. The steeper slope (high value of n) of fatigue line for Mix 7 with low fatigue life compared to Mix 8 might have been caused by the result of the variability in stiffness of the mix of the weak test specimen. The reasons for the weakness of Mix 7 have been discussed above.

The strain-at-break values (investigated in Chapter 6) for the foam mixes are also indicated in Table 5.13. In comparison it can be seen that Mix 8 is stronger (more flexible) compared to Mix 7 and Mix 9. However, this does not fully concurs with the investigation on the fatigue performances on these mixes. Nevertheless, it shows the correlation between fatigue life and strain-at-break properties

5.6 EFFECTIVE FATIGUE TRANSFER FUNCTION FOR FOAMED BITUMEN MIXES

Using strain-at-break values (investigated in Chapter 6) and tensile strain from laboratory fatigue test the critical parameter (strain ratio) for the foam mixes was calculated and presented as presented in Tables 5.14, 5.15 and 5.16. The effective fatigue life and strain ratio was then plotted to investigate if strain-at-break is a normalizing parameter of the foam mixes fatigue properties Figure 5.9.

Table 5.14: Strain ratio and effective fatigue life of Mix 7(C-75C-0%) at 5°C and 10Hz

Beam specimen	Strain level ($\mu\epsilon$)	Strain Ratio (ϵ/ϵ_b) at $\epsilon_b = 1790\mu\text{m/m}$	Fatigue life Load reps to failure
D5	470	0.26	3 942
C1	450	0.25	7 680
D3	430	0.24	2 390
D4	400	0.22	22 550
D6	380	0.21	34 400
B4	350	0.20	42 000
D1	330	0.18	66 000
B3	300	0.17	420 000
B5	250	0.14	3 420 000
D2	230	0.13	732 820
A6	200	0.11	1 620 000
A5	180	0.10	3 600 000

Table 5.15: Strain ratio and effective fatigue life of Mix 8 (C-75C-1%) at 5°C and 10Hz

Beam Specimen	Strain level ($\mu\epsilon$)	Strain Ratio (ϵ/ϵ_b), at $\epsilon_b = 2495\mu\text{m/m}$	Effective fatigue life Load reps to failure
A4	470	0.19	19 000
B5	450	0.18	16 460
A2	400	0.16	155 000
B3	380	0.15	58 200
A3	350	0.14	122 000
B2	330	0.13	91 000
A1	300	0.12	840 000
B4	280	0.11	550 000
A5	250	0.10	3 310 000
B1	230	0.09	822 000
A6	200	0.08	1 236 000
B6	180	0.07	5 680 000

Table 5.16: Strain ratio and effective fatigue life of Mix 9 (C-75M-0%) at 5°C and 10Hz

Beam specimen	Strain level ($\mu\epsilon$)	Strain Ratio (ϵ/ϵ_b), at $\epsilon_b = 1271 \mu\text{m/m}$	Fatigue life load reps to failure
C5	470	0.37	19 300
C4	450	0.35	14 790
B4	400	0.31	26 000
A3	380	0.30	39 600
A1	350	0.28	205 000
C2	330	0.26	310 762
A2	300	0.24	212 588
C3	280	0.22	194 177
A6	250	0.20	830 000
B5	230	0.18	410 000
A5	200	0.16	1 980 000
B6	180	0.14	3 520 000

As already discussed for the emulsion mixes, the foam mix with addition of active filler Mix 8 (C-75C-1%), has shown a low strain ratio caused by a high strain-at-break value. The translation of fatigue life of this mix in a pavement layer might results in high fatigue life compared to the mixes with low strain at break values (Mix 7 and 9). However, superimposition of effective fatigue models of foam bitumen Mix 7 (C-75C-0%), Mix 8 (C-75C-1%), and Mix 9 (C-75M-0%) (Figure 5.9) shows significantly differences in effective fatigue performance of these mixes, do not concur with the investigation in laboratory fatigue lives. Mix 8 with small strain ratios due to high strain at break values has a lower effective fatigue life for the same strain ratio compared to Mix 7 and 9 with lower strain-at-break values. The inverted behaviour in fatigue performance of the cold mixes using strain ratio parameters indicates that strain-at-break property does not demonstrate (normalize) the relationship between the laboratory fatigue properties and the related field response.

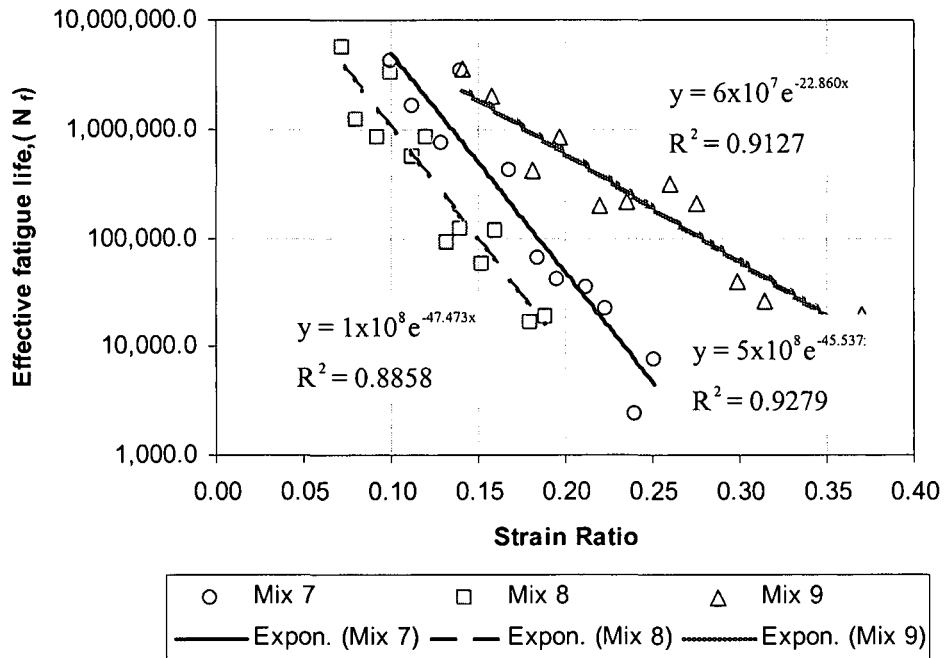


Figure 5.9: Effective fatigue life transfer function for Mix 7(C-75C-0%), Mix 8(C-75C-1%) and Mix 9(C-75M-0%) at 5°C

The summary of the effective fatigue life transfer function in Figure 5.9 of the selected foam mixes is presented in Table 5.17

Table 5.17: Effective fatigue life transfer function for selected foamed bitumen mixes

Mix Type	Linear Regression (Exponential)	R2	Transfer Function*
7: C-75C-0%	$y = 5 \times 10^8 e^{-45.537x}$	0.93	$N_f = 10^{\left(\frac{8.699 - 19.776 \frac{\epsilon}{\epsilon_b}}{\epsilon_b} \right)}$
8: C-75C-1%	$y = 1 \times 10^8 e^{-47.473x}$	0.89	$N_f = 10^{\left(\frac{8.000 - 20.617 \frac{\epsilon}{\epsilon_b}}{\epsilon_b} \right)}$
9: C-75M-0%	$y = 6 \times 10^7 e^{-22.860x}$	0.91	$N_f = 10^{\left(\frac{7.778 - 9.928 \frac{\epsilon}{\epsilon_b}}{\epsilon_b} \right)}$

* y is substituted by N_f , and x by ϵ / ϵ_b in exponential regression equation after solving the logarithmic relationship.

5.7 COMPARISON OF FATIGUE PERFORMANCE BETWEEN BITUMEN EMULSION AND FOAMED BITUMEN MIXES

The comparison of different parameters associated with fatigue test results of the selected mixes, give an insight on the characterization of the cold mixes. The results of the fatigue tests carried out on similar blends treated with either bitumen emulsion or foamed bitumen are superimposed in Figure 5.10, 5.11 and 5.12 for intrinsic comparison on the fatigue properties of these mixes.

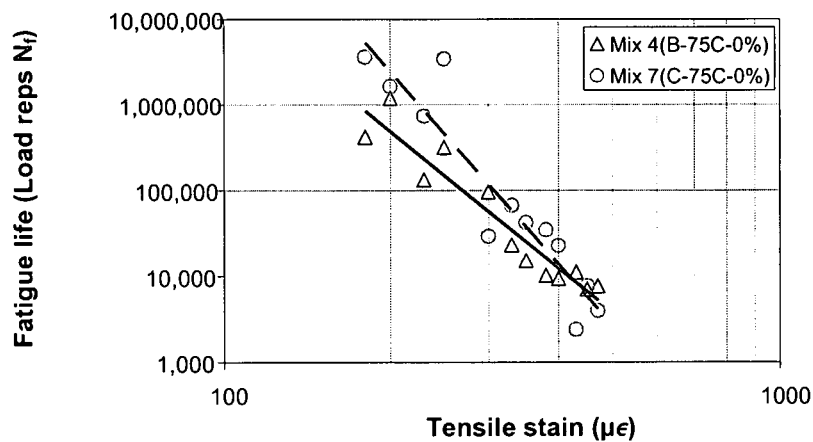


Figure 5.10: Fatigue models of emulsion Mix 4(B-75C-0%) and foam Mix 7(C-75C-0%) at 5°C and 10Hz

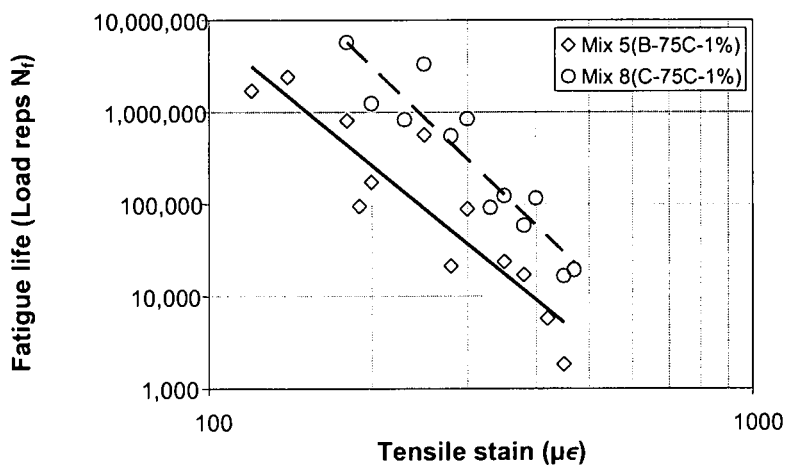


Figure 5.11: Fatigue models of emulsion Mix 5(B-75C-1%) and foam Mix 8(C-75C-1%) at 5°C and 10Hz

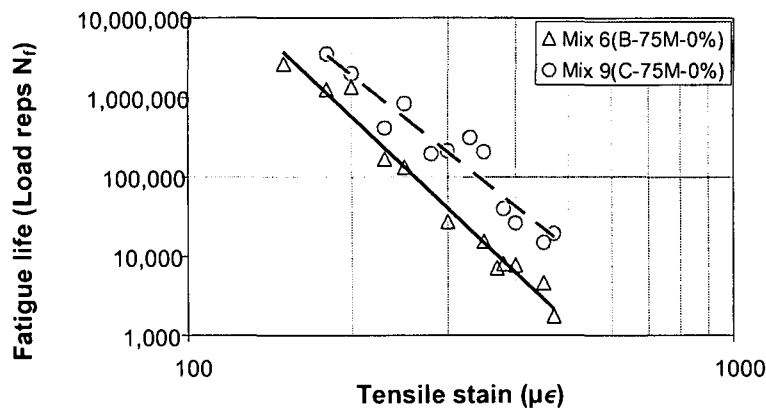


Figure 5.12: Fatigue models of emulsion Mix 6(B-75M-0%) and foam Mix 9(C-75M-0%) at 5°C and 10Hz

The different blends and binder (emulsion and foamed bitumen) provide fatigue life lines that appear to be parallel except for the 75% limestone blend with no cement (Mix 4 and Mix 7). Figure 5.10 shows that there is no significant difference in fatigue performance at high strain levels. However, a significant shift is noted for the foamed bitumen mixes with the addition of active filler (Mix 8). This might be due to improvement in dispersing characteristics of foamed bitumen by active filler, which resulted in the increase of the cohesive strength of the mix and consequently improved in fatigue performance.

The blends with high percentage of RAP treated with foamed bitumen (Mix 9) indicate good performance compared to emulsion (Mix 6). However, when bitumen emulsion or foamed bitumen was used in the experiment for treatment of the mixes with high percentage of millings asphalt (RAP), a lower percentage of residual binder was applied to the mix. This was arbitrary selected to ensure good binder dispersion and compaction characteristics without over-rich mixes. Whether the difference of performance of the mixes with high to low percentage of RAP is due to adhesion properties of new binder to the old existing asphalt or the residual binder content of fresh bitumen is not apparent. This requires further investigations.

The fatigue cracking of the pavement layer occurs at the bottom of the base layer. Brown (2000) indicated that the critical tensile strain for cold mixes lay on a range of 200 microstrain. It is also assumed that load application at 400 microstrain provide significant weakening of cold mixes. The comparison of the fatigue properties of the selected blends treated with either bitumen emulsion or foamed bitumen basing on the critical tensile strain at the bottom of the base layer provide an insight on the ranking of these mixes in fatigue performance. Figure 5.13 present the superimposition of fatigue functions of all selected mixes.

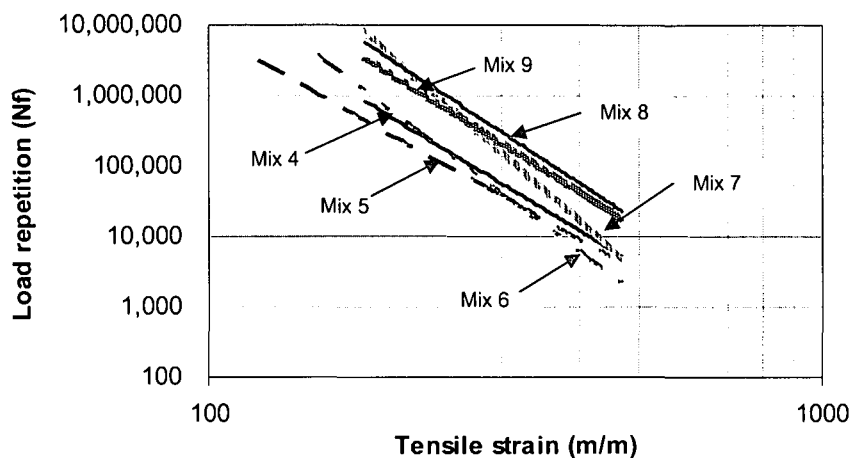


Figure 5.13: Superimposition of fatigue function of the selected Mix 4, Mix 5, Mix 6, Mix 7, Mix 8, Mix 9

The fatigue function of the all mixes, Mix 4(B-75C-0%), Mix 5(B-75C-1%) and Mix 6(B-75M-0%) crosses at 250microstrain. Similar although at high shift fatigue function for Mix 7(C-75C-0%), Mix 8 (C-75C-1%), and Mix 9(C-75M-0%) also crosses at 250microstrain. Based on laboratory fatigue life obtained from critical strain levels, the selected mixes were ranked as presented in Table 5.18. The comparison of the ranking of the selected mixes according to the fatigue test and strain-at-break is presented in Figure 5.14.

Table 5.18: Ranking of selected mixes fatigue performance at critical strain and strain-at-break

Mix type	Fatigue life at Nf,200 (Load reps)	Fatigue life at Nf,400 (Load reps)	Strain-at-break ($\mu\epsilon$)
Mix 4	1,177,900 (5)	9,323 (4)	1,845 (2)
Mix 5	172,000 (6)	7,400 (6)	994 (5)
Mix 6	1,345,510 (3)	7,706 (5)	921 (6)
Mix 7	1,620,000 (2)	22,550 (3)	1,790 (3)
Mix 8	1,236,000 (4)	115,000 (1)	2,495 (1)
Mix 9	1,980,000 (1)	26,000 (2)	1,271 (4)

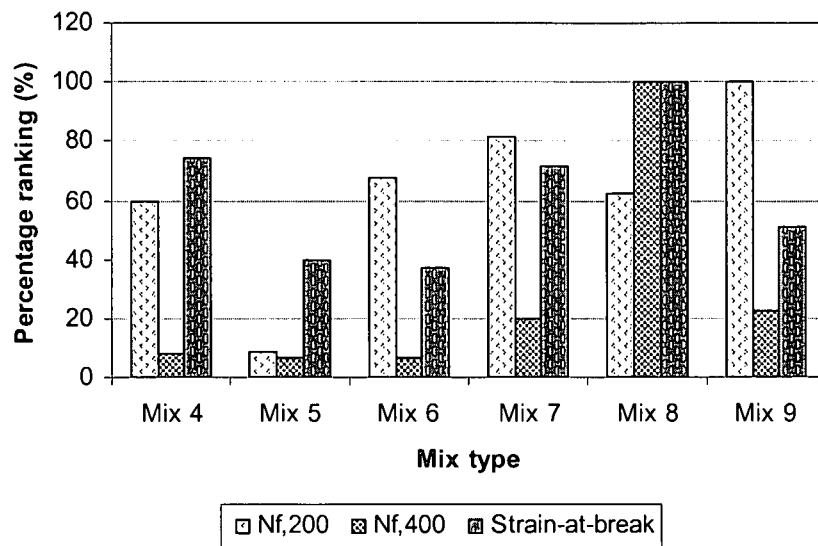


Figure 5.14: Graphs for ranking selected mixes in relation to fatigue performance at 200 $\mu\epsilon$, 400 $\mu\epsilon$ and strain-at-break properties

The plot Figure 5.14 provides a clear ranking of mixes in terms of critical loading condition and intrinsic relationship between fatigue and stain-at-break performance of the selected mixes. It can be seen that at lower strain level (200) Mix 8 (C-75C-1%) which is ranked as high in fatigue and strain-at-break has lower percentage ranking on 200 microstrain compared to Mix 6(B-75M-0%), Mix 7(C-75C-0%), and Mix 9(C-75M-0%). This might have occurred due to extrapolations of the fatigue results of these mixes where a beam fails to reach 50% reduction of initial stiffness. This indicates that ranking or characterization of fatigue performance of the mixes based on the single fatigue results might not be appropriated due to significant variability in the four- point beam fatigue test.

Due to the lack of standardized fatigue performance guideline for cold bituminous treated materials, it is apparent that characterization of fatigue performance for cold mixes can be done relative to the guideline prepared for the HMA. This however might substantiate the understanding in fatigue performance of the cold mixes when comparing different binder type.

The comparison of the fatigue performance of the selected materials treated with either bitumen emulsion or foamed bitumen is based on the limits defined for HMA by CSIR (2000).

The guideline Figure 5.13 defines the upper limit as good fatigue performance of the mixture and lower limit is poor fatigue performance while intermediate is defines as good-medium or medium-poor. The fatigue properties models of emulsion mixes described previously are superimposed on HMA limits as presented in Figure 5.13.

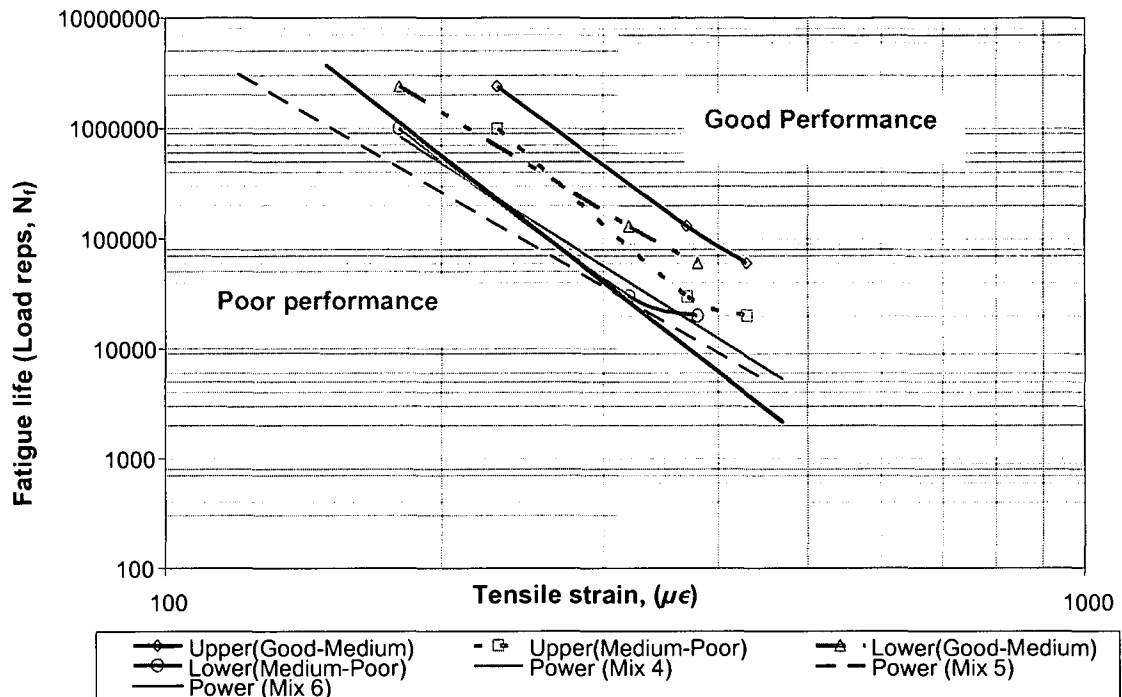


Figure 5.13: Fatigue performance of bitumen emulsion mixes at 5°C and 10Hz

The fatigue performances of bitumen emulsion Mix 4(B-75C-0%) (Figure 5.13) can be characterized as medium-poor in relation to HMA at the same strain levels. This mixture shows a boundary condition of medium-poor at low strain levels due to load sensitivity. However, any improvement in binder content might give a significant shift into medium fatigue performance at all strain regimes. The Mix 5(B-75C-1%) can be characterized as poor in fatigue performance at the same strain levels with HMA. This was unexpected; however, the fact that this mixture shows consistency of poor performance at all strain regimes indicates that the addition of cement impaired the cohesive strength of this mix.

The Mix 6(B-75M-0%) can be characterized as medium-poor in fatigue performance. The mixture shows a consistent boundary condition at all levels of strain regimes. This mixture indicates that any improvement on binder-aggregates-moisture interaction will result into good-medium performance. In pavement layer the cold mix is provided as thicker layers relative to HMA in that factor emulsion mixes should be ranked as good-medium in fatigue performance.

For the foamed bitumen mixes the fatigue properties models described previously are superimposed on the HMA limits as presented in Figure 5.11.

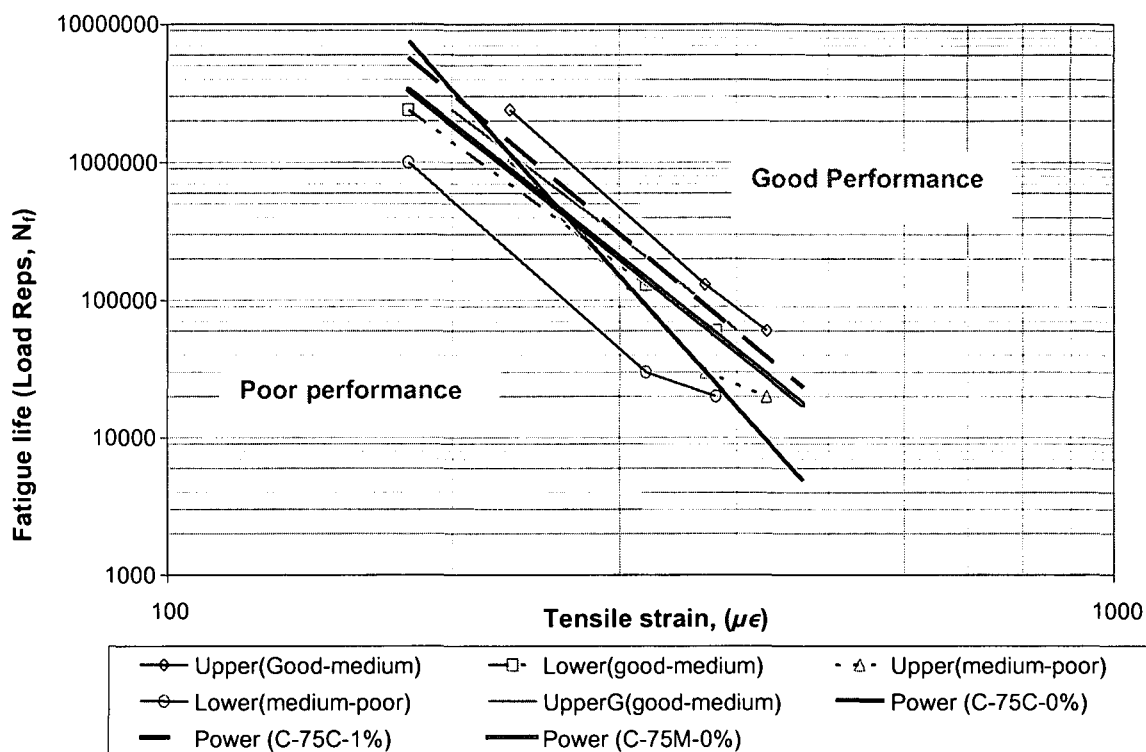


Figure 5.14: Fatigue performance of foamed bitumen mixes at 5°C and 10Hz

The fatigue performance of foamed bitumen Mix 7 (C-75C-0%) Figure 5.14 can be characterized as good-medium in fatigue performance in relation to HMA at the same strain levels. However, at higher strain levels this mixture lay at the upper limit of medium-poor performance. This indicates that any improvement in binder-mineral aggregates interaction will influence the shift in the mix fatigue performance.

The Mix 8(C-75C-1%) can be characterized as good-medium in fatigue performance at the present broad demarcated limits of strain regimes. However applying the second upper limit line in Figure 5.14 presents the actual field strain levels for the pavement layer. As mentioned previously, Mix 8 can be characterized as good in fatigue performance in relation to HMA at the same strain levels. The fact that this mixture shows consistency of high fatigue resistance at all strain regimes indicates that the additional of active filler (1% cement) has a significant role in the improvement of the fatigue characteristics of some foamed bitumen treated materials.

Mix 9 (C-75M-0%) can be characterized as good-medium in fatigue performance. This mixture shows a good-medium fatigue performance at the low strain regime and lies at the lower boundary of the good-medium fatigue performance.

The comparison of the selected materials treated with bitumen emulsion and foamed bitumen in fatigue performances in relation to HMA indicates that the bitumen emulsion can be characterized as medium-poor in performance and foam bitumen as good-medium. However, in the general practice the cold mix layers in a pavement structure are provided as thicker layer compared to HMA. This gives an indication that emulsion mixes can be characterized as good-medium and foam mixes as good in fatigue performance. The findings related to the other properties such as strain-at-break properties concurred with this characterization.

The research on cold mixes to determine effective fatigue life has been carried out using HVS tests (field) and laboratory tests. The researched ferricrete materials treated with foamed bitumen, (Long and Theyse, 2001) or bitumen emulsion, (Liebenberg, 2002) at residual bitumen content of 1.8% and addition of 2% cement, and sand materials (Schmidt et al., 1973) treated bitumen emulsion at 3.5% residual bitumen and addition of 1.3% cement, will be used to compare with the selected Mix 8(C-75C-1%)(foam) and Mix 5(B-75C-1%)(emulsion), treated with 3.6% residual bitumen and 1% cement. The comparison will provide an intrinsic relationship on the fatigue performances of these mixes. The superimpositions of effective fatigue life of these mixes are presented in Figure 5.15

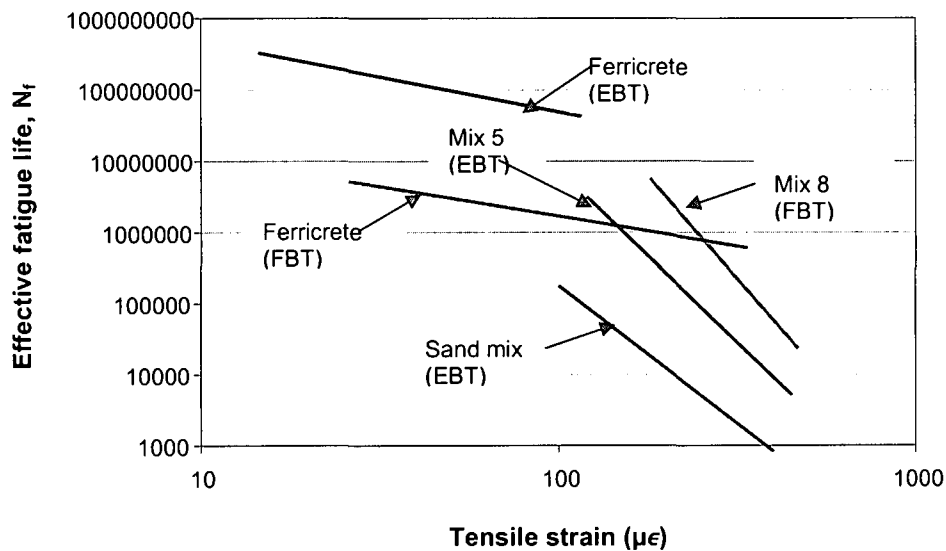


Figure 5.15: Superimposition of effective fatigue life model for Ferricrete, Sand mix, Mix 5, and Mix 8.

The effective fatigue life models for the ferricrete mixes, shows incomparable fatigue performance at the same strain levels with sand mix or limestone blends (Mix 5(B-75C-1%) and Mix 8(C-75C-1%). However, the sand mix shows good comparison on fatigue performance with limestone blends (Mix 4 and Mix 8) (see Figure 5.15). This significant difference in slope of the fatigue lines for ferricrete mixes with other mixes is not expected for this kind of materials. However, the

contributing factors might have been due to extrapolation of the transfer function for the lower strain established from high strain test of the HVS load repetition. The notable shift of increase in fatigue lines for Mix 5 (B-75C-1%) and Mix 8 (C-75C-1%) compared to sand mix is expected. This is due to fact that Mix 5 and Mix 8 incorporate high quality materials compared to sand, and therefore at the same binder content high quality materials will have good cohesive strength compared to sand, hence resulting in high fatigue resistance.

The effective fatigue life transfer function of the limestone blends and ferricretes are compared. However the low strain-at-break values of inferior quality ferricrete materials give high strain ratio at the same tensile strain compared to high strain-at-break of the selected limestone blends. The factors contributing to the lower strain-at-break properties of ferricretes mixes are discussed in Chapter 6 of this thesis. These include specimen preparation, method of test and interpretation of results.

The effective fatigue life transfer functions superimposed for ferricrete mixes, Mix 5 (C-75C-1%) and Mix 8 (C-75C-1%) is presented in Figure 5.16.

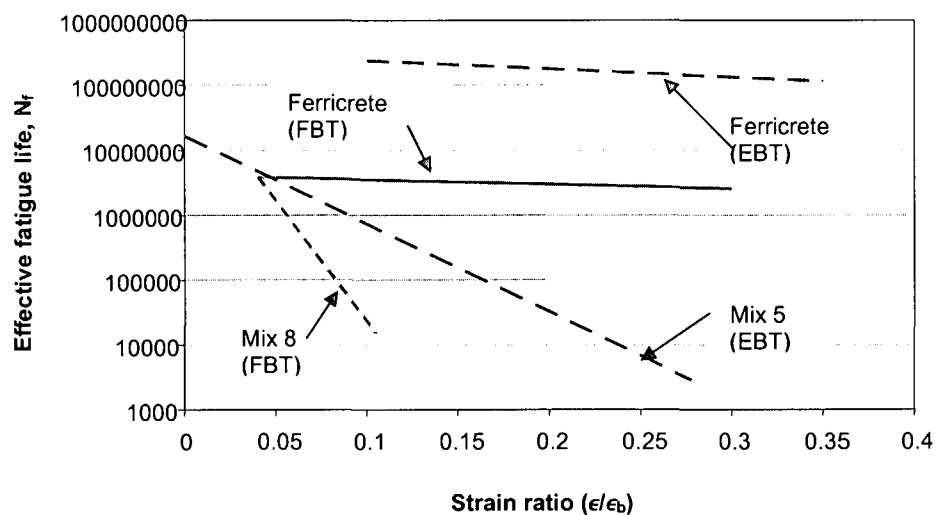


Figure 5.16: Superimposition of fatigue life transfer function for Ferricrete mixes (emulsion and foam), Mix 5 and Mix 8

In Figure 5.16, it can be seen that there is significant difference in fatigue performance of these mixes at the same strain ratio. The differences in slopes of the fatigue lines are incomparable for these mixes, as in case for fatigue line as a function of strain level. This indicates that strain-at-break properties do not normalize the fatigue performance of cold mixes. It should be noted that the ferricrete mixes required significant extrapolation of the results to plot strain ratios below 0.4. This is due to the exceptionally low strain-at-break values obtained for these mixes.

5.8 CONCLUSIONS

The fatigue performance of the selected mixes treated with either bitumen emulsion or foamed bitumen is influenced by the interaction of binder, mineral aggregates, moisture as well as the use of active filler. By using the four-point beam testing apparatus, the results of the test beams methods were obtained. However, the characterization of fatigue performance requires a number of test specimens sufficient to develop a level of reliability for the acquired fatigue results. In this study, twelve beams were used to develop fatigue properties of the selected mixes.

The protocol for sample preparations and testing on the selected mixes were similar. This enabled intrinsic comparison of the mixes' fatigue performance. The characterization of fatigue performance of bitumen emulsions and foamed bitumen treated mixes therefore, has led to the following conclusions:

5.8.1 Fatigue properties

- The selected cold bituminous treated materials tested in displacement controlled mode at selected loading time (frequency) and temperature shows that fatigue life is dependent on the loading rates. On a log-log plot, linear fatigue functions are obtained, as is the case with many HMA mixes.
- The behaviour of emulsion mixes with 75% limestone blend shows an increase in flexural stiffness as strain decreases. This is unexpected for the fatigue test of the visco-elastic materials. However, the combination of mixture variability, test conditions, and sensitivity of equipment might contribute to this behaviour, but further investigation is recommended.
- The quality of the test beam specimen, testing method and extrapolation of captured fatigue results influences the variability of the fatigue results. Cold mixes' binder distribution is not as uniform as HMA. The weakness of the mixes might result in the spalling of the beam edges and faces during sawing. The beam fatigue test is designed, through its geometry, to initiate cracks at its centre with uniform stress concentration; therefore, for a cold mix beam, the decrease in stiffness during fatigue testing depends on the location of weakness in specimen where micro-cracking initiates or where cracking occurs. Failure of test beams to reach 50% reduction of its initial stiffness after many load repetitions have resulted in premature stoppage of the test and extrapolation of fatigue results. The combination of these parameters leads to higher variability in the estimation of fatigue life for cold mixes than HMA. Therefore, twelve beams specimen in each blend were tested to develop a fatigue function of statistical significance.

- The advantage of determining the Wöhler parameters (fatigue model) for HMA is to easily relate the fatigue characteristics of different mixes in term of fatigue resistance and sensitivity to overloading. The high n-value implies increasing fatigue resistance and sensitivity to overloading of the pavement layer and vice-versa for the low n-value. However, the variability in the fatigue results of the selected mixes resulted in parameters that do not consistently follow the definition or concurring to the fatigue properties and strain-at-break properties for both emulsion and foam mixes.

5.8.2 Strain-at-break function

- The fatigue property is influenced by among others the cohesive strength of the mixes. The strain-at-break function however, provides a balance in the mix design by introducing a flexibility consideration as opposed to strength requirements. It should not be considered to be a normalizing parameter for the fatigue analysis of cold mixes. The fatigue properties of the selected cold mixes (emulsion and foam) normalized by strain-at-break function did not effectively improve the laboratory characterization of fatigue properties of these mixes. The mixes with high fatigue life after being normalized were inverted to low relative fatigue life.
- The comparison of the fatigue properties and strain-at-break properties of the selected mixes shows that strain-at-break properties are inconsistent in providing a link to mix type for analysis of the fatigue life. The relative strain-at-break properties of the selected mixes compared to fatigue properties were not consistently observed in all the mixes.

5.8.4 Fatigue performance

- The selected cold mixes (emulsion and foam) provide fatigue life lines that appear to be parallel except for the 75%limestone blend with no cement (Mix 4 and Mix 7). These mixes show no significant difference in fatigue life with respect to binder type at high strain levels. However, the addition of a small quantity of cement (1%) a notable shift in fatigue life line for the foam mixes occurs with an increase in fatigue life, compared to that of emulsion mixes.
- When cold mixes (emulsion or foam) are used for the treatment of the mixes with high percentage of milling asphalts (RAP) a lower percentage of residual bitumen is applied to the mix. However the difference of fatigue performance of the mixes with high or low percentage of the RAP is due to different blending of virgin aggregates to old existing asphalt or the different residual binder contents which cannot clearly discerned from these test results. The influence of the binder type on binder adhesion for RAP versus crushed aggregates is likely to play a role in this phenomenon. Further investigation in this aspect is recommended.

- Ranking of the selected mixes (emulsion or foam) according to critical maximum tensile strain ($200\mu\epsilon$ and $400\mu\epsilon$) indicates that foamed mixes perform better than emulsion mixes. However the formed mixes with addition of cement Mix 8 which is ranked as higher in fatigue and strain-at-break performance shows that at lower strain level has significantly lower performance compared to Mix 6,7 and 9. This might have occurred due to variability expected from the four-point beam test. It is therefore not appropriate to rank mixes using single value of the fatigue test.
- The fatigue performance of the selected mixes (emulsion or foam) was compared using the guideline developed for HMA. According to defined limits, emulsion mixes were characterized as medium-poor in fatigue performance at the same strain levels as for HMA and foam mixes as good-medium fatigue performance. However in practice a cold mix layer in the pavement structure is thicker compared to HMA, this probably allows the characterization of the selected mixes be good to medium for emulsion mixes and good for the foam mixes.
- The fatigue performance of the mixes that lie on the boundary of the developed fatigue limits demonstrate that optimization of binder content, mineral aggregates, active filler and moisture content will improve the fatigue performance with fatigue life line significantly shifting to good fatigue performance.
- The comparison of fatigue life models for ferricrete materials with sand mix or limestone blends, Mix 5 (C-75C-1%) and Mix 8(C-75C-1%) shows a significant difference. Such differences in fatigue performance are not expected for this kind of materials. However, extrapolated fatigue function model from HVS test at lower strain levels might have contributed unexpected high fatigue performance of these mixes. The sand mix however, shows good comparison with limestone blends, Mix 5(B-75C-1%) and Mix 8(C-75C-1%). The shift of increasing fatigue of Mix 5 (B-75C-1%) and Mix 8(C-75C-1%) indicate that sand mix has a lower fatigue life compared to Mix 5 and Mix 8. This is due to the difference in the quality of materials on these mixes.

5.9 REFERENCES

AUSTROADS. 2001. **Fatigue life of compacted bituminous mixes subject to repeated flexural bending**. Manual AST03. Sydney, Australia.

ASPHALT ACADEMY. 2002. **The design and use of foamed bitumen treated materials**. TG2, Interim Technical Guideline. Pretoria, South Africa.

- CSIR, 2000. **Interim guideline for the design of hot-mix asphalt in South Africa**, prepared as part of the Hot-Mix Asphalt Design Project, Transportek, CSIR, Pretoria, South Africa.
- IPC (Industrial Process Control Ltd), 1998. **Beam fatigue apparatus**. Reference Manual. Boronia, Australia.
- JENKINS J.K., 2000. **Mix design consideration for cold and half-warm bituminous mixes with emphasis on foamed bitumen**. PhD Dissertation, University of Stellenbosch, South Africa.
- LONG F.M., 2002. **The development of structural design models for foamed bitumen treated pavement layers**. Contract Report CR-2001/76, Transportek, CSIR, Pretoria, South Africa.
- LONG F.M AND THEYSE H.L., 2001. **Laboratory testing for the HVS section on P243-1**. Contract Report CR-2001/32. Transportek, CSIR, Pretoria, South Africa.
- LONG F.M AND VENTURA D.F.C., 2003. **Laboratory testing for HVS test section on the N7. TR11/1**. First Draft for review. Contract Report CR-2003/56. Transportek, CSIR, Pretoria, South Africa.
- LONG F.M, 2001. **Interim guidelines: the design and use of foamed bitumen treated bases**. Road Pavement Forum, Pretoria, South Africa.
- LIEBENBERG J.J.E., 2002. **the influence of various emulsion and cement content on an emulsion treated ferricrete from the HVS test section on road P234/1**. Contract Report, CR-2001/77, Transportek, CSIR, Pretoria, South Africa
- LIEBENBERG J.J.E., 2003. **A structural design procedure for emulsion treated pavement layers**. Master Dissertation, University of Pretoria, South Africa.
- MEDANI T.O. and MOLENAAR A.A.A., 2003. **Estimation of fatigue characteristics of asphalt mixes using simple tests**. Werkbouwkundige werksdagen, The Netherlands.
- SCHMIDT RJ, SANTUCCI LE, and COYNE LD., 1973. **Performance characteristics of cement-modified asphalt emulsion mixes**. Proceedings of Association of Asphalt Paving Technologists, Technical session, Houston, Texas.
- THEYSE H.L., 2000. **Overview of the South African mechanistic pavement design methods**. South African Transport Conference, Pretoria, South Africa.

THEYSE H.L., 1998. **Towards guidelines on the structural design of pavement with emulsion treated layers.** Contract Report CR-97/045, Transportek, CSIR, Pretoria, South Africa.

THEYSE H.L et al., 1995. **Testing of the fatigue characteristics of bound wearing courses to more accurately predict pavements behaviour and field performance in design.** Report No. RR 95/565, Department of Transport, Pretoria, South Africa.

VOSKUILEN J.L.M, VAN DE VEN M.F.C and WIERINGEN J.B.M., 2004. **Experiences with half-warm foam bitumen treated process in the Netherlands.** Conference on Asphalt Pavements for Southern Africa CAPSA'04, Sun City, South Africa.

CHAPTER 6

6. STRAIN-AT-BREAK PROPERTIES AND TRANSFER FUNCTION

6.1 INTRODUCTION

The failure mode of every type of material is linked to critical parameters at a specific position in the pavement structure under loading. For cold bituminous treated materials, one of the major failure modes is fatigue cracking under repeated loading and the critical parameter for effective fatigue life is the strain ratio. This is similar to the model developed for cemented materials. The strain ratio is the ratio of the horizontal tensile strain (ϵ) at the bottom of the layer and strain-at-break (ϵ_b) determined from flexing beam tests.

The strain-at-break test and strain ratio have been used to determine the effective fatigue life of cemented materials. The transfer function shown in equation 6.1 for the effective fatigue life of cemented layer relates the strain ratio to the number of load repetition to reach the equivalent granular state (Theyse, 2000).

$$N_{\text{eff}} = 10^{\left(c - b \left(\frac{\epsilon}{\epsilon_b} \right) \right)} \quad (6.1)$$

Where:	N_{eff}	= effective fatigue life (Load repetition)
	c, b	= regression coefficients
	ϵ/ϵ_b	= strain ratio
	ϵ	= maximum horizontal tensile strain at the bottom of the layer
	ϵ_b	= strain-at-break from laboratory testing

Some researchers have indicated that cold mixes when included in pavement layer exhibit phases in fatigue life similar to cemented materials. The first phase is when the layer is stiff and provides resistance to fatigue. This phase ends when stiffness reduction of the layer reaches an equivalent granular state or effective life (see Figure 6.1). However, this is not apparent for the cold mixes. Because a large percentage of rutting that takes place early in the pavement life and fatigue cracking (reduction in stiffness) that begins slowly and accumulates with time as materials flex under traffic load.

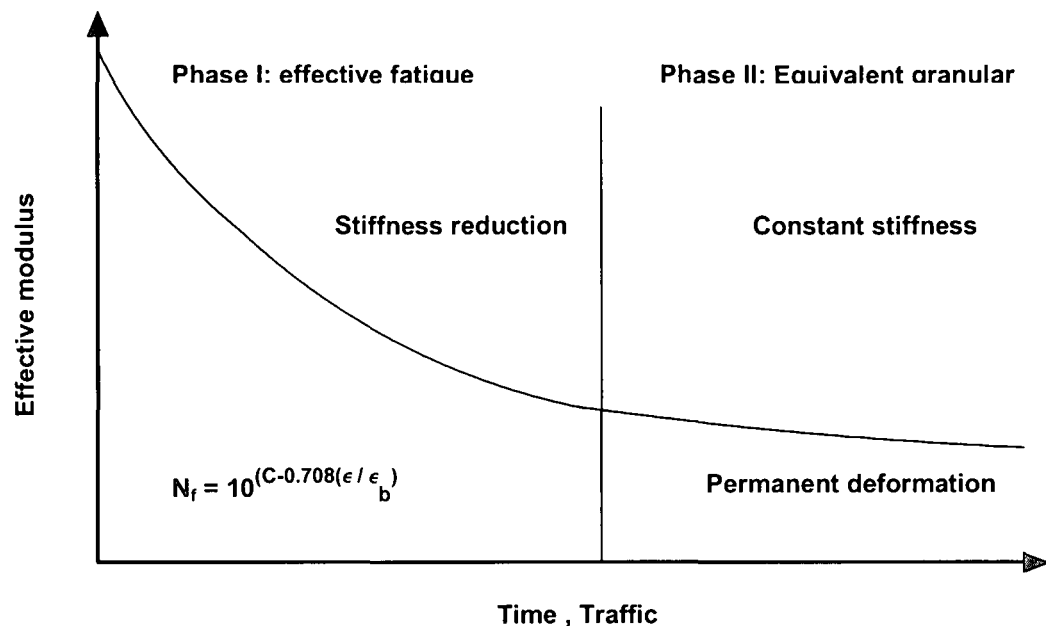


Figure 6.1: Behaviour of cold mixes (foam) in a pavement (TG2, Asphalt Academy, 2002)

The strain-at-break test using monotonic loading has been used in the recent research as a measure of the “flexibility” of the cold mixes. However some practitioners are still questioning the applicability, reliability and relevance of the flexibility function in cold mix design and its link to the fatigue performance. In this study some of these points will be reviewed and discussed.

Past researchers of cold mixes have indicated that the cold mixes exhibit small strain-at-break values. However, factors such as specimen preparation including mixing, compaction, curing and cutting of beam, and methods of testing should be taken into account as it might contribute to these results. Theyse (2000) conducted laboratory tests on the natural gravel (sandstone conglomerate) and Premamix (ash waste materials) treated with emulsion including 2.5% residual binder and 1% cement, and 1.5% residual binder with 1% cement respectively. He found that the strain-at-break results were “erratic” due to difficulties in specimen preparations. The Premamix specimens broke prematurely, however the average strain-at-break values found were $244\mu\epsilon$ at 1550Kg/m^3 dry density for natural gravel and $128\mu\epsilon$ at 2110Kg/m^3 for Premamix.

Liebenberg (2002) conducted laboratory tests on milled ferricrete (RAP) from road section P243/1 treated with bitumen emulsion, where the residual binder varied from 1.8% to 3% and cement content varies from 0% to 2%. He found that the mixes with no cement broke under their own weight. However an increase in cement content from 0 to 1% at a given binder content shows a significant increase in strain-at-break to $677\mu\epsilon$. But increase in cement content to 2% had an effect on the stiffness of the materials in the sense that it reduced the strain-at-break value to $235\mu\epsilon$. Table 6.1 shows strain-at-break tests results of these mixes.

Liebenberg (2002) further recommended that G5 and G7 materials according to the TRH 14 classification (SABITA, 1993) treated with emulsion should have a strain-at-break value of $145\mu\epsilon$ (for 2% residual bitumen) and $230\mu\epsilon$ (for 3.5% residual bitumen). In light of this research, these values are seen to be too low to classify as base material in the opinion of the Author. Hence revision is necessary.

**Table 6.1 Summary of the strain at break tests from four point beam tests;
(Liebenberg, 2002)**

Cement content (%)	Test Parameter	Net bitumen content (%)		
		0	1.8	3.0
0		-	Samples broke under own weight	
1	Strain at break ($\mu\epsilon$)	96	336	677
	Stress at break (kPa)	38	25	53
	Energy to break (mJ/m^3)	2.66	6.48	41.4
	Initial stiffness (MPa)	1428	235	275
	Stiffness at break (MPa)	496	85	95
2	Strain at break ($\mu\epsilon$)	183*	141*	235*
	Stress at break (kPa)	273	360	307
	Energy to break (mJ/m^3)	45.1	32.2	53.2
	Initial stiffness (MPa)	4921*	4731*	3919*
	Stiffness at break (MPa)	1600*	2655*	2200*

* From the work of Long and Thyese (2002)

Long (2001), Long and Theyse (2002) and Long and Ventura (2003) conducted laboratory tests on the milled (RAP) ferricrete materials taken from road section P243/1 and Hornfels materials taken from road section N7 (TR11/1) treated with foamed bitumen (varying binder content 1.8-3% and cement contents 0-2%). They found that an increase in residual binder in the mix or lower cement to binder content ratio, results in an increase of strain-at-break 'flexibility' and therefore higher fatigue resistance. However, in contrast an increase in the cement content or higher cement to binder content ratio results in an increase in stiffness; hence reduce the strain-at-break. Figure 6.2 illustrates the strain-at-break laboratory tests results of those mixes.

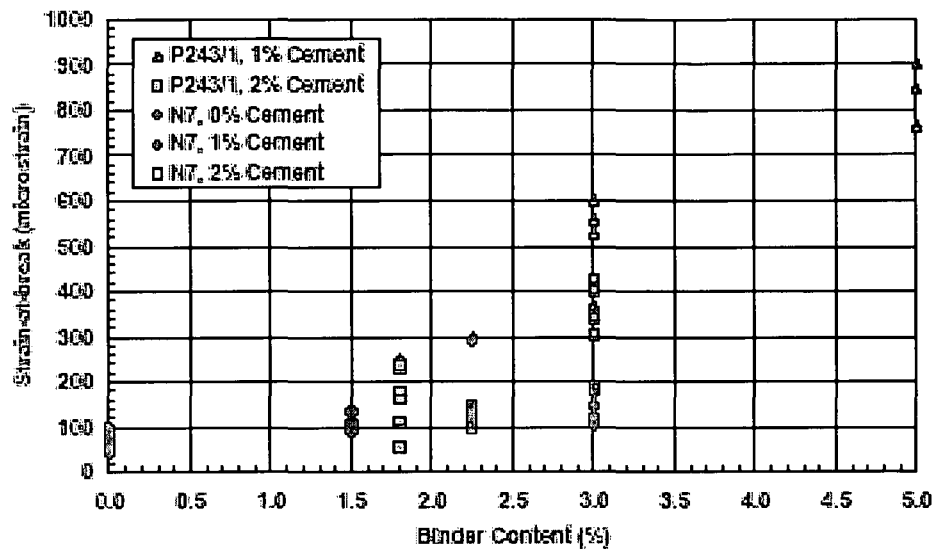


Figure 6.2 Strain-at-break results of foamed treated materials, (Long and Theyse 2001, 2002), Long and Ventura, 2003)

The analysis of a pavement layer for the effective fatigue life (stiffness reduction phase) to develop transfer functions for foamed bitumen mixes was linked to the model developed for the cement treated materials established by Long (2000). Long considered a two-phase approach of the fatigue performance; firstly, stiffness reduction to reach a steady state resilient modulus and secondly predominantly permanent deformation of granular state after reaching steady state condition. Therefore the transfer function for effective fatigue “stiffness reduction phase” of foamed bitumen treated materials relates the ratio of the tensile strain at the bottom of the foamed bitumen layer and the strain-at-break to the number of load repetitions to reach the equivalent granular state. The tensile strain at the bottom of the layer is related to the maximum controlled strain, ϵ applied to the beam specimen in laboratory test on fatigue test. Strain-at-break, ϵ_b is determined in a monotonic test on a beam specimen where the applied load and vertical displacement are measured during the test. Figure 6.3 illustrates the transfer function principal.

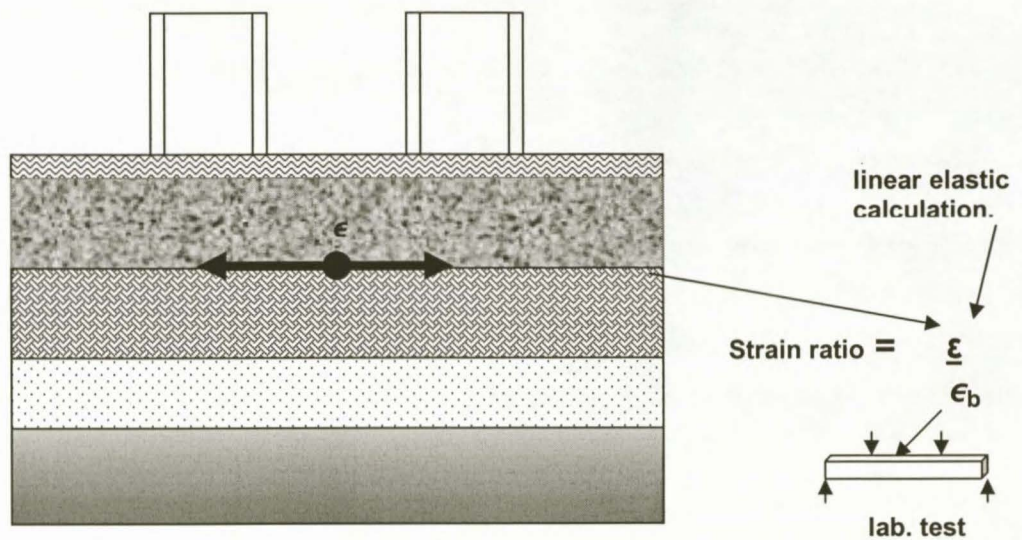


Figure 6.3: Maximum horizontal tensile strain at the bottom of the layer, (Long, 2000)

The transfer function for foamed bitumen treated materials with 1.8% residual binder and 2% cement content, was developed by Long, (2000) using back calculated stiffness module from multi-depth deflectometer (MDD) data. The models (equations 6.2) are similar to the ones of cemented materials that are based on the category of the road for certain levels of reliability. Category A allows five percent of the design section to have failed at the end of structural design life. Category B, C and D allow 10, 20 and 50 respectively (also see transfer function, Figure 6.4).

$$\begin{aligned}
 \text{Category A: } N_{f,FB} &= 10^{\left[6.339-0.708\left(\frac{\epsilon}{\epsilon_b}\right)\right]} \\
 \text{Category B: } N_{f,FB} &= 10^{\left[6.499-0.708\left(\frac{\epsilon}{\epsilon_b}\right)\right]} \\
 \text{Category C: } N_{f,FB} &= 10^{\left[6.579-0.708\left(\frac{\epsilon}{\epsilon_b}\right)\right]} \\
 \text{Category D: } N_{f,FB} &= 10^{\left[6.619-0.708\left(\frac{\epsilon}{\epsilon_b}\right)\right]}
 \end{aligned} \tag{6.2}$$

Where:

- $N_{f,FB}$ = Effective fatigue life of foamed bitumen layer.
- ϵ/ϵ_b = strain ratio
- ϵ = maximum tensile strain at the bottom of the layer from linear elastic calculations.
- ϵ_b = strain at break from laboratory testing.

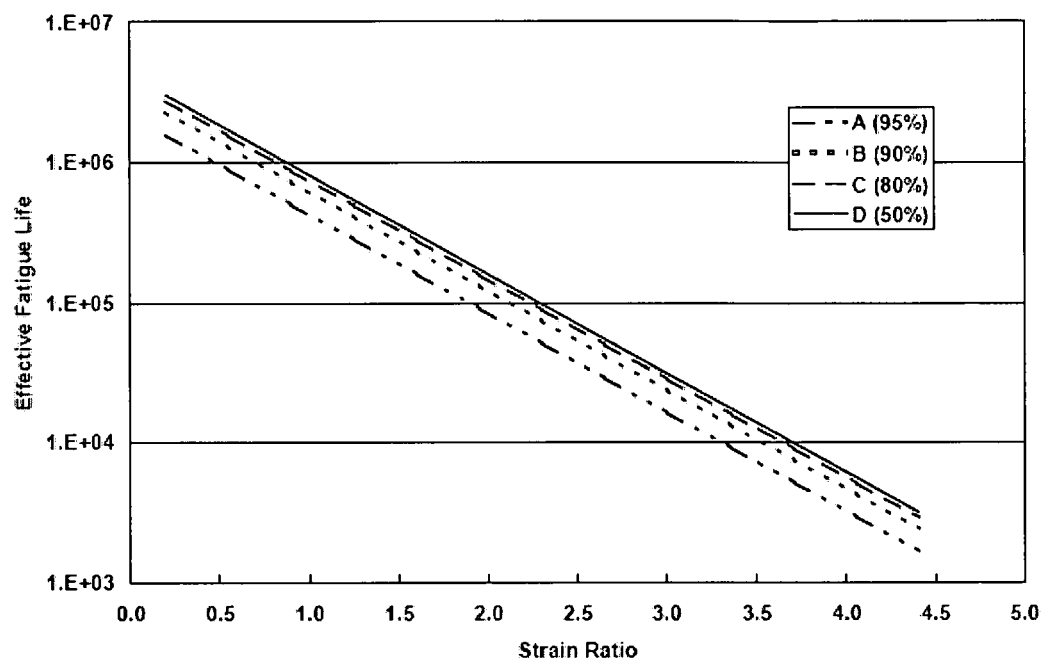


Figure 6.4: Graphical effective fatigue life transfer function of foamed bitumen treated materials, (Long, 2002)

Liebenberg (2003) back-calculated effective stiffness from the MDD data to determine a point in the life of emulsion treated base layer (ETBM) where it would start to behave in a similar way as granular material. However, no good fit could be obtained in the data. Using probabilistic methods at 95% confidence the transfer functions for effective fatigue life of emulsion treated layer at four different road categories were determined as follows:

$$\begin{aligned}
 \text{Category A: } N_{f,A} &= 10^{\left[7.9183-1.2775\left(\frac{\epsilon}{\epsilon_b}\right)\right]} \\
 \text{Category B: } N_{f,B} &= 10^{\left[8.0331-1.2775\left(\frac{\epsilon}{\epsilon_b}\right)\right]} \\
 \text{Category C: } N_{f,C} &= 10^{\left[8.1747-1.2775\left(\frac{\epsilon}{\epsilon_b}\right)\right]} \\
 \text{Category D: } N_{f,D} &= 10^{\left[8.5066-1.2775\left(\frac{\epsilon}{\epsilon_b}\right)\right]}
 \end{aligned} \tag{6.3}$$

Where: The variables are as described in equation 6.2 above.

The two-phase consideration for the determination of effective fatigue life transfer function for the cold mixes and in particular foamed bitumen mixes overestimates the actual field response on these mixes. Jenkins et al., (2005) indicated that one of the problems with a two phased approach to describe the effective behaviour of foamed bitumen mixes is that rutting accumulation generally follows a hyperbolic linear function and that fatigue damage follows a cumulative frequency

distribution curve shape as shown in Figure 6.5. This means that a high percentage of the rutting takes place early in the pavement life where as the fatigue begins slowly and accumulates with time as materials flex under traffic load. Notwithstanding this, the two-phase concept places the fatigue mechanism ahead of the rutting mechanism contrary to the in-situ pavement layer response. This shows that the two-phase concept and the use of strain-at-break in defining the effective life transfer function for cold mixes need to be critically analysed before it become apparent to be applied in the mix type analysis of the layer in the pavement structure.

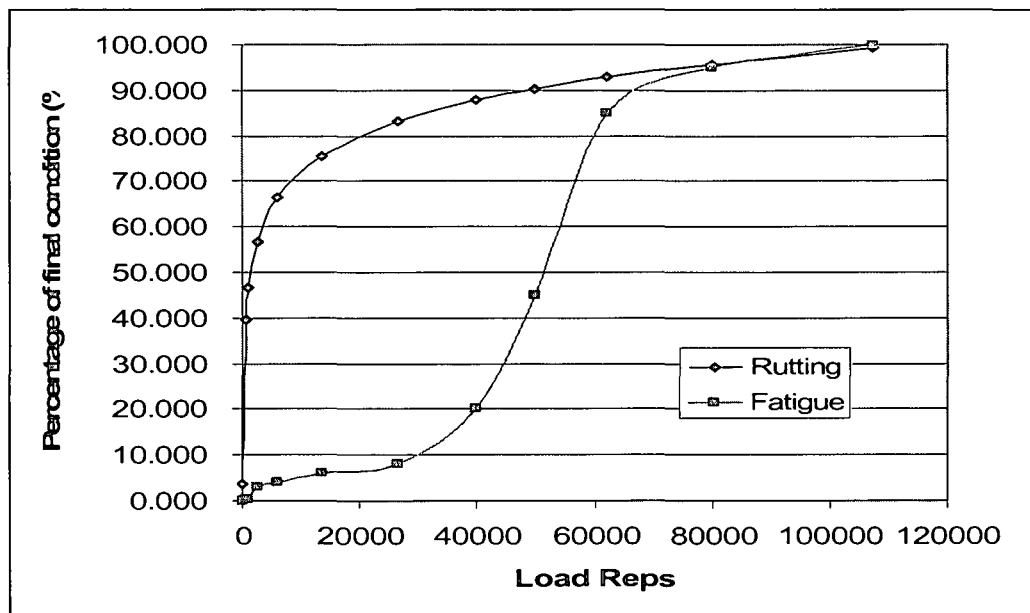


Figure 6.5: Evolution of rutting versus cracking mechanism of foam mixes, (Jenkins et al, 2005)

6.1.1 Strain-at-break materials classification

The shear strength and tensile strength properties of bitumen emulsion and foamed bitumen treated materials play an important role in the long term performance of these materials because of the interaction between the flexibility and resistance to permanent deformation of these mixes. During the mix design process it is preferred that shear strength and strain-at-break (or tensile strength) properties be established through triaxial testing and flexural beam tests. These methods give more insight on the mixture performance in terms of fatigue and strain-at-break properties. However, such tests are seldom feasible due to the specialised equipment required and the time consuming process of testing.

In South Africa bitumen emulsion and foamed bitumen treated materials are classified in terms of UCS and ITS. However, the strain-at-break test as other parameter for classification is still under the investigation. If this parameter accurately reflects the fatigue properties of the cold mixes it

can be linked to the mix type for analysis of the layer fatigue live and easily be implemented. Table 6.2 and 6.3 illustrate the current classifications, TG2, (Asphalt Academy, 2002).

Table 6.2: Classification of foamed bitumen treated materials.

FB Classification			
Material Code		ITS (kPa)	
		100-300	>300
UCS (kPa)	700-1400	FB4	FB3
	>1400	FB2	FB1
Foamed bitumen treated material classes, FB1, FB2, FB3, FB4			

Table 6.3: Classification of bitumen emulsion treated materials.

EB Classification			
Material Code		ITS (kPa)	
		100-300	>300
UCS (kPa)	400-1200	EB4	EB3
	>1200	EB2	EB1
Bitumen emulsion treated materials classes, EB1, EB2, EB3, EB4			

The classification approach was an attempt to capture the complex behavioural characteristics of these materials, i.e. shear and flexural characteristics. Verhaeghe and Long, (2004) indicate that although a distinction is made between class FB2/EB2 and FB3/EB3 materials the early indication of the structural behaviour of these materials is similar. The classification therefore does not imply that class FB2/EB2 is better materials quality than class FB3/EB3. Hence recommended classification basing on "strain-at-break values" on these classes as presented in Table 6.4.

Table 6.4: Material properties for foamed bitumen and bitumen emulsion, (Verhaeghe and Long, 2004)

Material classification	Foamed Bitumen		Bitumen Emulsion*	
	FB2	FB3	EB2	EB3
Stiffness (MPa)	1200-2100	680-1625	2680	1360
Strain at break ($\mu\epsilon$)	120-230	390-590	178	553

*Based on the material properties for road P243/1

However the recommended classification values Table 6.4 is an indication of the performance of the specific project, but not a representative of the general performance of the cold mixes.

In this chapter, the strain-at-break testing protocol will be discussed and the determination of strain-at-break values will be addressed. The analysis of strain-at-break results on both emulsion and foam mixes will be presented and discussed and finally the characterization of flexibility properties of the selected materials treated with emulsion or foam will be compared and discussed, and lastly conclusions will be drawn.

6.2 4PB STRAIN-AT-BREAK TESTING

6.2.1 Monotonic beam testing

The strain-at-break is not a standard test for the cold mixes. The 4PB testing apparatus (BFA) (Figure 4.17 Chapter 4) was also used for monotonic testing (strain-at-break). The sample preparation of beam specimen, and testing set-up were similar to testing procedure described for the fatigue testing in Chapter 5.

The specimens are conditioned at 5°C in the controlled temperature cabinet for duration of at least four hours prior to testing. This duration is needed to allow specimens to stabilise at the testing temperature. Before inserting the specimen into the loading frame (central loading support), it is positioned at the maximum actuator span (+9mm) due to downward loading. Then the specimen is inserted in the BFA and the outer support levels balanced by inserting 2.5mm spacers. The specimen is then allowed to settle under the clamping stresses for the period of 30 to 40 minutes before commencing the test. Specimen's set-up procedures are included in Appendix A.

The monotonic loading is applied on a beam specimen which has dimensions of 63.5 ± 0.5 mm width 50 ± 0.5 mm thickness and 380 ± 0.5 mm length. The vertical downward loads are applied at two positions at a distance equal to one third of the length of the beam. The testing of specimen is performed under controlled strain mode and the magnitude of the load is determined using a load cell measuring the resistance of the beam as it is flexed.

The vertical displacement or downward deflection of the central section of the beam during the test is measured by linear variable displacement transducer (LVDT) positioned above the specimen with the deflections being measured on the specimen's top surface. The actuator LVDT also measures deflection of the specimen and is located at the bottom of the beam with the load cell. The actuator LVDT measures the total deflection of the beam, whereas the on-specimen

LVDT measures approximately half of the actual peak deflection of the test beam and goes out of range as the test progresses. Appendix B illustrates the mathematical relationship of the values capture by the on-specimen LVDT relative to the actual peak deflection. Due to the fact that the on-specimen LVDT goes out of range, the deflection captured by actuator LVDT was used for strain at break calculations.

6.2.2 Testing parameters and recording of results

Using IPC (UTM 12) computer software, several in-put test parameters are entered to instruct the CDAS to control and monitor the specimen loading function and data acquisition from testing. Amongst others in-puts parameters the most relevant ones are:

- Specimen : beam identifications and dimensions (measured precisely using vernier calliper at five locations)
- Mode of loading : displacement control
- Loading rate : 1mm/min or 0.0167mm/s
- Termination condition : a maximum allowable time (say 540seconds) to failure, and / or actuator maximum span (9mm) , whichever reached first during the test

The loading frame provides a free rotation at all four-point and free longitudinal translation at the two reactions (support) points which is separated at a distance typically 355.5 mm. The third - point is supported at the span of 118.5 mm. Although free translation movement is allowed, the outer two supports remained fixed during testing, with no vertical movement, while the central section of testing frame and therefore two central supports are able to move vertically downwards. The specimen clamping system of end points is servo-pneumatic controlled and vertical middle points are servo-motor driven.

The software records and measures the applied load and vertical displacement of the beam during the test and transferred to the PC to be stored and plotted. Various parameters are calculated from the acquired data as the test proceeds and record amongst other the following values: Time of loading, actuator LVDT displacement, load, on-specimen LVDT displacement as well as calculating maximum tensile stress.

6.3 STRAIN- AT-BREAK CALCULATION

The strain-at-break calculation as a non standard test uses IPC (UTM 21) formula to calculate tensile strain at fatigue test. The software uses on-specimen LVDT to determine the beam deflection. However, as per the set-up of the 4PB the on-specimen deflection value is only a half of the peak beam deflection as previously discussed. Appendix B illustrates the mathematical relationship of the values capture by the on-specimen LVDT relative to the actual peak beam deflection.

A monotonic 4PB test set-up for strain-at-break is illustrated in Figure 6.6

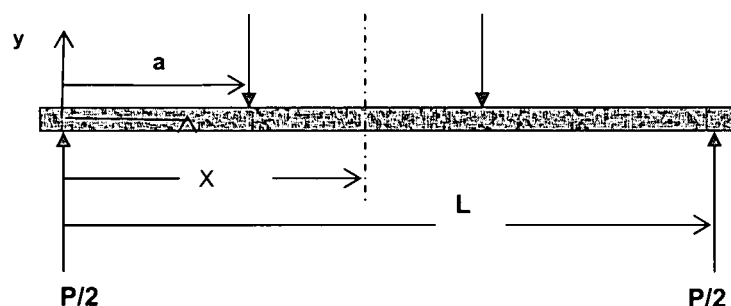


Figure 6.6: Monotonic 4PB set-up for strain at break

The deflection captured by the on-specimen LVDT maximum at the third point loading is given as:

$$\omega(L/6) = \frac{23PL^3}{1296EI} \quad (6.4)$$

The actual (peak) beam deflection at the centre is given as;

$$\omega(L/2) = \frac{23PL^3}{648EI} \quad (6.5)$$

Where:	ω	= deflection of beam due to applied load, (mm)
	P	= applied load, (KN)
	x	= distance along the beam neutral axis, (mm)
	y	= distance across the beam neutral axis, (mm)
	L	= distance between centre support of beam, (mm)
	I	= area moment of inertia of beam, ($I=bh^3/12$), (mm^4)
	E	= elastic modulus of material, F/L^2 (MPa)

The data captured by the actuator LVDT mounted adjacent to load cell at the bottom of the beam is used to determine the actual deformation at break. The BFA loading frame is set to apply

monotonic load downwards and actuator LVDT measures peak deflection as the on specimen LVDT runs out of range. The acquired values are imported to a spreadsheet and the load versus actuator LVDT values are used to plot the deformation curve. Regression equation is fit in the data and the maximum or peak value in the curve is determined as the deformation at break. The regression fit however does not properly define the peak deflection due to scattering of the values. Therefore, extrapolation is necessary to ensure that better maximum value is depicted. Figure 6.7 indicates a typical curve of load versus beam deformation captured by actuator LVDT.

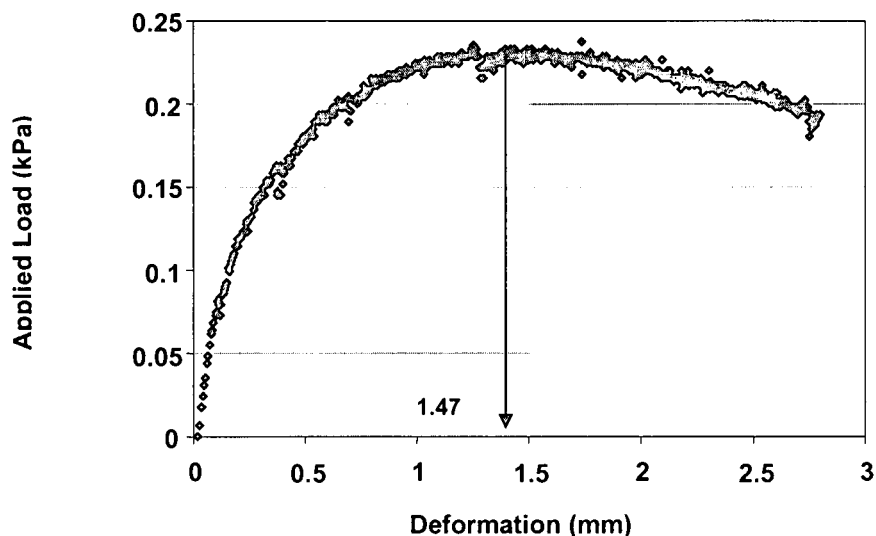


Figure 6.7: Typical graph of load viz deformation from 4PB monotonic test.

The determined or extrapolated deformation at break value from the graph is then used in the four point beam fatigue testing equation expressed in IPC (UTM 21), (equation 6.5) to determine the beam strain-at-break. Appendix C illustrates the derivations of strain calculation for the four point loads.

$$\text{Maximum Tensile Microstrain, } \epsilon_b = \frac{12\delta_c h \times 10^6}{(3G_o^2 - 4G_i^2)} \quad (6.6)$$

Where

- ϵ_b = Strain-at-break (microstrain)
- δ_c = $\omega(L/2)$, on-specimen LVDT peak deflection at the center of beam (mm)
- h = average beam height (mm)
- G_o = Outer gauge length, outer span (355.5mm)
- G_i = Inner gauge length, inner span (118.5mm)

Theyse (2000) indicated that the strain-at-break point can be obtained by plotting stress vs strain data calculated from force and vertical displacement recorded during flexing 4PB tests. See figure

6.8, where the turning point on the curve indicates failure of specimen and the strain at that point is regarded as the strain-at-break, and stress at that point is regarded as stress at break.

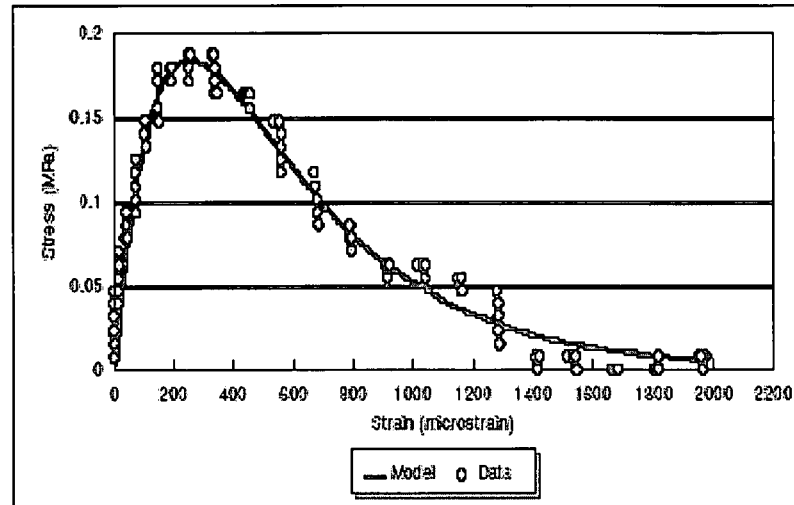


Figure 6.8: Stress-Strain plot from flexural beam 4PB test. (Theyse, 2000)

Theyse (2000) further, proposed the following mathematical model to fit the data from flexing beam tests;

$$\sigma = P(e^{-D\epsilon} - e^{-Q\epsilon}) \quad (6.6)$$

Where:

- σ = stress
- ϵ = strain
- e = natural logarithm
- P, D, Q = regression coefficients.

Equation 6.6 shows that maximum stress can be determined by taking the first derivative of equation 6.6, equate this to zero and solve the maximum tensile strain (ϵ). The maximum strain that can be sustained before failure of beam is strain-at-break can be obtained as follows:

$$\epsilon_b = \frac{\ln(D/Q)}{D - Q} \quad (6.7)$$

The maximum stress, (σ_{max}) and the value of maximum strain-at-break (ϵ_b), gives the effective stiffness of the beam at failure i.e. ($S_{eff} = \sigma_{max} / \epsilon_b$). The amount of energy required to break the beam, (area under strain-at-break curve) gives an indication of the toughness of materials on applied load. The energy required is obtained by integrating the original function Equation 6.6 between zero to strain-at-break point as presented in the Equation 6.8.

$$\begin{aligned} \text{Energy} &= \int_0^{\epsilon_b} \sigma \partial \epsilon = \int_0^{\epsilon_b} P(e^{-D\epsilon} - e^{-Q\epsilon}) \partial \epsilon \\ &= P \left(\frac{e^{-Q\epsilon_b} - 1}{Q} - \frac{e^{-D\epsilon_b} - 1}{D} \right) \end{aligned} \quad (6.8)$$

Where: The variables are as explained in equation 6.6 above

The strength and flexibility of the mixture determines the amount of energy required to break the beam. The mixture with high strength and flexibility show increasing strain-at-break values compared to stiff and elastic behavioural materials.

6.4 STRAIN-AT-BREAK PROPERTIES OF BITUMEN EMULSION MIXES

This section presents and discusses the strain-at-break results of beam tests for three selected blends treated with bitumen emulsion. Due to variability in estimation of the 4PB monotonic test results three beams were used to model the results to increase the statistical significance.

The summary of the determined strain-at-break values for bitumen emulsion mixes; Mix 4 (B-75C-0%), blend of 75%limestone and 25% milling asphalts (RAP) with no cement, is presented in Table 6.5. Mix 5 (B-75C-1%), blend of 75%limestone and 25% asphalts milling (RAP) with 1% cement, is presented in Table 6.6 and Mix 6 (B-75M-0%), blend of 25%limestone and 75% asphalt millings (RAP) with no cement, is presented in Table 6.7. The summaries include the BRD's of tested beam specimens, the determined peak deflections, and the calculated strain-at-break values. Detailed graphs of the strain-at-break LVDT results are presented in Appendix E.

Table 6.5: Strain at break results for bitumen emulsion Mix 4 (B-75C-0%) at 5°C

Beam*	BRD's (Kg/m3)	Peak Deflection (mm)	Strain at break ($\mu\epsilon$)
1C	2.239	0.84	1545
5C	2.241	1.23	2315
6C	2.240	0.90	1674
Average	2.240	0.99	1845
Std Dev.	0.001	0.21	412
CoV	0.05%	21.1%	22.3%

* Three beams were tested for repeatability.

Table 6.6: Strain-at-break results for bitumen emulsion Mix 5 (B-75C-1%) at 5°C

Beam	BRD's (Kg/m ³)	Peak Deflection (mm)	Strain at break ($\mu\epsilon$)
1D	2.202	0.58	1093
2D	2.233	0.63	1172
3D	2.238	0.38	717
Average	2.224	0.53	994
Std Dev	0.019	0.13	243
CoV	0.8%	24.5%	24.4%

Table 6.7: Strain-at-break results for bitumen emulsion Mix 6 (B-75M-0%) at 5°C

Beam	BRD's (Kg/m ³)	Peak Deflection (mm)	Strain at break ($\mu\epsilon$)
2C	2.134	0.45	833
5C	2.151	0.43	806
6C	2.128	0.60	1122
Average	2.138	0.49	921
Std Dev	0.013	0.09	175
CoV	0.6%	18.4%	19%

The repeatability on strain-at-break tests for Mix 4(B-75C-0%), Mix 5(B-75C-1%), and Mix 6(B-75M-0%) shows a fair amount of variability in strain-at-break values which shows in the CoV, (Table 6.5 and 6.6). This is expected due non-homogeneity (non-uniform dispersion of the binder) of the mixes and condition's of the beams (spalling of edges and faces during sawing), which greatly contributes to variability. A beam dimension is another significant factor for the variability, an increase or decrease in beam depth see equation 6.5 cause a big increase or decrease in strain-at-break values. The specimen preparation protocol in Chapter 4 describes measures to be taken to improve cutting process of the beams.

The characterization of strain-at-break properties (flexibility) of Mix 4(B-75C-0%) and Mix 5(B-75C-1%) found to be significant different. The comparison of these mixes shows that Mix 4 with no cement is 46% stronger (more flexible) than similar mix with 1% cement. This is high because the addition of cement in the mix (Mix 5) should have shown some level of improvement not negative behaviour on the mix. However, looking at the fatigue properties of these mixes (see Figure 5.3 Chapter 5) this amount of difference between the mixes is not reflected.

The comparison of Mix 4(B-75C-0%) with Mix 6(B-75M-0%) also shows a significant difference, where Mix 4 is 50% stronger (more flexible) than Mix 6 of high percentage of asphalt millings

(RAP). This difference does also not concur with the findings of the fatigue properties of these mixes (see Figure 5.4 Chapter 5).

However, an interesting point to note is that when the fatigue properties are normalized by strain-at-break values the mentioned differences in these mixes type become real in fatigue performance. The reversed orders of these mixes indicate that mix with high fatigue life becomes low and vice versa. As discussed in Chapter 5, the normalization of fatigue properties using strain-at-break does not reflect the mix type analysis of the layer fatigue life in the pavement structure accurately. Also the rate of loading on strain-at-break test which is arbitrary selected as 1mm/min does not indicate any relevance to cold mixes flexibility in terms of the field response. Therefore appropriate loading should be selected to represent the field pavement layer response.

From these observations, it can be commented that strain-at-break test is not accurately reflecting the fatigue properties of these mixes. So it cannot stand independently to characterize the mix type fatigue life for the mix design purposes. Therefore, the test protocol needs further development or adjustment before it can be considered to provide a meaningful relationship with fatigue life of the cold mixes.

The improvement on the specimen preparation, especially the cutting process and testing methods might provide better comparison and correlation of these properties. The compaction effort and specimen preparation also contributes to the strain-at-break performance. Table 6.7, 6.8 and 6.9 shows that the mix with high average relative bulk densities show increasing in strain-at-break values. Good compaction reduces void content, packs the mineral aggregate properly, and increases the cohesive strength of the mix skeleton with residual bitumen.

The strain-at-break values in this study when compared to the previous research, shows that cold mixes might have significant differences in performance even at very good mix composition. It all depends on the specimen preparation process, method of test and interpretations of results. It follows that the review of the proposed strain-at-break values for emulsion classification is required.

6.5 STRAIN-AT-BREAK PROPERTIES FOR FOAMED BITUMEN MIXES

This section present and discusses the strain-at-break results of beam tests for three selected blends treated with foamed bitumen. Three beam specimens was also used for modeling of results

The summary of the determined strain-at-break values of foamed bitumen mixes; Mix 7(C-75C-0%), blend of 75%limestone and 25% milling asphalts (RAP) with no cement, is presented in Table 6.8. Mix 8(C-75C-1%), blend of 75%limestone and 25% asphalts milling (RAP) with 1% cement, is presented in Table 6.9 and Mix 9(C-75M-0%), blend of 25%limestone and 75% asphalt millings (RAP) with no cement, is presented in Table 6.10. The summaries include the specimen BRD's, peak deflections, and the calculated strain-at-break values. Details of the strain-a-break graphs are presented in Appendix E.

Table 6.8: Strain-at-break results for foamed bitumen Mix 7(C-75C-0%) at 5°C

Beam	BRD's (Kg/m3)	Peak Deflection (mm)	Strain at break ($\mu\epsilon$)
2C	2.070	0.82	1511
5C	2.057	0.91	1697
6C	2.035	1.16	2163
Average	2.054	0.96	1790
Std Dev	0.17	0.18	336
CoV	0.8%	18.8%	18.8%

Table 6.9: Strain-at-break results for foamed bitumen Mix 8 (C-75C-1%) at 5°C

Beam	BRD's (Kg/m3)	Peak Deflection (mm)	Strain at break
1C	2.028	1.55	2897
5C	2.100	1.32	2427
6C	2.027	1.16	2160
Average	2.052	1.34	2495
Std Dev	0.042	0.20	373
CoV	2%	14.9%	14.9%

Table 6.10: Strain-at-break results for foamed bitumen Mix 9 (C-75M-0%) at 5°C

Beam	BRD's (Kg/m3)	Peak Deflection (mm)	Strain at break
1B	1.985	0.54	989
2B	2.011	0.72	1356
2B	2.031	0.78	1469
Average	1.998	0.68	1271
Std Dev	0.018	0.13	251
CoV	0.9%	19.1%	19.7%

The strain-at-break values of Mix 7(C-75C-0%), Mix 8(C-75C-1%) and Mix 9(C-75M-0%) Table 6.8 6.9 and 6.10 shows a fair repeatability in average and CoV.

The strain-at-break values of Mix 7(C-75C-0%) and Mix 8(C-75C-1%) seem to be significant different. Mix 8 with one percent cement is 28% stronger (more flexible) than the similar mix without cement. This could be possible but the correlation with other properties such as fatigue properties and stiffness master curve does not reflect the same difference as presented in Figure 5.7 Chapter 5, and Figure 7.10 Chapter 7. However the reason for high strain-at-break value might be the effect of cement that improved the dispersion of foamed bitumen in the mix, hence results in increase in cohesive strength of the mixture.

The comparison of Mix 8(C-75C-1%) with Mix 9(C-75M-0%) shows that Mix 8 is 49% stronger than Mix 9 (higher percentage of RAP). This also does not concur to the finding of other properties of these mixes such as fatigue properties (see Figure 5.8, Chapter 5).

However normalization of the fatigue properties using strain-at-break values reflect these differences which is a reversing of the fatigue properties of these mixes obtained from the 4PB fatigue tests. Therefore, the comment for this behaviour is as recorded for the emulsion mixes above.

The strain-at-break values for foam mixes when compared to the past research also found to be much higher. This shows that the classification limits for the cold mixes guideline need to be reviewed.

6.6 COMPARISON OF STRAIN-AT-BREAK PROPERTIES FOR THE BITUMEN EMULSION AND FOAMED BITUMEN MIXES

Flexibility can defined as ability of the mixture (structure) to resist cracks or fracture under the applied load. Flexibility is a function of the inverse of stiffness corollary that cracking or fracture of the materials must not occur. Flexibility is a function of the ratio of bending displacement due to applied load within the tensile strength range of material.

The laboratory strain-at-break test using monotonic loading gives a relationship of displacement against applied load until cracking occurs. However, the field performance of the pavement structure has the effect of multiple loads applied by traffic. The laboratory fatigue test at defined displacement level, gives a relationship of stiffness and number of load repletion until cracks

occur. These tests try to measure the flexibility of the mixture under repeated loading before failure. However, the meaningful relationship between these tests is not apparently obvious.

The comparison of strain-at-break results of the bitumen emulsion and foamed bitumen mixes give an insight on the suitability of these mixtures to withstand a level of deformation under applied load before cracking occurs.

The amount of energy (area of the curves to maximum deformation) required to break the test beams specimen give an indication of the cohesive strength properties or stiffness of the mixture before failure due to the applied load, Figure 6.9 and 6.10 presents the superimposition of the graphs of load versus deformation for the emulsion mixes and foam mixes respectively.

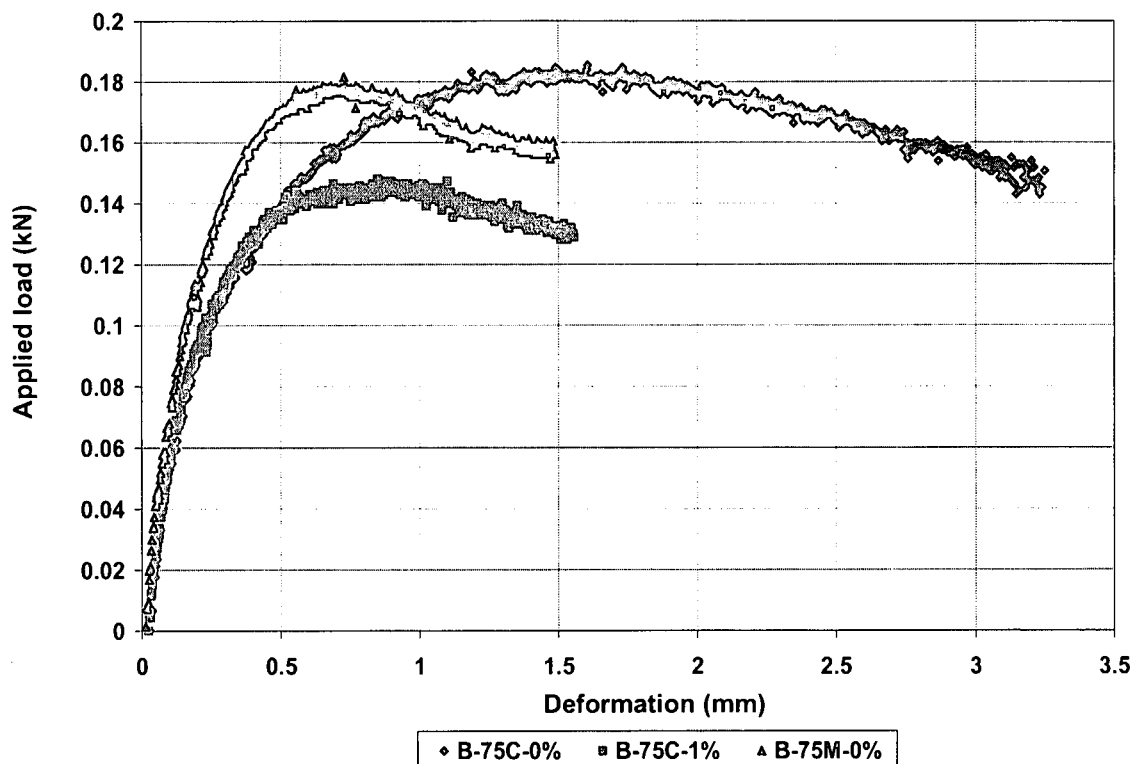


Figure 6.9: Strength properties of emulsion mixes; Mix 4, Mix 5 and Mix 6 at 5°C

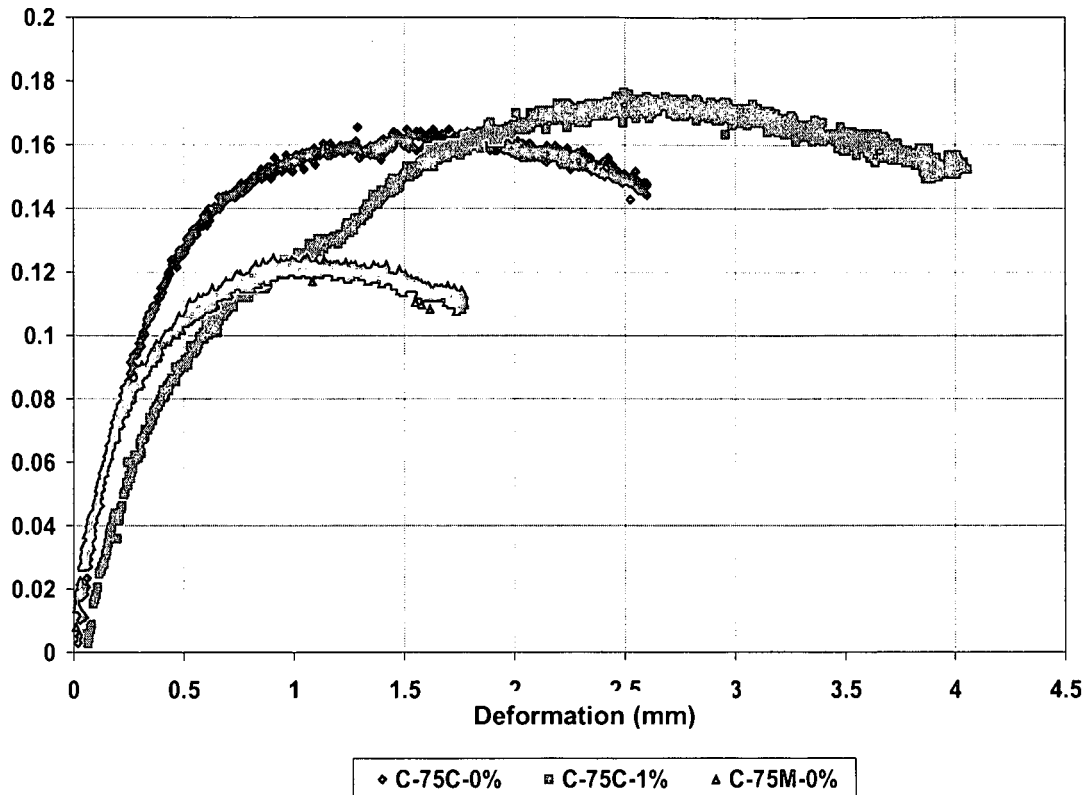


Figure 6.9 and 6.10 illustrate the beam deformation as a function of strength of the mixture. The results show that mixes with higher flexibility (combination of deformation and load) required more energy to reach the deformation at break. Emulsion Mix 4(B-75C-0%) shows higher deformation at break (strain-at-break) than Mix 5 and 6. This indicates that the mix is much stronger (more flexible) compared to Mix 5(B-75C-1%) and Mix 6(B-75M-0%).

Mix 5(B-75B-1%) shows larger deformation at break under small applied load compared to Mix 4. This shows that Mix 5 is stiffer compared to Mix 4. However, Mix 6(B-75M-05) shows small deformation at break (strain-at-break) compared to Mix 5(B-75C-1%), but requires a large load to reach the deformation at break. This shows that Mix 6 is stiff (less flexible) compared to Mix 4 and 5. The comparison on the cohesive strength of these mixes and the energy required to reach deformation at break concur with the findings in other properties such as stiffness and fatigue, where mixes with high strength (more flexible) show increasing fatigue life and stiff mixes show high flexural stiffness master curve.

The characterization of strain-at-break properties of the selected emulsion and foam mixes (Mix 4, 5 and 6 and Mix 7, 8 and 9 respectively) give an insight in the comparison of the flexibility function and the relative performance of these mixes. The superimposition of strain-at-break values as a

function of binder, cement, and percentage asphalt millings (RAP) are presented in Figure 6.9, 6.10 and 6.11 respectively.

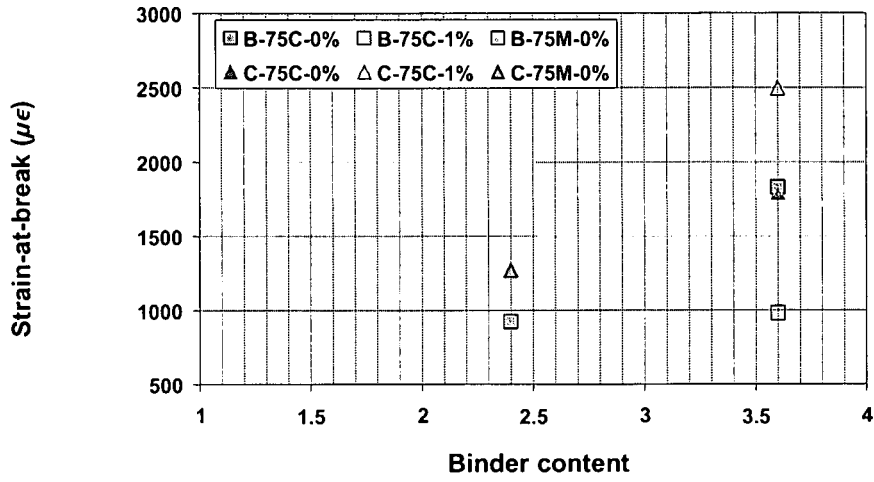


Figure 6.11: Strain-at-break as a function of binder content

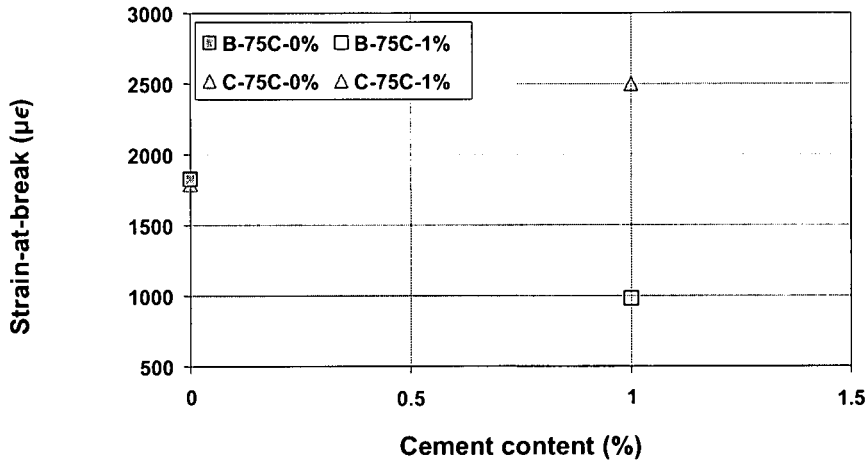


Figure 6.12: Strain-at-break as a function of cement content (%)

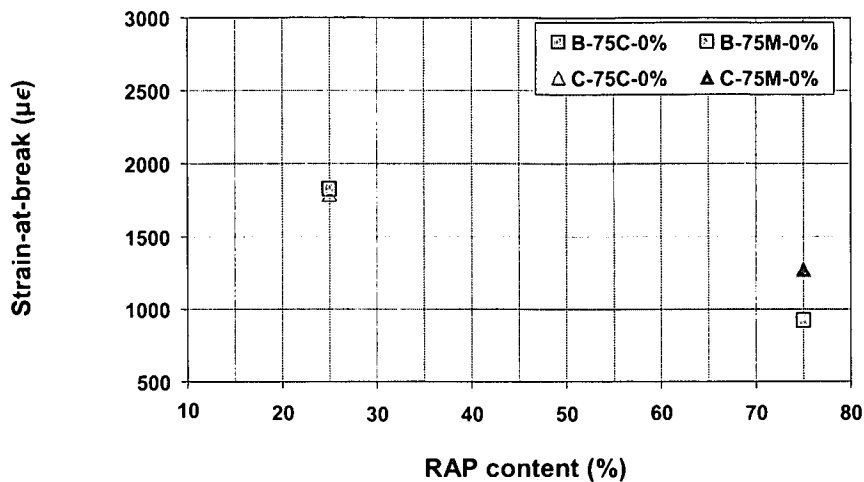


Figure 6.13: Strain-at-break as function of percentage asphalt millings (RAP)

The strain-at-break properties are shown in relation to the variables binder, mineral aggregates and active filler in Figure 6.11. The results indicate that the mixes (both emulsion and foam) with higher binder contents have increasing strain-at-break values, which is consistent with behaviour of HMA. However, the emulsion mixes with addition of active filler do not subscribe to this trend, which is unexpected. The addition of higher percentage RAP in the mixes shows a reduction in strain-at-break properties. This might possibly be the result of reduced “fresh” binder content being applied to the mixes. It is essential therefore, for strength and flexural parameters to be balanced and optimized in the mix design through laboratory testing to achieve the maximum load spreading and fatigue resistance in pavement layer.

The strain-at-break properties have shown that emulsion mixes with no cement is approximately the same than the similar mix treated with foamed bitumen. The foamed bitumen mix with 1% cement is 61% stronger than the similar mix treated with emulsion. The foamed bitumen mix with the high percentage of RAP is 27% stronger than the similar mix treated with emulsion. These differences do not fully concur with the findings of the fatigue performance of these mixes

However, notwithstanding this, it is essential to have a parameter that reflects the positive influence of increased bitumen content rather than just a strength test, which encourages excessive amount of cement to be used in cold mixes. This could be possible by reviewing the strain-at-break test.

The comparisons of the selected mixes (emulsion and foam) in terms of strain-at-break properties in relation to the past research on cold mixes provide an intrinsic comparison of the performances of these mixes. The superimposition of strain-at-break properties for Hornfels milled material

treated with foamed bitumen. Ferricrete milled materials treated with either emulsion or foam and selected limestone blends treated with emulsion, (Mix 4(B-75C-05), Mix 5 (B-75C-15), and Mix 6(B-75M-05)) or treated with foamed bitumen (Mix 7(C-75C-0%), Mix 8(C-75C-1%), and Mix 9(C-75M-0%) as a function of residual bitumen is presented in Figure 6.14 and as a function of cement contents in Figure 6.15.

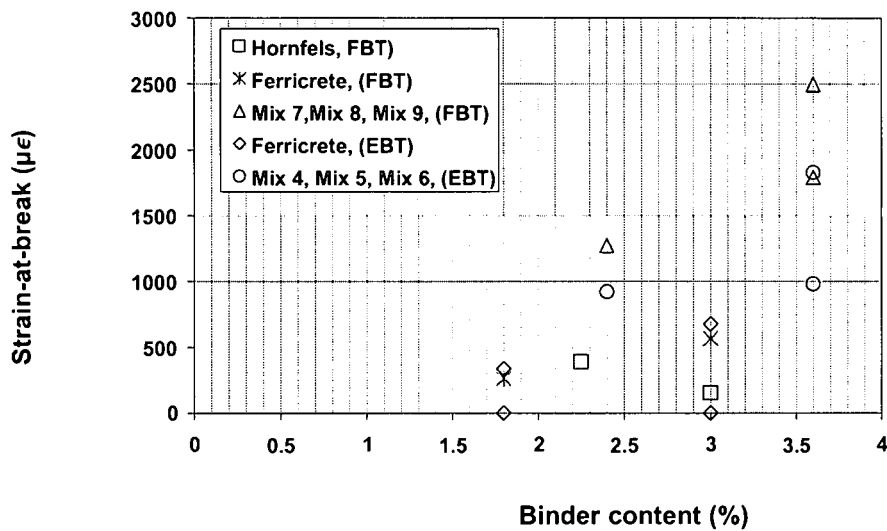


Figure 6.14: Superimposition of strain-at-break properties of selected mixes and past researches as function of binder contents.

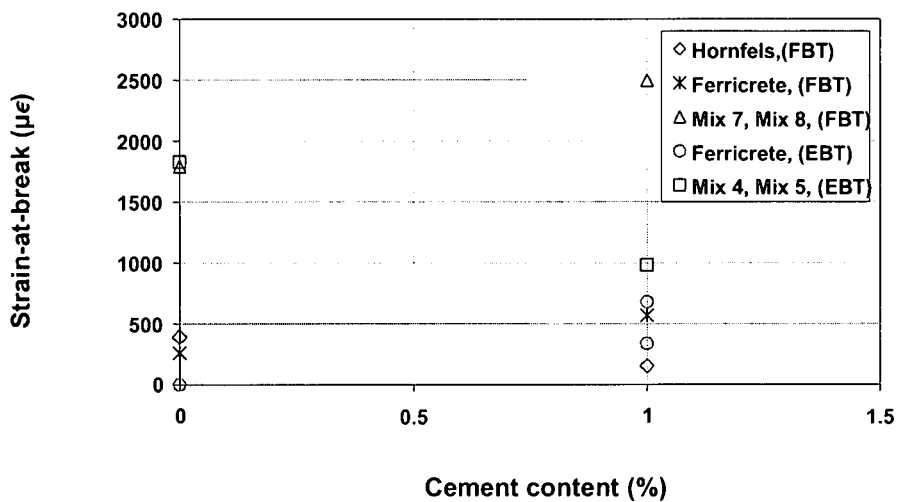


Figure 6.15: Superimposition of strain-at-break properties for selected mixes and past research as function of cement contents

The strain-at-break properties for Mix 4(B-75C-0%), Mix 5(B-75C-1%) and Mix 6(B-75M-0%), Mix 7(C-75C-0%), Mix 8(C-75C-1%) and Mix 9(C-75M-0%) show significant higher strain-at-break

values compared to Hornfels mixes, Ferricretes mixes with similar binder or cement contents (Figure 6.13 and Figure 6.14). This significant difference in strain-at-break properties for these mixes was not expected. However, the contributing factors might have been; blending and quality of mineral aggregates, binder contents, specimen preparation and method of testing as previously discussed.

There is an overall trend of increase in strain-at-break as the binder content increases, which is to be expected. Notable is the variability in results, which brings into question the reliability of strain-at-break test as a flexibility measure for the cold mixes.

6.7 CONCLUSIONS

The strain-at-break test is a non standard test, but it can be used for the characterization of flexibility properties of the cold bituminous treated materials. It is in this regard that reliability, relevance and applicability of the test is still a key question for practitioners that need to be addressed. The study on strain-at-break properties of the selected materials treated with either bitumen emulsion or foamed bitumen has led to the following conclusions being drawn:

6.7.1 Specimen preparation and testing

- The strain-at-break properties of the mixes have shown to be influenced by the interaction of binder, active filler mineral aggregates, and moisture content. Therefore, specimen preparation including mixing, compaction, curing and cutting, and methods of test are important factors for achieving better and more reliable results.
- Testing variables amongst others are a contributing factor to the variability of test results. Testing at low temperature is complicated with 4PB pneumatic servo-operating system. The interruptions in air supply due to icing up of condensation water in the pipes affects the smooth operation of the actuator. This results in a jumping motion or failure to reach maximum span (weak stroke) due insufficient air supply. Therefore, improvement to account for these ambiguities is recommended as suggested in testing methodology Chapter 4.

6.7.2 Strain at break properties

- The strain-at-break properties have shown in relationship to variables such as binder, active filler, and mineral aggregates. The results indicate that the mixes with high binder content have increasing strain-at-break values. However, emulsion mixes with addition of cement do not

subscribe to this trend, which is unexpected. The mixes with a high percentage of RAP show a reduction in strain-at-break properties. This is possibly the result of reduced “fresh” binder content being applied to these mixes. It is essential, therefore, for strength and flexural parameters to be balanced and optimized in the mix design through laboratory testing to achieve the maximum load spread and fatigue resistance in the pavement layer.

- The strain-at-break test makes use of monotonic loading. The strain-at-break properties have been used as a measure of the “flexibility” of the cold mixes. However, the strain-at-break properties of emulsion mixes show significant differences in comparison with the foamed bitumen mixes. The emulsion mixes with no cement (Mix 4(B-75C-0%)) has shown to be 46 percent more flexible compared to similar mixes with one percent cement (Mix 5(B-75C-1%)). The opposite is for the foam mixes; the mix with one percent cement (Mix 8(C-75C-1%)) has shown to be 28 percent more flexible than similar mix with no cement Mix 7(C-75C-0%). For the mixes with a high percentage of asphalt millings (RAP), treatment with foamed bitumen results in 27 percent higher strain-at-break values compared to similar mix treatment with emulsion.
- The significant differences in strain-at-break properties of the selected mixes indicate that the strain-at-break does not accurately reflect the fatigue properties of cold mixes. It can therefore not be used independently to characterize the mix type fatigue life for the mix design purposes. Therefore, the test protocol and rate of loading needs further development or adjustment before it can be considered to provide a meaningful relationship with fatigue life of the cold mixes.
- The comparison of the strain-at-break properties of the selected mixes (emulsion and foam) from this research with past research shows significant difference at the same binder or cement content. This show that standardization of strain-at- break test in terms of specimen preparation such as mixing, compaction, curing and, methods of testing and interpretation of results is of paramount importance and requires more attention.

6.8 REFERENCES

AUSTROADS. 2004. **Sample preparation-compaction of asphalt slabs suitable for laboratory characterization.** Commentary to AG:PT/T220, Sydney, Australia.

AUSTROADS. 2001. **Fatigue life of compacted bituminous mixes subject to repeated flexural bending.** Manual AST03.Sydney, Australia.

ASPHALT ACADEMY. 2002. **The design and use of foamed bitumen treated materials**. TG2, Interim Technical Guideline. Pretoria, South Africa.

EBELS L.J, JENKINS K.J and COLLINGS D., 2005. **Cold mix (bitumen stabilization) technology in Southern Africa into the 21st Century**. Proceedings of International symposium on pavement recycling, Sao, Paulo, Brazil.

IPC (Industrial Process Control Ltd), 1998. **Beam Fatigue Apparatus**. Reference Manual. Boronia, Australia.

JENKINS K..J., 2000. **Mix design considerations for cold and half-warm bituminous mixes with emphasis on foamed bitumen**. PhD Dissertation, University of Stellenbosch, South Africa.

LONG F.M., 2001. **The development of structural design models for foamed bitumen treated pavement layers**. Contract Report CR-2001/76, Transportek, CSIR, Pretoria, South Africa.

LONG F.M and THEYSE H.L., 2001. **Laboratory testing for the HVS section on P243-1**. Contract Report CR-2001/32. Transportek, CSIR, Pretoria, South Africa.

LONG F.M and VENTURA D.F.C., 2003. **Laboratory testing for HVS test section on the N7. TR11/1**. First Draft for review. Contract Report CR-2003/56. Transportek, CSIR, Pretoria, South Africa.

LONG F.M, 2001. **Interim guidelines: the design and use of foamed bitumen treated bases**. Road Pavement Forum, Pretoria, South Africa.

LIEBENBERG J.J.E., 2002. **The influence of various emulsion and cement content on an emulsion treated ferricrete from the HVS Test section on Road P234/1**. Contract Report, CR-2001/77, Transportek, CSIR, Pretoria, South Africa

LIEBENBERG J.J.E., 2003. **A structural design procedure for emulsion treated pavement layers**. Master Dissertation, University of Pretoria, South Africa.

SABITA, 1993, **GEMS: The design and use of granular emulsion mixes**, Manual 14, SABITA, Cape Town, South Africa.

THEYSE H.L., 2000. **Laboratory design models for materials suited to Labour-Intensive construction**. Volume I: Report, Contract Report CR-99/038. Transportek, CSIR, Pretoria, South Africa.

THEYSE H.L., 2000. **Overview of the South African mechanistic pavement design methods.** South African Transport Conference, Pretoria, South Africa.

THEYSE H.L., 1998. **Towards guidelines on the structural design of pavement with emulsion treated layers.** Contract Report CR-97/045, Transportek, CSIR, Pretoria, South Africa.

THEYSE H.L et al., 1995. **Testing of the fatigue characteristics of bound wearing courses to more accurately predict pavements behaviour and field performance in design.** Report No. RR 95/565, Department of Transport, Pretoria, South Africa.

VERHAEGHE B.M.J.A and LONG F.M., 2004. **Cold in-place recycling with bitumen emulsion and foamed bitumen: a South African perspective¹.** International Seminar on Asphalt Pavement Technologies II. Kuala Lumpur, Malaysia.

CHAPTER 7

7. DEVELOPMENT OF STIFFNESS MASTER CURVES

7.1 INTRODUCTION

The fatigue performance of the bituminous materials is strongly related to the stiffness characteristics. This Chapter is provided to give an indication of the selected mixes stiffness modulus for better insight on characterizing and comparing the mixes fatigue performance.

Bituminous treated materials are neither purely elastic nor purely viscous. However when loaded extremely rapidly (or at low temperature) they exhibit elastic response and when loaded very slowly (or at high temperature), viscous response prevails. For intermediate loading rate a response is a combination of the two, called visco-elastic behaviour (Francken, 1977). Figure 7.1 illustrate that behaviour.

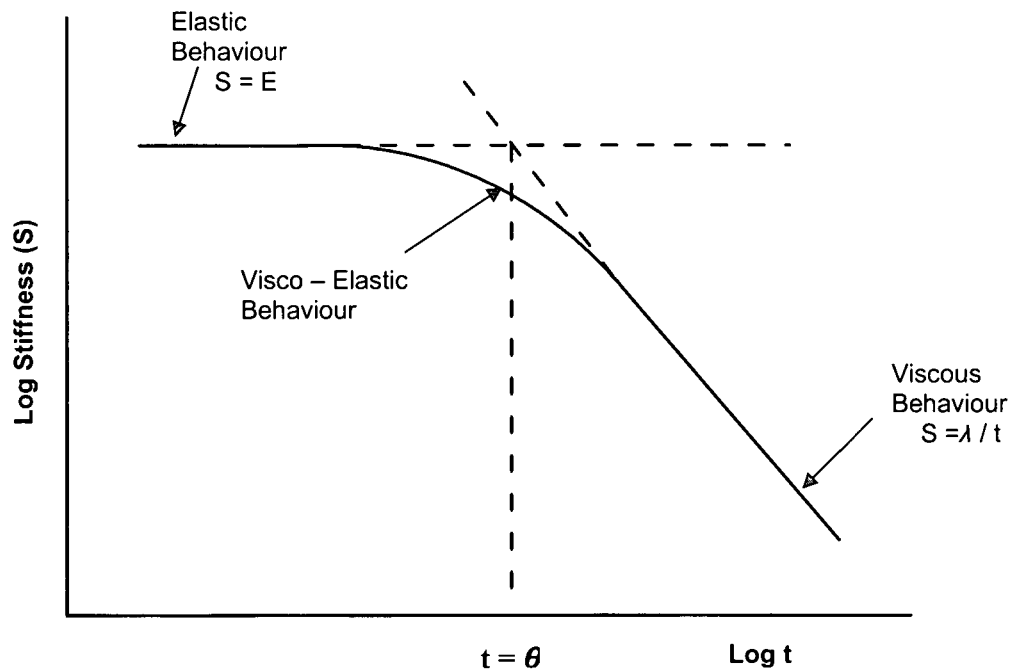


Figure 7.1: Stiffness of rheological materials as a function of loading time, (Francken, 1977)

Due to visco-elastic properties of bituminous treated materials, stiffness characteristics of the mixture needs to be determined in order to evaluate the behaviour of the mix in both load induced and thermal stress and strain distribution in pavement layer (Medani et al.,2003). Stiffness has

been used as an indicator of mixture quality for pavements and mixture design in order to evaluate damage and age-hardening trends of bituminous mixture both in laboratory and the field, (Epps et al., 2000).

The mix stiffness is estimated from the master curve i.e. the relationship between the mix stiffness, loading time (frequency) and temperature. In practice, the indirect tensile test or the 4PB-beam testing is used to determine this relationship, (Medani et al., 2003 and Fritz et al., 1999). However, laboratory techniques have limitations in defining a complete set of stiffness values over the whole loading time range at a particular temperature. Therefore laboratory testing is done by measuring the stiffness of the mixture over a small loading time range (frequencies) but at a number of different temperatures, (Francken, 1977).

Generally the stiffness modulus of bituminous mixes increases with decreasing temperature and increasing loading frequency. Airey, (1995) investigated the influence of primary variables (deflection and loading frequency) and secondary variables (temperature and loading waveform) on the stiffness and fatigue life of beam test specimens, using the four point beam bending apparatus. He indicated that, since maximum strain is a good criterion for defining crack initiation, stiffness plays a predominant role in determining the fatigue behaviour of bituminous bound materials.

Stiffness of mixture, defined as the ratio of stress amplitude to strain amplitude is dependent on the temperature and rate of loading. Keeping the temperature and loading wave constant under varying primary variables, indicates that as loading frequency decreases the stiffness values of the mixture decrease. Lower strain rates and decreasing frequencies causes the bituminous materials to behave increasingly viscous and resulting in a decrease in elastic nature and consequently a decrease in mixture stiffness. Table 7.1 illustrate this behaviour for fatigue performance and stiffness at various frequencies.

Table 7.1: Fatigue performance and Stiffness of asphalt mix at various frequencies at 0.5mm deflection (Airey, 1995)

Test No.	Freq (Hz)	Load Reps (N_f)	Stiffness (MPa)	Strain ($\mu\epsilon$)
1	20	56 600	3 575	1260
2	10	53 100	3 281	1260
3	5	65 700	3 052	1260

By varying the secondary variables (temperature and loading wave), Airey indicated that as temperature increases the stiffness of the bituminous mixes decreases. This is due to its viscoelastic nature where an increase in temperature results in an increase in the viscous nature

and decreases in the elastic nature of the bituminous mixture and consequently decreases the stiffness. Table 7.2 indicates this behaviour. Airey (1995) further commented that from the results it can be seen that crack initiation seems to occur more readily (lower number of load repetitions to crack initiation) at higher temperature. Crack propagation is stress concentration dependent and will result in an increase in crack propagation at higher stress and lower temperature under controlled displacement conditions.

Goodrich, (1991) indicated that at high temperature the fatigue resistance of the binder can be attributed to its retained elastic properties and at low temperature to its retained viscous (flow) properties. The decrease in the fatigue life of test specimens as the test temperature increases may be ascribed to the fact that when the cohesive strength of the binder decreases as the binder softens, the stiffness of the specimen also decreases.

Table 7.2: Fatigue performance and stiffness asphalt mix at various temperatures at 20Hz loading frequency and 0.5mm deflection (Airey, 1995)

Test No.	Temperature (°C)	Load reps (N_f)	Stiffness (MPa)	Strain ($\mu\epsilon$)
1	5	56 600	3 575	1260
2	10	78 000	3 056	1260
3	15	23 200	2 290	1260
4	19	25 000	2 141	1260

The stiffness modulus master curve may be developed from any arbitrary chosen reference temperature, T_{ref} in the experimental range. By shifting the different experimental curves (graph of stiffness modulus versus loading time (frequency) for various temperatures) horizontally with respect to chosen curve as reference, a complete stiffness modulus-time behaviour curve at a constant, arbitrarily chosen, reference temperature T_{ref} can be assembled.

The master curve is a function of the reduced frequency from which it is possible to determine a particular value of stiffness modulus corresponding to any frequency and temperature in the realistic condition range (Francken, 1977). It is always an increasing function (see Figure 7.2) of the reduced frequency tending to an upper asymptotic limit. In the lower frequency (higher temperature) range, the reduced stiffness modulus increases exponentially with logarithm of reduced frequency. While in the medium range the reduced stiffness depends linearly on the logarithm of the reduced frequency. The slope of the line may be predicted from the asphaltene content or Penetration Index of the bitumen used. At the higher frequency (low temperature) range the reduced stiffness modulus tends to an asymptotic relationship with the logarithm of the reduced frequency.

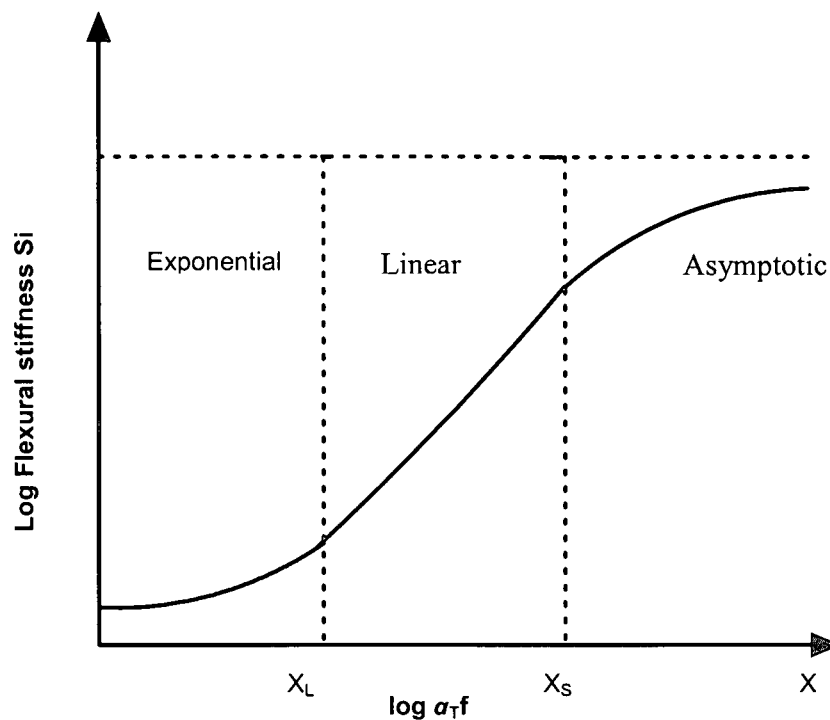


Figure 7.2: Schematic representation of reduced stiffness modulus at frequency range (low, medium and high) After (Francken, 1977)

The objective of this chapter is to develop the stiffness modulus master curve for the selected cold bituminous mixes. The chapter describe the methodology used to construct the stiffness modulus master curves from frequency sweeps tests. The flexural beam stiffness values are determined from frequency sweeps tests (varying frequencies and temperatures) using IPC, 4PB Apparatus (1998).

The sample preparation methodology of beam test specimens of the selected mixes is detailed in Chapter 4. The typical Arrhenius model is used to characterise the stiffness properties of the mixture, which believed to give reasonable estimates for the mix stiffness at any arbitrary loading frequency. The stiffness properties of the mixes are then presented and discussed.

7.2 TIME-TEMPERATURE SUPERPOSITION PRINCIPLE

A quantitative mathematical model that describe the time-temperature dependency of asphalt binder is needed for calculating materials properties for a wide range of loading time and temperatures from limited measurements made in a laboratory. Three dimensional non-linear constitutive relationships for time-temperature dependent material models are often complicated mathematically; therefore traditional approaches reduce the three dimensional characterisation,

i.e. modulus, time and temperature to two dimensional problems by imposing time-temperature superposition, (Mihai et al., 1996).

The technique for determination of the master curve is based on the principle of time-temperature superposition, or thermo-rheological simplicity. In this manner the modulus or other visco-elastic moduli are expressed as a function of reduced time. This implies that the stiffness modulus values of the mixes can be obtained either at low temperatures (non-equilibrium behaviour) or at high temperature (Newtonian behaviour) or intermediate region (linear visco-elastic behaviour). Chehab et al.,(2002) have shown that this property based on the work of Schapery et al., (1997) and that the time-temperature superposition principle may hold even if the linear visco-elastic conditions are violated.

The stiffness modulus data collected at different temperature are plotted as logarithm of the modulus versus the logarithm of loading time and the resultant data are “shifted” relative to the time of loading (or frequency), until the different experimental curves merge into single function called “Master Curve”. The master curve can be constructed using an arbitrary selected reference temperature, (T_{ref}) to which all data are shifted. At the reference temperature, the shift factor is equal to one (=1).

The shift factor may simply be reported in graphical or tabular format or regressed to fit some predetermined function such as Arrhenius or Williams-Landel-Ferry equations, etc.

The researchers have indicated that the stiffness modulus master curve can be mathematically modelled by function described as:

$$\log f_{eq} - \log f = \log \alpha_t \quad (7.1)$$

Where:

f_{eq}	= the frequency where the master curve should be read (Hz)
f	= actual frequency of loading test (Hz)
α_t	= shift factor

In the literature, among other methods three methods are commonly used for determination of shift factor (α_t) for the development of the master curve these includes:

- Graphical shifting of experimental results,
- Using the Arrhenius type equation,
- And using the Williams-Landel-Ferry (WLF) equation.

These methods are described as follows;

7.2.1 Graphical shifting of experimental results

The experimental stiffness data are plotted versus log frequency or log loading time. After choosing a reference temperature the data of the other temperature are shifted horizontally until they fit the curve for the reference temperature (shift factor can be obtained by inter-or extrapolation). Then the data obtained at other temperatures are shifted until they fix the extended reference curve. This procedure was described by Germann and Lytton (1977) as shown in Figure 7.3

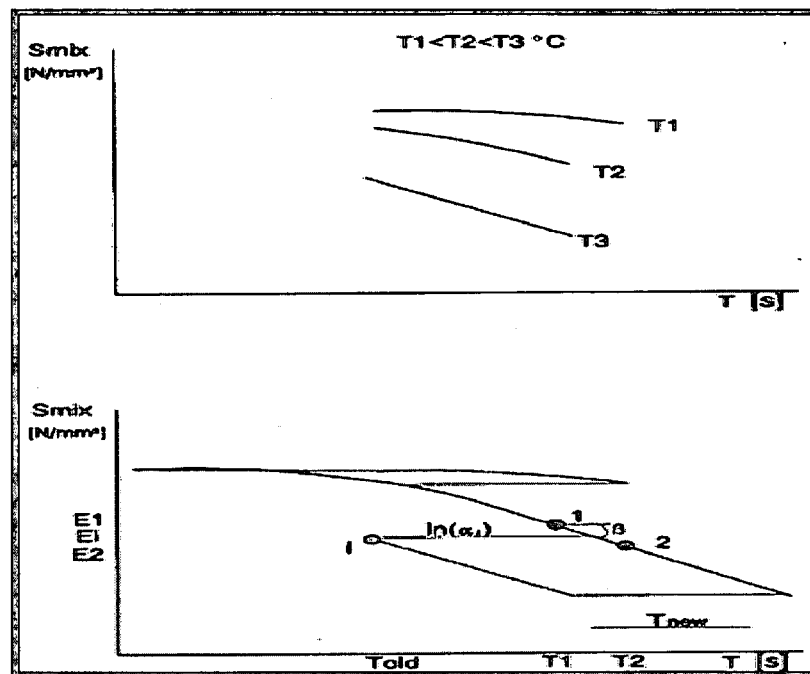


Figure 7.3: Setting up of master curve using fitting of experimental curves methods, after Germann and Lytton, (1997).

From Figure 7.3, the graphical shifting of experimental results can be done as follows:

$$T_{\text{master}} = e^{(\ln(T_{\text{old}}) - \ln(\bar{\alpha}_i))} \tag{7.2}$$

Where

$$\ln(\bar{\alpha}) = \frac{\sum_{i=1}^m \ln(\alpha_i)}{m}, \tag{7.3}$$

and $\ln(\alpha_i) = \ln(T_{\text{old},i}) - \ln(T_{\text{new},i})$

$$\text{Thus } T_{\text{new},i} = 10^{(\log T_2 - \Delta x_i)} \quad (7.4)$$

$$\text{Where } \Delta x_i = \frac{\Delta y}{\tan \beta} = \frac{\delta x}{\delta y} \cdot \Delta y$$

$$\text{and } \delta x = (\log(T_1) - \log(T_2)) \quad (7.5)$$

$$\text{and } \delta y = (\log(E_1) - \log(E_2))$$

$$\text{and } \Delta y = (\log(E_i) - \log(E_2))$$

$T_{\text{new},i}$ is the individually shifted time-value of data point i , shifted over $\ln(\alpha_t)$, such that it exactly matches the reference curve. T_{master} is the shifted time-value of point i , shifted over the average shift factor for that temperature $\ln(\alpha_t)$.

7.2.2 Arrhenius type equation

A commonly used formula for the shift factor is an Arrhenius type equation (Francken et al., 1988, Jacobs 1995, Lytton et al., 1993). The shift factor is described as follows:

$$\begin{aligned} \log f_{\text{eq}} - \log f &= \log \alpha_t \\ \log \alpha_t &= C \cdot \left(\frac{1}{T} - \frac{1}{T_{\text{ref}}} \right) = \log e \cdot \frac{\Delta H}{R} \left(\frac{1}{T} - \frac{1}{T_{\text{ref}}} \right) \end{aligned} \quad (7.6)$$

Where:

- T = experimental or test temperature (K)
- T_{ref} = the reference temperature selected (K)
- C = constant (K)
- ΔH = activation energy (J/mol)
- R = ideal gas constant, 8.314(J/(mol.K))

Other variables are as previously defined.

In literature, different values were reported for the constant C.

- C = 10920 K, Francken et al., (1988)
- C = 13060 K, Lytton et al., (1993)
- C = 7680 K, Jacobs, (1995)

7.2.3 Williams-Landel-Ferry (WLF) equation

Another formula for the calculation of the shift factor is the Williams-Landel-Ferry (WLF) equation (Williams et al., 1955) described as follows:

$$\log f_{eq} - \log f = \log a_1$$

$$\log a_1 = -\frac{C_1 \cdot (T - T_{ref})}{C_2 + (T - T_{ref})} \quad (7.7)$$

Where: T = experimental or test temperature (K)
 T_{ref} = the reference temperature selected (K)
 C_1, C_2 = empirical constants
 Other variables are as previously defined.

According to Sayegh, (1967) the $C_1 = 9.5$ and $C_2 = 95$. It has also been reported by Lytton et al, (1993) that $C_1 = 19$ and $C_2 = 92$.

7.3 CONSTRUCTION OF MASTER CURVES

The Arrhenius model has been applied to construct the stiffness master curve for the selected cold bituminous treated materials in this study. It is believed that the model gives reasonable estimates of the mix stiffness at any arbitrary loading frequency, when the difference between temperature to be shifted and reference temperature ($T-T_{ref}$) is less or equal to 20°C, (Medani et al., 2003). Typical Arrhenius method of shifting experimental stiffness curves is illustrated in Figure 7.4

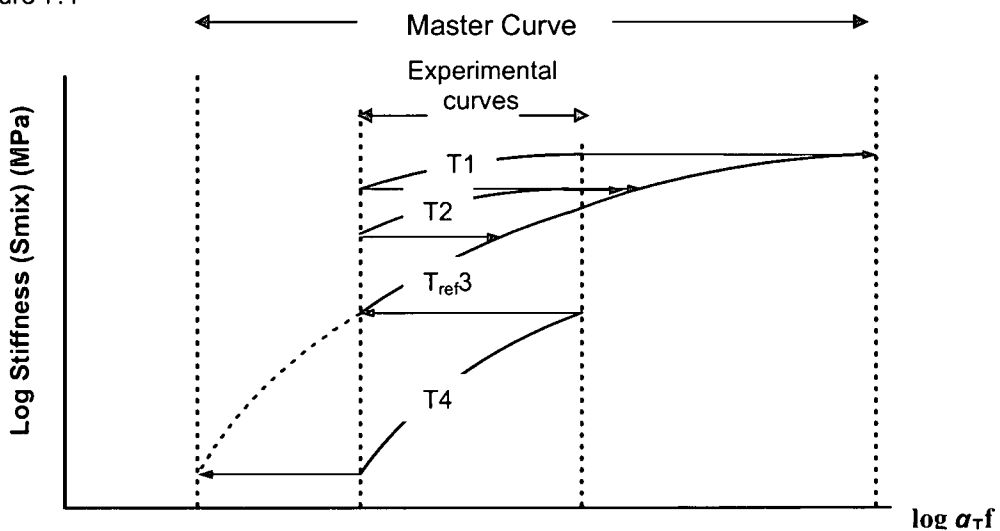


Figure 7.4: Master curve from frequency sweeps test (varying temp and freq) for determination of stiffness modulus (Franken, 1977).

7.3.1 Determination of the mix stiffness at different temperature and frequencies

The stiffness modulus of the selected cold bituminous treated mixes was investigated using the IPC, 4PB Apparatus (1998). The advantage of using the 4BP apparatus in the developing master curves is that similar specimen preparation of beam test specimens is similar to the fatigue testing and that testing procedures as described in Chapter 4 and Appendix A respectively are also applicable to the frequency sweep tests.

Generally flexural beam stiffness values determined with the 4BP Apparatus show relatively high variations. To account for that a repeat test of temperature-frequency sweeps was carried out on two (2) selected beam specimens for each mix. The tests conditions were as follows:

Type of test	= displacement controlled
Frequencies	= 0.5Hz, 1Hz, 2Hz, 5Hz, and 10Hz
Temperature	= 5°C, 10°C, 15°C, 20°C and 25°C
Strain amplitude	= 70µm/m
Loading wave	= haversine
Stiffness measurement	= after 50 pulse (cycles)
Termination condition	= 300 cycles

In order to minimise the damage of the beam specimens during testing, the tests were carried out at lower strain levels (70µm/m) and terminated at a maximum numbers of 300 cycles. The tests commenced at the lower temperature and higher frequencies. The initial flexural stiffness S_i from 4PB tests is defined as being a measure from regression relationship of the data at the 50th pulse, (see Figure 7.5). These values are then used to construct the experimental stiffness curves.

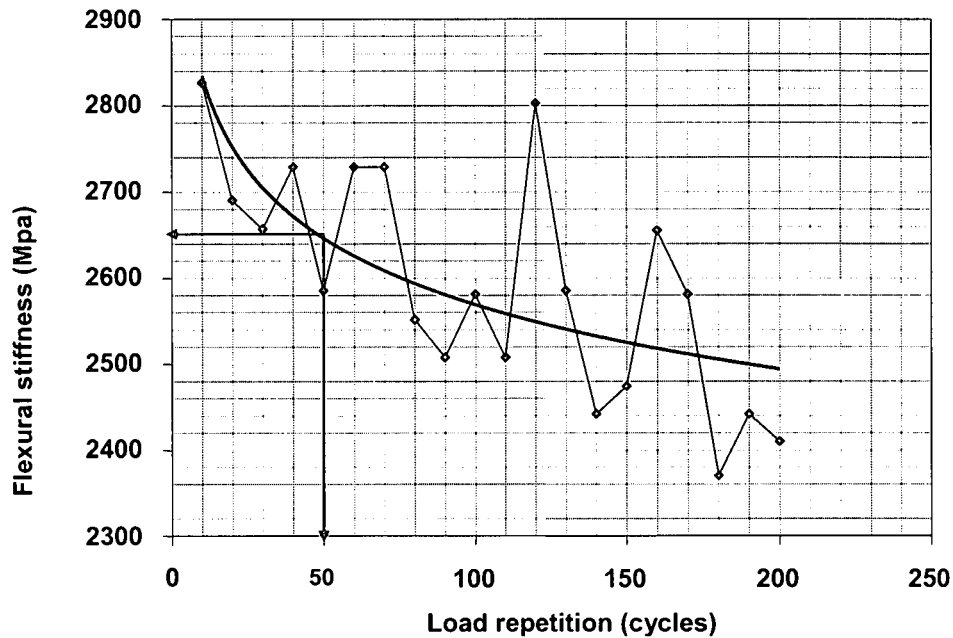


Figure 7.5: Initial flexural stiffness from frequency sweep tests at controlled displacement 4PB.

7.3.2 Fitting the experimental results using Arrhenius type equation

A reference temperature of 20°C was chosen to fit the experimental stiffness curves to fit the Arrhenius type model. Cheung, (1995) showed that if the difference between the temperature to be shifted and reference temperature ($T-T_{ref}$) is less or equal to 20°C the Arrhenius type equation gives the best fit. When ($T-T_{ref}$) is more that 20°C the William-Landel-Ferry (WLF) equation gives a better fit. Therefore since the difference between the temperature to be shifted and the reference temperature is less than 20°C for the tested data, the Arrhenius type equation was applied for determination of shifting factor. The Arrhenius shifting factor is described in equation 7.2 as follows:

$$\log \alpha_t = C \cdot \left(\frac{1}{T} - \frac{1}{T_{ref}} \right) = \log e \cdot \frac{\Delta H}{R} \left(\frac{1}{T} - \frac{1}{T_{ref}} \right) \quad (\text{as 7.2})$$

The frequency where the master curve should be read f_{eq} is defined above as:

$$\log f_{eq} - \log f = \log \alpha_t \quad (\text{as 7.1})$$

Where: = The variables are as previously defined.

The Francken's constant ($C=10920$) was used for the Arrhenius equation. Jenkins (2000) indicated that this constant yielded a good fit for the master curve of Half-Warm Foamed bitumen treated materials, hence it was found to be applicable for this study too. Jenkins (2000) shows that

the use of other constants does not improve the correlation coefficient sufficiently to justify their use. Some variation from the regression line is to be expected, not only from random error influence, but also from the assumption that C and ΔH are independent of temperature. Saygeh, (1967) found this assumption thermodynamically inconsistent as the activation energy can be reduce by some 60% with a 60°K increase in temperature from 253°k.

7.4 STIFFNESS MASTER CURVE MODELS OF BITUMEN EMULSION MIXES

This section presents and discusses the results from frequency sweeps tests on all three emulsion treated mixes. The test is used to determine stiffness modulus master curve of the bituminous treated materials. The summary of the stiffness values in a log-log plot of frequencies versus flexural stiffness for all emulsion mixes are presented in Appendix F. The stiffness modulus repeat test on each beam of bitumen emulsion treated mixes: Mix 4(B-75C-0%), Mix 5(B-75C-1%) and Mix 6(B-75M-0%) are summarized in Table 7.3. This table allows a direct comparison of stiffness values and the trends of the repeat test on two beams at each mix.

Table 7.3: Flexural stiffness modulus for the bitumen emulsion mixes.

Test temp. (deg)	Frequency (Hz)	Flexural stiffness modulus per mix type (MPa)					
		B-75C-0%		B-75C-1%		B-75M-0%	
		Beam D3	Beam D4	Beam D5	Beam D6	Beam C3	Beam C4
5	0.5	2029	2010	2419	2460	1863	2330
	1	2329	2167	2561	2565	1965	2336
	2	2481	2310	2702	2813	2090	2522
	5	2950	2543	2910	3114	2386	2854
	10	3393	2828	3273	3354	2667	3179
10	0.5	1816	1610	1935	2046	1646	1854
	1	1997	1800	2000	2176	1790	2018
	2	2075	1950	2115	2335	1932	2232
	5	2451	2180	2396	2643	2105	2528
	10	2649	2355	2728	2853	2335	2710
15	0.5	1324	1290	1567	1690	1449	1526
	1	1475	1440	1731	1846	1550	1575
	2	1609	1520	1811	1947	1664	1777
	5	1775	1720	1942	2130	1822	1968
	10	1955	1850	2229	2315	2030	2076
20	0.5	1129	1044	1138	1303	1171	1217
	1	1224	1128	1423	1484	1286	1324
	2	1355	1303	1364	1540	1397	1416
	5	1467	1468	1542	1710	1552	1603
	10	1600	1625	1779	1852	1686	1716
25	0.5	1020	916	1059	1108	983	1028
	1	1029	1091	1160	1175	1094	1095
	2	1080	1087	1178	1258	1193	1202
	5	1180	1135	1268	1406	1206	1286
	10	1221	1266	1383	1558	1333	1444

The stiffness results of two beams for each mix Table 7.3 provides similar trends of increasing stiffness as the frequency increase and decreased in stiffness as the temperature increase, although with some variations. At low temperature and high frequencies it is apparent that all mixes experience increasing stiffness behaviour. This can be expected for the visco-elastic materials. However variation in repeatability test might be ascribed by the non homogeneity of the mixture (non-uniform dispersion of the binder) which results into localised weakness of the mixes. The stiffness of the mix is a function of stress and strain value. The strain value in the outer fibres of beam is a function of the beam dimensions and the beam deflection. Therefore imperfection of the specimen resulted from spilling of edges and faces might affect an area of peak deflection hence resulting in variation in stiffness values.

The repeatability results are difficult to be compared directly to account for the variability. But using a cumulative distribution graph of the ratio of the difference between the measured stiffness and the average stiffness of the two beams gives good indication of the variability of the stiffness values for the two repeat test (see Figure 7.6).

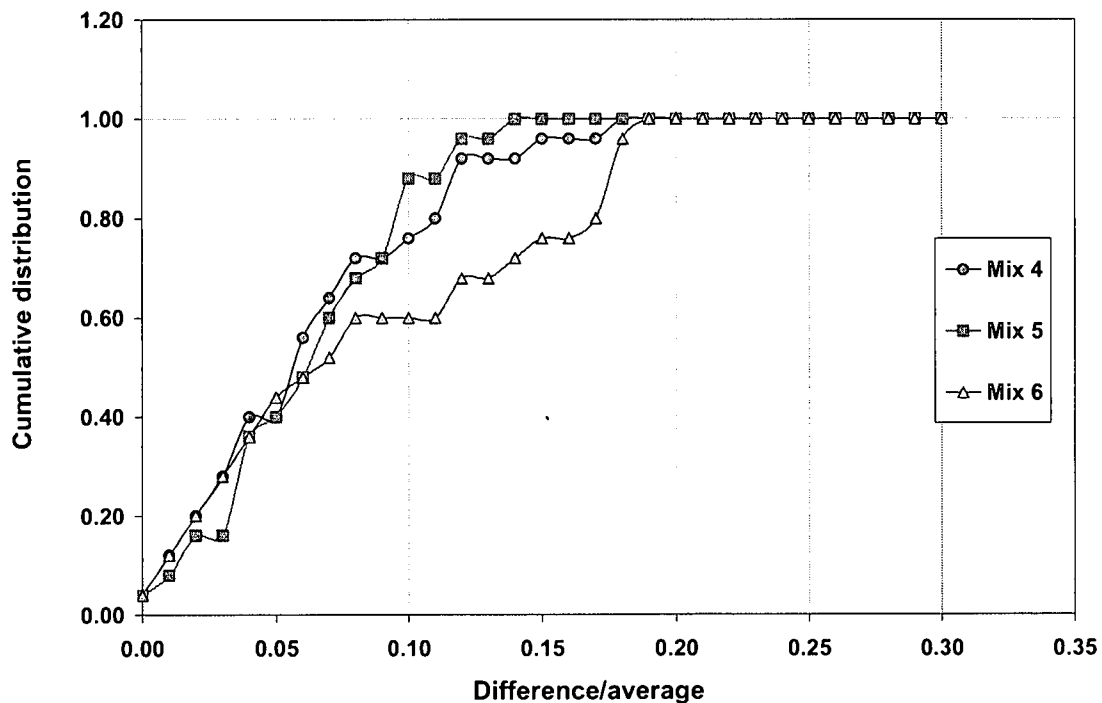


Figure 7.6: Cumulative distribution of variation ratio per mix.

In Figure 7.6 it can be seen that the stiffness values of the two repeat tests for each mix compare fairly well, a low ratio indicates good repeatability. Mix 4(B-75C-0%) and Mix 5(B-75C-1%) show the variation on stiffness values of about 15% for all data points (25). Mix 6(B-75M-0%) stiffness values show the variation of 8% for the 60% of the data points (15) and 18% for the remaining 40% of the data points (10). The variation of each mix show that the stiffness values for the

determination of the stiffness modulus master curve does not result in a significant difference for the purpose of comparison of the mixes stiffness behaviour.

The stiffness modulus master curve using Arrhenius' equation describes the time-temperature dependency for the characterization of the stiffness modulus of the emulsion mixes. The shifted experimental curves for the master curve model of emulsion Mix 4(B-75C-0%), Mix 5(B-75C-1%) and Mix 6(B-75M-0%) at a reference temperature chosen as 20°C are presented in Figure 7.7, 7.8 and 7.9 respectively.

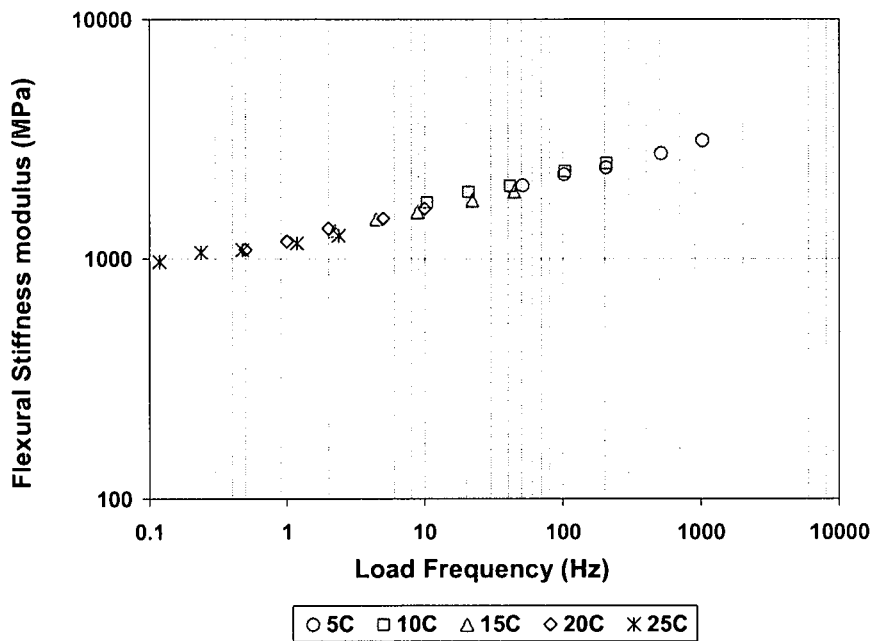


Figure 7.7: Stiffness master curve model for Mix 4(B-75C-0%) at 20°C ref. temperature

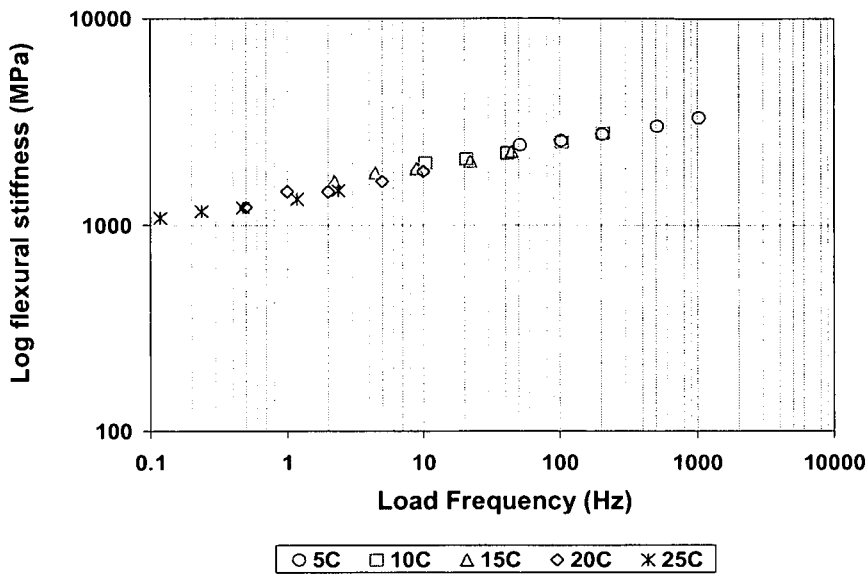


Figure 7.8: Stiffness master curve for Mix 5(B-75C-1%) at 20°C ref. Temperature

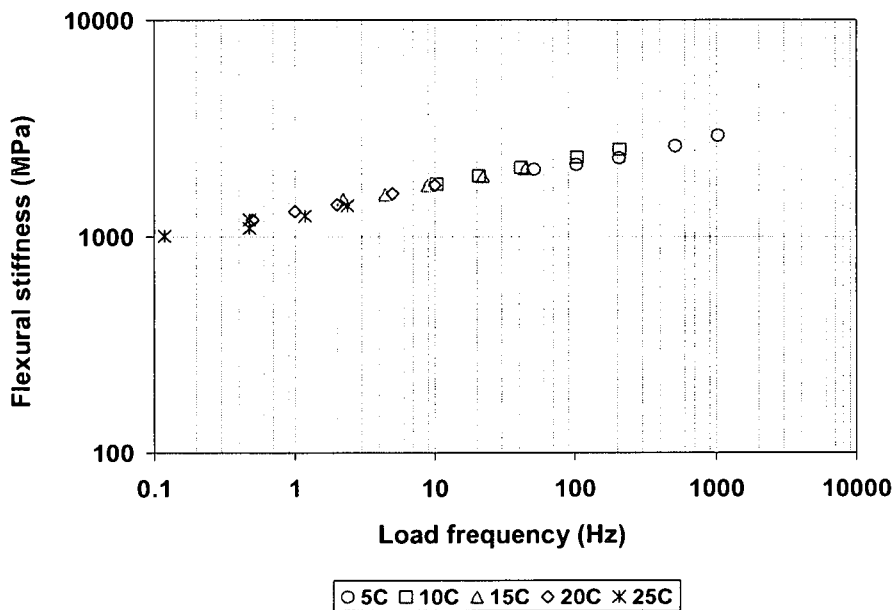


Figure 7.9: Stiffness master curve for Mix 6(B-75M-0%) at 20°C ref. temperature

A stiffness modulus master curve is an increasing function of the reduced frequency tending to an upper limit. The shifted experimental curves as stiffness modulus versus logarithm of reduced frequencies fit the model quite well. This shows that the Arrhenius approach yields satisfactory results in terms of master curve fit. This indicates that the models obtained for these mixes offer a reasonable accurate tool for describing the stiffness characteristics of bituminous mixes at limited testing ranges of frequencies and temperatures.

The superimposition of the master curves of all three bitumen emulsion mixes in the same graph provides an intrinsic comparison of the flexural stiffness behaviour of these mixes, (see Figure 7.10).

In Figure 7.10 it can be seen that a notable shift upwards of the flexural stiffness of Mix 5(B-75C-1%) is evident at all range of reduced frequencies compared to other mixes. Mix 4(B-75C-0%) show low stiffness behaviour compared to Mix 5 and 6. While Mix 6(B-75M-0%) shows an intermediate stiffness characteristics at low load frequency with the other mixes and a similar stiffness as Mix 4 at high load frequencies.

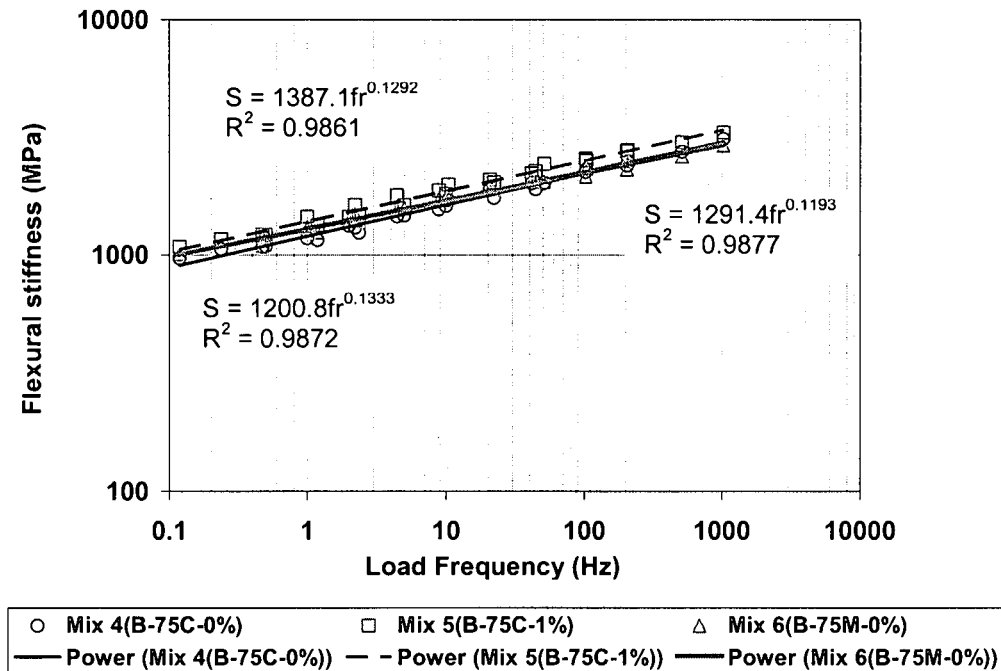


Figure 7.10: Superimposition of emulsion mixes master curves models

The stiffness properties of emulsion mixes, Figure 7.10 can be characterized and compared fairly well in terms of stiffness behaviour from the presented stiffness models. The stiffness values in Table 7.3 indicate that the emulsion mixes exhibit high stiffness characteristics. From Figure 7.10 Mix 4(B-75C-0%) can be characterized as having fairly low stiffness behaviour compared to Mix 5(B-75C-1%) and no significant difference with Mix 6(B-75M-0%). This concurs with the finding of the fatigue performance and strain-at-break properties of these mixes.

7.5 STIFFNESS MASTER CURVE MODELS OF FOAMED BITUMEN MIXES

This section presents and discusses the results of the frequency sweep tests on all three foamed bitumen treated mixes. The summary of the stiffness values on a log-log plot of frequencies versus flexural stiffness for all foamed bitumen mixes are presented in Appendix F.

The stiffness modulus repeat tests of each beam of foamed bitumen treated mixes: Mix 7(B-75C-0%), Mix 8(B-75C-1%) and Mix 9(B-75M-0%) are summarized in Table 7.4 for direct comparison of the repeat beam tests.

Table 7.4: Flexural stiffness modulus of the foamed bitumen mixes.

Test temp. (deg)	Frequency sweep (Hz)	Flexural stiffness modulus per mix type (MPa)					
		C-75C-0%		C-75C-1%		C-75M-0%	
		Beam C3	Beam C4	Beam C2	Beam C4	Beam C3	Beam C4
5	0.5	1822	1788	1725	2017	1423	1448
	1	1937	1905	1750	2028	1573	1493
	2	2130	1970	1872	2079	1601	1584
	5	2333	2234	2029	2157	1714	1672
	10	2477	2430	2106	2291	1758	1762
10	0.5	1607	1682	1451	1692	1210	1261
	1	1741	1786	1533	1756	1324	1348
	2	1805	1895	1537	1811	1374	1422
	5	2000	2013	1573	1933	1538	1510
	10	2194	2249	1585	1973	1570	1594
15	0.5	1251	1392	1260	1373	1069	1054
	1	1381	1436	1335	1469	1154	1100
	2	1532	1536	1387	1501	1180	1144
	5	1650	1669	1421	1605	1232	1314
	10	1751	1901	1497	1662	1300	1320
20	0.5	1082	1174	1087	1220	984	977
	1	1181	1267	1183	1284	1041	957
	2	1256	1358	1190	1343	950	989
	5	1345	1460	1238	1430	1099	1053
	10	1445	1555	1265	1479	1156	1061
25	0.5	999	1053	957	1000	919	781
	1	1039	1072	1012	1089	937	859
	2	1077	1136	1054	1043	904	887
	5	1198	1087	1065	1062	888	871
	10	1289	1151	1128	1110	939	866

In Table 7.4 it can be seen that the foam mixes show dependency of temperature and rate of loading. By increasing loading rate and keeping other variables constant during testing, the stiffness modulus of the mixes increases. By increasing the temperature of the mixes the stiffness modulus of the mixes reduces. This is consistent with the behaviour of HMA.

The variability of the repeat tests on foam mixes has been expressed as a ratio of the difference between the measured stiffness in the two repeat tests and the average stiffness of the two

beams. For easy assessment and comparison of the mix repeat test as well as other mix types (see Figure 7.11).

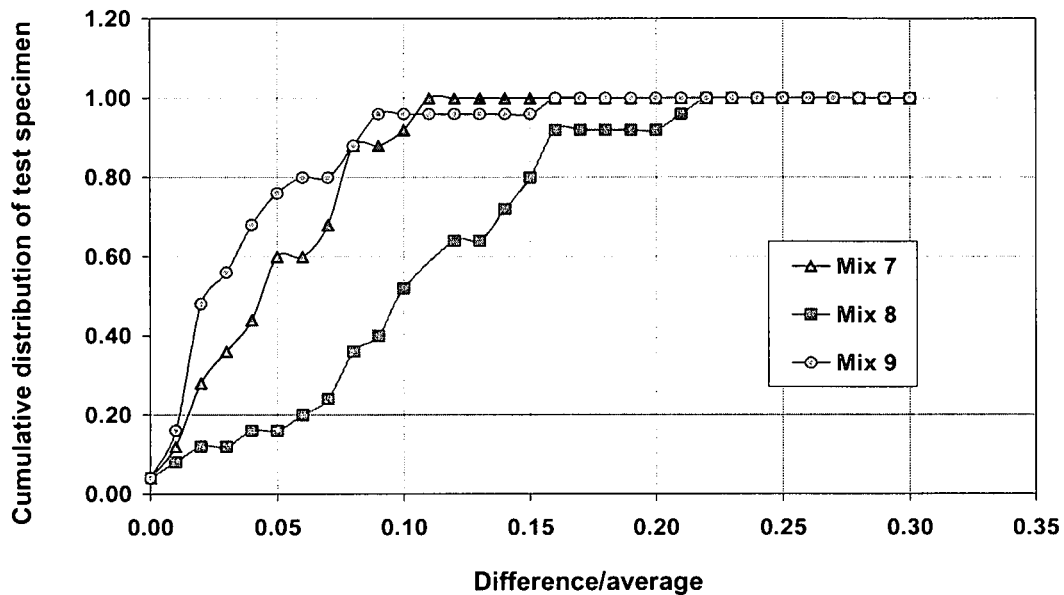


Figure 7.11: Cumulative distribution of variation ratio per mix.

The stiffness values of the two repeat tests for each mix compare fairly well. As low ratio indicates good repeatability Mix 7(C-75C-0%) and Mix 9(C-75M-1%) shows less variation on stiffness values. Mix 7 shows 11% variation on all (25) data points and Mix 9 show 8% variation of 98% of the data points. However, Mix 8 shows a fairly high variation of 15% for 95% data points. This indicates that apart from improving cohesive strength in the mix, the additional of cement makes the mixture also more sensitive to loading and temperature change. The variation of the stiffness values of the repeat tests of each mix, as noted for the emulsion mixes, are not significant for averaging repeat values in order to determine the stiffness modulus master curve of the mix.

The shifted experimental curves for the master curve models for foamed bitumen Mix 7(C-75C-0%), Mix 8(C-75C-1%) and Mix 9((C-75M-0%) at a reference temperature chosen as 20°C are presented in Figure 7.12, 7.13 and 7.14 respectively.

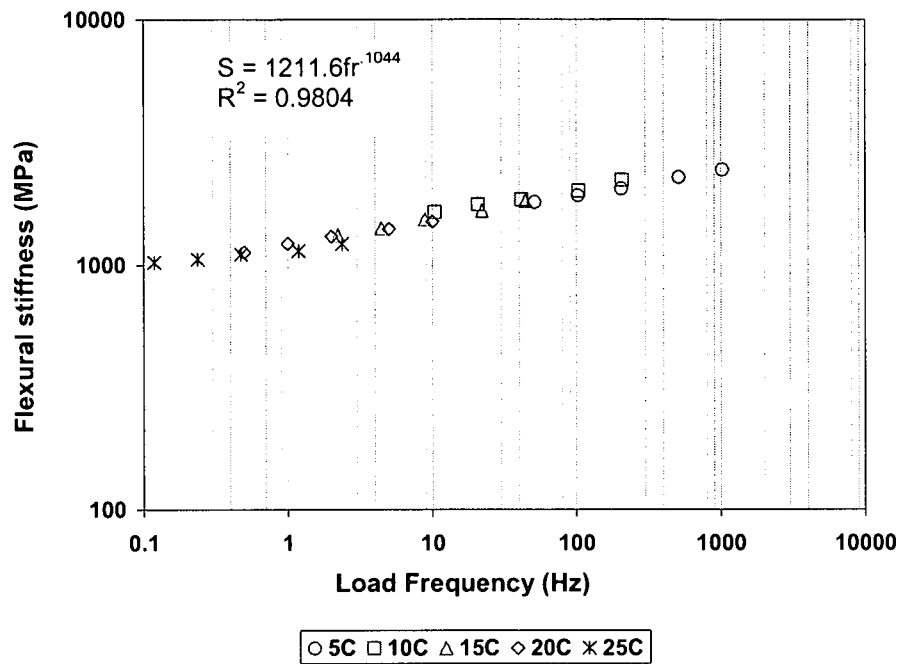


Figure 7.12: Stiffness master curve for Mix 7(B-75C-0%) at 20°C ref. temperature

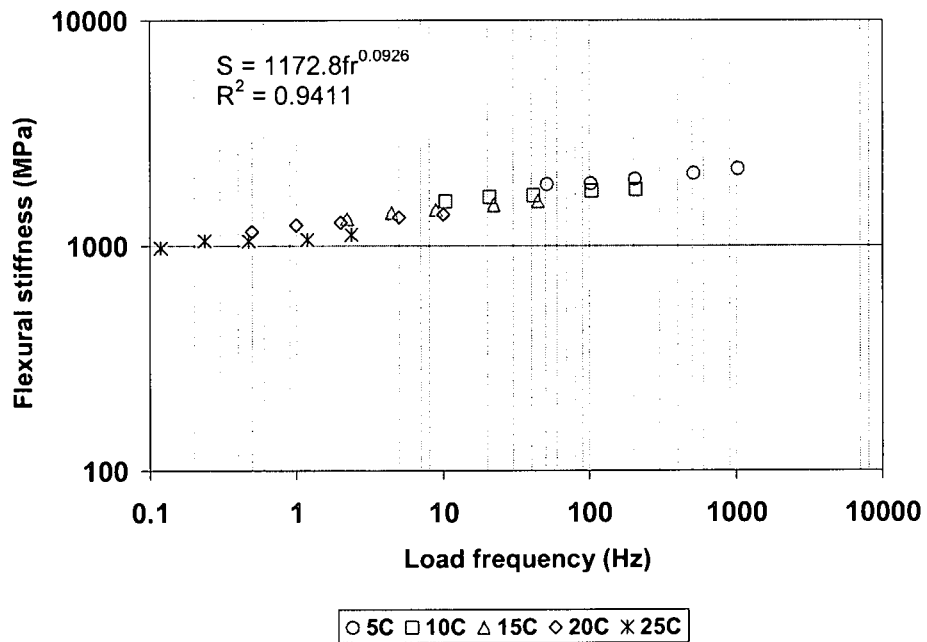


Figure 7.13: Stiffness master curve for Mix 8(B-75C-0%) at 20°C ref. temperature

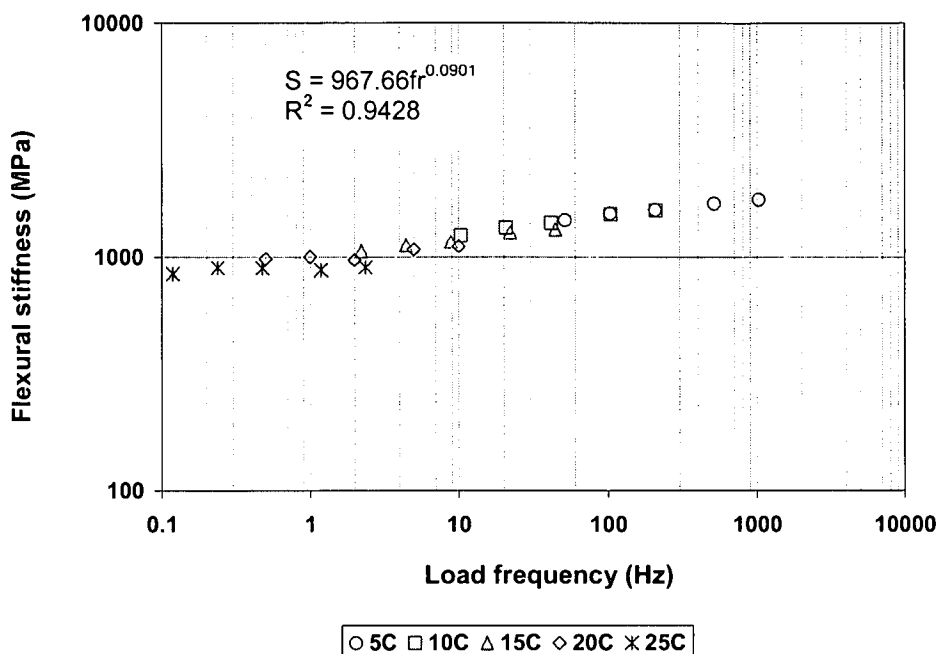


Figure 7.14: Stiffness modulus master curve for Mix 9(C-75C-0%) at 20°C ref. temperature

The shifted experimental curves of average stiffness modulus versus logarithm of reduced frequencies for the selected mixes fit the models quite well. However, the variability at high temperature indicates that as temperature increases the binder softens and the cohesive strength of the mix decreases, hence leading to the complex behaviour of stiffness reduction in the mixes. The models obtained for the foamed bitumen mixes offer a reasonable accurate tool for describing the stiffness characteristics of cold mixes at a limited testing range of frequencies and temperature. In that regard, the Arrhenius approach yields satisfactory results in terms of stiffness master curve fit of foamed bitumen mixes too.

The superimposition of the master curves of all three foamed bitumen mixes in the same graph provides intrinsic comparisons of the flexural stiffness behaviour of these mixes, (see Figure 7.15). There is a notable shift in the flexural stiffness of Mix 7 compared to Mix 8 and Mix 9. Low stiffness characterisation of Mix 8 might be due to influence by addition of active filler which improves the cohesive strength of the mixes and resulting flexibility. However, the decrease in flexural stiffness of Mix 9 with high percentage of RAP might have been caused by binder interaction (new and old) or high percentage of RAP. The respect still needs further actual fact needs investigation.

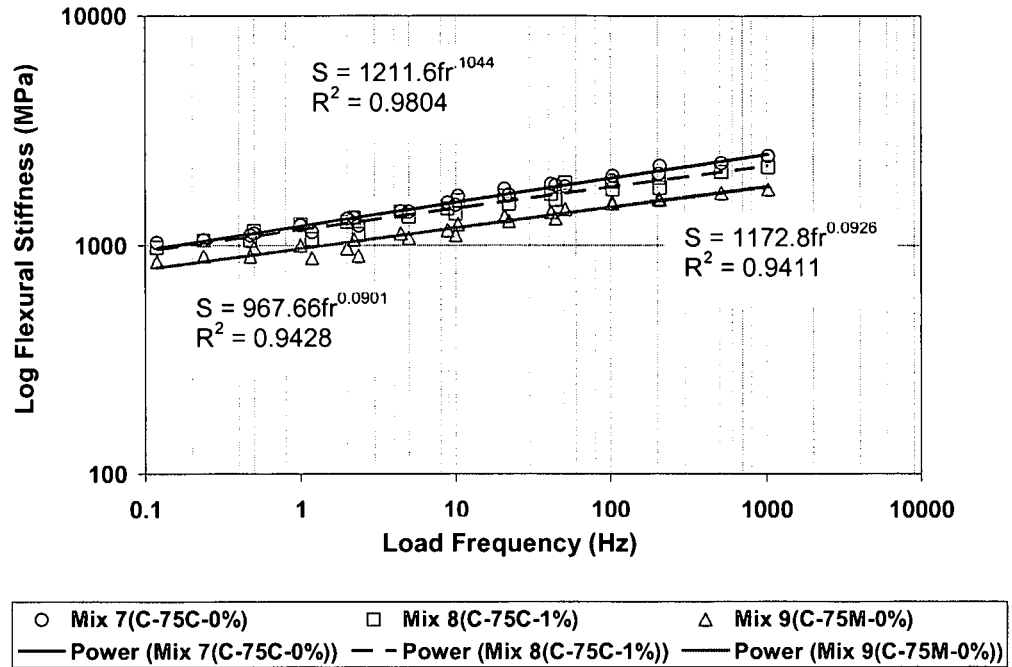


Figure 7.15: Stiffness characteristics of foam mixes at various frequencies and temperature

7.6 COMPARISON OF STIFFNESS MASTER CURVE FOR BITUMEN EMULSION AND FOAMED BITUMEN MIXES

The superimposition of the stiffness master curves of selected mixes (emulsion and foam) provides intrinsic comparison of these mixes and their flexural stiffness characteristics. The comparisons of these mixes are based on the similarity of the selected mix blend treated with either bitumen emulsion or foamed bitumen. Figure 7.16 superimpose the flexural stiffness models of Mix 4 (emulsion) and Mix 7 (foam) without cement. Figure 7.17 compares Mix 5(emulsion) and Mix 8(foam) with addition of 1% cement and Figure 7.18 compare Mix 6(emulsion) and Mix 9(foam) with high percentage of RAP with no cement.

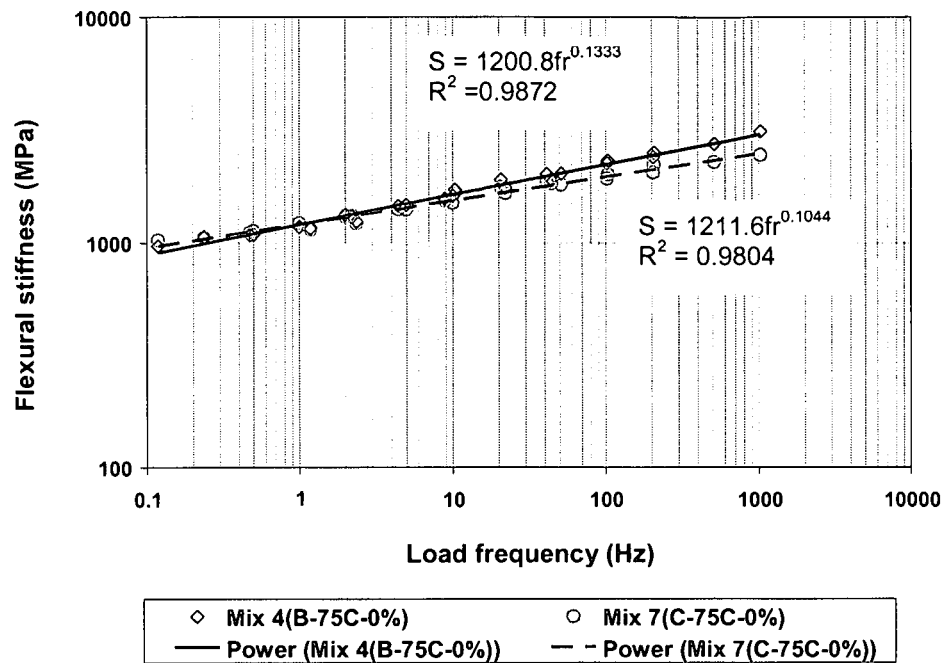


Figure 7.16: Superimposition of stiffness master curves for Mix 4(B-75C-0%) and Mix 7(C-75C-0%)

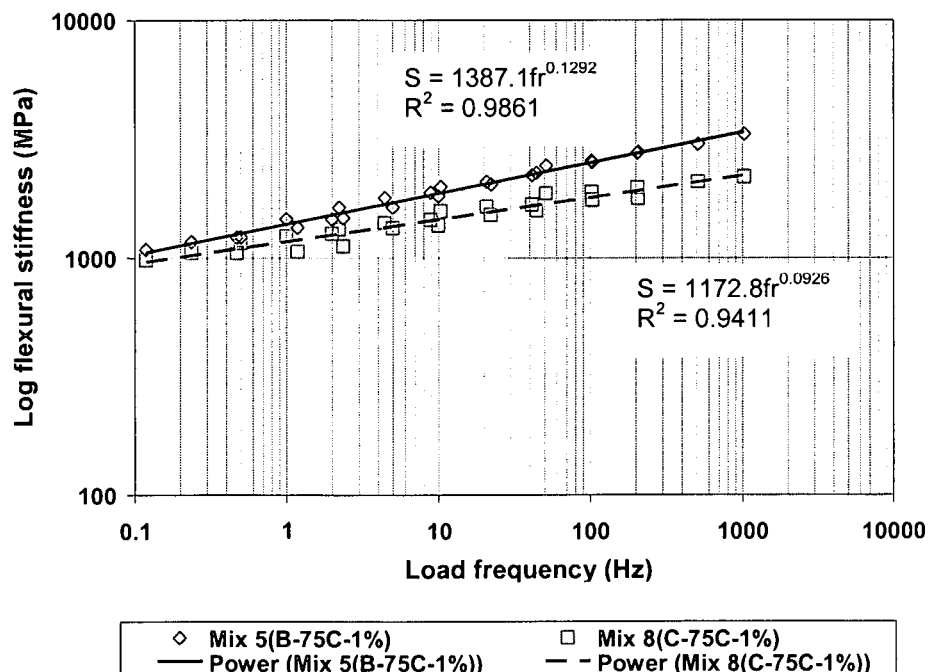


Figure 7.17: Superimposition of stiffness master curves for Mix 5(B-75C-1%) and Mix 8(C-75C-1%)

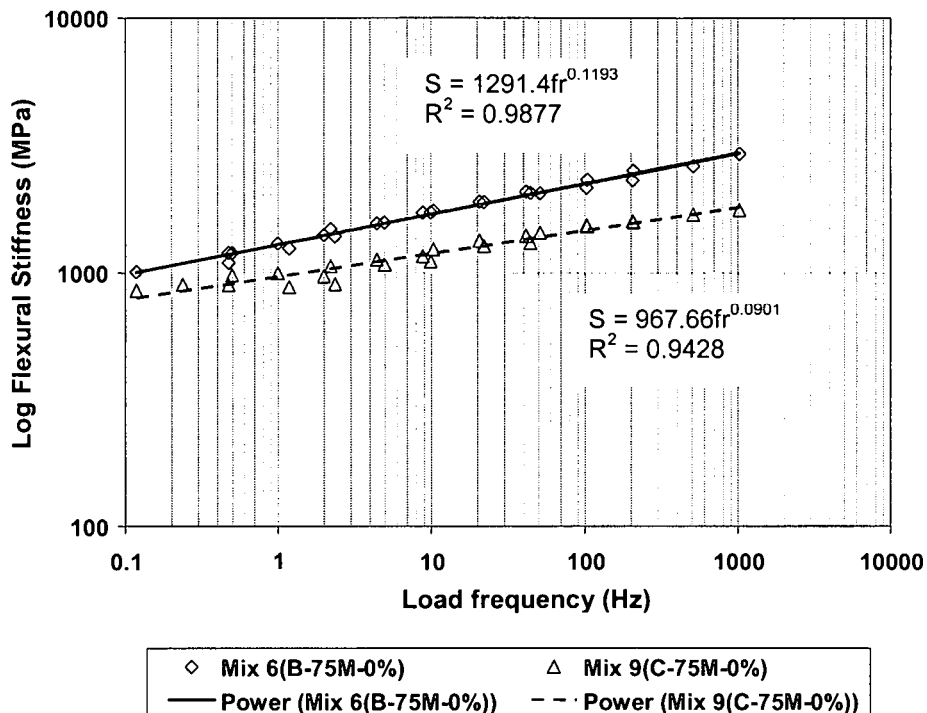


Figure 7.18: Superimposition of stiffness master curves for Mix 6(B-75M-0%) and Mix 9(C-75M-0%)

The flexural stiffness of emulsion and foamed bitumen mixes shows a dependency on temperature and rate of loading. By increasing the loading and keeping other variable constant during the test, the stiffness increases. By increasing the temperature of the mixes the stiffness modulus of the mixes reduces. This is consistent with the behaviour of HMA, however the slope of the master curve for cold mix is significantly flatter than for HMA.

The relevance of the differences in flexural stiffness shown by the master curves is apparent, particularly considering the fatigue resistance under extended loading time, i.e. low and medium frequencies and high temperatures. A pavement structure with cold mix (thick layer) under traffic loading indicates that as the stiffness of the mixes increase the fatigue life decreases. The strain loading however can be reduced significantly. Therefore, the overall performance of the mixture improves. However, for thin layers (not commonly for cold mixes) as the stiffness increases the fatigue life decreases and strain loading increases. Therefore so the overall performance of the mixture becomes poorer.

The ranking of emulsion and foamed bitumen mixes in terms of flexural stiffness indicates that the emulsion mixes have a higher stiffness than foamed bitumen mixes. This needs to be accounted for in the analysis of pavement life. Depending on the pavement layer support conditions,

emulsion mixes might carry higher traffic loads than foamed bitumen mixes. However, at low loading times foamed bitumen mixes might have longer fatigue lives than emulsion mixes. However, this becomes apparent during pavement analysis.

The flexural stiffness of the selected mixes (bitumen emulsion and foamed bitumen) can be characterized by the following comparison models (Table 7.5 and Table 7.6). This model might also be used to estimate flexural stiffness modulus of the materials based on Arrhenius type equation at various temperature and loading frequencies.

Table 7.5: Models for estimation of stiffness modulus of bitumen emulsion mixes

Mix Type	Stiffness Models	R ²
Mix 4 (B-75C-0%)	$S_i = 1200.8fr^{0.1333}$	0.99
Mix 5 (B-75C-1%)	$S_i = 1387.1fr^{0.1292}$	0.99
Mix 6 (B-75M-0%)	$S_i = 1291.4fr^{0.1193}$	0.99

Table 7.6 Models for estimation of stiffness modulus of foamed bitumen mixes

Mix Type	Stiffness Models*	R ²
Mix 7 (C-75C-0%)	$S_i = 1211.6fr^{0.1044}$	0.99
Mix 8 (C-75C-1%)	$S_i = 1172.8fr^{0.0926}$	0.94
Mix 9 (C-75M-0%)	$S_i = 967.66fr^{0.0901}$	0.94

* S_i = initial flexural stiffness (MPa), fr = load frequency (Hz) and a, n = experimental parameters.

The Laboratory Central des Point et Chaussees (LCPC) conducted stiffness modulus master curve tests on fine graded (maximum of 14mm) and a medium graded (maximum of 20mm) mixes treated with different binder, i.e. bitumen (GB) and foamed bitumen (GM). The test were normalised at 10°C, (Brosseau et al., 1997). Jenkins (2000) conducted a test on stiffness modulus master curve on Half-warm foamed bitumen mixes. The superimposition of these mixes (LCPC), HW-FBT and Mix 4(emulsion) and Mix 7(foam) master curves provide intrinsic comparison of the stiffness properties these mixes Figure 7.19.

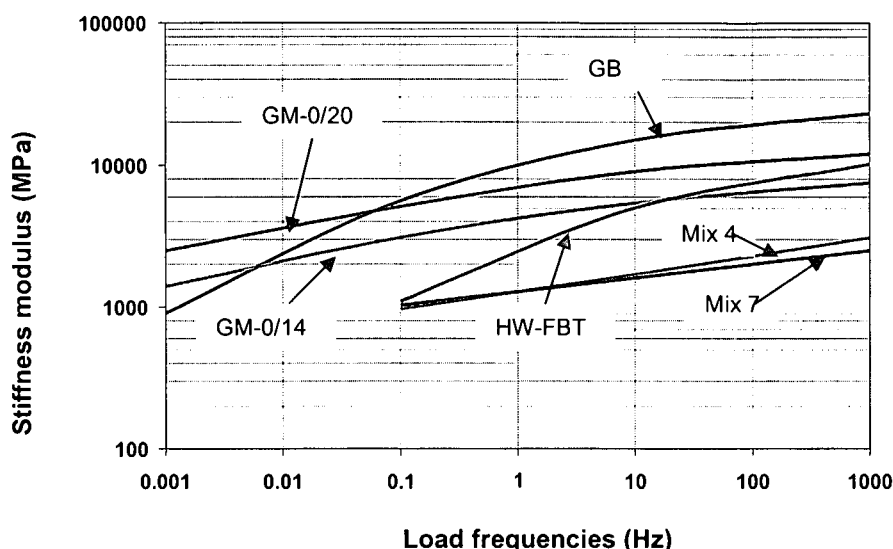


Figure 7.19: Superimposition of stiffness modulus master curve for LCPC (GB and GM), M4 and M7

The stiffness modulus master curves for limestone blends Mix 4 (B-75C-0%) and Mix 7 (C-75C-0%) are compared with LCPC Mix GB (HMA) and Mix GM (foam), Figure 7.19. Mix 4 and 7 shows significantly lower stiffness modulus values. The binder content for hot asphalt mix (GB) was 4% and foam mix (GM) was 3.5%; the mineral aggregates used were graded crushed quartz. The binder content of these mixes (bitumen emulsion and foamed bitumen) are similar, but the quality of GM mineral aggregates used might contribute the significant shift on the increase of the stiffness master curve compared to blend of mineral aggregates (limestone and RAP) used in Mix 4 and 7. However the slope of the master curves for both GM's Mix 4 (B-75C-0%) and Mix 7 (C-75C-0%) found to be similar and flat compared to bitumen Mix GB and HW-FBT. This endorses the perception that cold mixes provide stiffness that are less susceptible to change in loading frequency than hot mix asphalt.

7.7 CONCLUSIONS

Several laboratory and field tests are used to determine the stiffness behaviour of bituminous mixes. In this study 4PB test was used to determine flexural stiffness of selected mixes. Amongst other models used for the determination of stiffness modulus master curve the, Arrhenius type equation was selected with Francken's shift-constant to construct the master curves by applying the time-temperature superimposition principle. The study of the flexural stiffness properties of these mixes (bitumen emulsion and foamed bitumen) has led to the following conclusion being drawn:

- The flexural stiffness of bitumen emulsion and foamed bitumen mixes shows a dependency of temperature and rate of loading. By increasing the loading and keeping other variables constant during the test, the stiffness increases. By increasing the temperature of the mixes the stiffness modulus of the mixes reduces. This is consistent with the behaviour of HMA, however the slope of the master curve for cold mix is significantly flatter than for HMA.

The ranking of emulsion and foamed bitumen mixes in terms of flexural stiffness indicates that emulsion mixes have a higher stiffness than foamed mixes. This needs to be accounted for in the design of pavement life. Depending on the pavement layer support condition emulsion mixes might carry higher traffic loads compared to foamed bitumen mixes, however at low loading foamed bitumen mixes may have a longer fatigue life than emulsion mixes. However these become apparent during pavement analysis.

- The flexural stiffness determined by four point bending testing beam seem to provide a fairly high variation (15-20%) in repeat tests. This could be caused by factors such as mixture variables (non-homogeneous) and condition of beam specimens (imperfection due to spalling of beam edges and faces during sawing) and interpretation of results. However, variability is accounted for by the repeat test on two beams which increase the statistical significance of the models.
- Characterization of the selected mixes (emulsion or foamed bitumen) using the Arrhenius type equation at 20°C reference temperature provides models which fit fairly well to the shifted experimental curves determined at different frequencies and temperature. The models obtained in the selected mixes offers a reasonable accurate tool for describing stiffness characteristics of emulsion and foamed bitumen mixes at a limited testing range of frequencies and temperature.
- The Arrhenius type approach yields satisfactory results in terms of stiffness master curve fit for both mixes. Therefore comparison with other models was not necessary in this study.
- The stiffness modulus for selected mixes, Mix 4(B-75C-0%), Mix 7(C-75C-0%), and LCPC (GM's) are comparable by showing similar slope and flat relative to asphalt mixes and Half-warm foam mixes. However there is a notable shift of increase in stiffness modulus for the LCPC mixes (GM's) compared to Mix 4(B-75C-0%) and Mix 7(C-75C-0%). This could be due to the high quality virgin materials treated with foamed bitumen that produce a mix with a higher stiffness modulus compared to the blend with millings asphalt RAP. This might affect the fatigue performance of these mixes in a pavement layer too.

7.5 REFERENCES

- AIREY G.D., 1995. **Fatigue testing of asphalt mixtures using the laboratory third-point loading fatigue testing system**. Masters Dissertation, University of Pretoria, Pretoria, South Africa.
- BROSSEAUD Y, GRAMSAMMER J-C, KERZREHO J-P, GOACOLOU H, LE BOURLOT F., 1997. **Expérimentation (première partie) de la Grave-Mousse® sur le manège de fatigue**. RGRA No. 752 du LCPC, June pp 66.
- CHEBA G.R., KIM Y.R., SCHAPERLY R.A., WITCZAK M.W., and BONAQUIST R., 2002. **Time-temperature superposition for asphalt concrete mixtures with growing damage in tension state**, Asphalt Paving Technology, Association of Asphalt Paving Technologists, Minneapolis, MN, U.S.A.
- CHEUNG C.Y., 1995. **Mechanical behaviour of bitumens and bituminous mixes**, Ph.D. Dissertation; University of Cambridge, Engineering Department, Cambridge, U.K.
- EPPE A., HARVEY J.T, KIM Y.R and ROUQUE R,. 2000. **Structural requirements of bituminous paving mixtures**. Millennium papers, Transportation Research Records.
- FRANCKEN L., 1977. **Composite materials technology “asphalt systems”**. Bulletin Centre de Recherches Routieres, Bruxelles.
- FRANCKEN L. and CLAUWAERT C., 1988. **Characterization and Structural Assessment of Bound Materials for Flexible Road Structures**, Proceedings 6th International Conference on the Structural Design of Asphalt Pavements, Ann Arbor, 1987; University of Michigan, pp 130-144, Ann Arbor, MI, USA.
- FRITZ J.J and CRAWFORD A., 1999. **Comparison of asphalt stiffness values obtained from different test methods**. Proceedings of the 7th International Conference on Asphalt Pavements for South Africa.
- GERMANN F.P., and LYTTON R.L., 1979. **methodology for predicting the reflection cracking life of asphalt concrete overlays**. Report No. TTI-2-8-75-207-5, Texas Transportation Institute of the Texas A&M University, College Station.

GOODRICH J.L., 1991. **Asphalt binder rheology, asphalt concrete rheology and asphalt concrete mix properties**. Proceedings, Association of Asphalt Paving Technology, Vol 60, pp 80-120.

IPC (Industrial Process Control Ltd), 1998. **Beam Fatigue Apparatus**. Reference Manual. Boronia, Australia.

JACOBS M.M.J., 1995. **Cracks growth in asphalt mixes**. PhD Thesis, Delft University of Technology, Netherlands.

JENKINS J.K., 2000. **Mix design consideration for cold and half-warm bituminous mixes with emphasis on foamed bitumen**. PhD Dissertation, University of Stellenbosch, South Africa.

LYTTON R.L., UZAN J., FERNANDO E.M., ROQUE R., HILTUNEN D. and STOFFELS S.M., 1993. **Development and validation of performance prediction models and specifications for asphalt binders and paving mixes**, SHRP Report A-357, SHRP/NRC, Washington DC, USA

MEDANI T.O. and HUURMAN M., 2003. **Constructing the stiffness master curves for asphaltic mixes**, Report 7-10-127-3, Faculty of Civil Engineering and Geosciences, Delft University of Technology.

MEDANI T.O., HUURMAN M and MOLENAAR A.A.A, 2003a. **On the computation of master curves for bituminous mixes**. Faculty of Civil Engineering and Geosciences, Delft University of Technology.

MIHAI M. and DAVID A., 1996. **Time-temperature dependency of asphalt binders-an improved model**. Proceedings of the Association of Asphalt Paving Technologists. Vol. 63

PELLINEN T.K., 1998. **The assessment of validity of using different shifting equations to construct a master curve of HMA**. University of Maryland, Department of Civil Engineering at College Park, MD, USA, 1998.

PELLINEN T.K., and WITCZAK M.W., **Stress dependent master curve construction for dynamic (complex) modulus**. Annual Meeting Association of Asphalt Paving Technologists, Colorado Springs, Colorado, USA,

SAYEGH G., 1967. **Visco-elastic properties of bituminous mixtures**. Proceedings of the 2nd International Conference on the Structural Design of Asphalt Pavements. Ann Arbor. MI, USA, University of Michigan, pp 743-755, Ann Arbor, MI USA.

WILLIAMS M.L., LANDEL R.F. and FERRY J.D., 1955. **The temperature dependence of relaxation mechanism in amorphous polymers and other glass forming liquids.** Journal of ACS, Volume 77, pp 370.

CHAPTER 8

8. CONCLUSIONS AND RECOMMENDATIONS FOR FUTURE WORK

8.1 INTRODUCTION

In this final chapter, the most important conclusions of this thesis are summarized. These conclusions are divided into the study of selected mixes with relevance to laboratory specimen preparations and testing procedures, fatigue, strain-at-break and flexural stiffness properties for characterization of the mix performance. In additions, where applicable the recommendations for the future research that is deemed necessary are provided in the findings of this thesis.

The summarized conclusions focus on the original primary objective of the study which is the characterization of fatigue performance of selected materials, blended at two different proportions. Either the limestone or RAP is the dominant portion (ie.75% content) with one percent active filler (1% cement) being added to some of the 75% limestone blends. The blends were treated with either bitumen emulsion or foamed bitumen. This objective was achieved through laboratory testing using a four point beam bending apparatus. The advantages of using this apparatus is that the similar same specimen and testing procedures apply for fatigue, strain-at-break and flexural stiffness testing, which saves time and amount of materials required to produce different specimens.

8.2 SPECIMEN PREPARATION AND TESTING PROCEDURES

In the study of the fatigue performance of the mixes, specimen preparation (i.e. mixing, compaction, curing and cutting) found to play a significant role in the prediction of the testing results. The sensitivity of air flow on the servo-pneumatic controlled system and the CDAS operation determined the quality of the captured test data. The salient features of these aspects are outlined as follows:

- The moisture content and filler percentage during mixing and compaction plays a vital role in the behaviour of the bitumen emulsion and foamed bitumen mixes. The moisture acts as a densification agent of individual particles in the mix after breaking of the bitumen emulsion and aids in the bitumen dispersion of foamed bitumen over the filler during mixing. This results in increasing cohesive strength of the mixes. The mixes with 75% limestone had a high affinity for water compared to the mix with 75% milled asphalt. The addition of moisture to 70% of OMC during mixing produces a fairly dry mix in case of foamed bitumen, which results in less workability for proper compaction. This had to be increased to 80% of OMC during mixing for

foamed bitumen mixes. For the emulsion mixes 70% of OMC was seen to produce fairly wet mixes resulting in a proposed decrease to 65% of OMC. This is due to fact bitumen in emulsion acts more like a compaction aid during compaction than the foamed bitumen.

- The addition of active filler (cement) improves the dispersion of foamed bitumen and breaking of bitumen emulsion, which is an advantage for the mixes. In such cases the addition of cement should be done in conjunction with emulsion or foamed bitumen to ensure the achievement of the role of cement in the mixes.
- The mixing technique utilized to agitate the aggregates during the application of foamed bitumen has a significant influence on the quality of the mix. However the twin-shaft pugmill mixer used in this laboratory research frequently got stuck by larger aggregates resulting in wasting of the mixes. Frequent mechanical work (repair) was therefore required, to keep it into good working order. It is proposed that the pugmilling mixes used be improved in order to prevent this problem in the future.
- The influence of compaction level and technique in the mix behaviour is significant. The use of a laboratory steel-wheel roller with both static and vibration action for compaction of the emulsion or foamed bitumen mixes was found to provide sufficient energy to compress measured materials in a slab mould (frames). The compaction level applied for emulsion mixes was 50-60 passes and 60-70 passes for foam mixes. For each 10 of the passes were vibratory. These passes were able to achieve a compaction level in excess of the target density of 98% MDD.
- The cutting technique utilized to produce and shape beam faces play a significant role in the condition and quality of beams. The materials treated with emulsion or foamed bitumen is too weak for wet cutting and therefore dry cutting is required. However this method produces excessive dust which is health hazardous and therefore needs extra attention. The normal laboratory saw cutter (fixed motor and sliding table) found to produce inferior quality beams and requires certain modifications. It is suggested, that an investigation into the appropriate laboratory saw cutter for cold bitumen treated mixes and dust prevention are conducted.
- The beam conditions and dimensions play a vital role in the quality and variability of the test results. The non-homogeneity of the cold mixes and imperfections of the beams results in spalling of the edges and faces of beam specimen during the sawing process. This aspect (spalling) needs to be addressed to ensure better results. The appropriate measure was found to be increasing the excess materials of the beam by increasing the thickness of the slab to 70mm instead of the current thickness of 60mm.
- The quality of the acquired data during testing relies on the smooth operation of the servo-pneumatic controlled system or load cell. Condensation in the air supplied at low temperature

results in excessive water in the pipes, which hinders the air flow. Icing up of this condensation water may result in interruption in the air supply and jumping of the actuator or causing a weak stroke. This causes damage to the beam specimen and consequently affects the captured data. The process of filtering supplied air to avoid excessive water in the system is required. Modifications were applied to the system to account for this problem by addition of extra filters and a heating element to the testing equipment, which is explained in section 4.32 of this Thesis.

- The increase or decrease of the test temperature affects the performance of the mixes. A test temperature of 5°C is prone to quick increase when opening the door of the climate chamber, especially during the summer period. This requires some improvement of the chamber by providing a suspended split curtain at the door, which will allow working with BFA while preventing high exchange of air in to and out of the climate chamber.

8.3 FATIGUE PROPERTIES

- The selected material blends treated with either bitumen emulsion or foamed bitumen under displacement control loading at selected loading times (frequency) and temperatures show that the fatigue life is dependent on the loading rate. On a log-log plot, linear functions are obtained, as is the case for many HMA mixes. The different blends and binder (emulsion and foam) provide fatigue lines that appear to be parallel except for the blend of 75% limestone with no cement. These blends show that there is no difference in fatigue performance at higher strain levels. However a significant shift is noted for the foamed bitumen mixes with active filler. This might be due to improved dispersion of the foamed bitumen due to the active filler, which results in an increase in the cohesive strength of the mix and consequently of the fatigue performance.
- The blends with the higher percentage of RAP (75%) treated with foamed bitumen exhibit a good fatigue performance compared to the emulsion mixes. However they show poor performance compared to the blends with a high percentage of limestone. When emulsion or foamed bitumen is used for the treatment of the mixes with the higher percentage of RAP lower residual bitumen content is applied to the mix. So whether the difference of performance of the mixes with high or low RAP is due to the adhesion properties of the new binder to the old existing asphalt or the residual fresh binder content is not apparent.
- Although HMA fatigue guideline can be used for the characterization and comparison of fatigue performance of the cold bituminous mixes, it does not provide a better indication of the cold mix performance in pavement layer. Because cold mixes are applied in thicker layers than HMA, It indicates that the need for specific fatigue guidelines for cold mixes is apparent.

- The comparisons of fatigue performance of ferricrete mixes with sand mix or limestone blends, Mix 5(B-75C-1%) and Mix 8(C-75C-1%) provide an insight in the fatigue behaviour of the cold mixes. The significant difference in fatigue life of ferricrete mixes compared with sand mix or limestone blends, Mix 5 and Mix 8 is unexpected. However extrapolation of fatigue model based on HVS testing. The decrease in fatigue life of the sand mix compared to limestone blends Mix 5(B-75C-1%) and Mix 8(C-75C-1%) is expected. This endorses that high quality materials used in cold mixes might produce mixtures with good fatigue resistance compared to inferior materials. Therefore, optimum design of inferior quality materials might produce equally excellent mixture as high quality virgin materials. However, the use of such type of materials will depend on the type of load that the pavement needs to carry.

8.4 STRAIN-AT-BREAK PROPERTIES

- The strain-at-break properties have been shown in relation to variables such as binder, active filler, and mineral aggregates. The results indicate that the mixes with high binder content have increasing strain-at-break values. However, emulsion mixes with addition of cement do not subscribe to this trend, which is unexpected. The mix with high addition of RAP shows a reduction in strain-at-break properties, possibly as a result of reduced “fresh” binder content being applied to the mixes. It is essential, therefore, for strength and flexural parameters to be balanced and optimized in the mix design through laboratory testing to achieve the maximum load spread and fatigue resistance in the pavement layer.
- The strain-at-break test using monotonic loading and has been considered as a measure of the “flexibility” of the cold mixes. However, strain-at-break properties of emulsion mixes show significant differences compared to the foamed bitumen mixes. The emulsion mixes with no cement (Mix 4(B-75C-0%)) have shown to be 47 percent more flexible compared to similar mixes with one percent cement (Mix 5(B-75C-1%)). The opposite is the for the foam mixes; the mix with one percent cement (Mix 8(C-74C-1%)) has shown to be 37 percent more flexible than the similar mix with no cement Mix 8(C-75C-1%). The mixes with a high percentage of asphalt millings (RAP) show that when treated with foamed bitumen the mix is 31 percent more flexible compared to the similar mix treated with bitumen emulsion.
- The anomalies in strain-at-break properties of the selected mixes indicate that the strain-at-break does not accurately reflect the fatigue properties of cold mixes. Therefore it cannot be used independently to characterize the mix type fatigue life for mix design purposes. Therefore, the test protocol and loading rate needs further development or adjustment before it can be considered to provide a meaningful relationship with fatigue life of the cold mixes.
- The comparison of the strain-at-break properties of the selected mixes (bitumen emulsion and foamed bitumen) with the results of past research shows a significant difference at the same binder or cement content. This shows that standardization of strain at break test in terms of

specimen preparation, such as mixing, compaction, cutting and cutting, and methods of testing and interpretation of results is of paramount importance and requires more attention.

8.5 RECOMMENDATION FOR THE FUTURE WORK

- This study has shown that the manner in which beam specimens for cold mixes are prepared and tested influence the characterization of fatigue, flexibility and flexural stiffness properties of the mixes to a greater extent. This makes the method of specimen preparation and the operation of the servo-pneumatic controlled BFA an important consideration. The modification of the saw cutting machine, dust prevention and addition of the filters and a heating element to the air supply system is an essential for the reliability of the test results in the future research.
- In conjunction with the modification in the specimen preparation and testing, the slab and wheel roller compaction should be standardised as beam production method and the thickness of the slab mould should be increase to 70mm for production of better beams in the future research.
- The behaviour of emulsion mixes with 75% limestone show an increase in flexural stiffness as strain decreases. This was unexpected for the fatigue testing of visco-elastic materials. However, the combination of mixture variability, test conditions, and sensitivity of equipment might contribute to this behaviour, but further investigations are recommended.
- The strain-at-break is not a standard test. The study has shown that strain-at-break properties of the selected materials have significant differences which do not reflect the fatigue properties of the mixes. This indicates that the test protocol needs further development or adjustment before it can be considered to provide a reliable link to the fatigue performance of cold mixes.
- When cold mixes (bitumen emulsion or foamed bitumen) are used for the treatment of the mixes with high percentages of milled asphalts (RAP) a lower percentage of residual bitumen is applied to the mix. However, whether the difference in fatigue performance of the mixes with a high or low percentage of the RAP is due to different blending ratio of virgin aggregates and milled existing asphalt or the different residual binder contents cannot be clearly discerned from this study. The influence of the binder type on binder adhesion to RAP or crushed aggregates appears to play a significant role in this phenomenon, but further investigation in this aspect is recommended.
- Fatigue cracking on four point beam is influenced by the test temperature. Testing at 5°C provide high possibility of beam failure at the area with high uniform stress concentration (central section of the test beam). However shift factor to relate laboratory fatigue life to the field response investigate in future research.

- The four point beam fatigue testing on cold bituminous mixes found to complex methodology to related the require laboratory measured fatigue life to that of in-situ performance. The investigation of these materials using rolling wheel fatigue is also recommended.

APPENDIX A

1. IPC 4PB TESTING PROCEDURE AND OPERATING THE BFA

1.1 GENERAL

Specimens shall be tested in accordance with the procedure detailed in this section. (Note: Details of operating procedure for the Beam Fatigue Apparatus (BFA) are provided in the Manufacturer's Operation Manual, and reference must be made to the Manual for any specific information.). The general procedure for testing each beam specimen is detailed in Section 1.2.

1.2 SET-UP AND CONDUCTING OF THE TEST

The following steps apply for each of the replicate specimens:

1. Measure the beam specimen width, and depth at the following five locations, within 20mm of each end, within 10mm at the centre of the beam and within 10mm of points located 90mm in either direction from the centre of the beam. The mean five measurements for each dimension shall be reported to the nearest 0.1mm. Reject the beam if any of the five measurements, for either width, or depth differs by more than 1.5mm from respective mean value.
2. Place the specimen in the controlled temperature cabinet and set the test temperature. Allow at least four hours for the specimen to stabilize at the test temperature.
3. Begin the test by switching the computer ON, then main air supply valve, CDAS and air valve to BFA. Close the test by the reverse order.
4. Use computer software (UTM 21) to input the following test control parameters:
 - i. Operator and test description,
 - ii. Specimen identification (beam label and number), dimensions and properties (beam condition)
 - iii. Select the mode of loading to be used (haversine or sine).
 - iv Loading frequency, (pulse)
 - v. Peak tensile strain, and
 - iv Termination criteria, a maximum allowable number of cycles and termination stiffness

5. Position the loading frame cradle in the centre of its stroke using jog up/down control. This is achieved when the level on Channel B is practically zero.
6. Insert location draw-bars provided, to set the pivot points to the correct spacing.
7. Position the beam specimen in the loading frame cradle so as the overhang at the either end is equal. However avoid hitting the on-specimen LVDT during inserting the specimen by check/adjust the transducer level. Activate (close) the side clamps (end plastic clamps) to hold the specimen ends in place.
8. Lower the outer and inner clamps at the four points to hold the specimen in place. Leave these jogs switch in lower position through out the test.
9. Remove the location draw-bars.
10. Adjust on-specimen displacement transducer to centre stroke.
11. Allow a minimum of 30 to 40 minutes to enable the specimen clamping stresses to be relieved before the commencement of test and the gaining of temperature equilibrium (outer/skin). Again check that on specimen transducer level is close to zero and adjust level, if necessary.
12. Secure the on-specimen transducer lock nut.
13. Check that the dummy specimen core temperature is at the target temperature within the tolerance specified prior to commencement of the test.
14. Start (RUN) the test.
15. In the course of test termination conditions should be confirmed. *Initial Flexural Stiffness* is the flexural stiffness calculated by the data acquisition software (CDAS) at the 50th load cycles. Check to confirm that the selected peak tensile strain level is achieved at the 50th cycle.
16. After the completion of the first 50 loading cycles, enter the required termination conditions, stiffness say approximately 40% of the initial stiffness of CDAS to ensure that the failure condition is achieved. The number of cycles should be artificially high, say 5million depending on the strain level. The test will run until the termination stiffness is reached or the required numbers of cycles have been applied.

17. On completion of the test remove the beam specimen.
18. Convert the test file to an ASCII file, and store both files in the hard drive or on a diskette.
19. Repeat steps (3) to (17) for remaining replicate specimens.

2. ADDITIONAL PROCEDURE FOR THE STRAIN-AT-BREAK TEST

The same procedure 1 to 3 and 8 to 14 similarly applied for the strain at break test.

The additional procedures are as follows:

4. Use computer software (UTM 12) to input the following test control parameters:
 - i. Operator and test description,
 - ii. Specimen identification (beam label and number), dimensions and properties (beam condition)
 - iii. Select the mode of loading to be used (displacement (actuator)).
 - iv. Loading rate, (1mm/min or -0.0167 mm/s)
 - v. Termination criteria, a maximum allowable time of loading 540 second and deformation actuator stroke 9mm, artificial maximum axial deformation of 2mm.
5. Position the loading frame cradle in the upper of its stroke using jog up/down control. This is achieved when the level on Channel B is practically on maximum side say ± 4.45 .
6. Insert location draw-bars provided, to set the pivot points to the correct spacing.
7. Position the beam specimen in the loading frame cradle so as the overhang at the either end is equal. However avoid hitting the on-specimen LVDT during inserting the specimen by check/adjust the transducer level.
- 8a. Insert the spacer bar at either end of the beam to raise the bottom of the outer cradles. Check to ensure that the beam bottom centre touches the cradles to avoid initial deformation during lowering the central loading cradle (frame). Activate (close) the side clamps (end plastic clamps) to hold the specimen ends in place.

Note: Procedure 13 above is not applicable for the strain-at-break test.

APPENDIX B

1. MOISTURE RECORDS FOR EMULSION MIXES

Table B1: Mixing moisture records

Slab no.	Mix type and moisture content (%)		
	Mix 4(B-75C-0%)	Mix 5(B-75C-1%)	Mix 6(B-75M-0%)
A	7.9	6.2	5.4
B	7.0	6.5	4.8
C	6.9	6.7	5.1
D	6.2	6.5	-
Average	7.0	6.5	5.1
Std dev	0.7	0.2	0.3
% of OMC*	93	87	100

* OMC for C-type aggr.= 7.5% and M-type aggr.=5.2%

Table B2: Compaction moisture records

Slab no.	Mix type and moisture content (%)		
	Mix 4(B-75C-0%)	Mix 5(B-75C-1%)	Mix 6(B-75M-0%)
A	Wet	8.0	6.8
B	Wet	7.7	7.2
C	Wet	7.6	7.2
D	6.7	7.2	-
Average	6.7	7.6	7.1
Std dev		0.4	0.2
% of OMC*	89	101	136

* Moisture measured by nuclear density equipment

Table B3: After the test moisture records

Slab no.	Mix type and moisture content (%)		
	Mix 4(B-75C-0%)	Mix 5(B-75C-1%)	Mix 6(B-75M-0%)
A	1.3	1.8	1.3
B	1.1	-	0.9
C	0.6	0.8	1.2
D	0.4	-	-
Average	0.85	1.3	1.1
Std dev	0.42	-	0.2
% of OMC*	10	17	21

2. BULK RELATIVE DENSITY (BRD's) AND PERCENTAGE Mod. AASHTO FOR EMULSION MIXES

Table B4: BRD's (Mg/m³) and % Mod. AASHTO for Mix 4(B-75C-0%)

Beam no.	Slab no			
	A	B	C	D
1	2.195	2.224	2.239	Broke
2	2.230	2.369	2.228	2.322
3	2.243	2.311	2.235	2.330
4	2.240	2.455	2.244	2.334
5	2.236	2.384	2.241	2.321
6	2.223	2.303	2.240	Broke
Average	2.228	2.341	2.238	2.327
Std dev.	0.02	0.08	0.01	0.01
% Mod. AASHTO*	103	108	104	107

* The (Mod.) MDD for C-type aggr = 2160 Kg/m³

Table B5: BRD's (Mg/m³) and % Mod. AASHTO for Mix 5(B-75C-1%)

Beam no.	Slab no			
	A	B	C	D
1	2.195	2.191	2.193	2.202
2	2.212	2.230	2.242	2.233
3	2.209	2.233	2.237	2.238
4	2.191	2.226	2.236	2.232
5	2.128	2.248	2.225	2.226
6	Broke	2.196	2.215	2.198
Average	2.187	2.221	2.225	2.222
Std dev.	0.03	0.02	0.02	0.02
% Mod. AASHTO	101	103	103	103

Table B6: BRD's (Mg/m³) and % Mod. AASHTO for Mix 6(B-75M-0%)

Beam no.	Slab no		
	A	B	C
1	2.124	2.124	2.100
2	2.137	2.168	2.134
3	2.142	2.159	2.152
4	2.140	2.159	2.154
5	2.134	2.160	2.151
6	2.103	2.131	2.128
Average	2.130	2.150	2.137
Std dev.	0.01	0.02	0.02
% Mod. AASHTO*	110	111	111

* The Mod. MDD for M-type aggr = 1930 Kg/m³

3. MOISTURE RECORDS FOR FOAM MIXES

Table B7: Mixing moisture records

Slab no.	Mix type		
	Mix 7(B-75C-0%)	Mix 8(B-75C-1%)	Mix 9(B-75M-0%)
A	5.2	5.7	4.0
B	3.7	5.4	4.4
C	5.7	5.0	4.6
Average	4.9	5.4	4.3
Std dev	1.0	0.3	0.3
% of OMC*	65	72	83

* OMC for C-type aggr.= 7.5% and M-type aggr.=5.2%

Table B8: Compaction moisture records

Slab no.	Mix type		
	Mix 4(B-75C-0%)	Mix 5(B-75C-1%)	Mix 6(B-75M-0%)
A	6.2	6.9	5.7
B	4.9	6.4	6.2
C	7.6	6.2	6.3
Average	6.2	6.5	6.1
Std dev	1.3	0.4	0.3
% of OMC*	83	87	117

* Moisture measured by nuclear density equipment

Table B9: After the test moisture records

Slab no.	Mix type and moisture content (%)		
	Mix 7(B-75C-0%)	Mix 8(B-75C-1%)	Mix 9(B-75M-0%)
A	0.6	0.5	0.8
B	0.4	-	0.6
C	0.4	0.7	0.9
Average	0.5	0.6	0.8
Std dev	-	0.3	0.2
% of OMC*	6	8	15

4. BULK RELATIVE DENSITY (BRD's) AND PERCENTAGE Mod. AASHTO FOR FOAM MIXES

Table B10: BRD's (Mg/m³) and % Mod. AASHTO for Mix 7(C-75C-0%)

Beam no.	Slab no		
	A	B	C
1	Broke	1.988	1.977
2	Broke	2.052	2.071
3	2.064	2.082	2.089
4	2.054	2.071	2.085
5	2.055	2.055	2.051
6	2.000	1.992	2.033
Average	2.043	2.040	2.051
Std dev.	0.03	0.04	0.04
% Mod. AASHTO	95	94	95

* The (Mod.) MDD for C-type aggr = 2160 Kg/m³

Table B11: BRD's (Mg/m³) and % Mod. AASHTO for Mix 8(C-75C-1%)

Beam no.	Slab no		
	A	B	C
1	2.047	1.946	2.025
2	2.142	2.035	2.088
3	2.098	Broke	2.088
4	2.150	2.069	2.113
5	2.124	2.074	2.100
6	2.046	1.947	2.027
Average	2.101	2.014	2.073
Std dev.	0.04	0.06	0.004
% Mod. AASHTO	97	93	96

Table B12: BRD's (Mg/m³) and % Mod. AASHTO for Mix 9(C-75M-0%)

Beam no.	Slab no		
	A	B	C
1	1.922	1.985	1.987
2	1.948	2.012	2.029
3	1.948	2.031	2.062
4	1.915	2.006	2.043
5	1.963	2.019	2.071
6	1.967	1.998	2.030
Average	1.943	2.008	2.037
Std dev.	0.02	0.02	0.03
% Mod. AASHTO	101	104	106

* The Mod. MDD for M-type aggr = 1930 Kg/m³

APPENDIX C

1 GRAPHS OF FATIGUE TEST RESULTS CAPTURED BY CADS FOR ANALYSIS OF LOAD REPETITION TO FAILURE (50% REDUCTION OF INITIAL STIFFNESS)

Note: The first 500cycles determine initial stiffness.

1.1 MIX 4 (B-75C-0%)

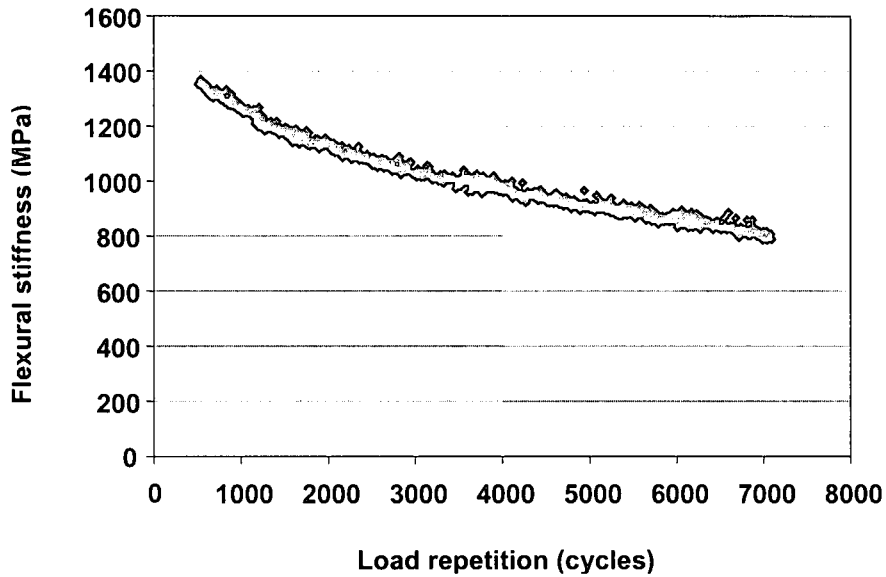


Figure C.1: Displacement control test at 470 microstrain of 5°C and 10Hz

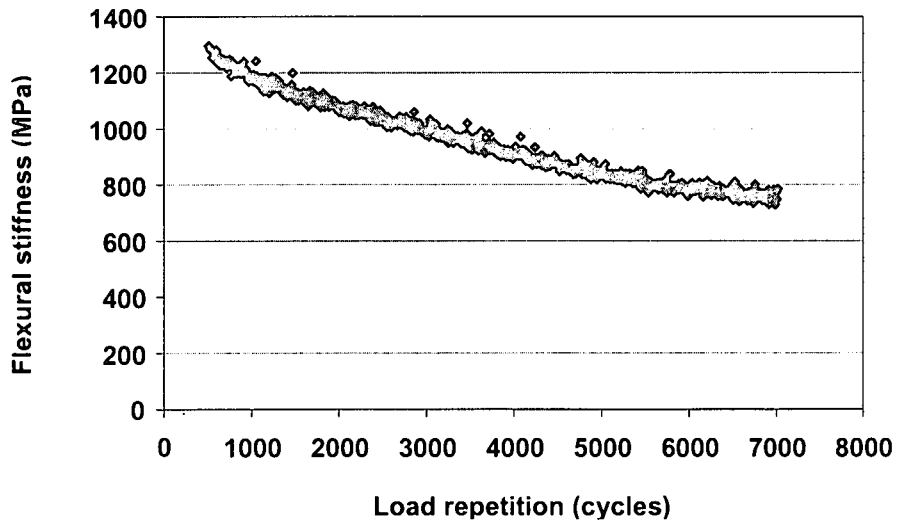


Figure C.2: Displacement control test at 450 microstrain of 5°C and 10Hz

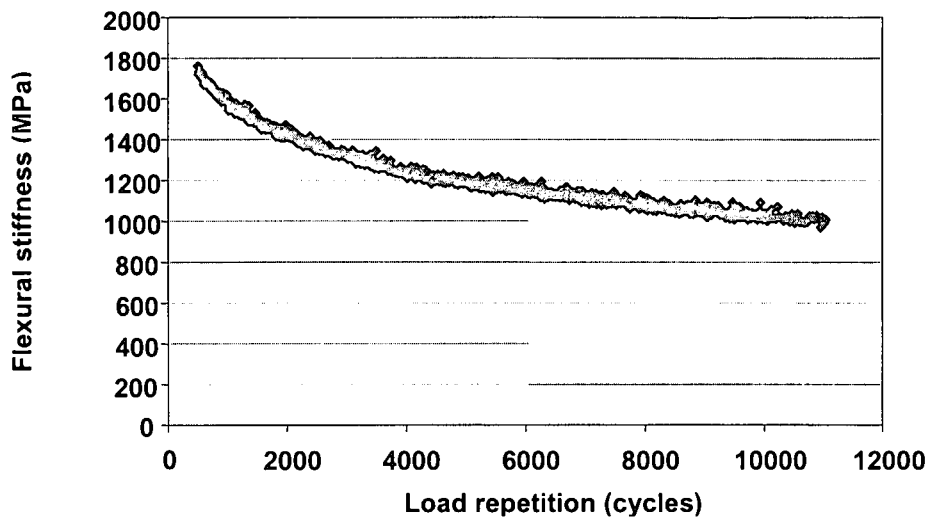


Figure C.3: Displacement control test at 430 microstrain of 5°C and 10Hz

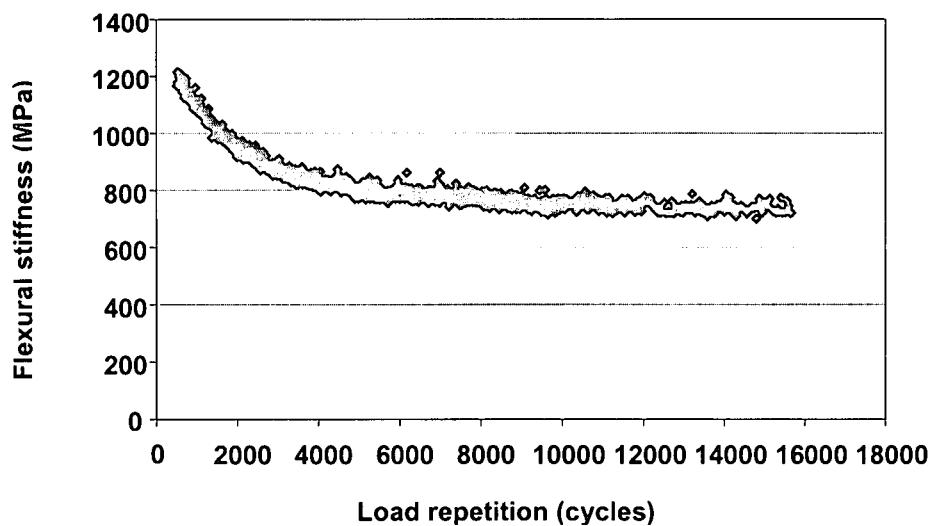


Figure C.4: Displacement control test at 400 microstrain of 5°C and 10Hz

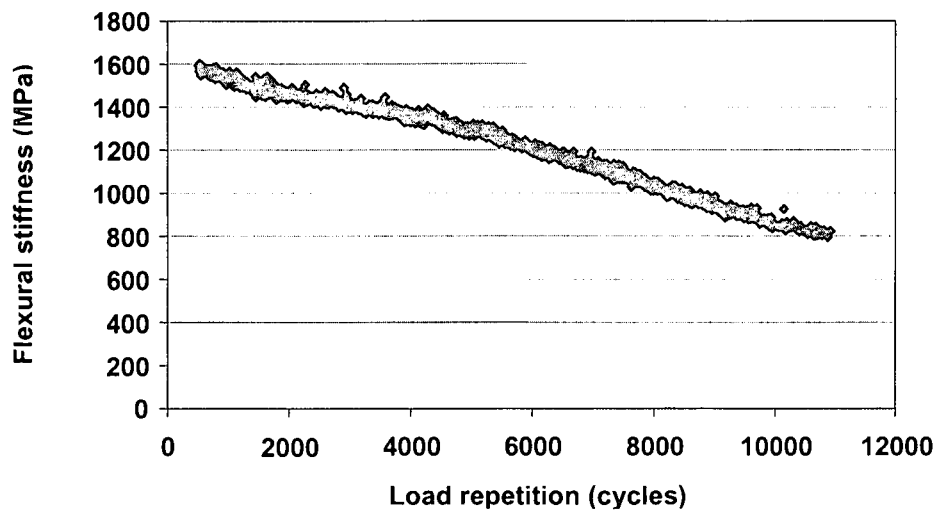


Figure C.5: Displacement control test at 380 microstrain of 5°C and 10Hz

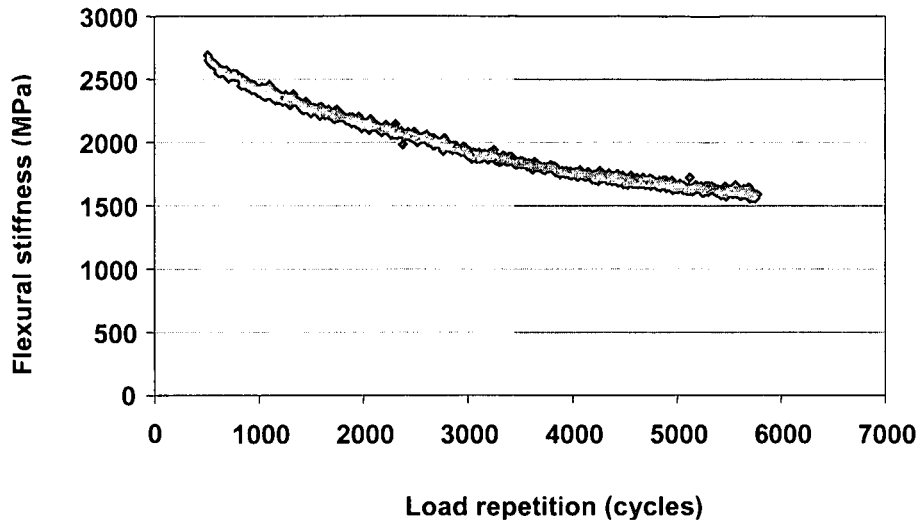


Figure C.6: Displacement control test at 350 microstrain of 5°C and 10Hz

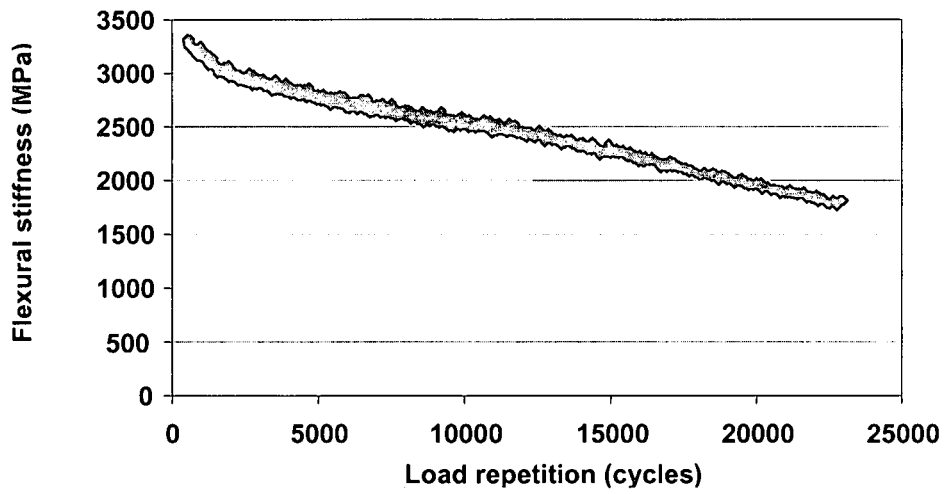


Figure C.7: Displacement control test at 330 microstrain of 5°C and 10Hz

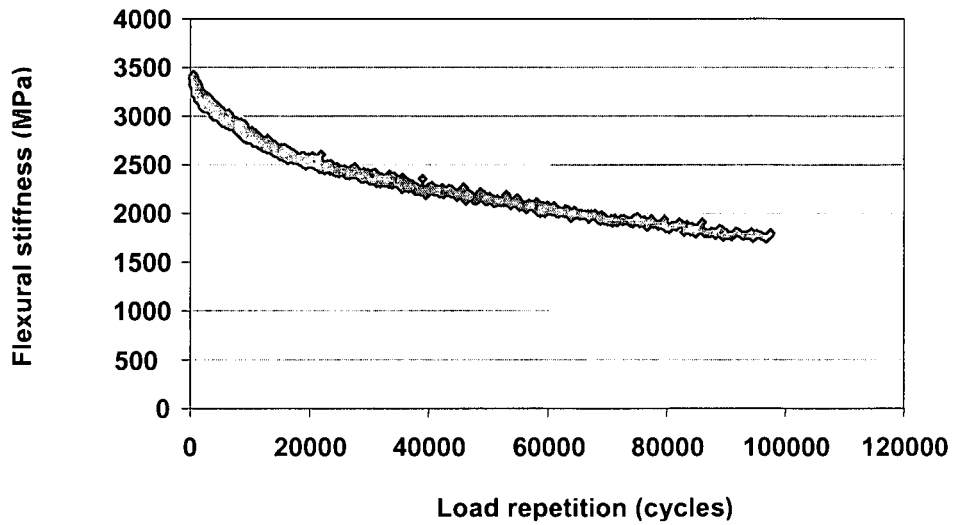


Figure C.8: Displacement control test at 300 microstrain of 5°C and 10Hz

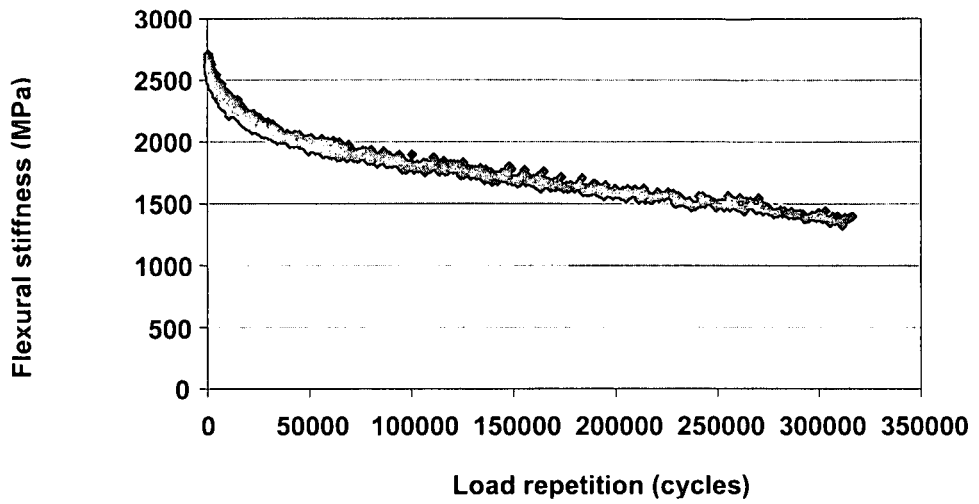


Figure C.9: Displacement control test at 250 microstrain of 5°C and 10Hz

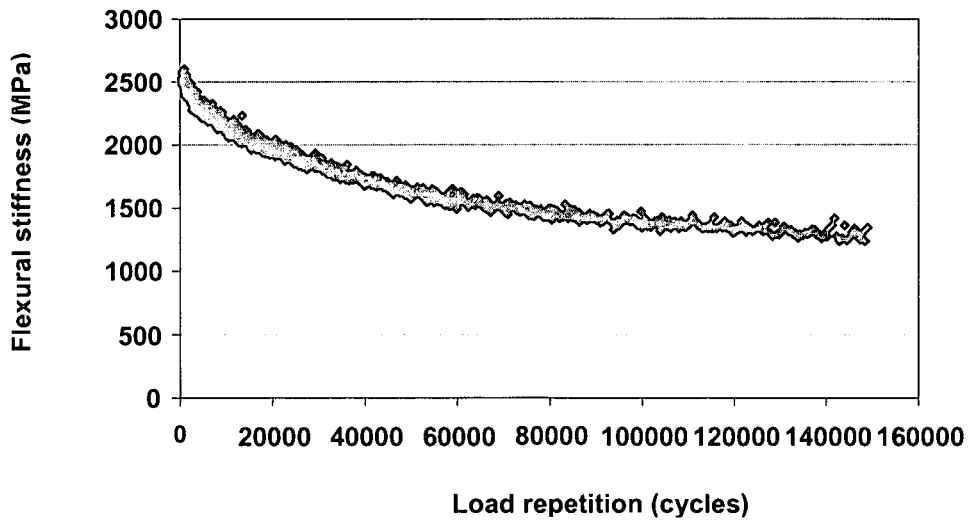


Figure C.10: Displacement control test at 230 microstrain of 5°C and 10Hz

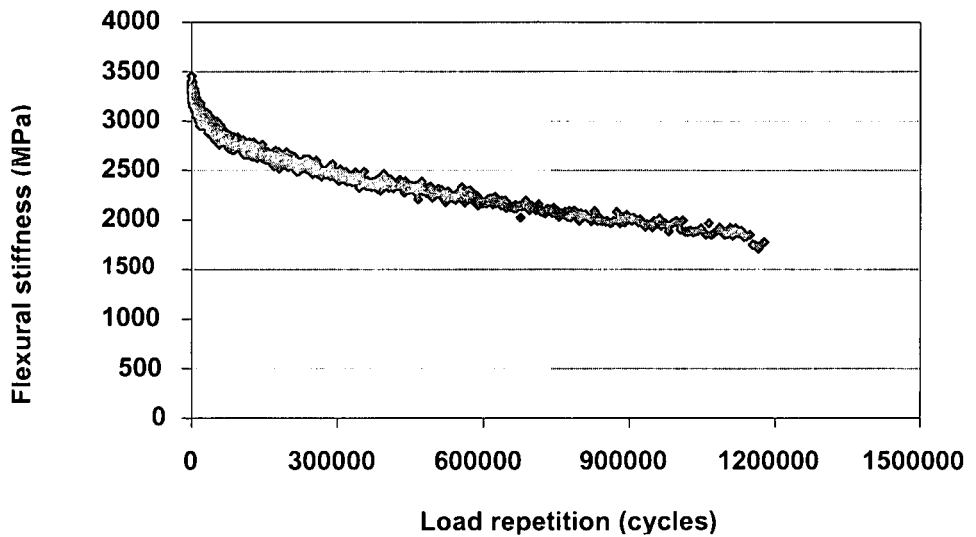


Figure C.11: Displacement control test at 200 microstrain of 5°C and 10Hz

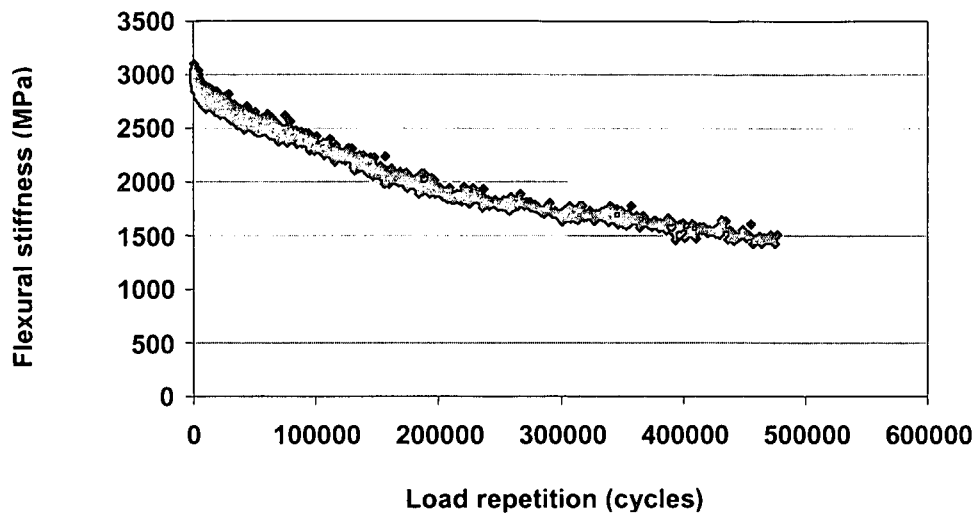


Figure C.12: Displacement control test at 180 microstrain of 5°C and 10Hz

1.2 MIX 5 (B-75C-1%)

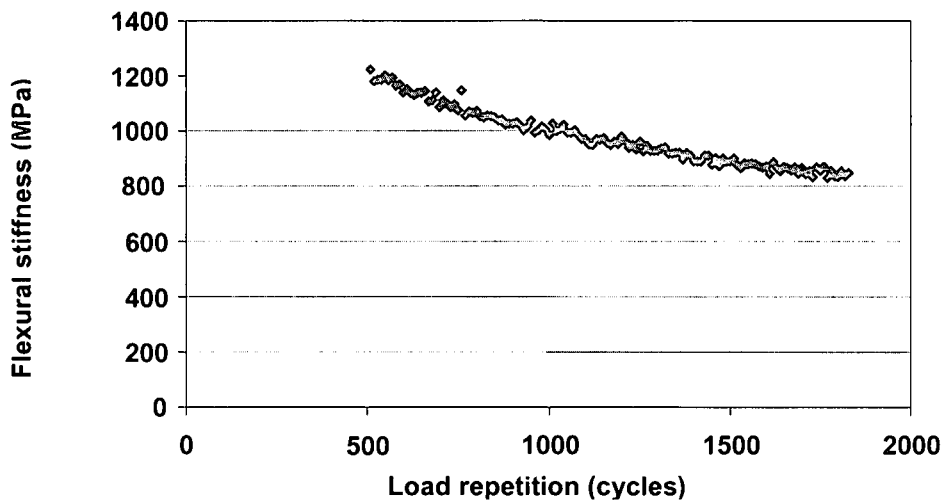


Figure C.13: Displacement control test at 450 microstrain of 5°C and 10Hz

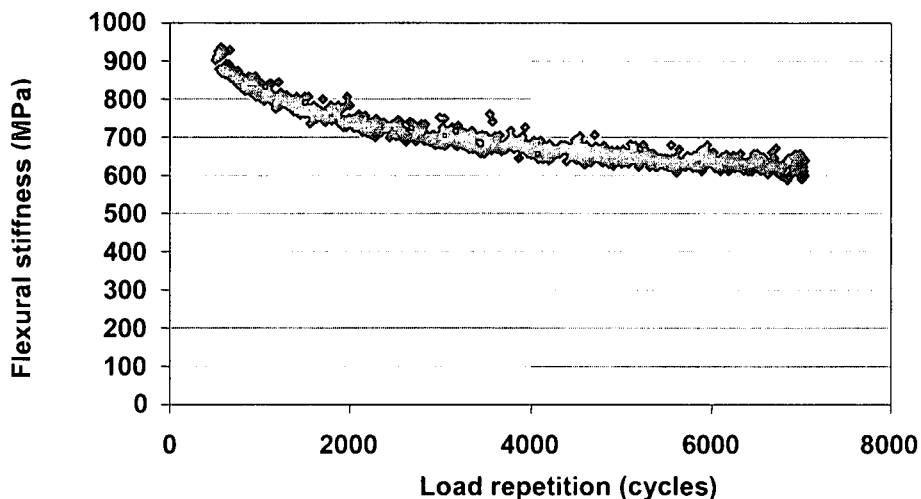


Figure C.14: Displacement control test at 420 microstrain of 5°C and 10Hz

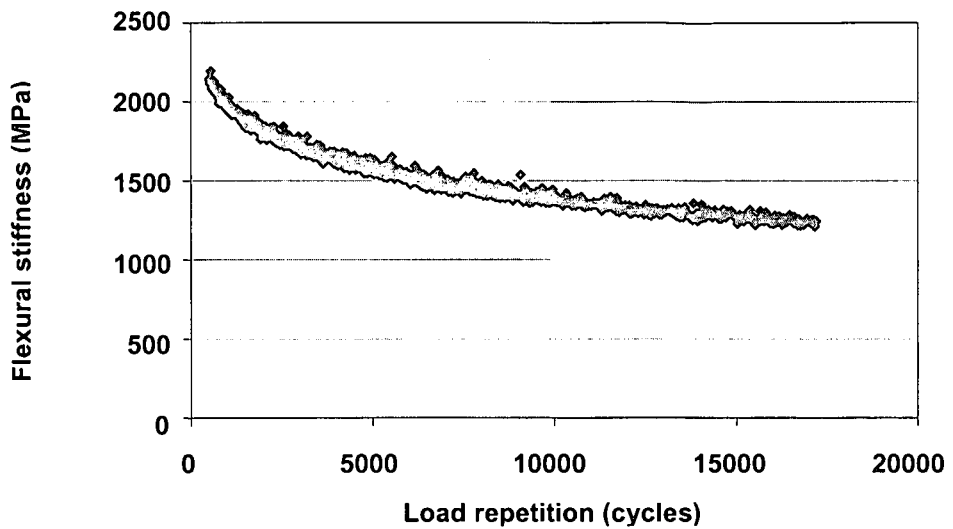


Figure C.15: Displacement control test at 380 microstrain of 5°C and 10Hz

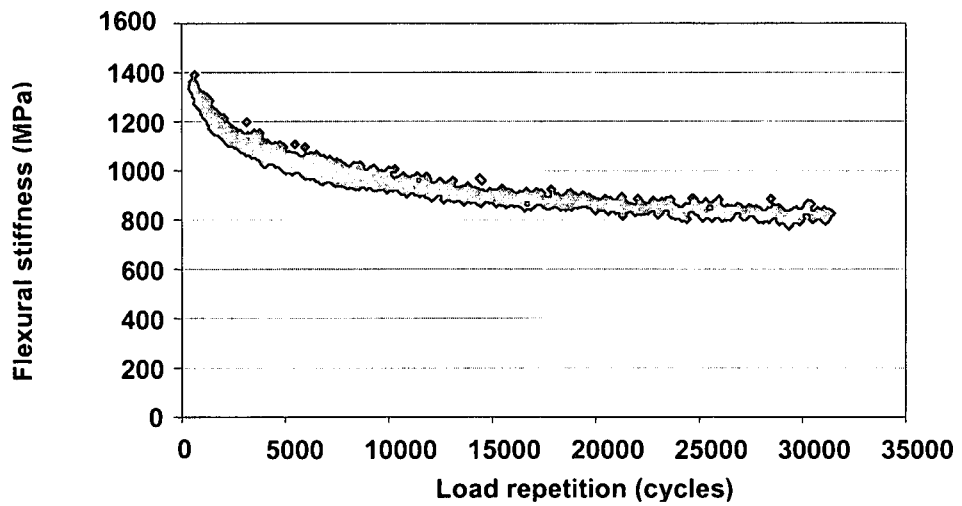


Figure C.16: Displacement control test at 350 microstrain of 5°C and 10Hz

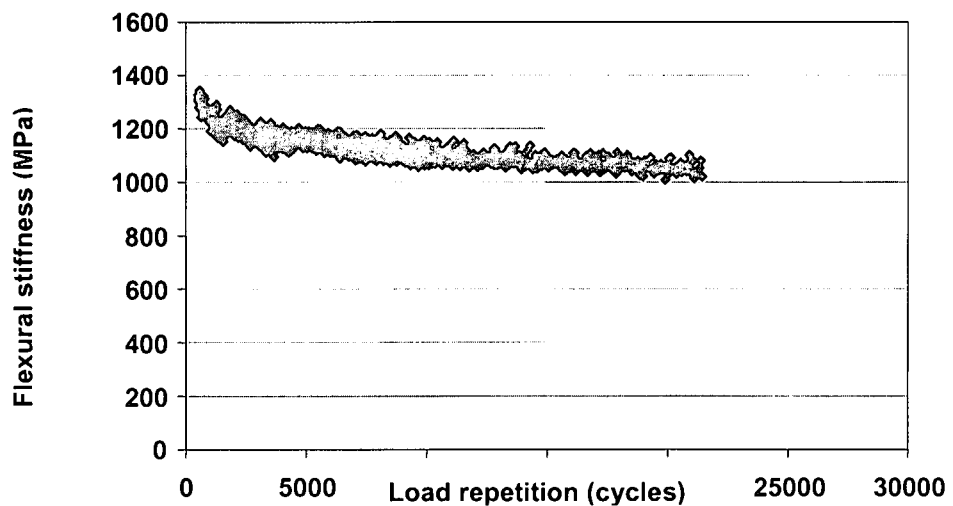


Figure C.17: Displacement control test at 300 microstrain of 5°C and 10Hz

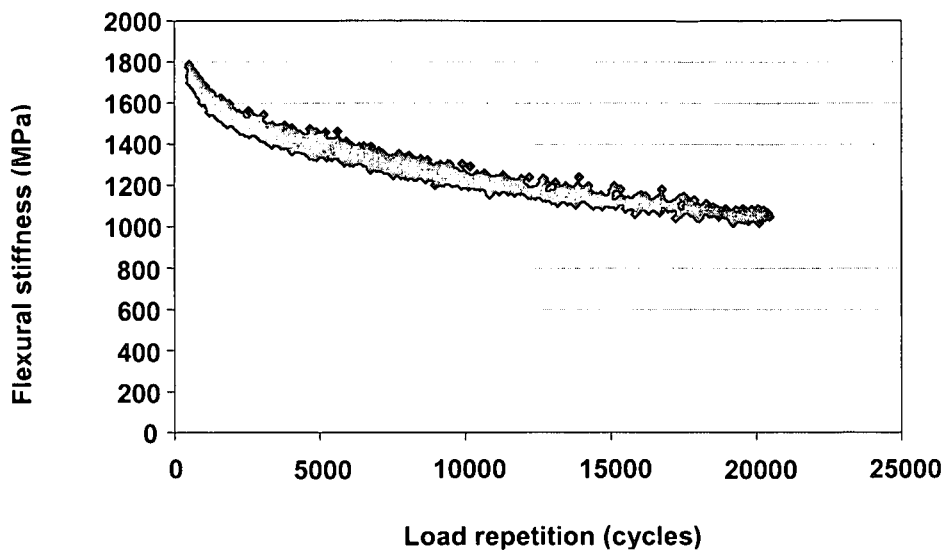


Figure C.18: Displacement control test at 280 microstrain of 5°C and 10Hz

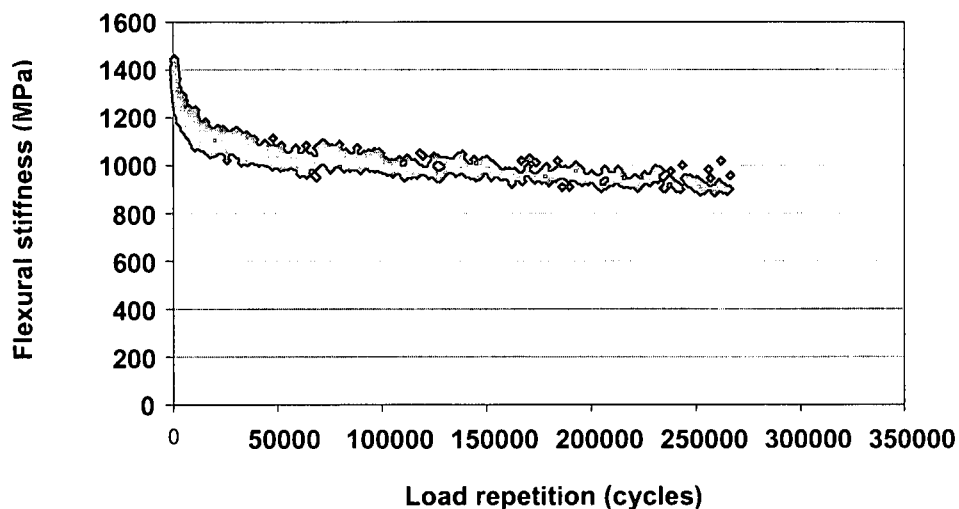


Figure C.19: Displacement control test at 250 microstrain of 5°C and 10Hz

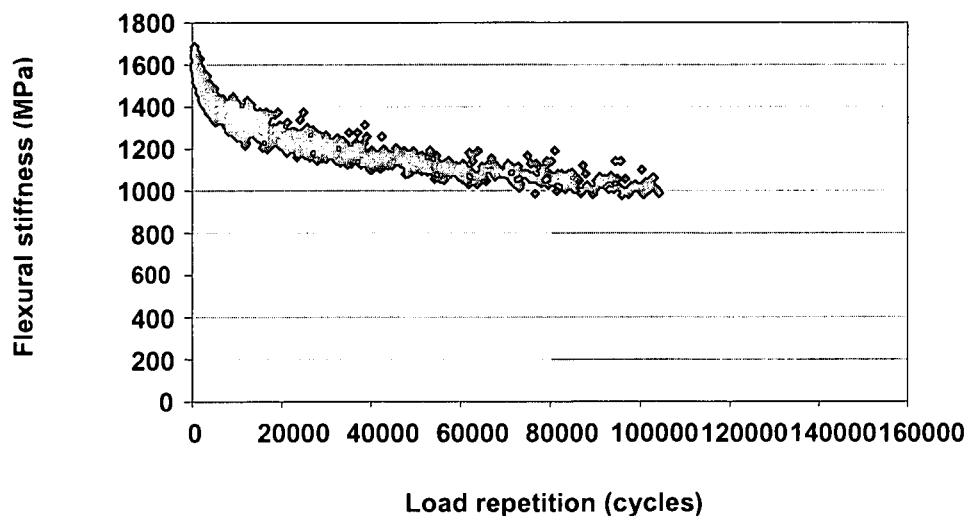


Figure C.20: Displacement control test at 200 microstrain of 5°C and 10Hz

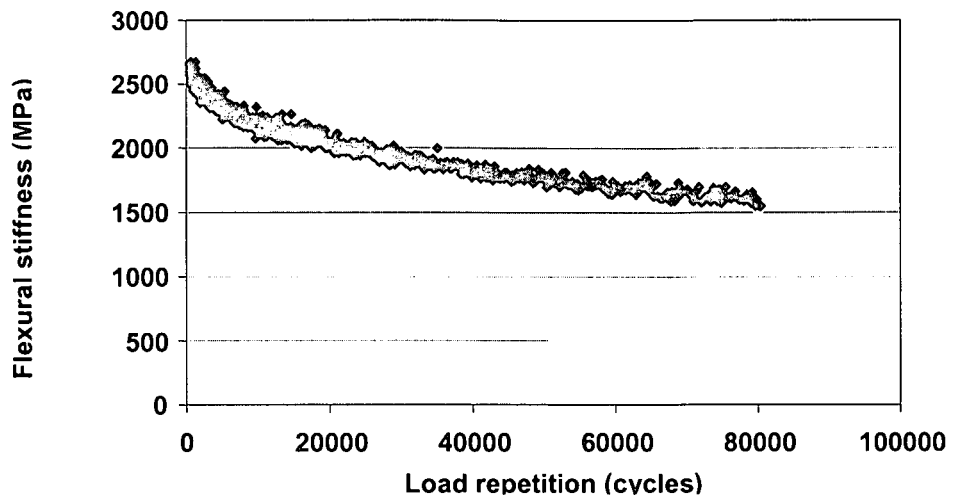


Figure C.21: Displacement control test at 190 microstrain of 5°C and 10Hz

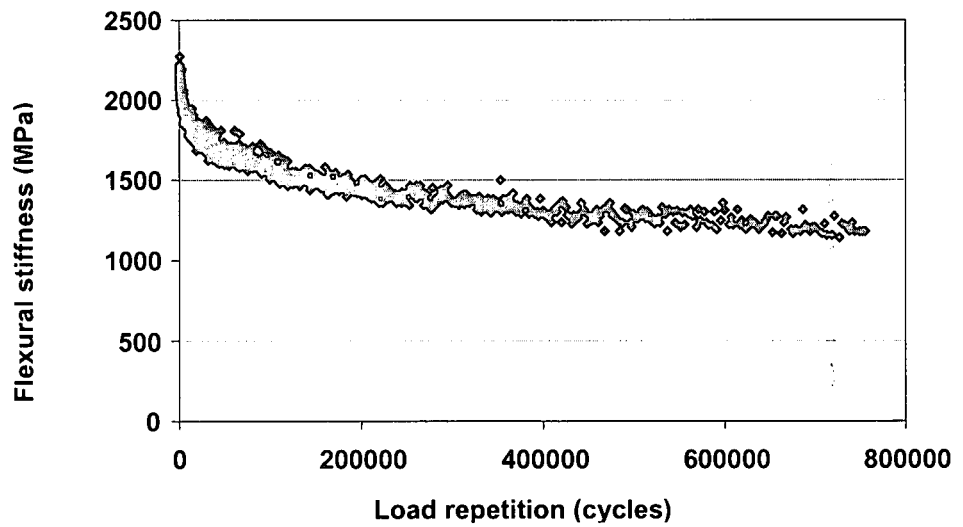


Figure C.22: Displacement control test at 180 microstrain of 5°C and 10Hz

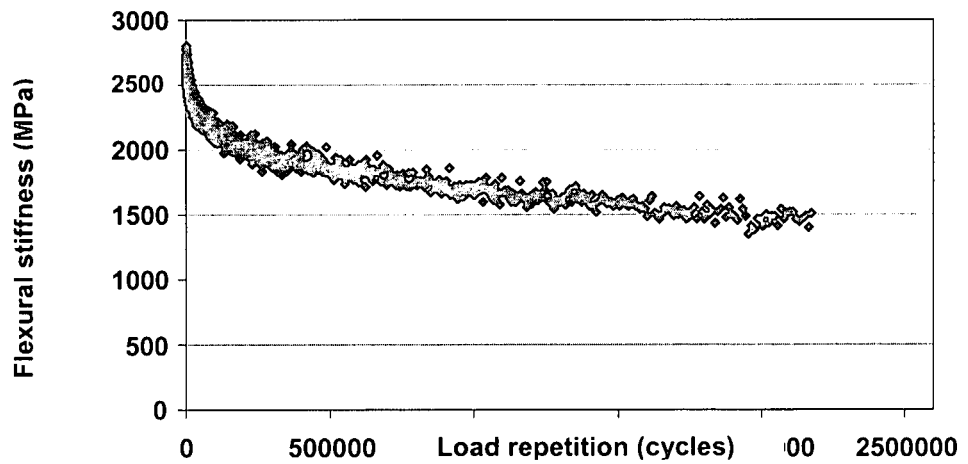


Figure C.23: Displacement control test at 140 microstrain of 5°C and 10Hz

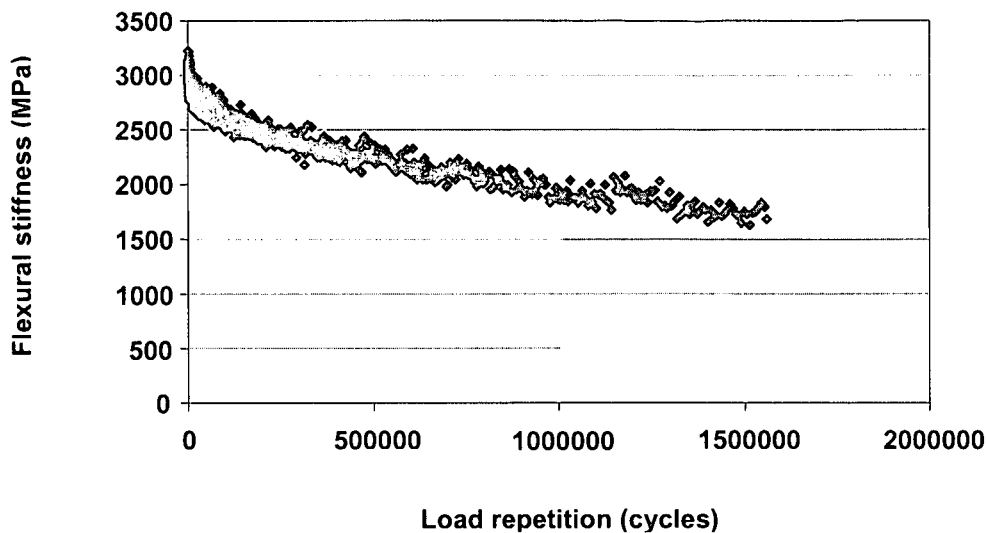


Figure C.24: Displacement control test at 120 microstrain of 5°C and 10Hz

1.3 MIX 6 (B-75M-0%)

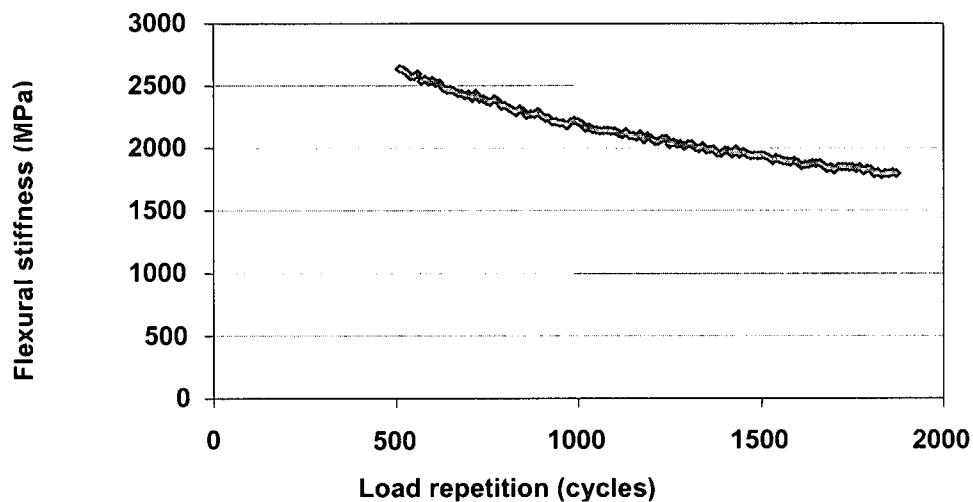


Figure C.25: Displacement control test at 470 microstrain of 5°C and 10Hz

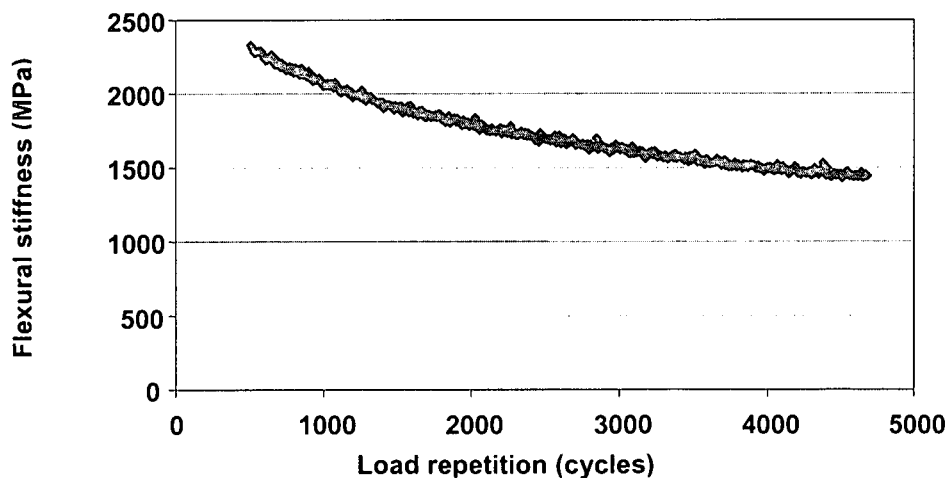


Figure C.26: Displacement control test at 450 microstrain of 5°C and 10Hz

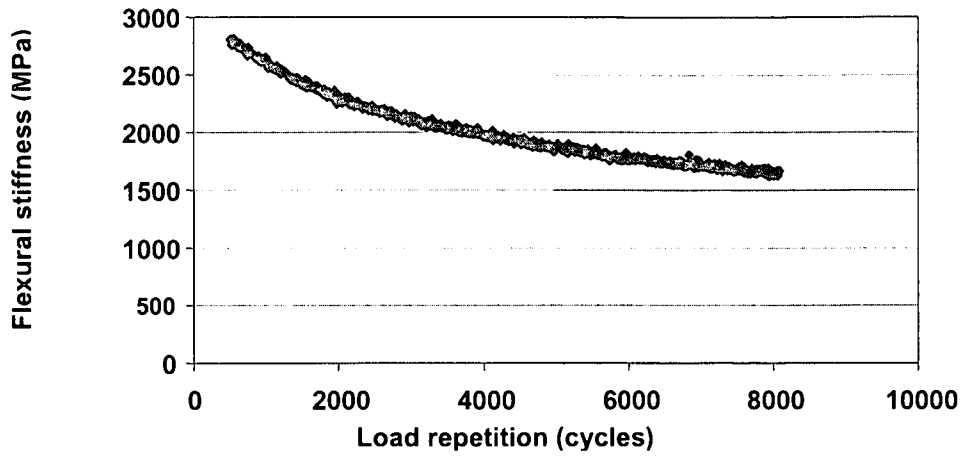


Figure C.27: Displacement control test at 400 microstrain of 5°C and 10Hz

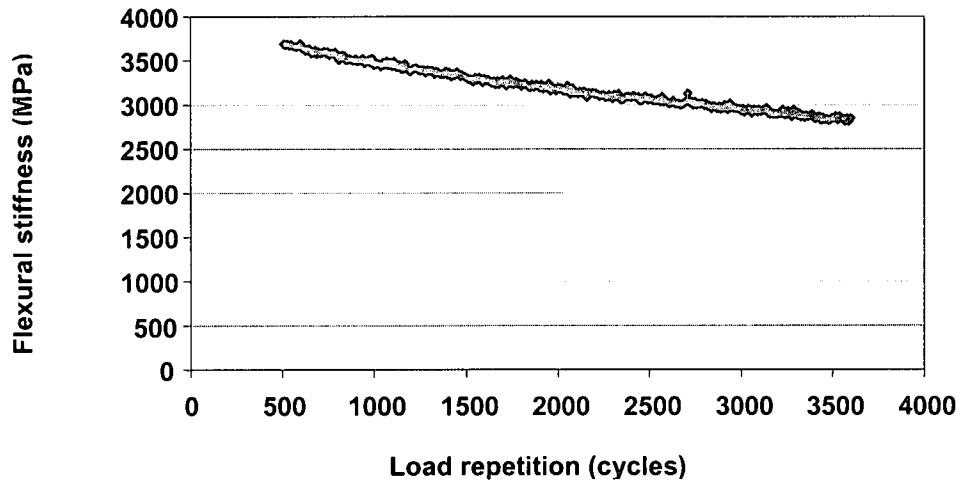


Figure C.28: Displacement control test at 380 microstrain of 5°C and 10Hz

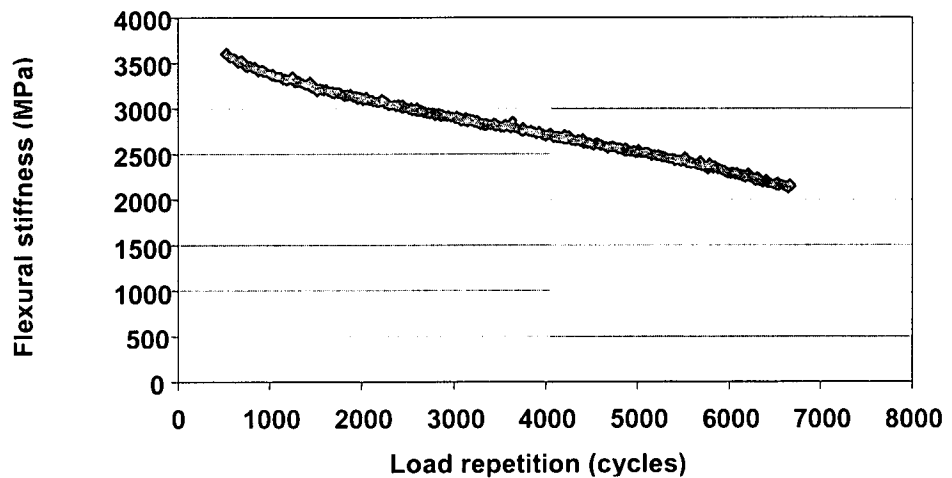


Figure C.29: Displacement control test at 370 microstrain of 5°C and 10Hz

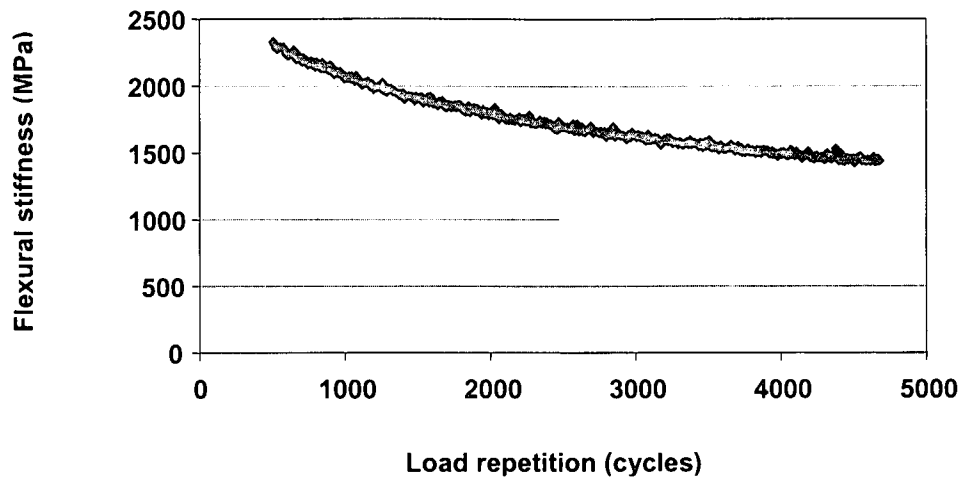


Figure C.30: Displacement control test at 350 microstrain of 5°C and 10Hz

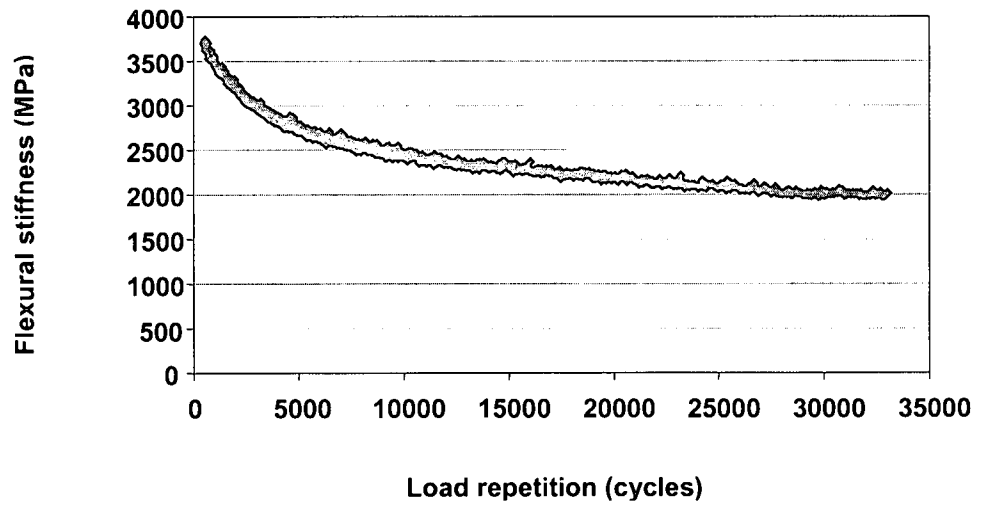


Figure C.31: Displacement control test at 300 microstrain of 5°C and 10Hz

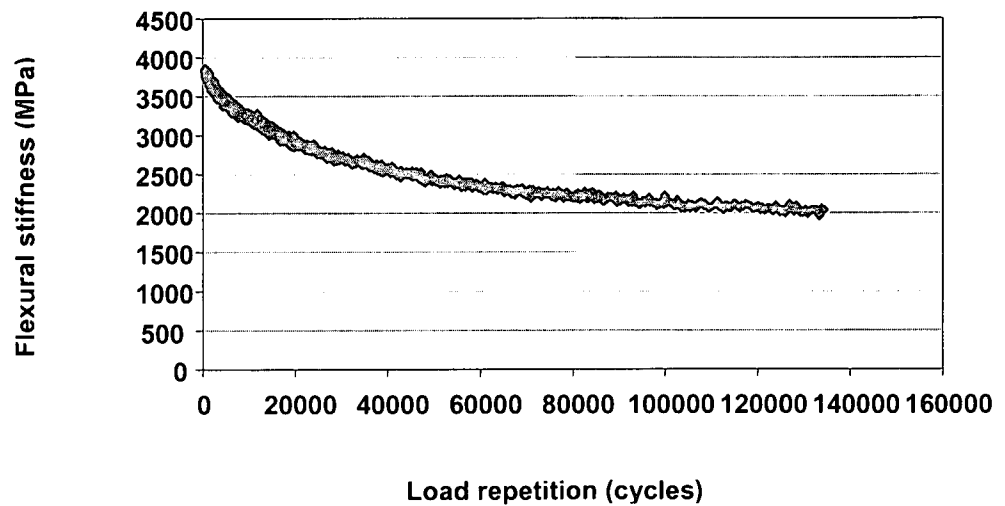


Figure C.32: Displacement control test at 250 microstrain of 5°C and 10Hz

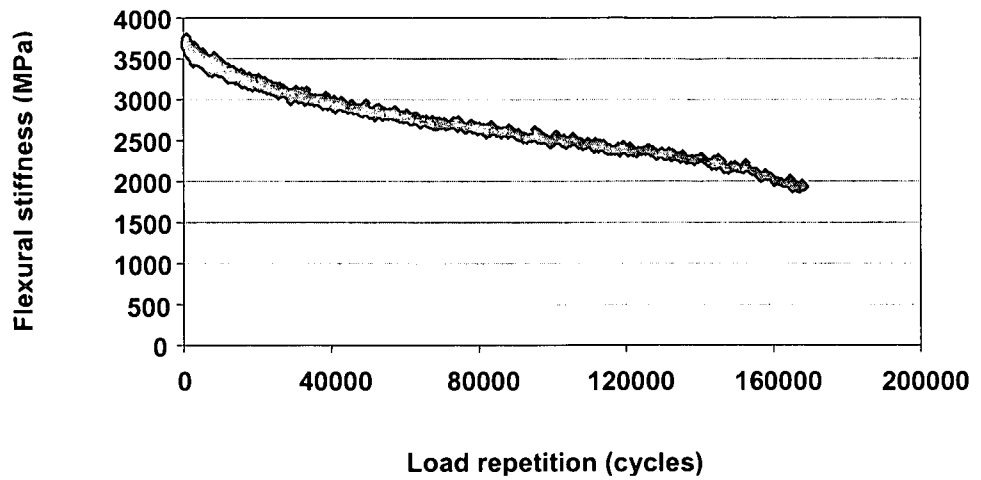


Figure C.33: Displacement control test at 230 microstrain of 5°C and 10Hz

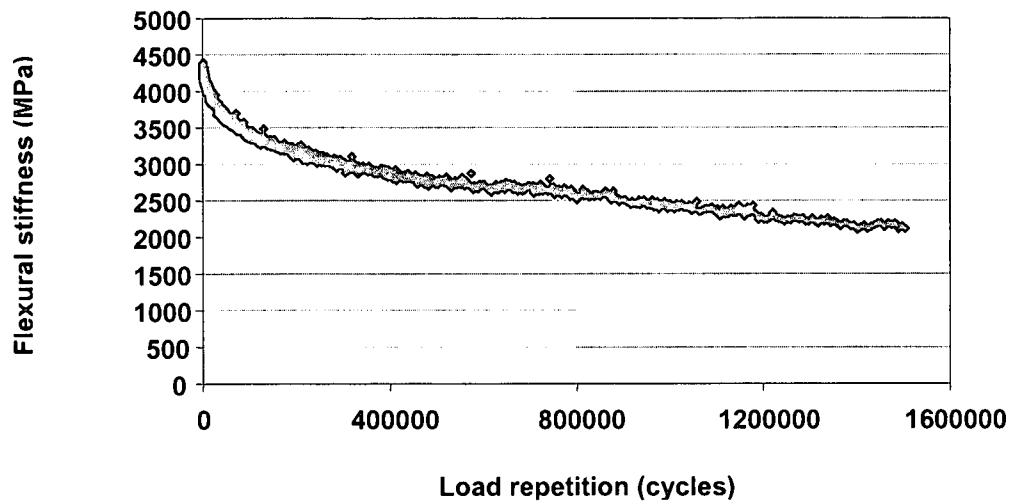


Figure C.34: Displacement control test at 200 microstrain of 5°C and 10Hz

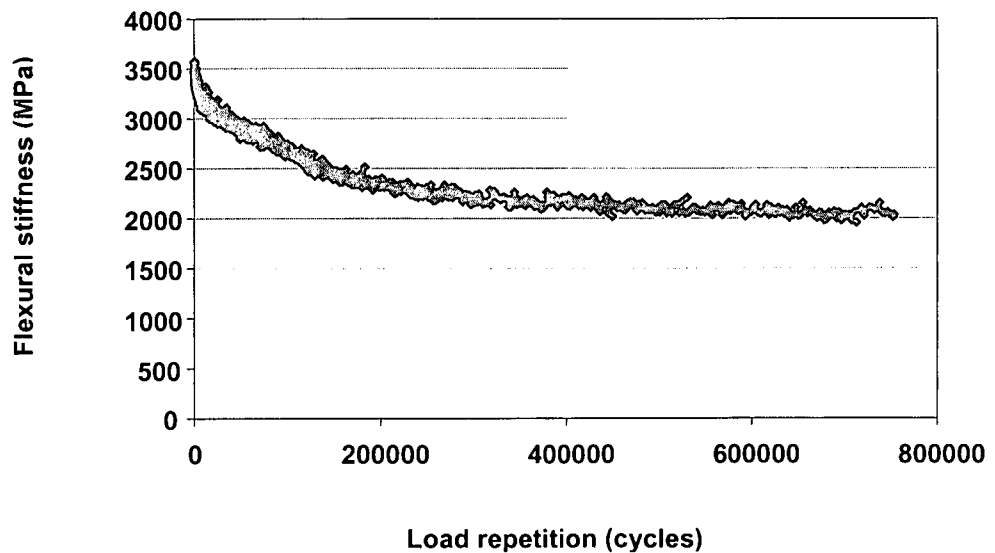


Figure C.35: Displacement control test at 180 microstrain of 5°C and 10Hz

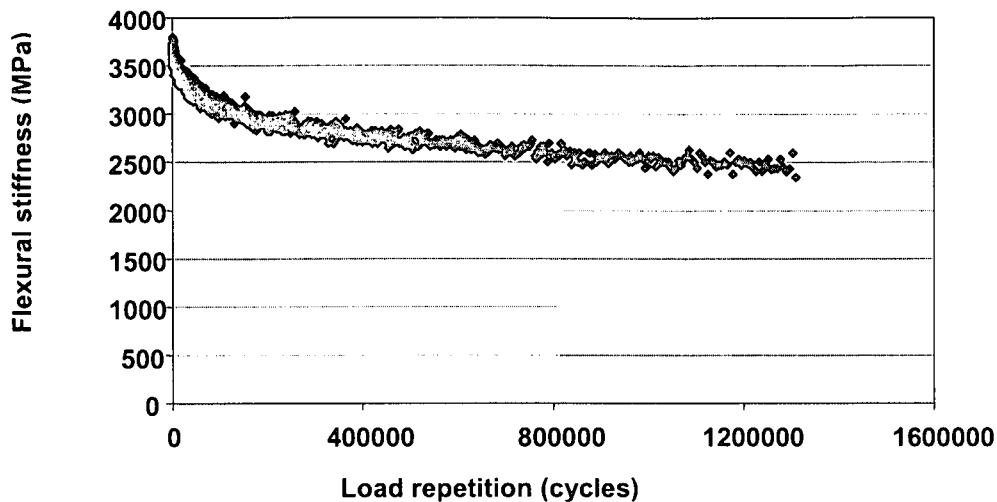


Figure C.36: Displacement control test at 150 microstrain of 5°C and 10Hz

1.4 MIX 7 (C-75C-0%)

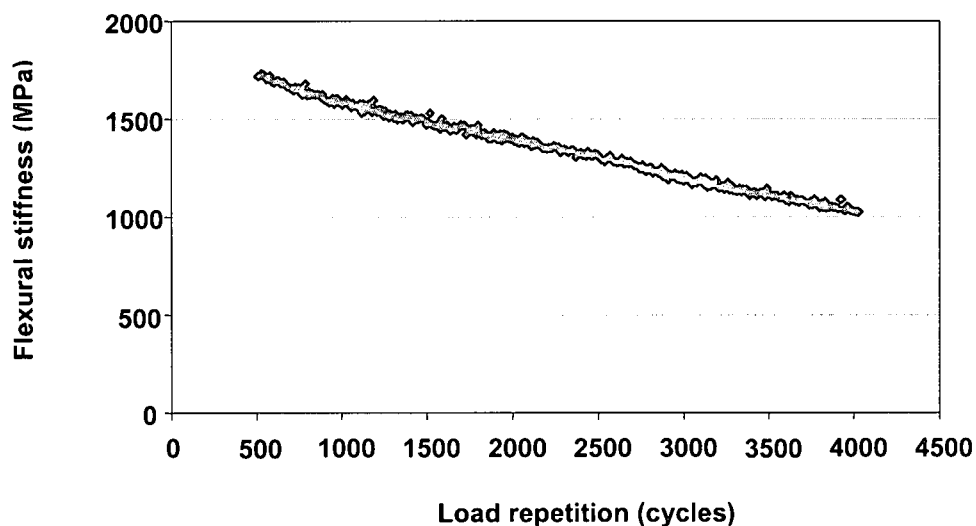


Figure C.37: Displacement control test at 470 microstrain of 5°C and 10Hz

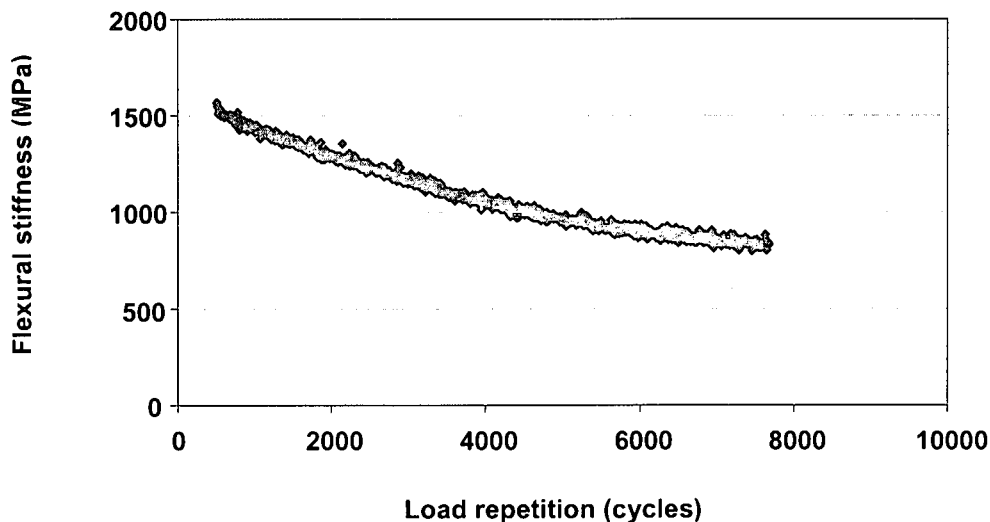


Figure C.38: Displacement control test at 450 microstrain of 5°C and 10Hz

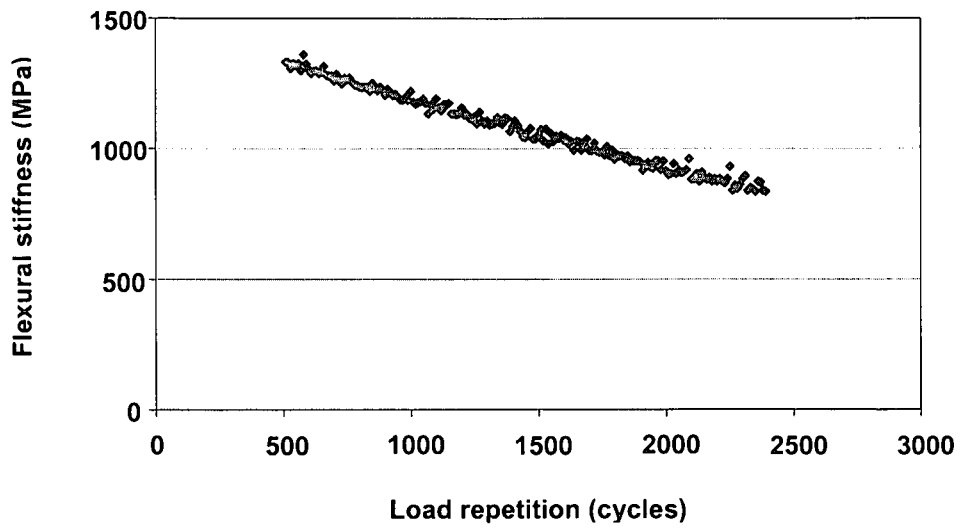


Figure C.39: Displacement control test at 430 microstrain of 5°C and 10Hz

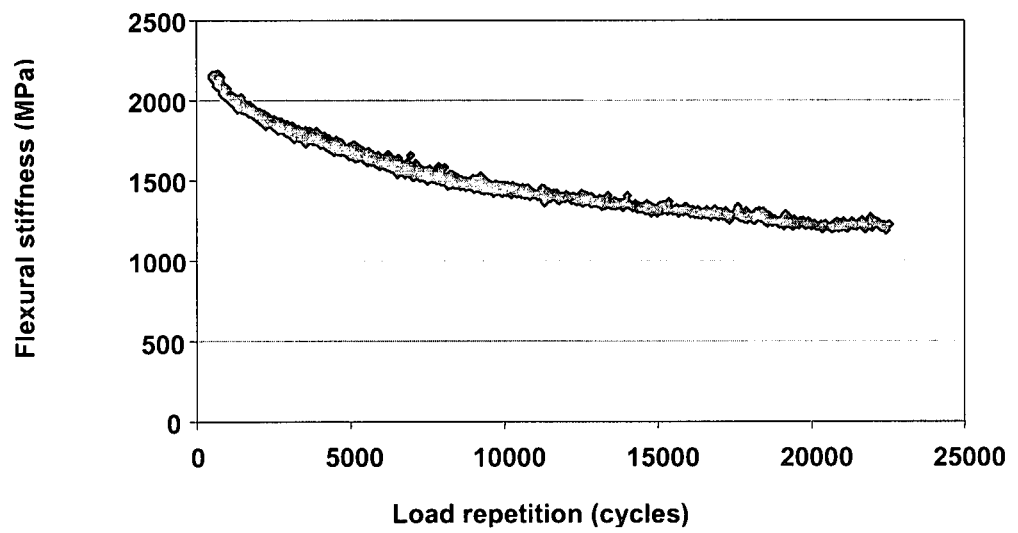


Figure C.40: Displacement control test at 400 microstrain of 5°C and 10Hz

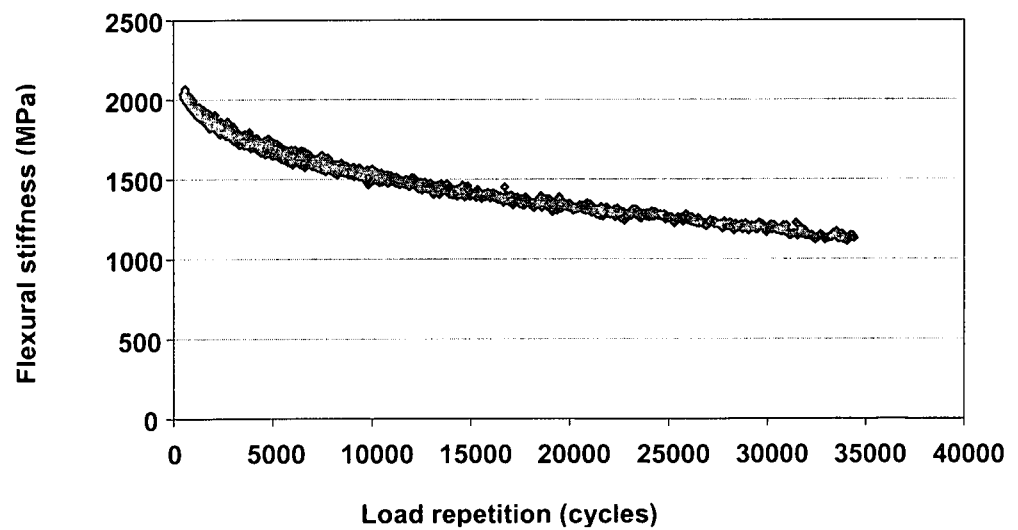


Figure C.41: Displacement control test at 380 microstrain of 5°C and 10Hz

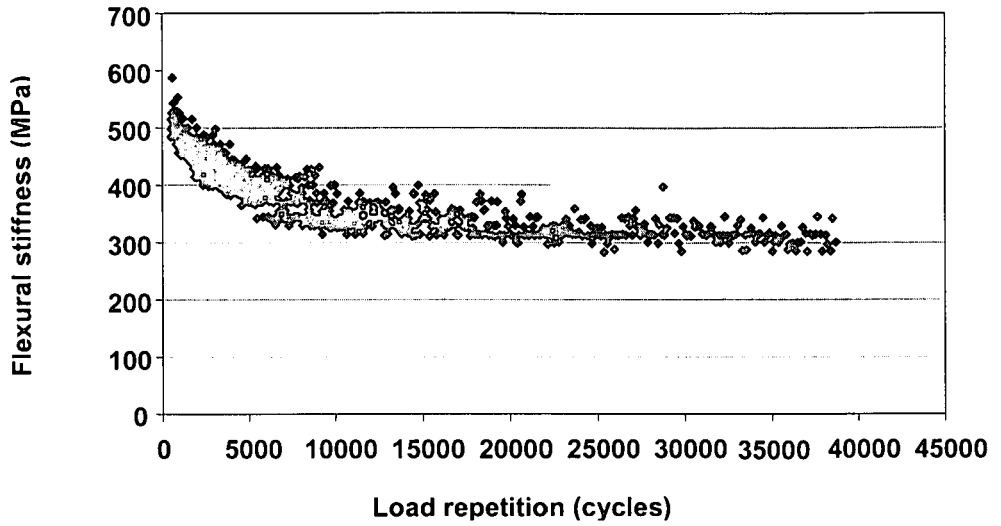


Figure C.42: Displacement control test at 350 microstrain of 5°C and 10Hz

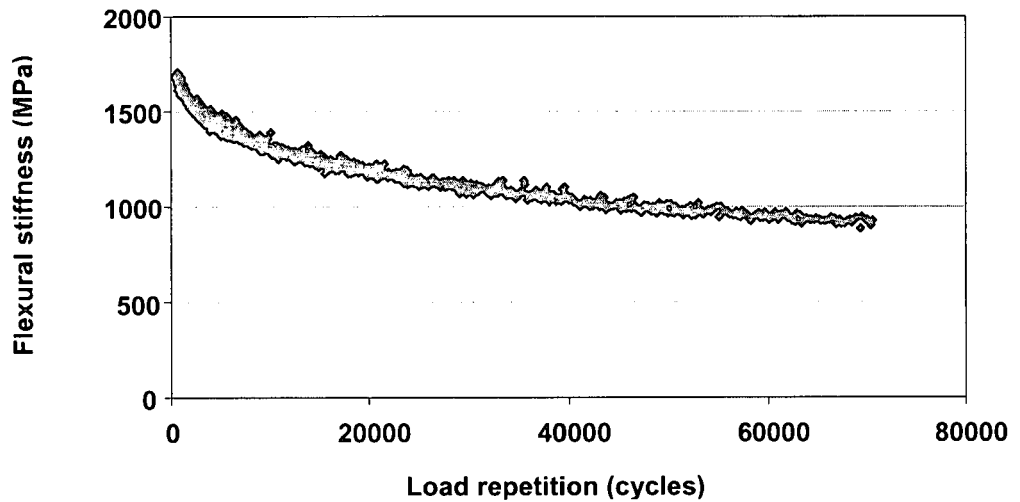


Figure C.43: Displacement control test at 330 microstrain of 5°C and 10Hz

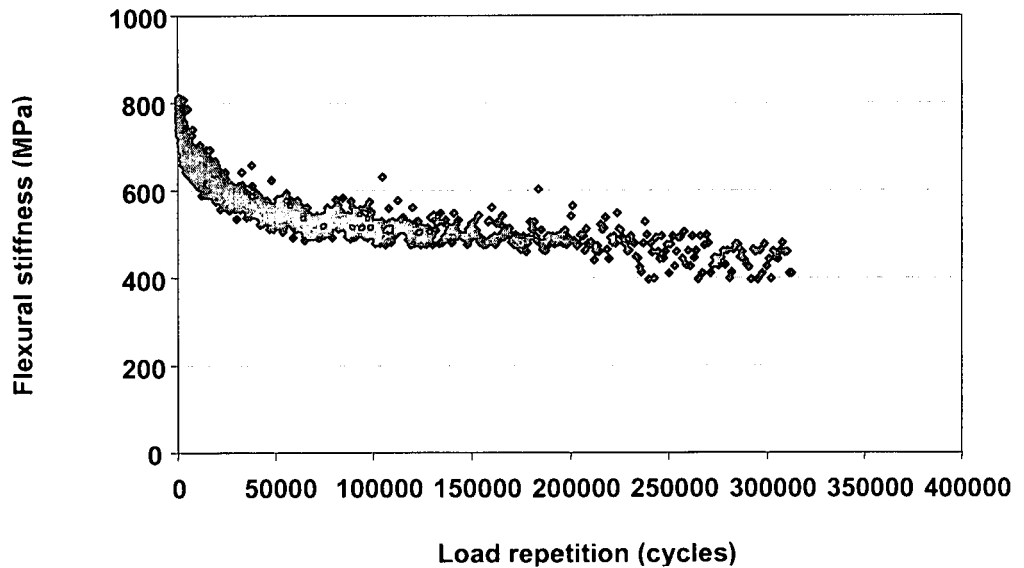


Figure C.44: Displacement control test at 300 microstrain of 5°C and 10Hz

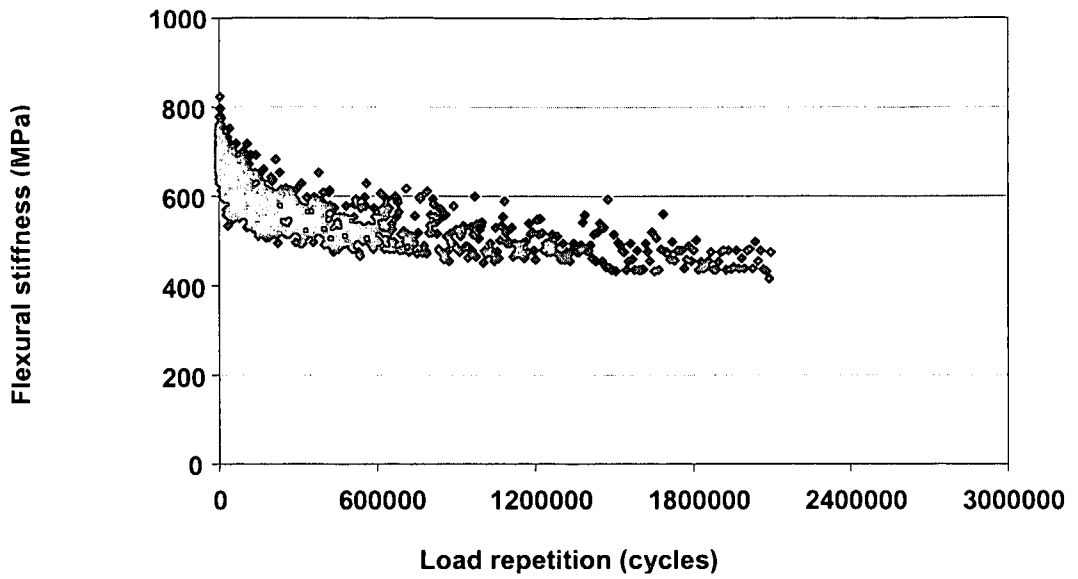


Figure C.45: Displacement control test at 250 microstrain of 5°C and 10Hz

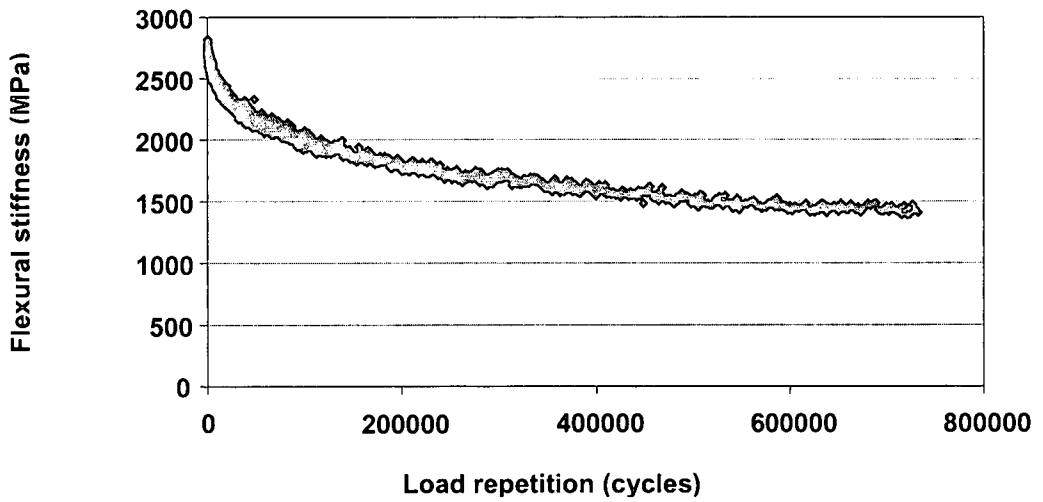


Figure C.46: Displacement control test at 230 microstrain of 5°C and 10Hz

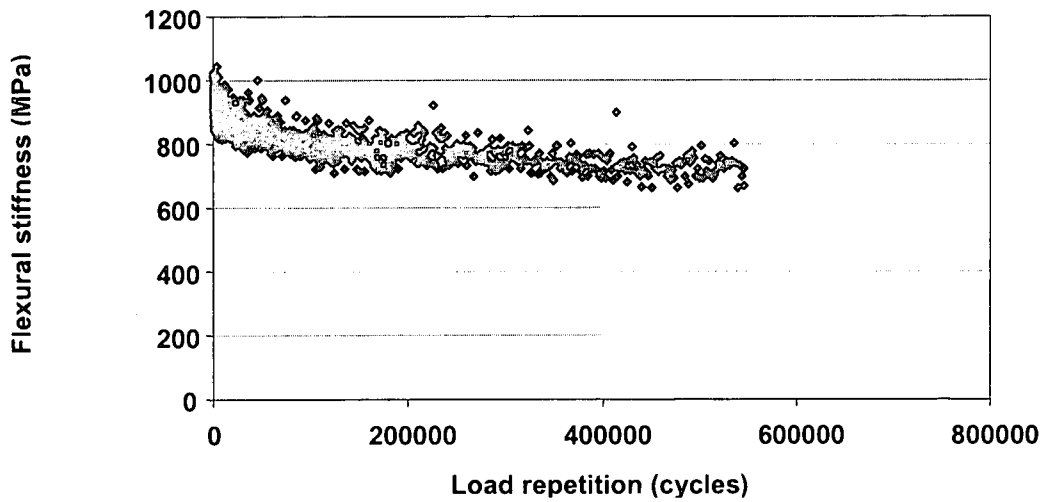


Figure C.47: Displacement control test at 200 microstrain of 5°C and 10Hz

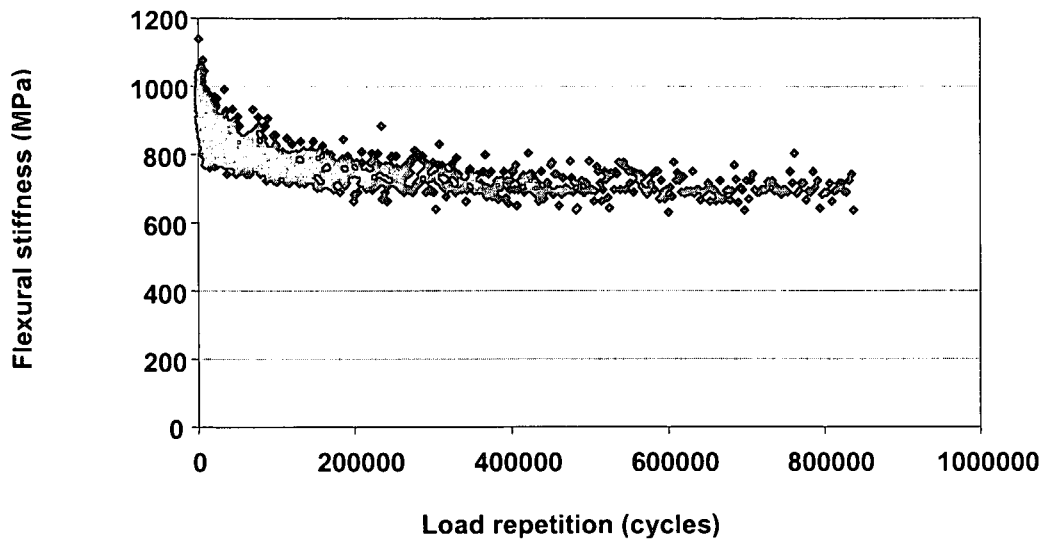


Figure C.48: Displacement control test at 180 microstrain of 5°C and 10Hz

1.5 MIX 8 (C-75C-0%)

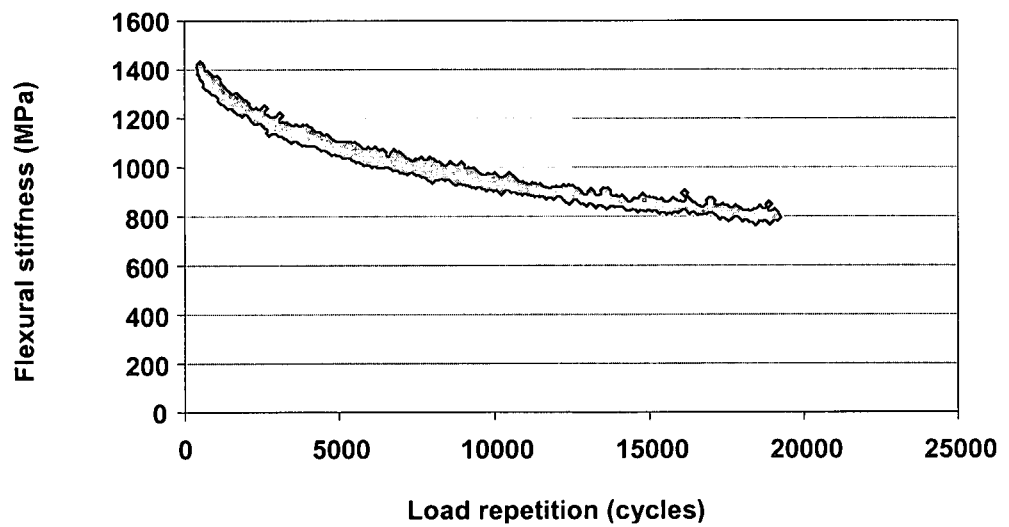


Figure C.49: Displacement control test at 470 microstrain of 5°C and 10Hz

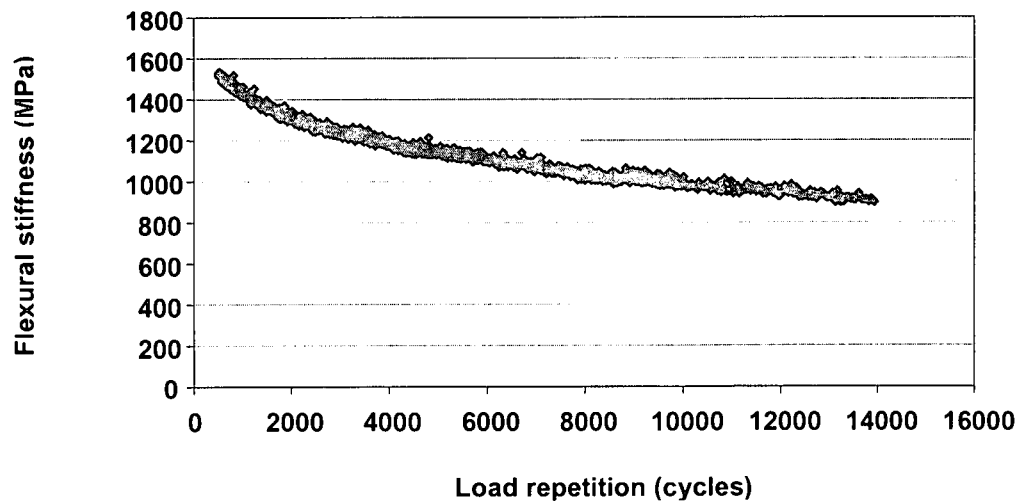


Figure C.50: Displacement control test at 450 microstrain of 5°C and 10Hz

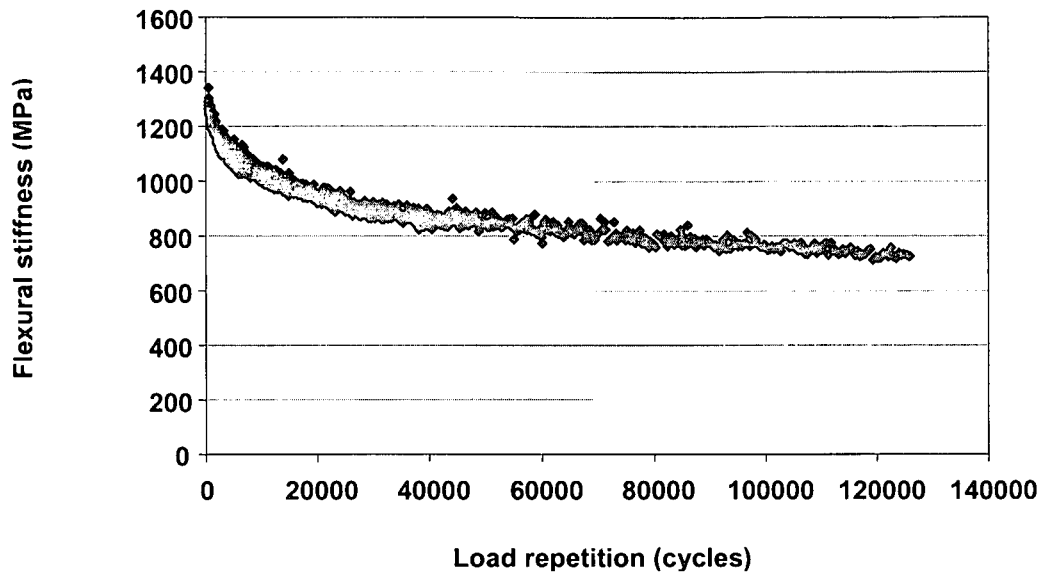


Figure C.51: Displacement control test at 400 microstrain of 5°C and 10Hz

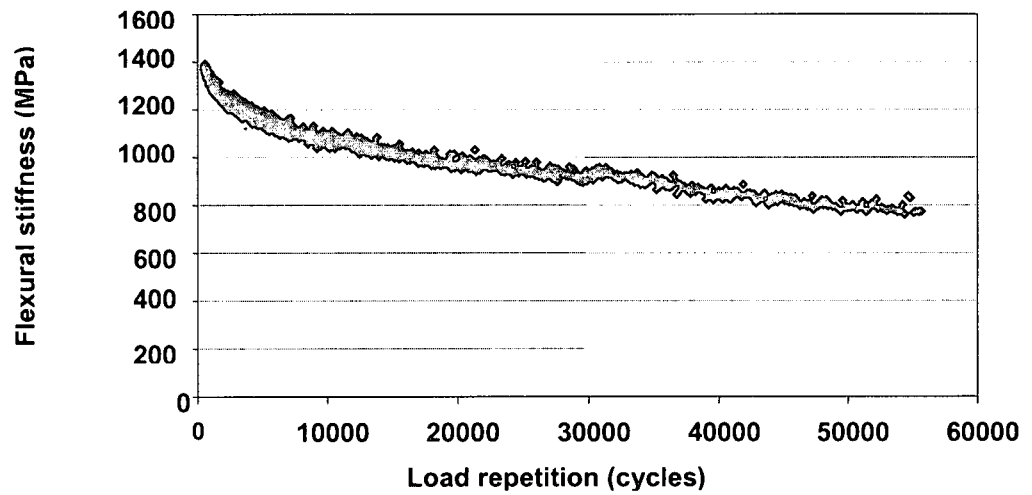


Figure C.52: Displacement control test at 380 microstrain of 5°C and 10Hz

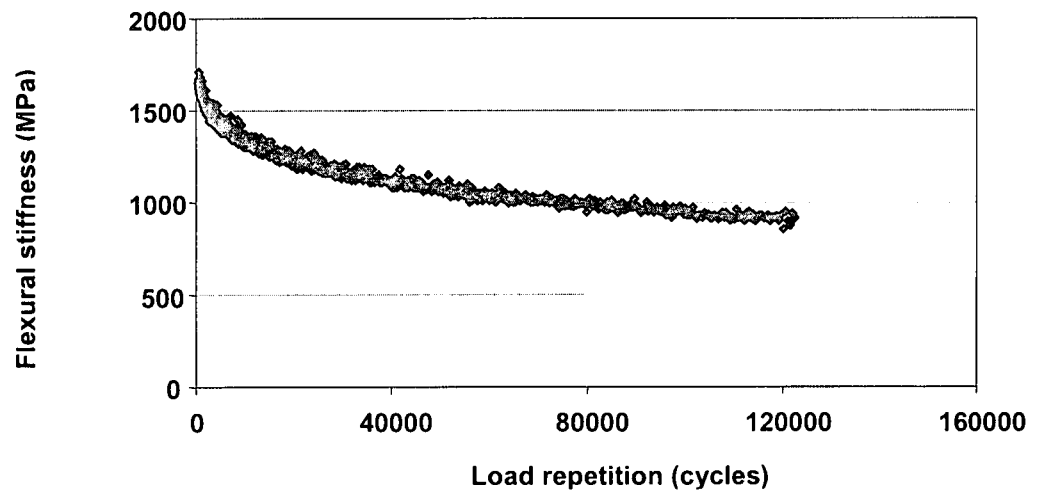


Figure C.53: Displacement control test at 350 microstrain of 5°C and 10Hz

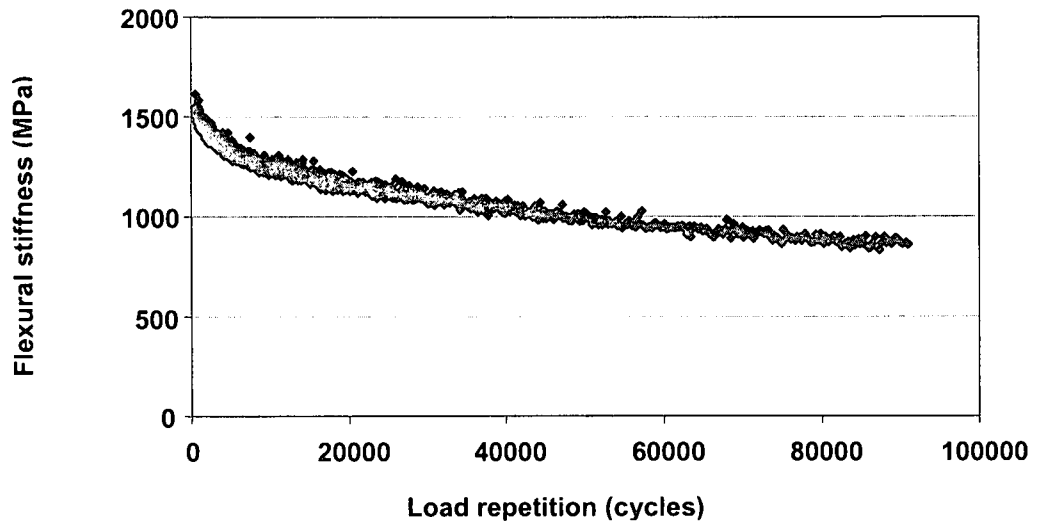


Figure C.54: Displacement control test at 330 microstrain of 5°C and 10Hz

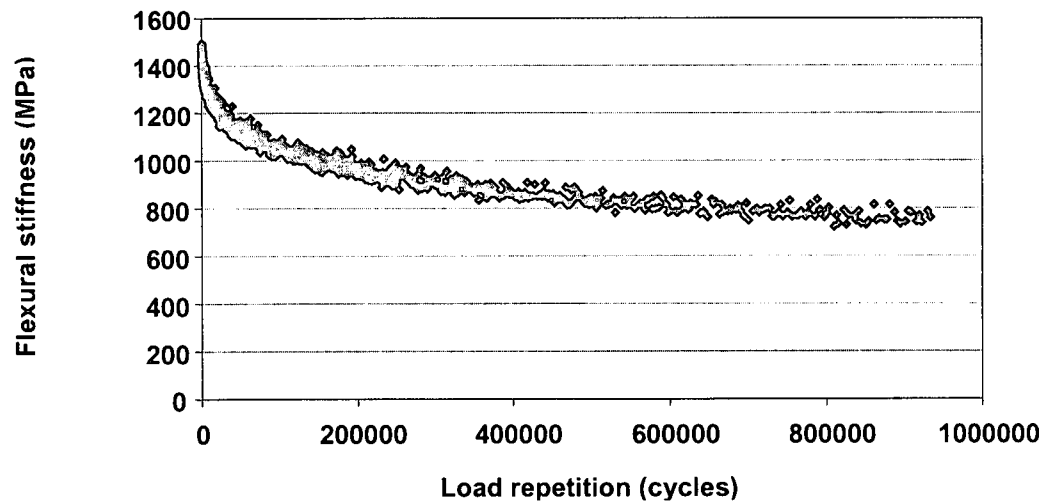


Figure C.55: Displacement control test at 300 microstrain of 5°C and 10Hz

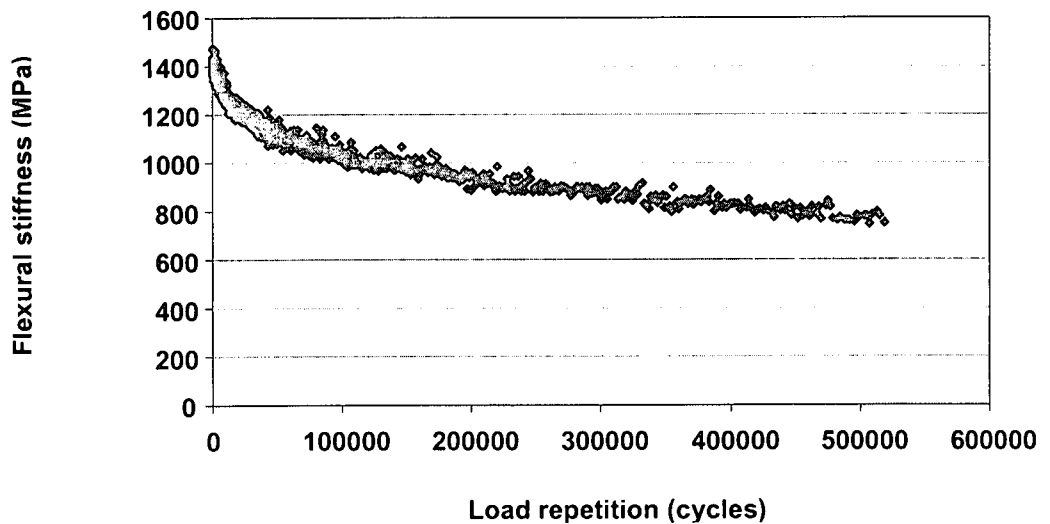


Figure C.56: Displacement control test at 280 microstrain of 5°C and 10Hz

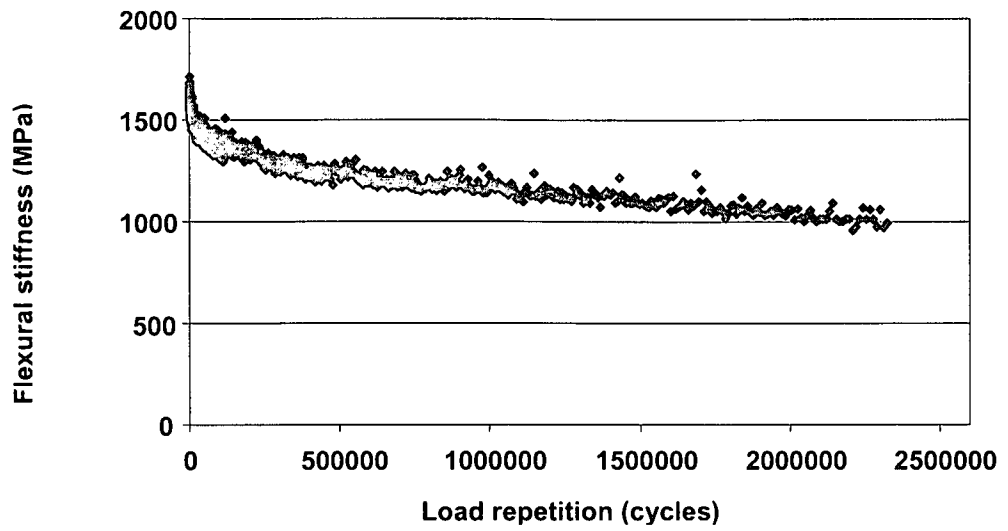


Figure C.57: Displacement control test at 250 microstrain of 5°C and 10Hz

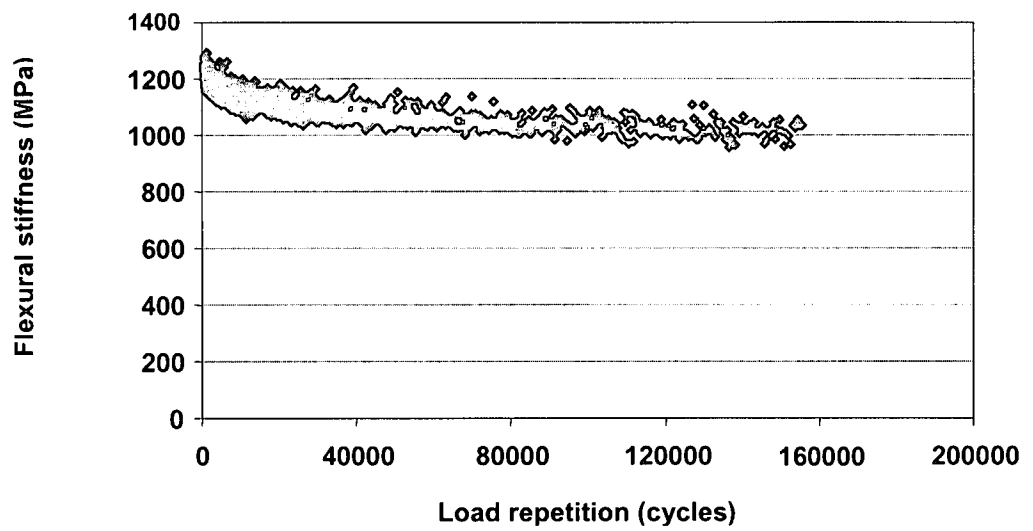


Figure C.58: Displacement control test at 230 microstrain of 5°C and 10Hz

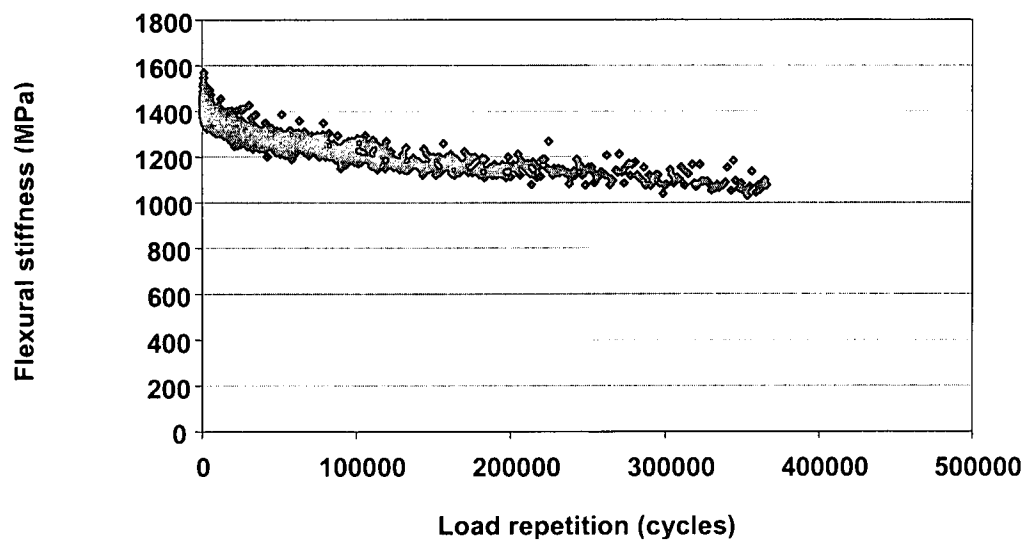


Figure C.59: Displacement control test at 200 microstrain of 5°C and 10Hz

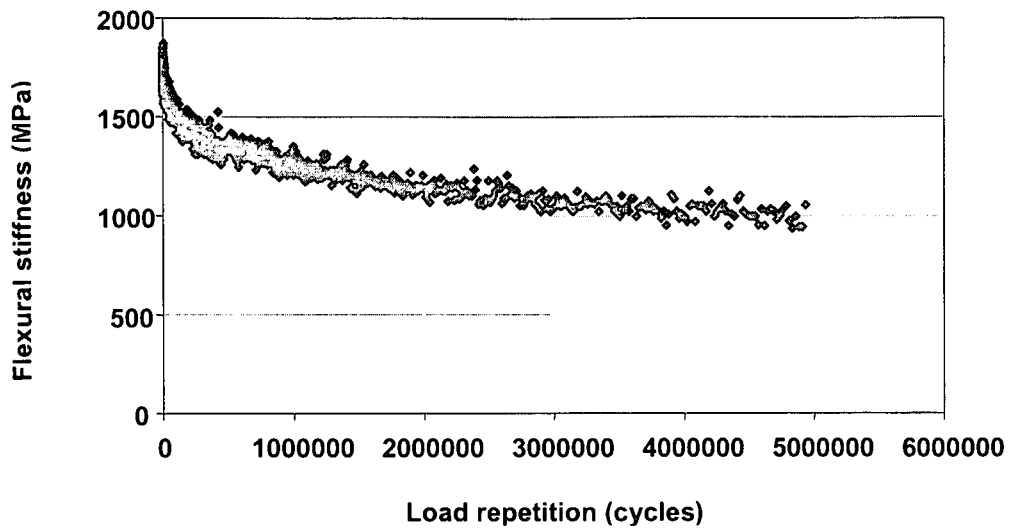


Figure C.60: Displacement control test at 180 microstrain of 5°C and 10Hz

1.6 MIX 9 (C-75M-0%)

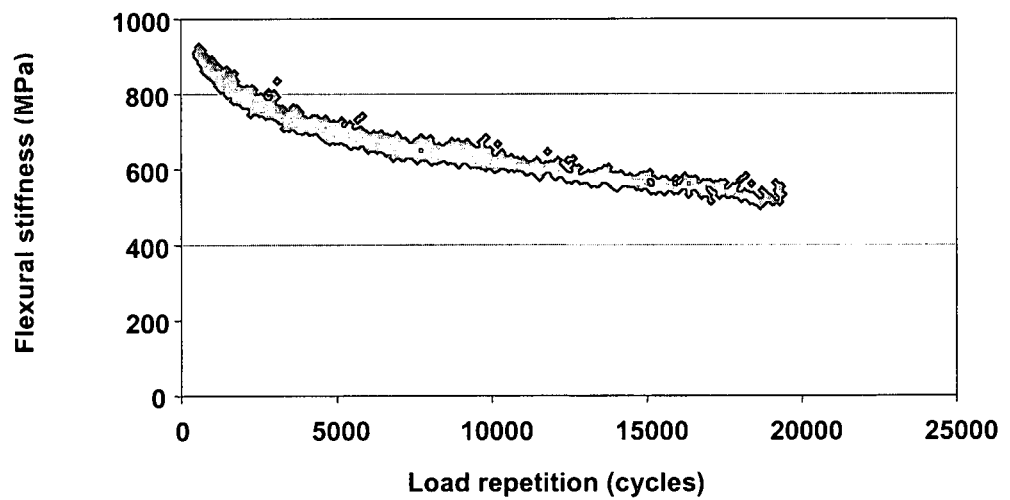


Figure C.61: Displacement control test at 470 microstrain of 5°C and 10Hz

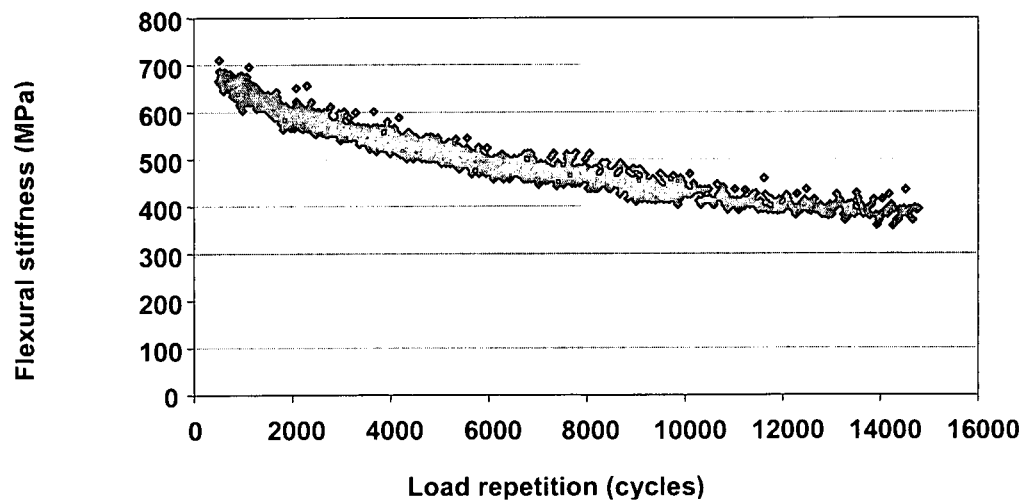


Figure C.62: Displacement control test at 450 microstrain of 5°C and 10Hz

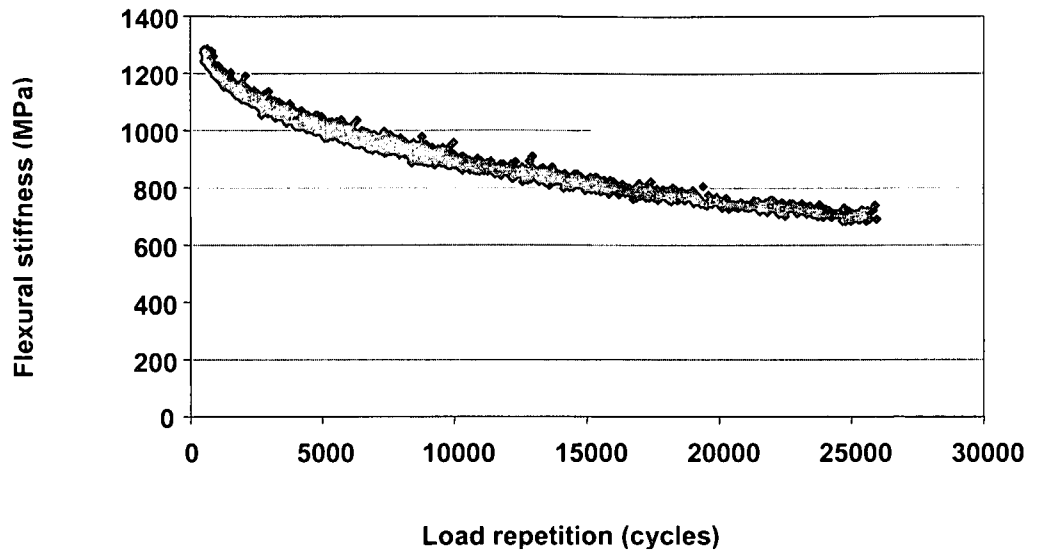


Figure C.63: Displacement control test at 400 microstrain of 5°C and 10Hz

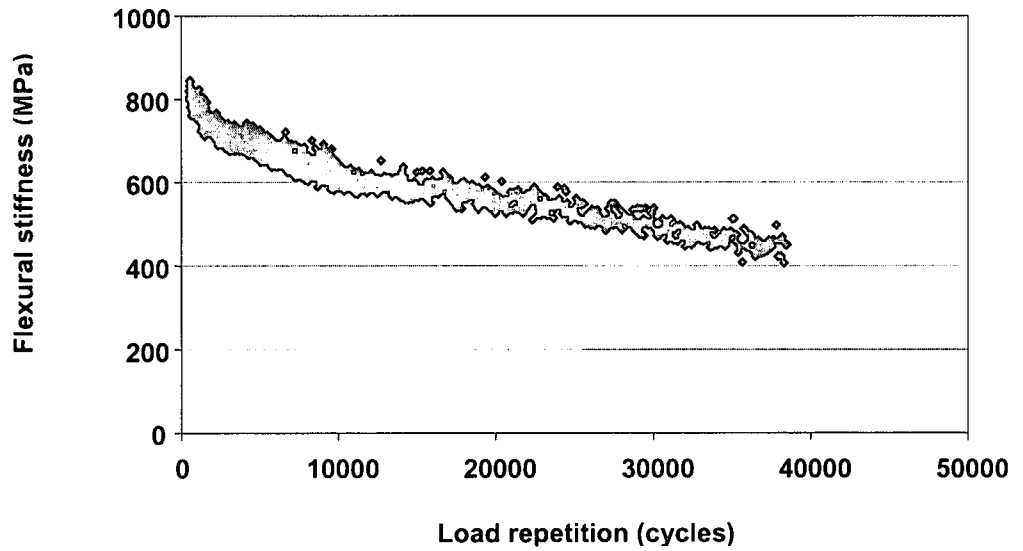


Figure C.64: Displacement control test at 380 microstrain of 5°C and 10Hz

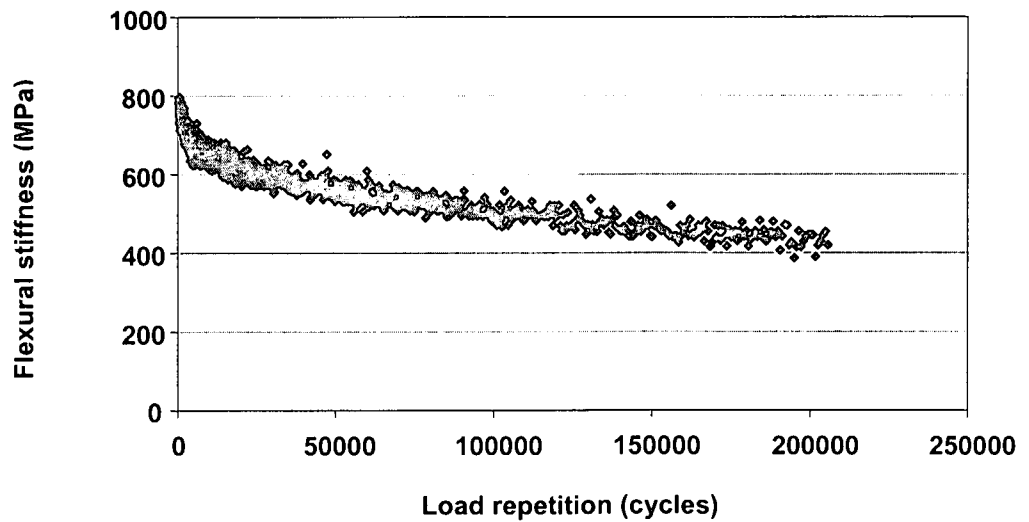


Figure C.65: Displacement control test at 350 microstrain of 5°C and 10Hz

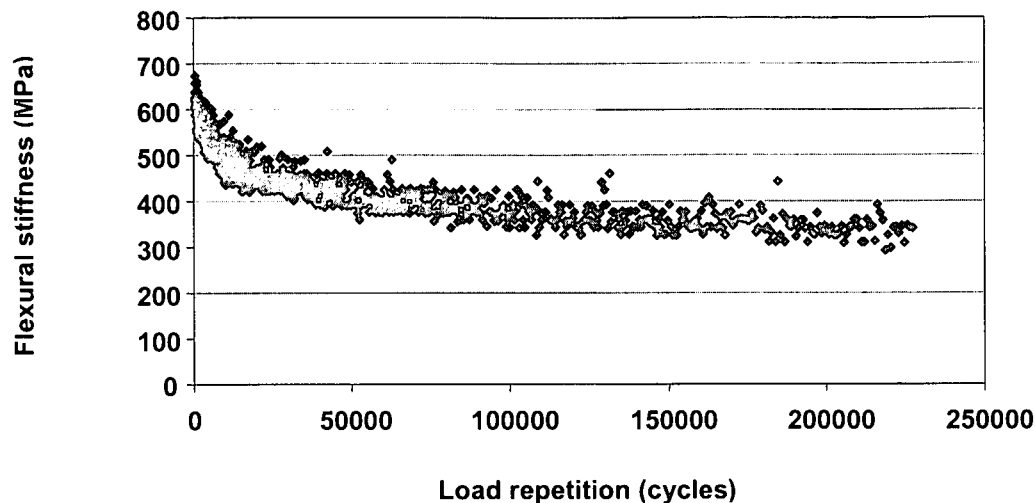


Figure C.66: Displacement control test at 300 microstrain of 5°C and 10Hz

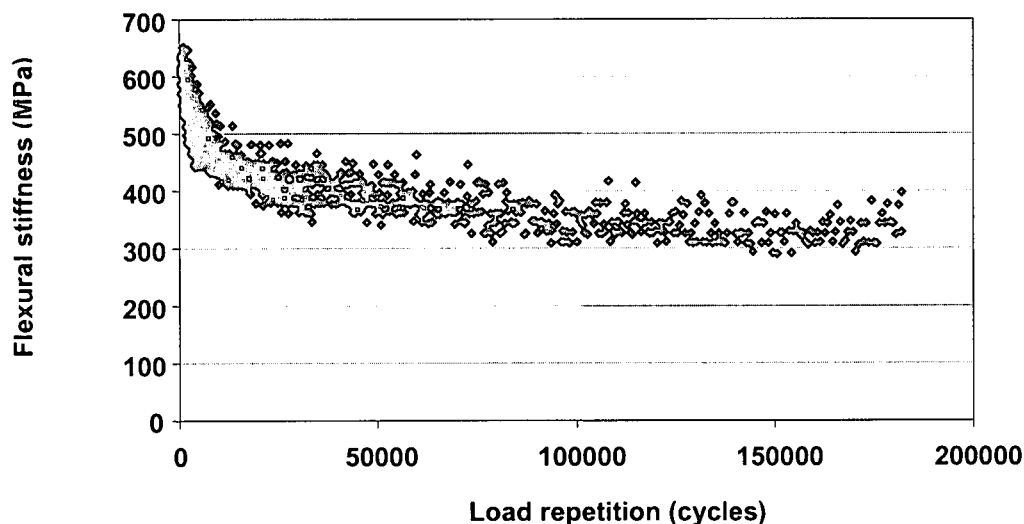


Figure C.67: Displacement control test at 280 microstrain of 5°C and 10Hz

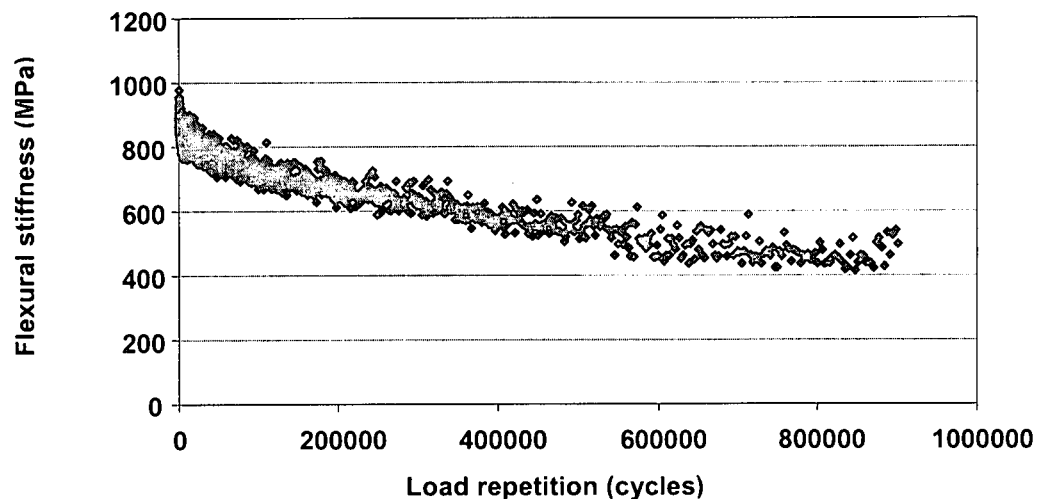


Figure C.68: Displacement control test at 250 microstrain of 5°C and 10Hz

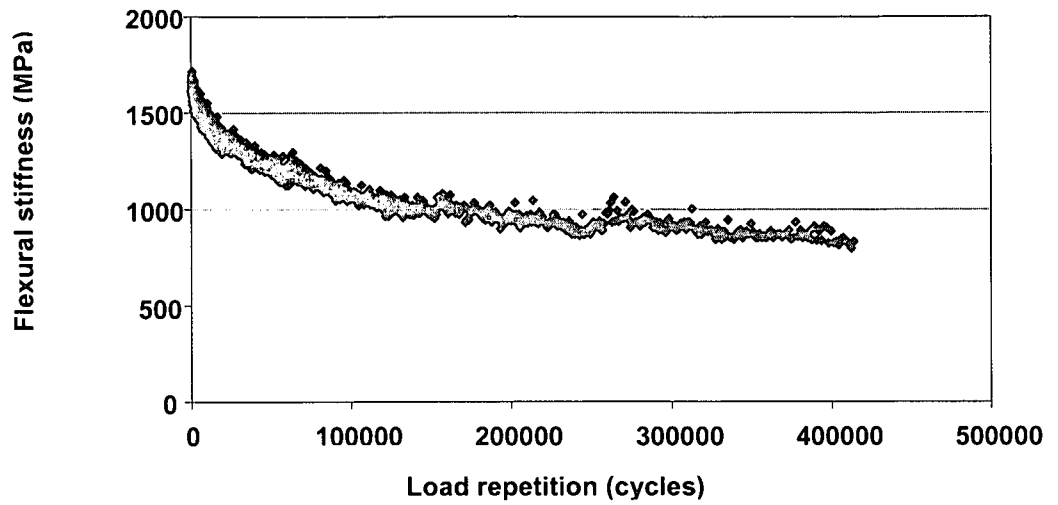


Figure C.69: Displacement control test at 250 microstrain of 5°C and 10Hz

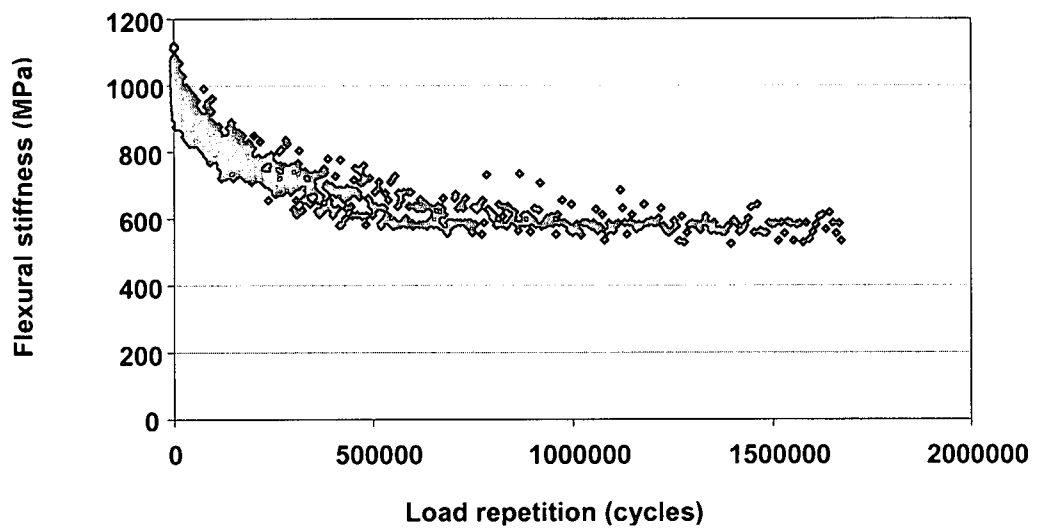


Figure C.70: Displacement control test at 200 microstrain of 5°C and 10Hz

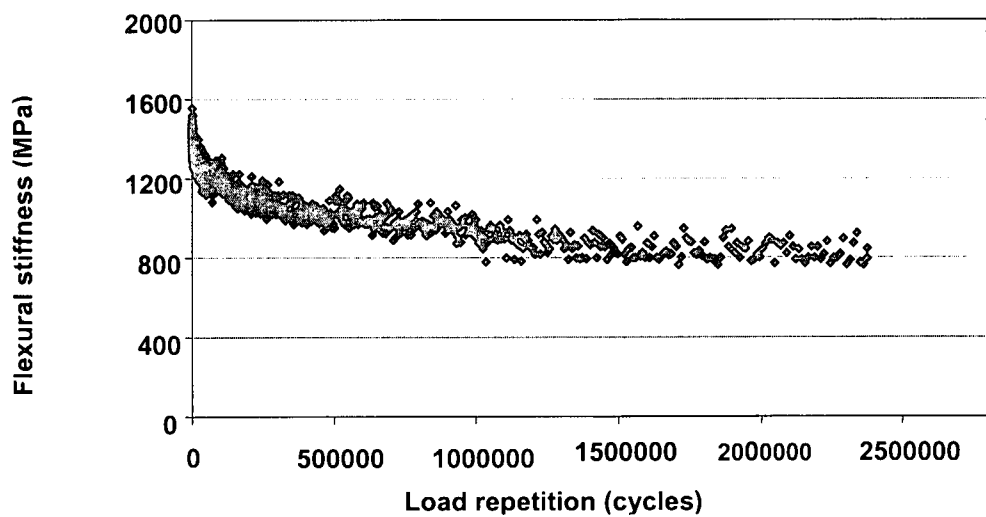


Figure C.71: Displacement control test at 200 microstrain of 5°C and 10Hz

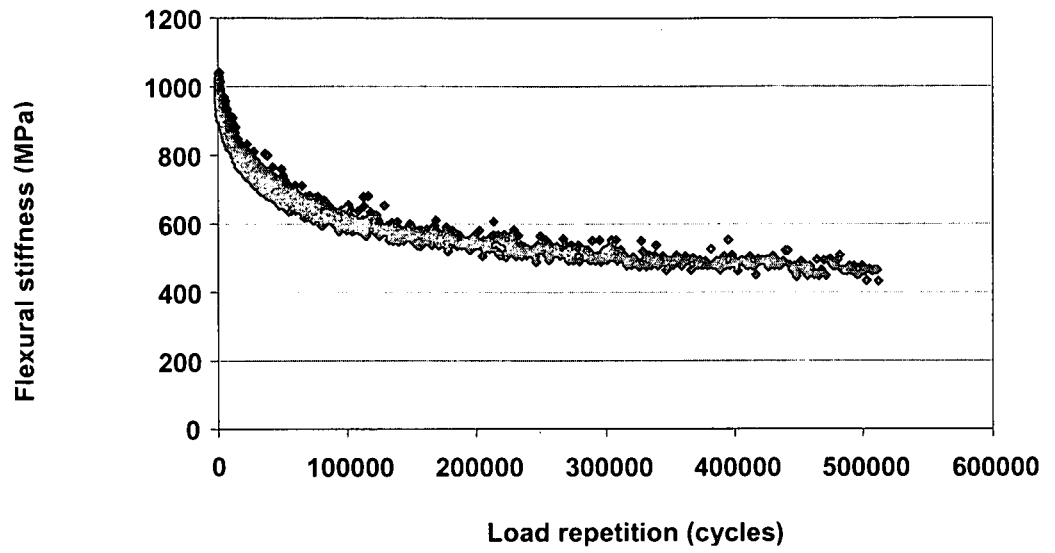


Figure C.72: Displacement control test at 330 microstrain of 5°C and 10Hz

APPENDIX D

1. CALCULATION OF PEAK DEFLECTION ON FOUR POINT BENDING BEAM LOADING

1.1 NOMECLATURE

P	= Applied load, P
M	= Moment due to applied load, PL
V	= Shear force due to applied load. P
x	= Distance along the beam neutral axis, L
y	= Distance across the beam neutral axis, L
ϕ	= Angle between tangent line, Radians
b	= Width of beam, L
h	= Depth of bam, L
L	= Distance between centre support of beam. L
A	= Cross sectional area of beam, $(A=bh)$, L^2
I	= Area moment of inertia of beam, $(I=bh^3/12)$, L^4
w	= Deflection of centre of beam due to applied load, L
E	= Elastic modulus of material, F/L^2
σ	= Normal stress applied at beam, P/A ,

1.2 DERIVATION

To determine a centre deflection $w(L/2)$, the loads are applied, which for this case is P at the four point of the beam. The applied load will generate shear force and moments as indicated in the Figure E1.

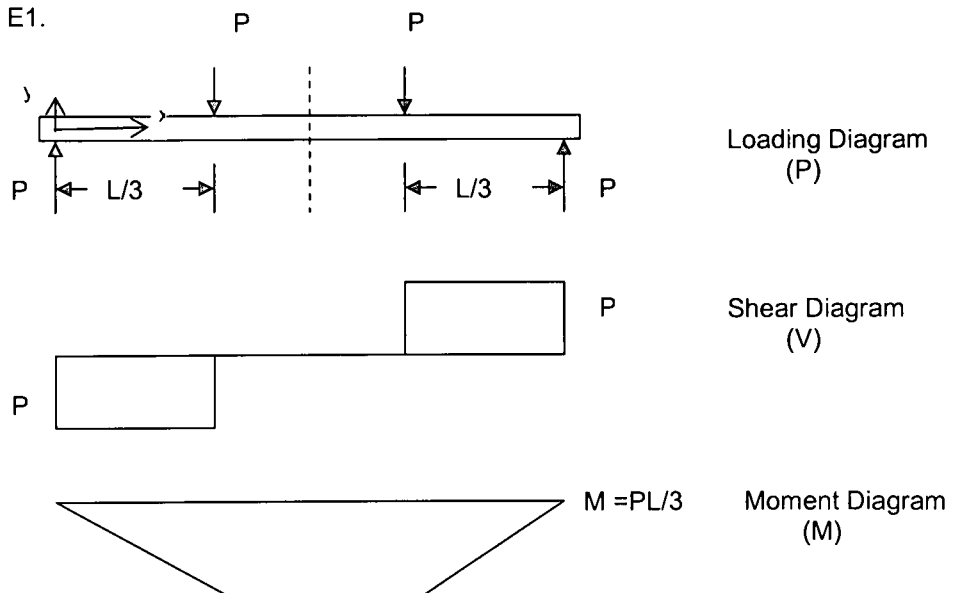
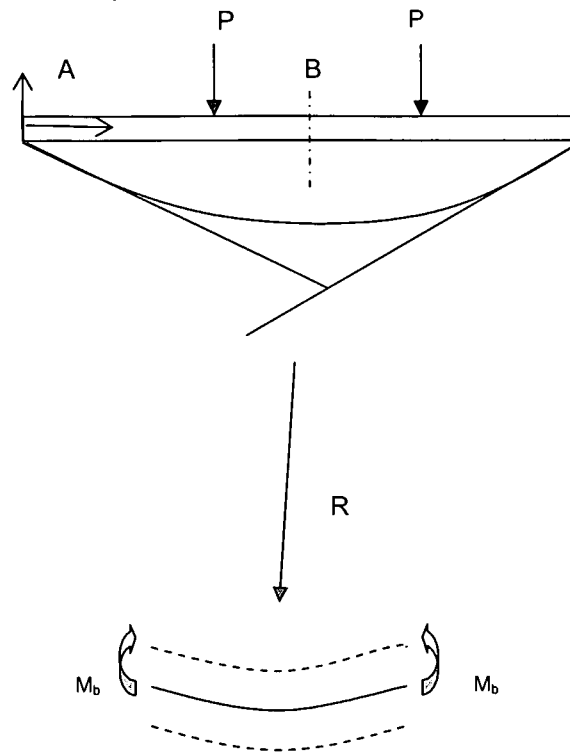


FIGURE D1: Shear and Moment diagrams due to applied load P at Four Point Bending

Consider a simple beam of rectangular cross-section, the deflection of beam curve due to applied loads is shown in Figure B3.



The significant stress is the normal stress on the x-axis, $\sigma_x = \frac{M_b \cdot y}{I}$, $I = \frac{bh^3}{12}$,

Bending Stiffness is defined as a product of EI. The change in slope of tangent line to deflection curve function $w(x)$ is given by;

$$\varphi_B = \varphi_A + \int_A^B \frac{M}{EI} \quad (\text{E.1})$$

- Where
- φ_B = Angle between tangent line to deflection $w(x)$ at B and centre.
 - $\varphi_B = 0$
 - φ_A = Angle between tangent line to deflection at A and centre (Max slope)
 - \int = Change in slope at any point in deflection curve between A and B

From Equation E.1:

$$0 = \varphi_A + \int_A^B \frac{M}{EI} \quad (\text{E.2})$$

$$\varphi_A = - \int_A^B \frac{M}{EI}$$

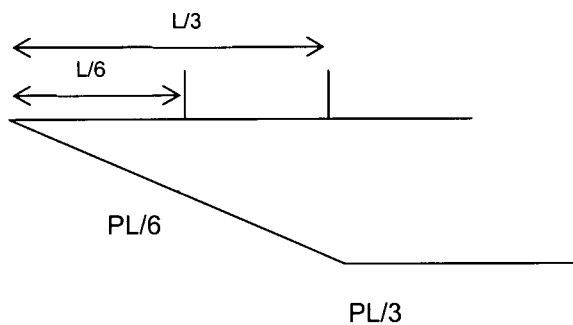
The Area under Bending Moment Diagram between A and B is equivalent to max slope given as:

$$\begin{aligned}\phi_A &= \frac{1}{2} \cdot P \frac{L}{3} + \frac{1}{3} \cdot P \frac{L}{3} \cdot \frac{L}{3} \\ &= - \frac{PL^2}{9EI}\end{aligned}\tag{E.3}$$

(-ve) sign indicate deflection is in opposite of y direction or downwards.

The deflection, $w(A)$ at point A (support) is equal to zero; $w(A) = 0$

However conventional Four Point Beam test is done with two loading geometry $a = L/3$ and $L/6$, thus;



$$\begin{aligned}\phi(L/6) &= \phi_A - \int_0^{L/6} \frac{M}{EI} dx \quad : \text{Area under } L/6 \text{ deflection is (-ve)} \\ &= - \frac{PL^2}{9EI} + \frac{1}{2} \cdot \frac{1}{EI} \cdot \frac{PL}{6} \cdot \frac{L}{6}\end{aligned}\tag{E.4}$$

$$\phi(L/6) = - \frac{7PL^2}{72EI}$$

Deflection at $a = L/6$:

$$\begin{aligned}\omega(L/6) &= \omega_A - \phi_A \cdot L/6 - \int_0^{L/6} \frac{M}{EI} \cdot \frac{L}{6} dx \\ &= 0 - \frac{PL^2}{9EI} \cdot \frac{L}{6} + \frac{7PL^2}{72EI} \cdot \frac{1}{3} \cdot \frac{L}{6} \\ \omega(L/6) &= \frac{23PL^3}{1296EI}\end{aligned}\tag{E.5}$$

$$\text{Slope at } a = L/3: \quad \varphi(L/3) = -\frac{PL^2}{9EI} + \frac{1}{2} \cdot \frac{PL}{3EI} \cdot \frac{L}{3} \quad (\text{E.6})$$

$$\varphi(L/3) = -\frac{PL^2}{18EI}$$

$$\begin{aligned} \text{Deflection at } a = L/3 \quad \omega(L/3) &= 0 + \frac{PL^2}{9EI} \cdot \frac{L}{3} - \frac{PL^2}{18EI} \cdot \frac{1}{3} \cdot \frac{L}{3} \\ &= \frac{5PL^3}{162EI} \end{aligned} \quad (\text{E.7})$$

The maximum deflection at the centre of beam

$$\begin{aligned} \text{Slope at } a = L/2 \quad \varphi(L/2) &= \varphi(L/3) + \int_{L/3}^{L/2} \frac{M}{EI} dx \\ &= -\frac{PL^2}{18EI} + \frac{PL}{EI} \cdot \frac{1}{2} \cdot \frac{L}{3} \\ &= 0 \end{aligned}$$

$$\begin{aligned} \text{Deflection at } a = L/2 \quad \omega(L/2) &= \omega(L/3) - j(L/3) \cdot \left(\frac{L}{2} - \frac{L}{3}\right) - \int_{L/3}^{L/2} \frac{M}{EI} dx \\ &= \frac{5PL^3}{162EI} + \frac{PL^2}{18EI} \cdot \frac{L}{6} - \frac{PL^2}{18EI} \cdot \frac{L}{12} \\ &= \frac{20PL^3}{648EI} + \frac{6PL^3}{648EI} - \frac{3PL^3}{648EI} \\ &= \frac{23PL^3}{648EI} \end{aligned} \quad (\text{E.8})$$

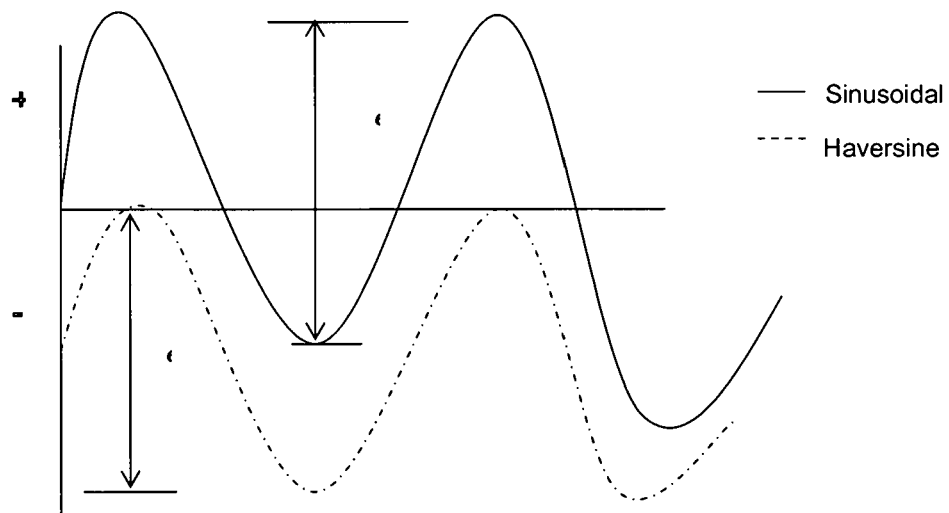
From Equation E.5 and E.8 it is clear that $\omega(L/2)$ is equal to $2x\omega(L/6)$. This indicates that the IPC On-Spacemen LVDT capture the $L/6$ deflection and not the maximum centre deflection. Therefore the peak deflections are evaluated from the actuator LVDT which measures the actual deflection mounted under the reaction frame.

APPENDIX D

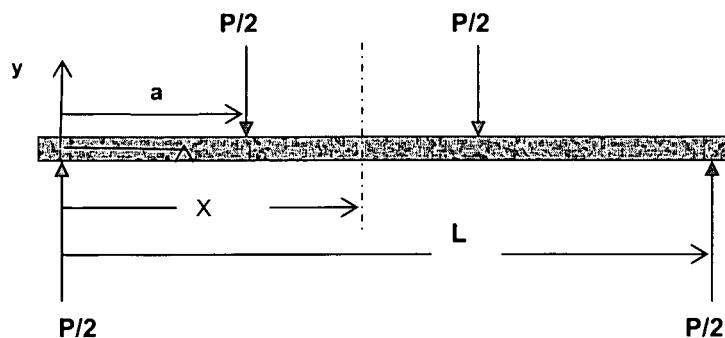
2. TENSILE STRAIN CALCULATION FOR THE FOUR POINT BENDING BEAM TEST (UTM 21 FEEDBACK CONTROLLED BEAM FATIGUE TEST CALCULATION).

2.1 DERIVATION

IPC testing software use default signals as haversine instead of normal sine i.e. the given stress/strain values are peak – peak values.



The fundamental of flexural beam bending using IPC BFA are illustrated in this appendix as follows:



From James M. Gere (Mechanics of Materials, 2001, page 895) it shows that the deflection of beam at any point between the inner loading points is given by:

$$y = \frac{Pa [3Lx - 3x^2 - a^2]}{12EI} \quad (\text{F.1})$$

For maximum deflection $x = L/2$ putting in Equation F.1 and replacing y by δ (taking modulus only) we get

$$\delta = \frac{Pa[3L^2 - 4a^2]}{48EI} \quad (\text{F.2})$$

Then replace E by Stress-Strain relation we get:

$$\delta = \frac{Pa[3L^2 - 4a^2]\epsilon}{48I \frac{Mc}{I}} \quad (\text{F.3})$$

Moment at the section along the center of the beam is given by:

$$M = \frac{Pa}{2}$$

Taking $c=h/2$, we get the deflection as follows:

$$\delta = \frac{Pa[3L^2 - 4a^2]\epsilon}{48 \frac{P}{2} \times \frac{h}{2}}$$

$$\delta = \frac{[3L^2 - 4a^2]\epsilon}{12h} \quad (\text{F.4})$$

$$\epsilon = \frac{12\delta h}{[3L^2 - 4a^2]}$$

IPC software use $L=Go$ as Outer Gauge length and $a=Gi$ as Inner Gauge length in the Calculation for the stress and strain given in Chapter 4.

APPENDIX E

1 GRAPHS OF STRAIN-AT-BREAK TEST RESULTS CAPTURED BY CADS FOR ANALYSIS OF DEFORMATION AT FAILURE

Note: Three beam were tested in each mix for repeatability

1.1 MIX 4 (B-75C-0%)

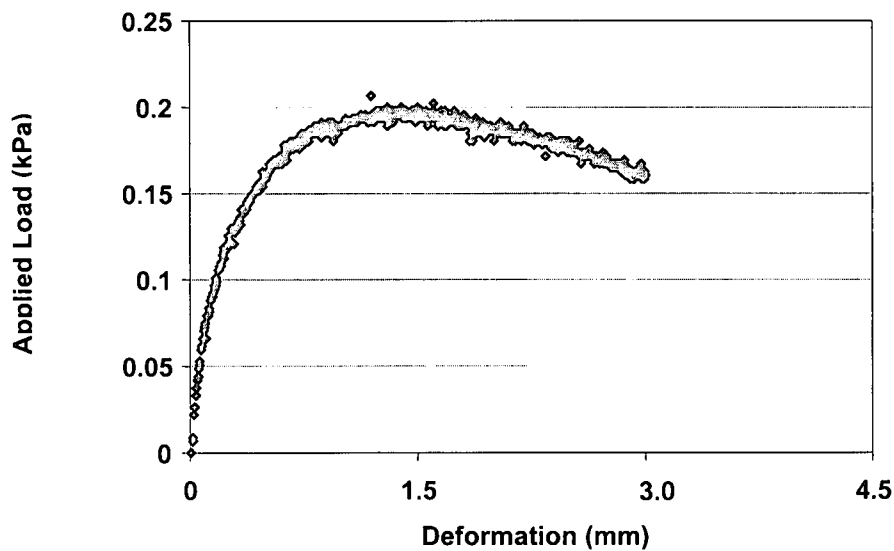


Figure C.1: Displacement control test at 1mm/min and 5°C

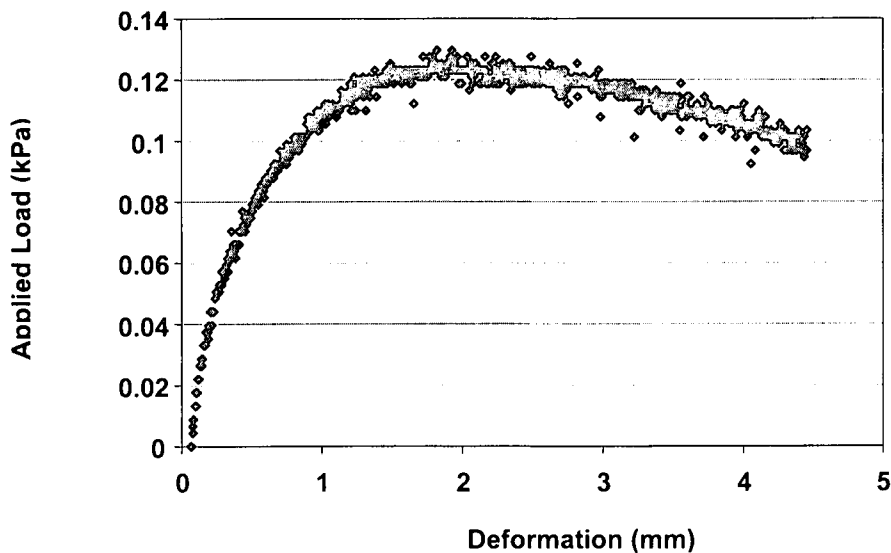


Figure C.2: Displacement control test at 1mm/min and 5°C

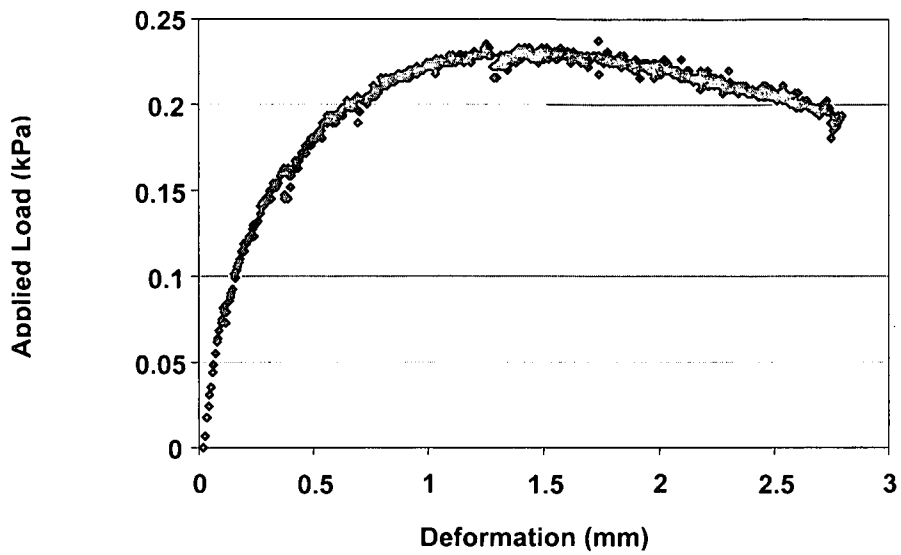


Figure C.3: Displacement control test at 1mm/min and 5°C

1.2 MIX 5 (B-75C-1%)

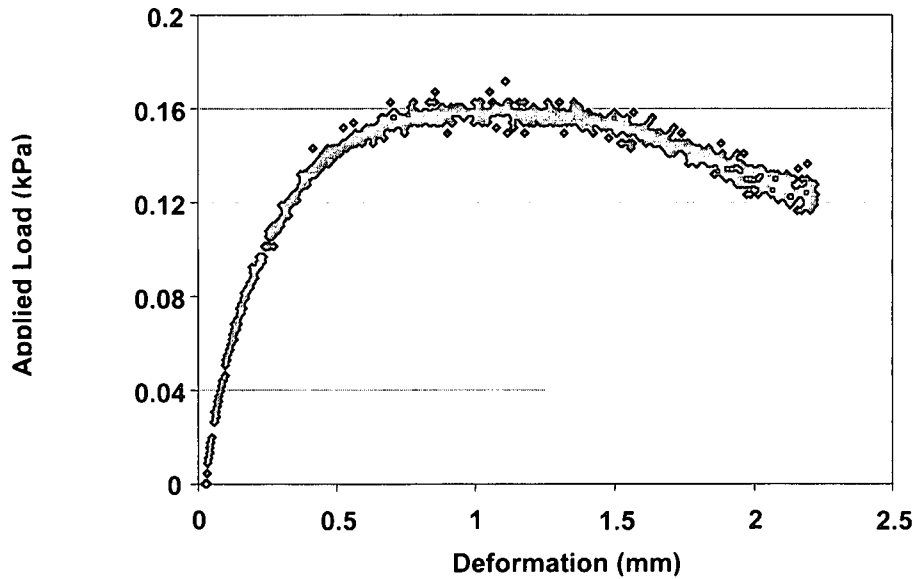


Figure C.4: Displacement control test at 1mm/min and 5°C

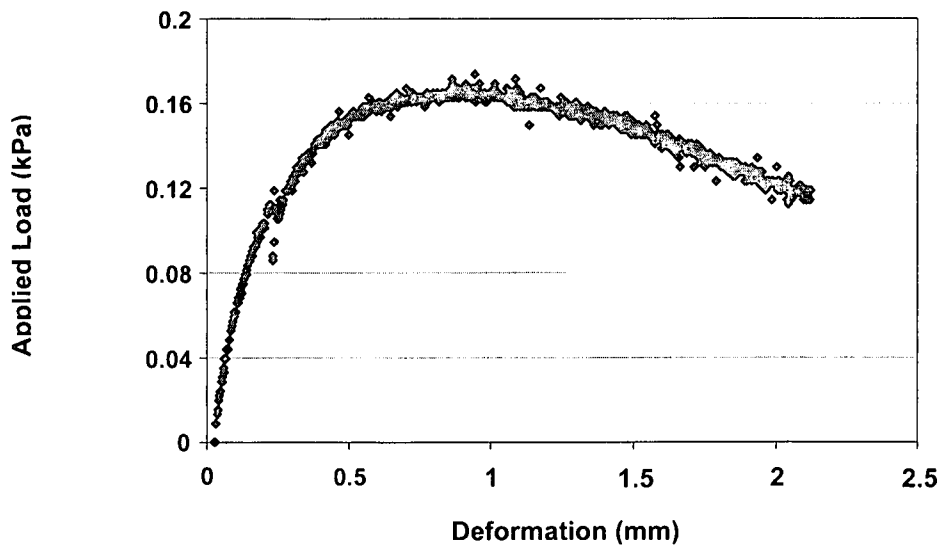


Figure C.5: Displacement control test at 1mm/min and 5°C

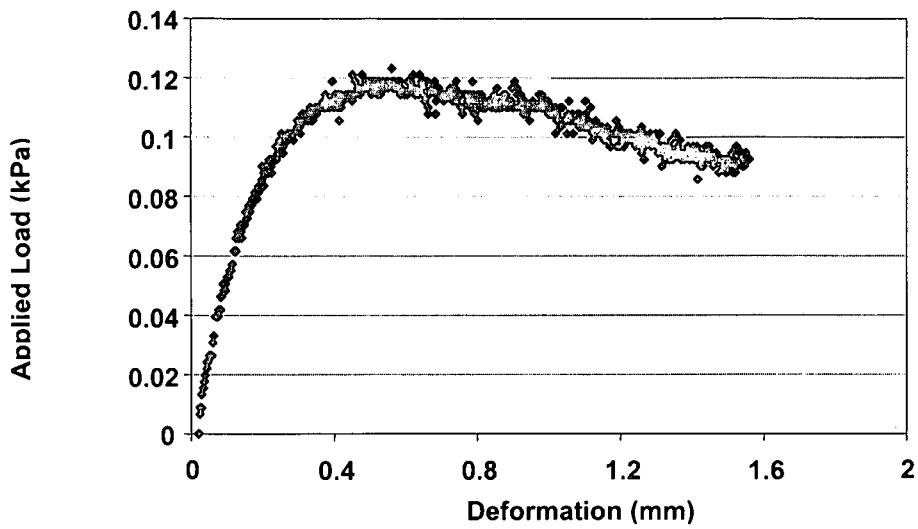


Figure C.6: Displacement control test at 1mm/min and 5°C

1.3 MIX 6 (B-75M-0%)

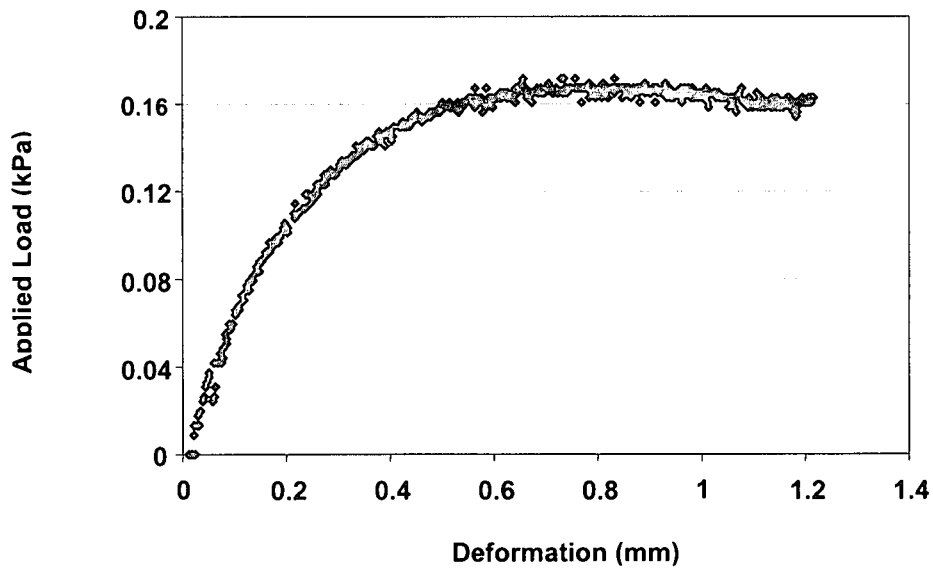


Figure C.7: Displacement control test at 1mm/min and 5°C

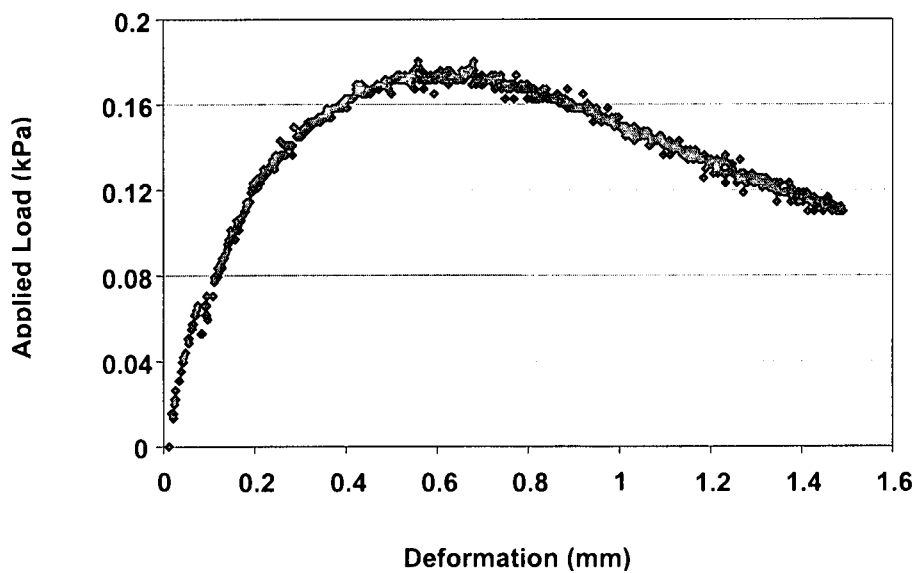


Figure C.8: Displacement control test at 1mm/min and 5°C

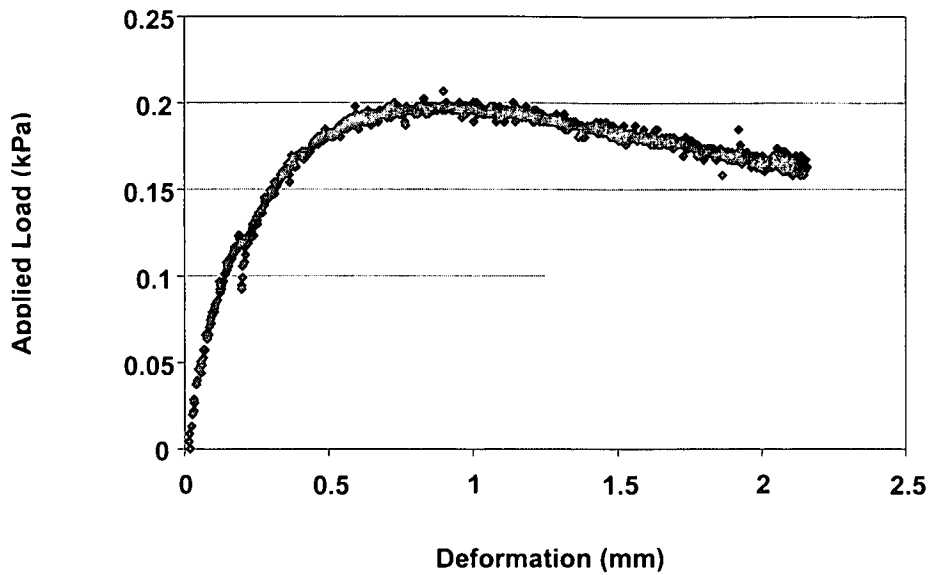


Figure C.9: Displacement control test at 1mm/min and 5°C

1.4 MIX 7 (C-75C-0%)

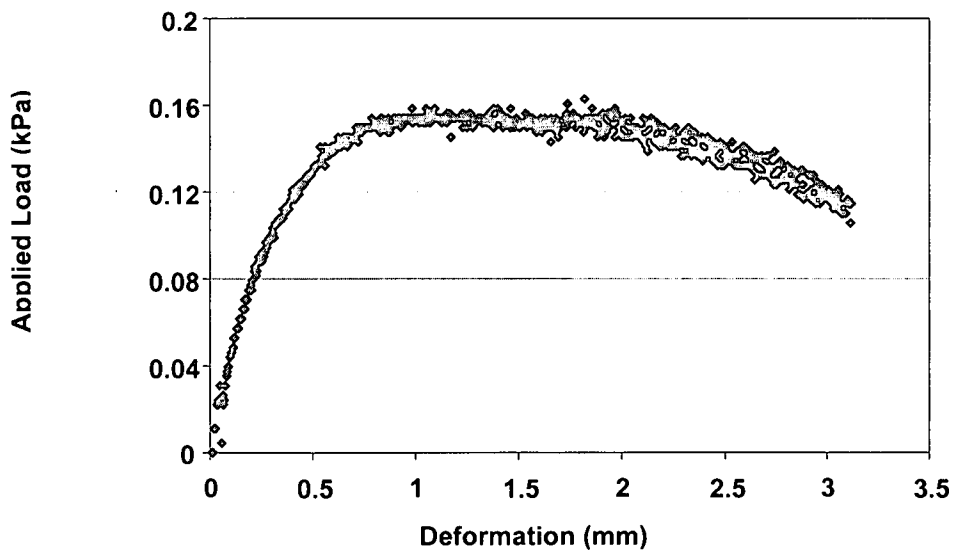


Figure C.10: Displacement control test at 1mm/min and 5°C

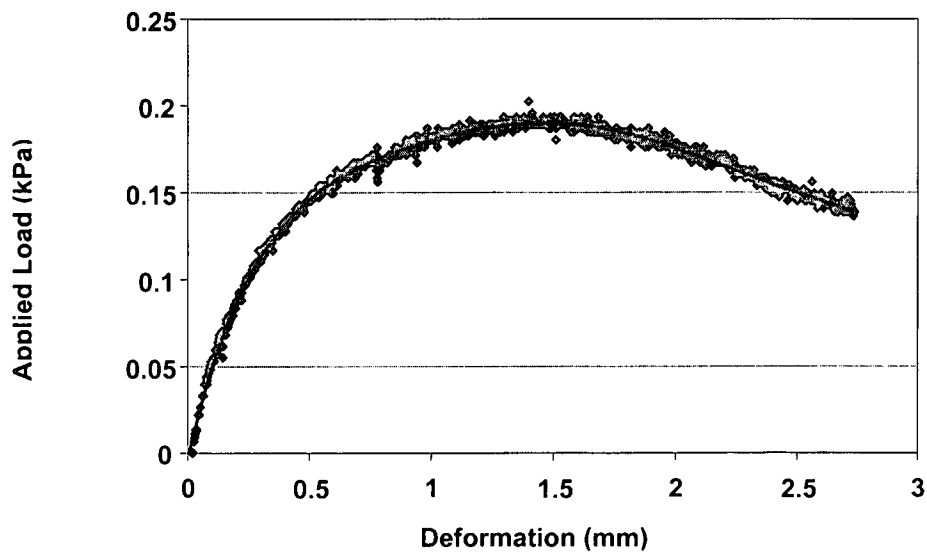


Figure C.11: Displacement control test at 1mm/min and 5°C

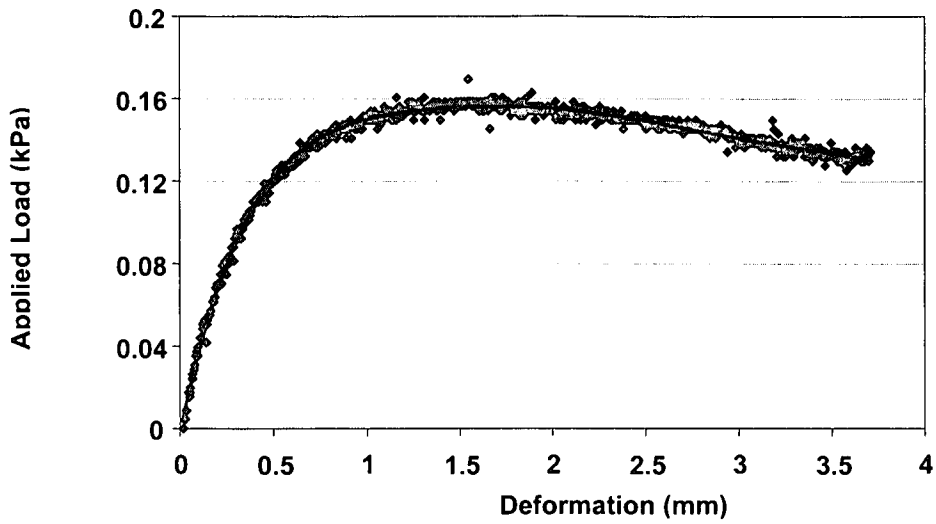


Figure C.12: Displacement control test at 1mm/min and 5°C

1.5 MIX 8 (C-75C-1%)

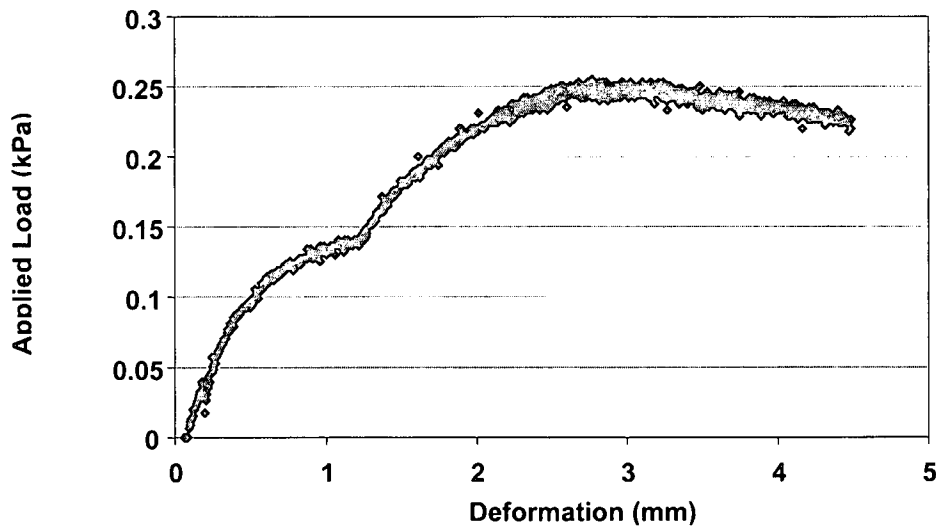


Figure C.13: Displacement control test at 1mm/min and 5°C

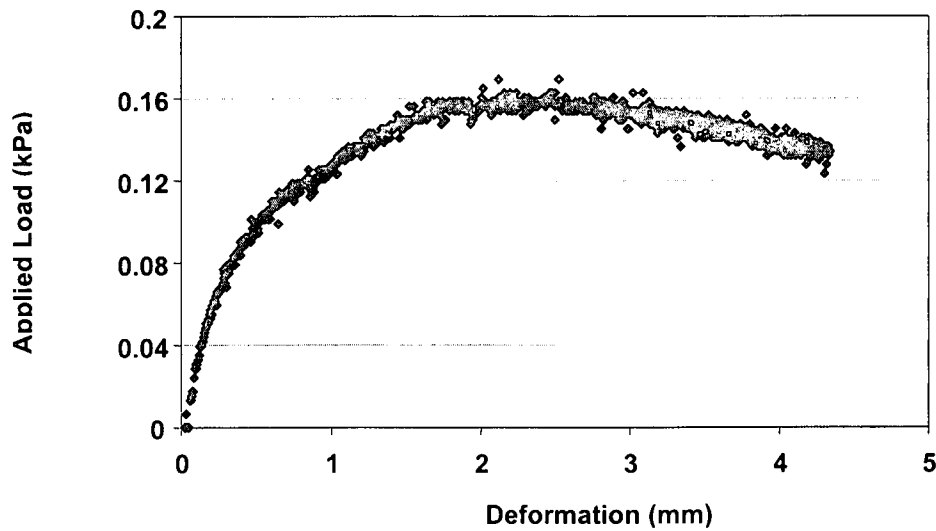


Figure C.14: Displacement control test at 1mm/min and 5°C

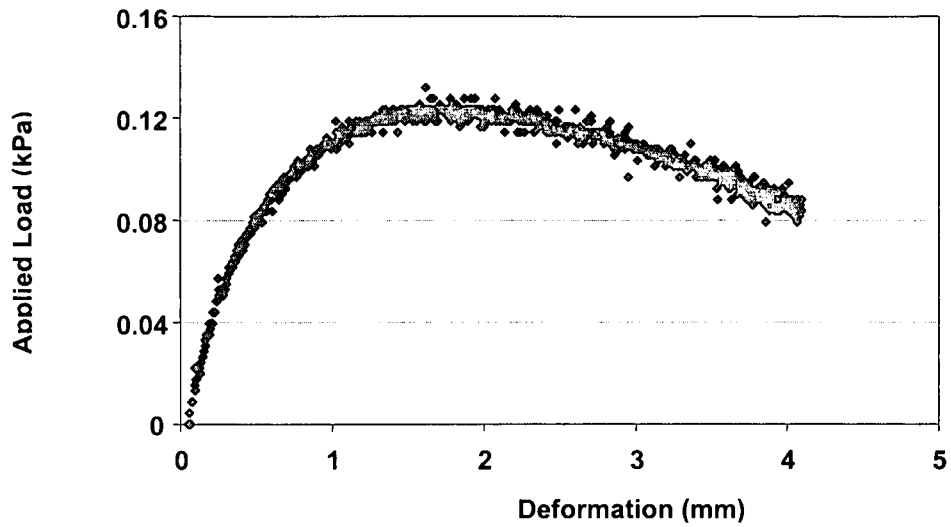


Figure C.15: Displacement control test at 1mm/min and 5°C

1.6 MIX 9 (B-75M-0%)

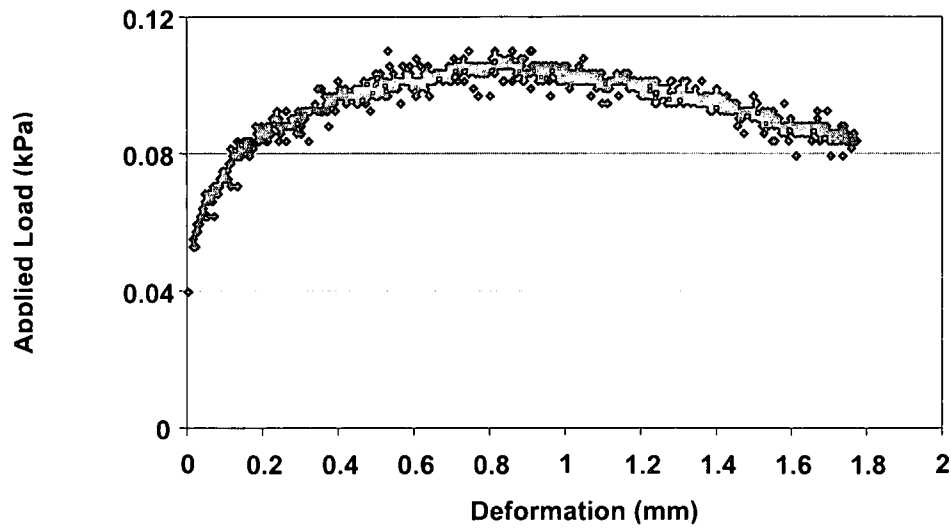


Figure C.16: Displacement control test at 1mm/min and 5°C

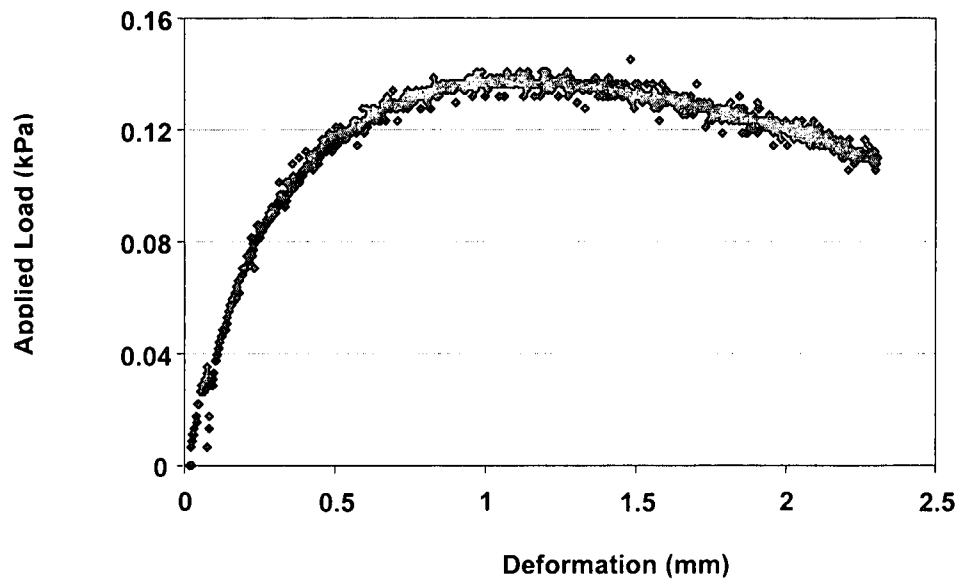


Figure C.17: Displacement control test at 1mm/min and 5°C

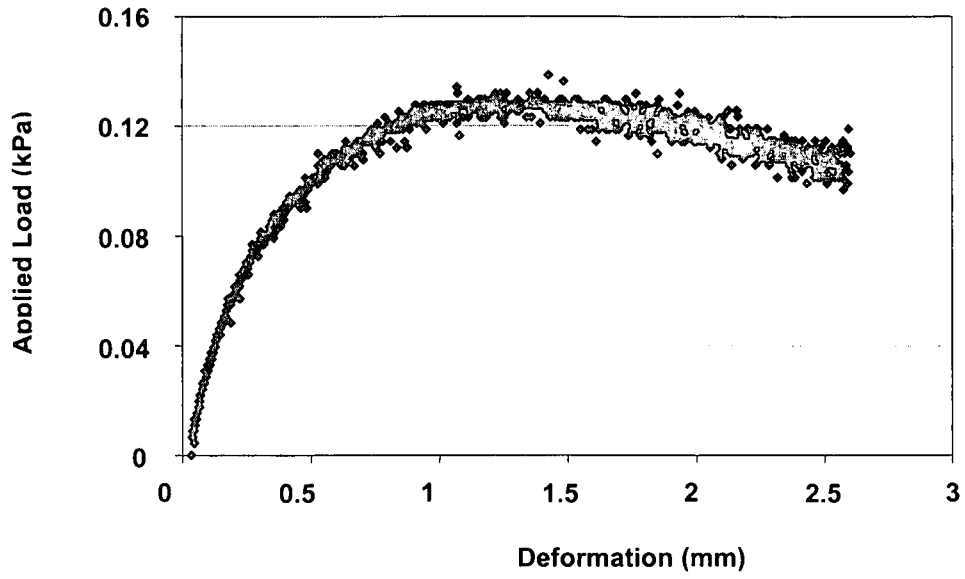


Figure C.18: Displacement control test at 1mm/min and 5°C

APPENDIX F

1. SUPERIMPOSITION OF FLEXURAL STIFFNESS MASTER CURVES OF REPEAT TEST FOR THE EMULSION MIXES

1.1 GENERAL

Specimens shall be tested in accordance with the procedure detailed in this section. (Note: Details of operating procedure for the Beam Fatigue Apparatus (BFA) are provided in the Manufacturer's Operation Manual, and reference must be made to the Manual for any specific information.). The general procedure for testing each beam specimen is detailed in Section 1.2.

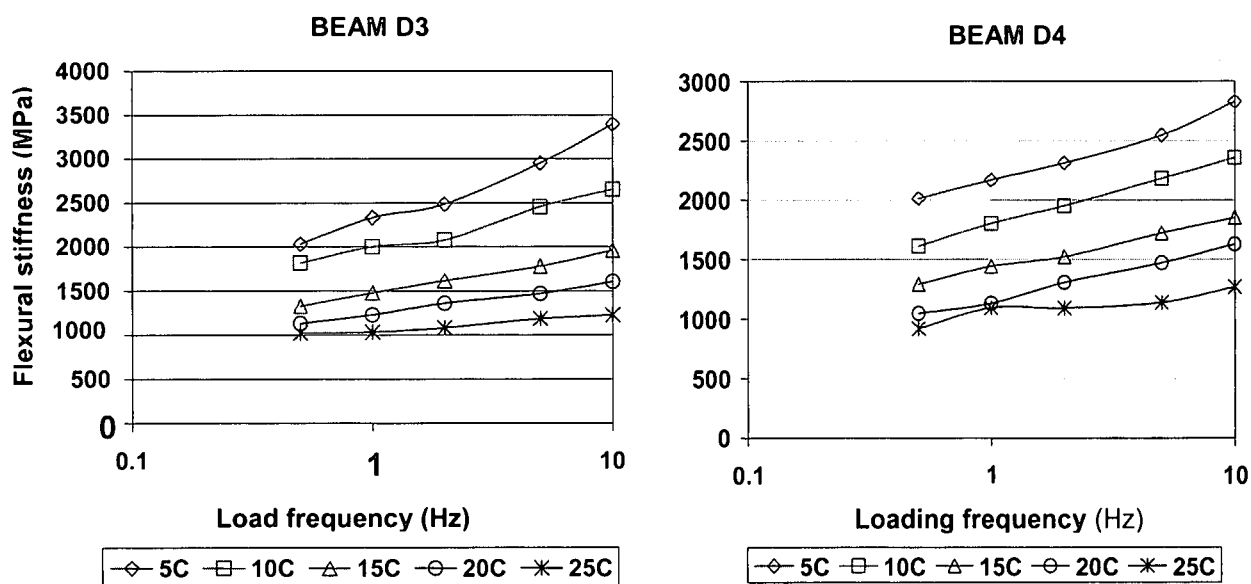


Figure F1: Stiffness modulus frequency sweep at various temperature of Mix 4(B-75C-0%)

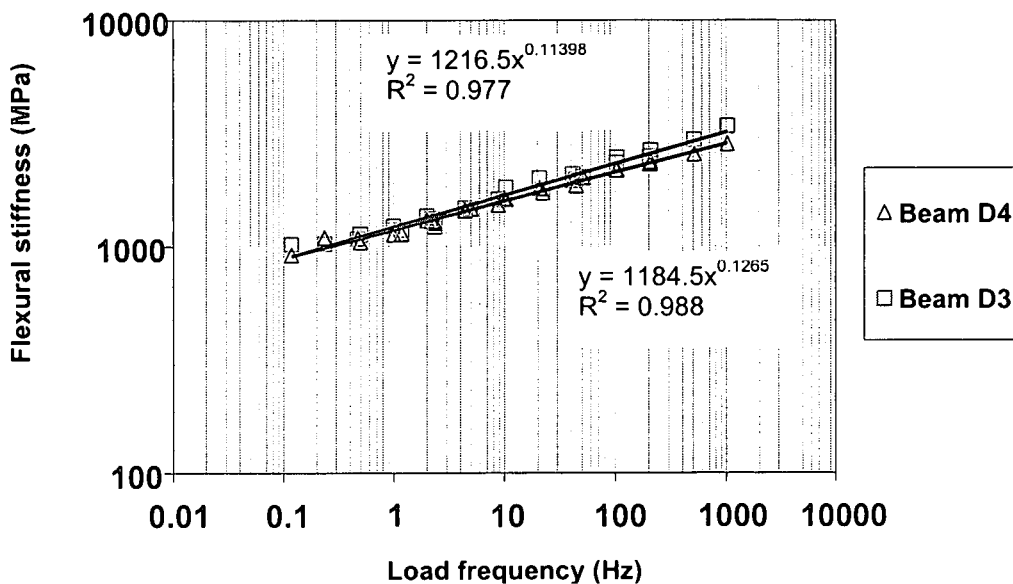


Figure F2: Stiffness characterisation of emulsion Mix 4(B-75C-0%) at various freq. and temp

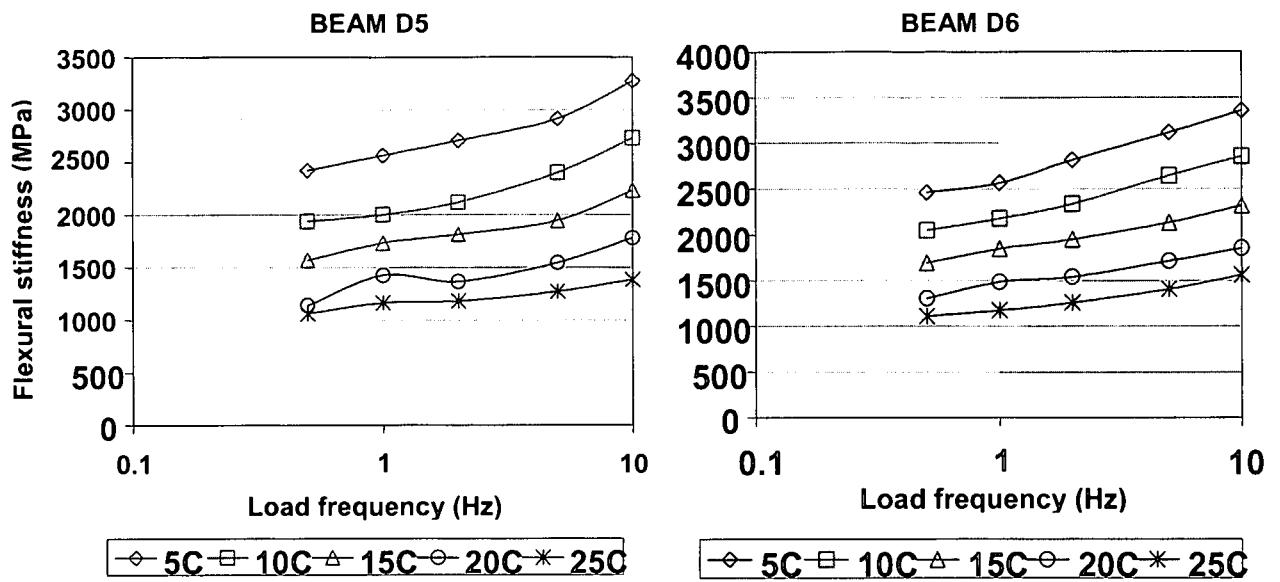


Figure F3: Stiffness modulus frequency sweep at various temperature of Mix 5(B-75C-1%)

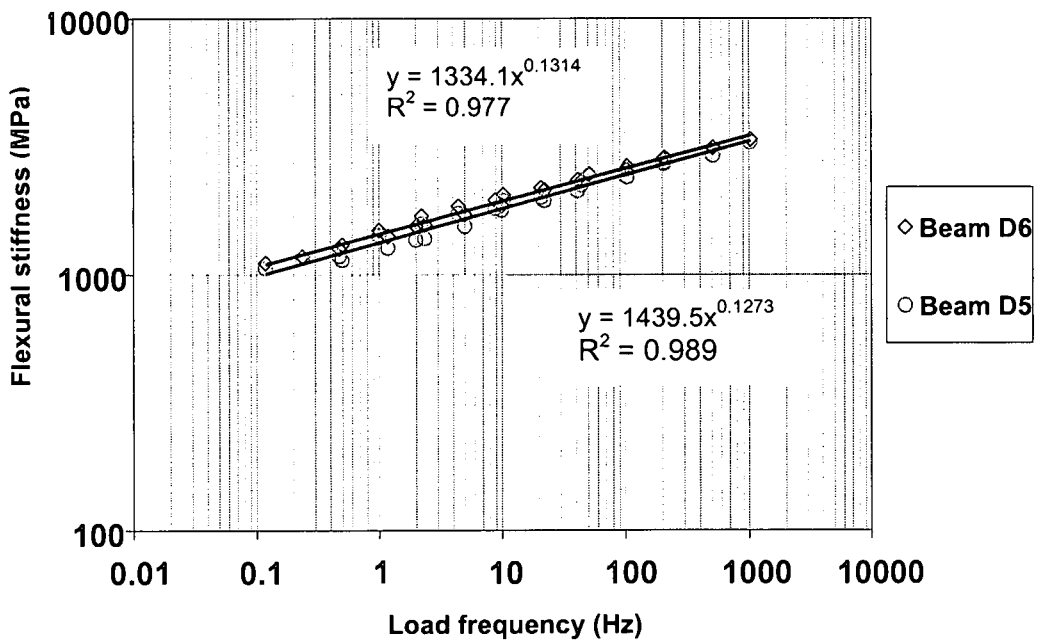


Figure F4: Stiffness characterisation of emulsion Mix 5(B-75C-1%) at various freq. and temp

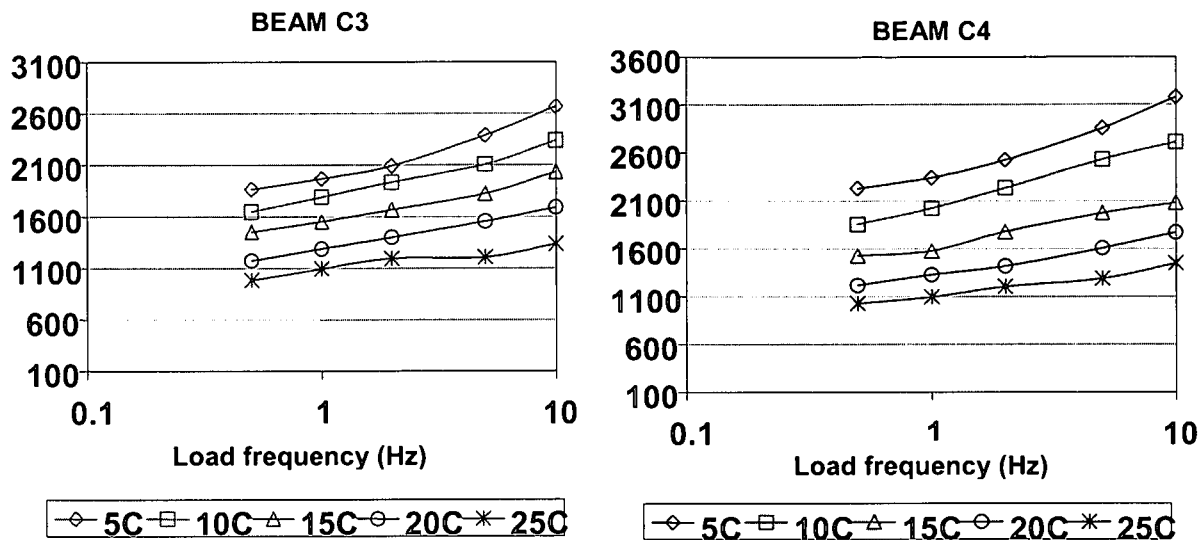


Figure F5: Stiffness modulus frequency sweep at various temperature of Mix 6(B-75M-0%)

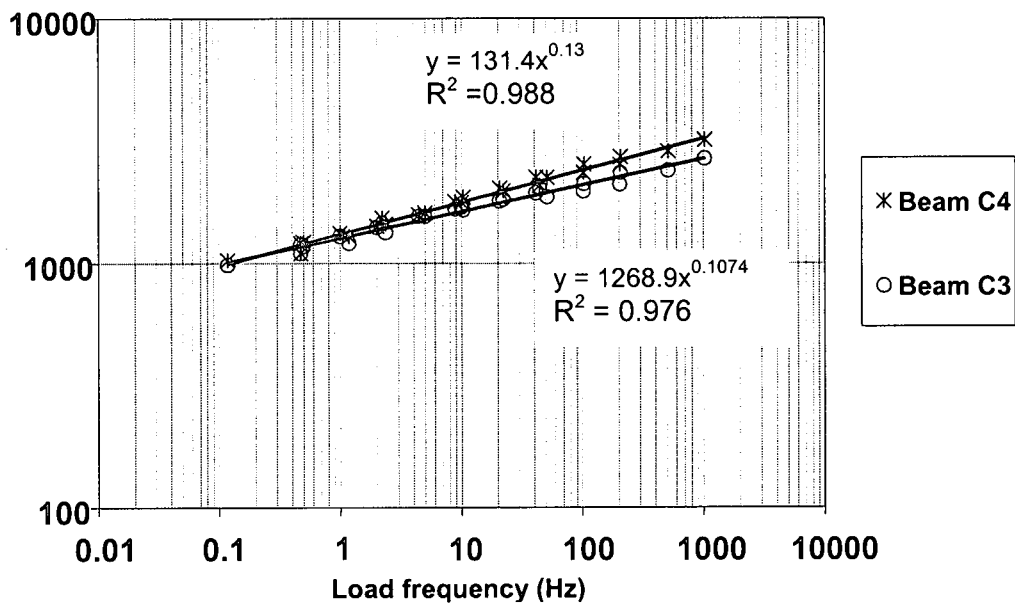


Figure F6: Stiffness characterisation of emulsion Mix 6(B-75M-0%) at various freq. and temp

2. SUPERIMPOSITION OF FLEXURAL STIFFNESS MASTER CURVES OF REPEAT TEST FOR THE FOAM MIXES

2.1 GENERAL

Specimens shall be tested in accordance with the procedure detailed in this section. (Note: Details of operating procedure for the Beam Fatigue Apparatus (BFA) are provided in the Manufacturer's Operation Manual, and reference must be made to the Manual for any specific

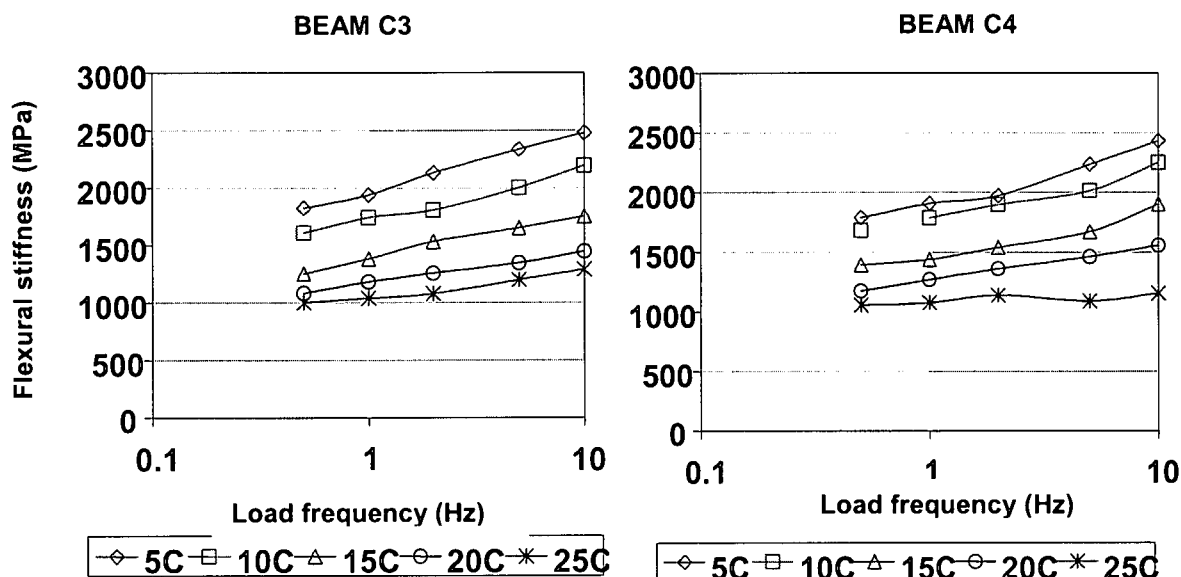


Figure F7: Stiffness modulus frequency sweep at various temperature of Mix 7(C-75C-0%)

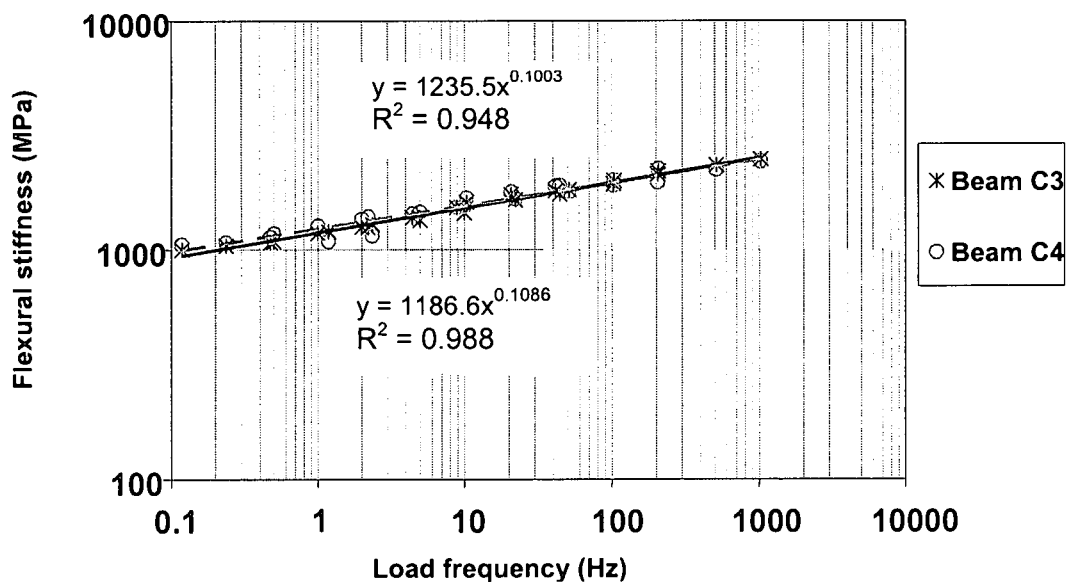


Figure F8: Stiffness characterisation of emulsion Mix 7(C-75C-0%) at various freq. and temp

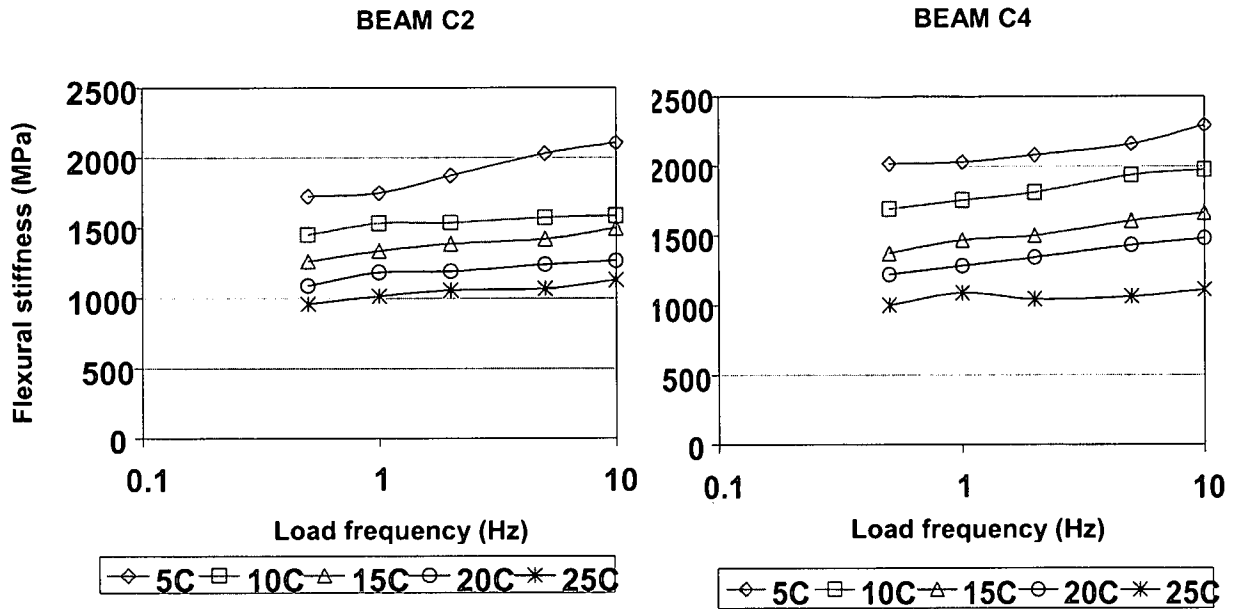


Figure F7: Stiffness modulus frequency sweep at various temperature of Mix 8(C-75C-1%)

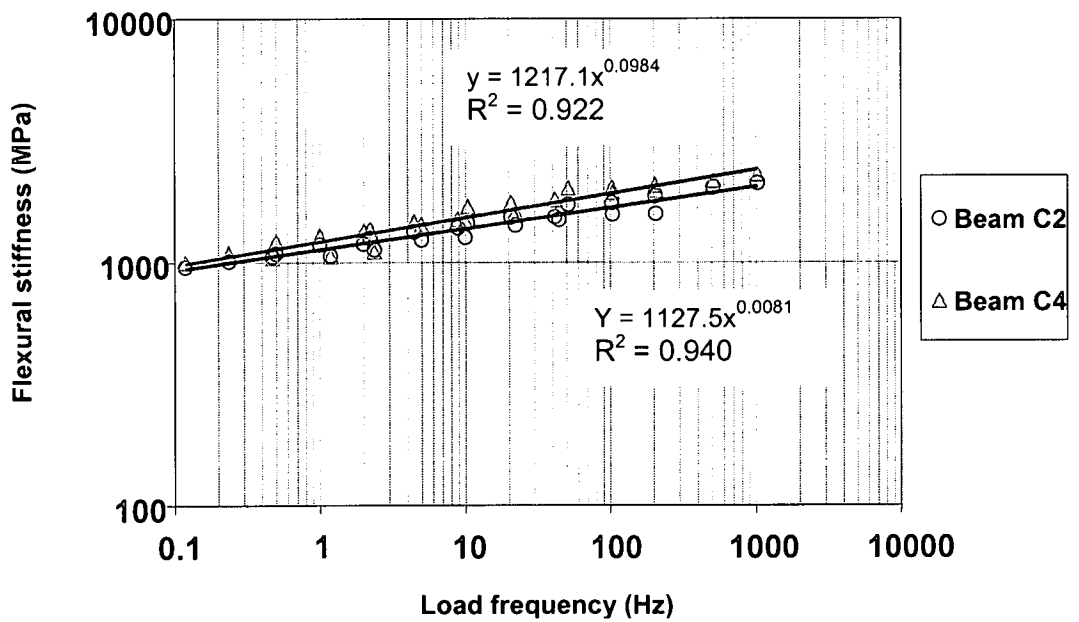


Figure F8: Stiffness characterisation of emulsion Mix 8(C-75C-1%) at various freq. and temp

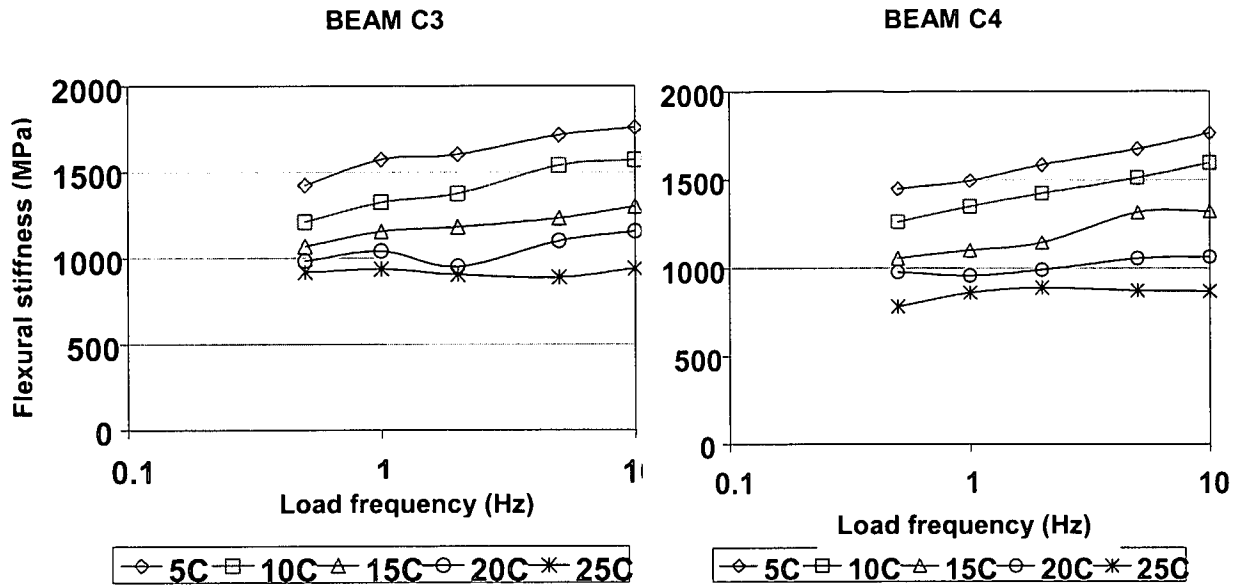


Figure F7: Stiffness modulus frequency sweep at various temperature of Mix 9(C-75M-0%)

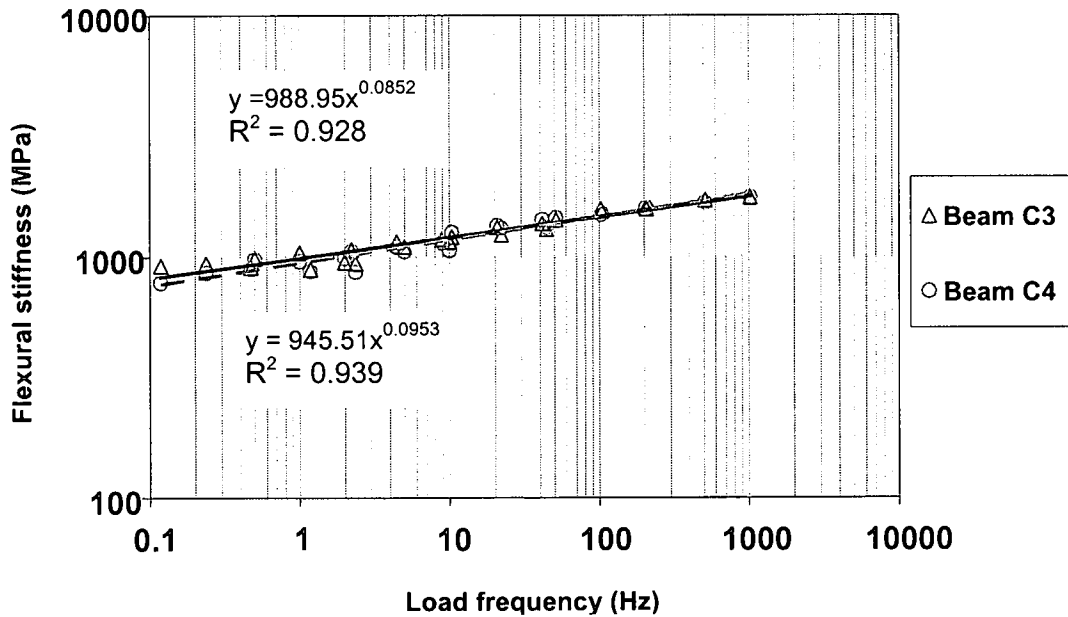


Figure F8: Stiffness characterisation of emulsion Mix 9(C-75M-0%) at various freq. and temp